COMPLEXITY OF GENOMIC ACTIONS CONTROLLED BY THYROID HORMONE RECEPTORS

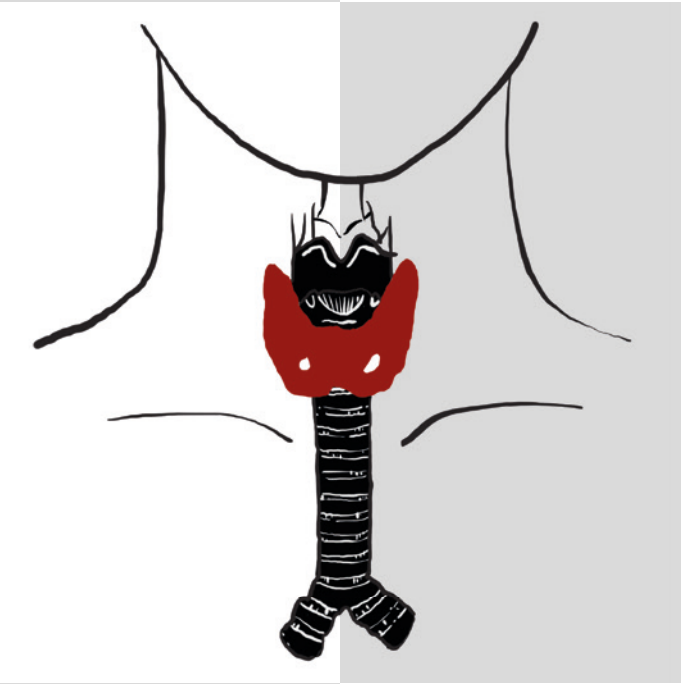

KARN WEJAPHIKUL

Complexity of Genomic Actions Controlled by Thyroid Hormone Receptors

Karn Wejaphikul

Cover design: Supuck Prugsiganont
Thesis layout: Karn Wejaphikul
Printing: Ridderprint BV, www.ridderprint.nl
ISBN: 978-94-6375-524-5

Complexity of Genomic Actions
Controlled by Thyroid Hormone Receptors

Complexiteit van genomische acties van
schildklierhormoonreceptoren

Thesis

to obtain the degree of Doctor from the
Erasmus University Rotterdam
by command of the
rector magnificus

Prof.dr. R.C.M.E. Engels

and in accordance with the decision of the Doctorate Board.

The public defense shall be held on

Wednesday 9 October 2019 at 9.30 hours

by

Karn Wejaphikul
born in Chiang Mai, Thailand

Erasmus University Rotterdam

DOCTORAL COMMITTEE

Promotor:	Prof.dr. R.P. Peeters
Other members:	Prof.dr. A.J. van der Lelij Prof.dr. A.C.S. Hokken-Koelega Prof.dr. A.S.P. van Trotsenburg
Co-promotors:	Dr. M.E. Meima Dr. W.E. Visser

Paranymphs:	Kasiphak Kaikaew Zhongli Chen

Those we love don't go away...
They walk beside us every day.
Unseen, unheard, but always near.
Still loved, still missed, and very dear.

- Anonymous -

In memoriam Prof.dr.ir. Theo J. Visser

Table of Contents

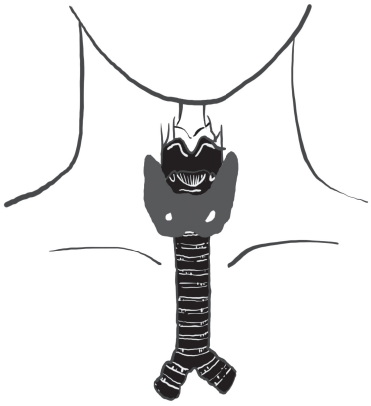

CHAPTER 1

General Introduction

1

Introduction

Thyroid hormone (TH) plays an important role in normal growth, development, and metabolic homeostasis. This is emphasized by severe growth retardation and neurodevelopmental impairment in patients with prolonged untreated congenital hypothyroidism or cretinism (1-4). Adults with hypothyroidism develop symptoms such as cold intolerance, constipation, fatigue, weight gain, bradycardia and depression (5). In contrast, heat intolerance, weight loss, and tachycardia are observed in hyperthyroid patients, illustrating the strong influence of TH in human metabolism (6,7).

TH is synthesized in the thyroid gland and released to the circulation under a tight regulation by the hypothalamic-pituitary-thyroid (HPT) axis. Two major forms of TH are produced, namely 3,3',5,5'-tetraiodothyronine or thyroxine (T4), and 3,3',5-triiodothyronine (T3). Both T3 and T4 are transported across the plasma membrane by multiple thyroid hormone transporters such as monocarboxylate transporter 8 (MCT8). Transcriptional gene regulation (genomic actions) is the principal action of TH, which is mediated by binding of TH to its nuclear thyroid hormone receptors (TRs). Since T3 binds to TRs with a high affinity, it is regarded as the biologically active TH. T4, despite being the most abundant in the circulation, is considered as a prohormone because of its lower biological potency. T4 is converted to T3 in peripheral tissues by outer ring deiodination (ORD) by the type 1 and type 2 deiodinase enzymes (DIO1 and DIO2).

Thyroid hormone synthesis and regulation

Thyroid hormone production

TH is produced by the thyroid gland. The process starts by active transport of iodide (I^-) into thyroid follicular cells via the Na^+/I^- symporter (NIS; SLC5A5) at the basolateral membrane. Intracellular I^- is then delivered into the follicular lumen using a transporter at the apical membrane, possibly Pendrin (PDS; SLC26A4). Next, I^- is oxidized by the membrane-bound thyroperoxidase (TPO) enzyme, which requires the presence of H_2O_2 generated by the dual oxidase enzyme DUOX2 and its specific maturation factor DUOXA2. Oxidized iodide is incorporated (organified) into tyrosyl residue of thyroglobulin (TG), a large glycoprotein that serves as a matrix for TH synthesis, to create two iodinated forms, namely, mono- and diiodotyrosine (MIT and DIT). TPO also catalyzes the coupling of MIT and DIT, and of two DIT molecules to form T3 and T4, respectively. The iodinated TG is subsequently internalized back into the follicular cells by micropinocytosis and endocytosis. After TG is hydrolysed in lysosomes, T3 and T4 are released into the circulation by transporters, including the TH transporter MCT8. MIT and DIT are deiodinated in the cytosol of thyroid follicular cells by the iodotyrosine dehalogenase (DEHAL1) enzyme to recycle iodine for further TH synthesis (Figure

1) (8-10). Genetic defects in each step of TH synthesis result in thyroid dyshormonogenesis, which causes approximately 15% of all cases of primary congenital hypothyroidism (11,12).

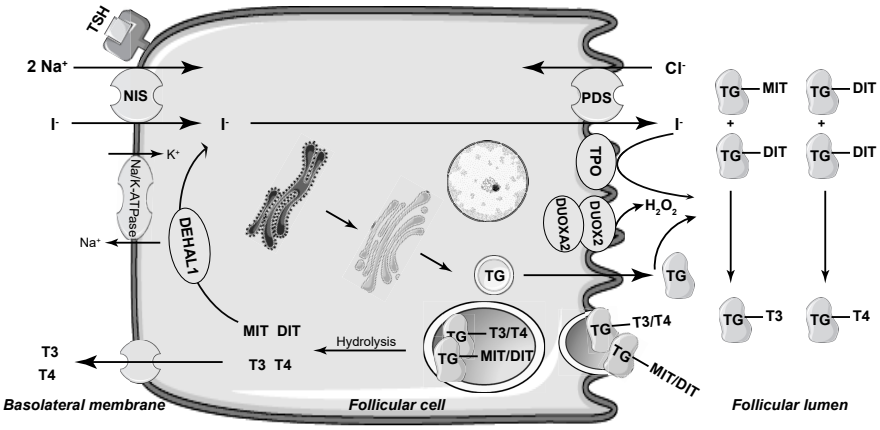

Figure 1. Steps in thyroid hormone synthesis.

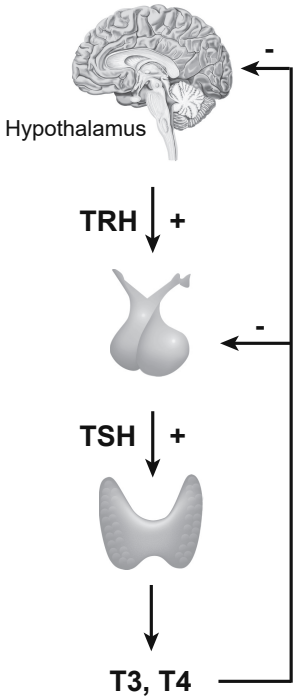

Figure 2. The hypothalamic-pituitary-thyroid axis.

Hypothalamic-Pituitary-Thyroid (HPT) axis

Thyroid hormone synthesis is stimulated by thyroid stimulating hormone (TSH; thyrotropin), a glycoprotein which is released from the anterior pituitary gland. TSH binds to the TSH receptor (TSHR), a G-protein coupled receptor at thyroid follicular cells, to promote multiple steps of TH synthesis, including iodide trapping in the thyroid gland, iodotyrosine and thyroglobulin synthesis, and thyroid hormone release. The concentration of TSH is controlled by thyrotropin-releasing hormone (TRH), produced in the TRH neurons in the paraventricular nucleus of the hypothalamus (13). High concentrations of TH can suppress the production of both TRH and TSH (Figure 2). Animal studies have shown that local conversion of T4 into T3 by the DIO2 in tanycytes, specialized glial cells lining the third ventricle, plays a crucial role in TRH suppression by TH (14,15). Local DIO2 in folliculostellate cells, agranular cells in the human anterior pituitary, converts T4 to T3 and transports T3 to thyrotrophs in a paracrine manner for TSH suppression (16,17). Via this negative feedback mechanism, circulating TH concentrations are maintained within the normal range.

Thyroid hormone transport

To facilitate its genomic action, TH has to enter the cells and bind to TRs. It was previously believed that TH entered the cells by passive diffusion because of its lipophilic property that would allow easy passage of TH through the phospholipid bilayers of the cell membrane. However, later evidence suggested that T3 and T4 are taken up into the cells by transporter proteins located at the plasma membrane of the cells. To date, several TH transporters have been identified, including the iodothyronine-specific transporters monocarboxylate transporters MCT8 (SLC16A2) (18,19) and MCT10 (SLC16A10 or TAT1) (20), the organic anion transporting polypeptide (OATP) family, especially OATP1C1 (SLCO1C1) (21), the Na^+-taurocholate co-transporting polypeptide (NTCP; SLC10A1) (22), and the L-type amino acid transporters LAT1 (SLC7A5) and LAT2 (SLC7A8) (23).

The importance of TH transport across the cell membrane is illustrated by the identification of patients carrying mutations in the TH transporters. The Allan-Herndon-Dudley syndrome (AHDS) was first described in 1944 in a large family with X-linked psychomotor retardation (24). Inactivating mutations in MCT8 were subsequently identified as a cause of this genetic syndrome (25,26). The clinical phenotype of AHDS includes cognitive impairment, intellectual disability, and central hypotonia. Thyroid function tests (TFTs) show low free and total T4, low reverse T3 (rT3), high free and total T3, increased T3/T4 and T3/rT3 ratio, and normal to mildly elevated TSH concentrations (18,27). Recently, Strømme et al. reported a homozygous missense mutation in OATP1C1 as a cause of developmental regression, progressive dementia, spastic diplegia, and cold intolerance in a 15-year-old girl with normal TFTs (28). Since OATP1C1 is important for TH transportation across the blood-brain barrier and into glia and neuronal cells in the brain, loss of the OATP1C1 function likely leads to brain-specific hypothyroidism and neurodegeneration.

Thyroid hormone metabolism: deiodination

As mentioned previously, T4 is the dominant form of TH that is secreted from the thyroid gland and is subsequently converted into the active form T3 at peripheral tissues. The deiodinase enzymes, a subfamily of three selenoproteins capable of removing an iodine atom from the inner (tyrosyl) or outer (phenolic) ring of TH, mediate this conversion (Figure 3). The DIO1, expressed in the liver, kidney, and thyroid gland, can deiodinate both the inner and outer ring of T4 to produce T3 and rT3, respectively. The DIO2, which is ubiquitously expressed in brain, pituitary, retina, brown adipose tissue, innate immune cells, and skeletal muscle, is only able to deiodinate the outer ring (5') of TH. The major role of DIO2 is therefore the conversion of T4 to T3 as well as the control of local tissue T3 concentration. The DIO3 is a TH-inactivating enzyme, as it can only deiodinate the iodine atom from the inner ring of T4 and T3. DIO3 is mainly expressed in fetal tissue and plays a crucial role in embryogenesis. It is also expressed in retina, neurons, pituitary gland, and various type of tumors, such as hemangioma, glioma and gliosarcoma, basal cell carcinoma, pituitary adenoma, and papillary thyroid carcinoma (29-32). Both DIO2 and DIO3 work antagonistically to control intracellular T3 concentrations. DIO2 converts T4 to T3 and therefore increases TH signaling, whereas DIO3 inactivates T4 and T3 and decreases TH signaling (33).

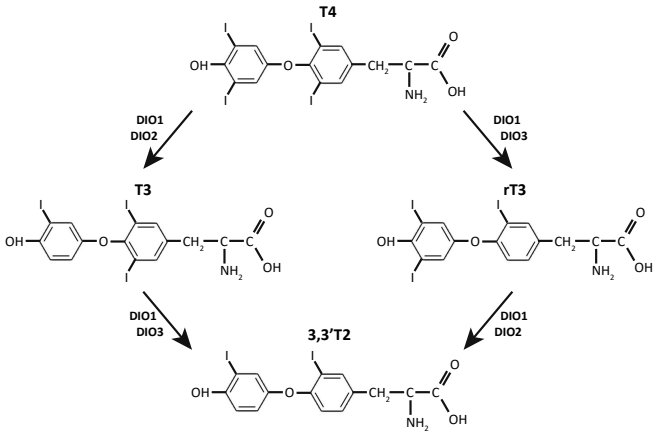

Figure 3. TH metabolism by deiodinase enzymes.

Thyroid hormone receptors and its genomic actions

Genomic actions of thyroid hormone are initiated by binding of T3 to TRs. TRs either homodimerize with the other TR or, more preferably, heterodimerize with retinoid X receptor (RXR) and bind to thyroid hormone response elements (TREs) in the promoter region of TH

target genes to regulate gene expression. In the absence of T3, the TRs recruit corepressor proteins that modify the chromatin structure, resulting in transcriptional repression of genes that are under positive control by TH. In the presence of T3, TRs then release the corepressors and recruit coactivators to induce gene transcriptional activation.

Multiple thyroid hormone isoforms

TRs are members of the nuclear receptor superfamily. Similar to other nuclear receptors, TRs consist of multiple functional domains, including an amino-terminal A/B domain, a central DNA-binding domain (DBD), a hinge region, and a carboxy-terminal ligand binding domain (LBD). There are multiple TR isoforms, generated from two different genes; however, only three functional isoforms have been described that are capable of binding T3 and controlling nuclear gene transcription, namely TRα1, TRβ1, and TRβ2 (Figure 4) (34-36). The structure of these three isoforms is highly homologous. TRα1 is encoded by *THRA* gene on chromosome 17. The alternative splice variant TRα2 is encoded by the same gene but has no T3-binding ability because of differences in length and amino acid composition in the C-terminal region. The *THRB* gene, located on chromosome 3, encodes two T3-binding TR isoforms, TRβ1, and TRβ2, which share high sequence homology in both DBD and LBD but differ in the length and amino acid sequences in the N-terminal A/B domain.

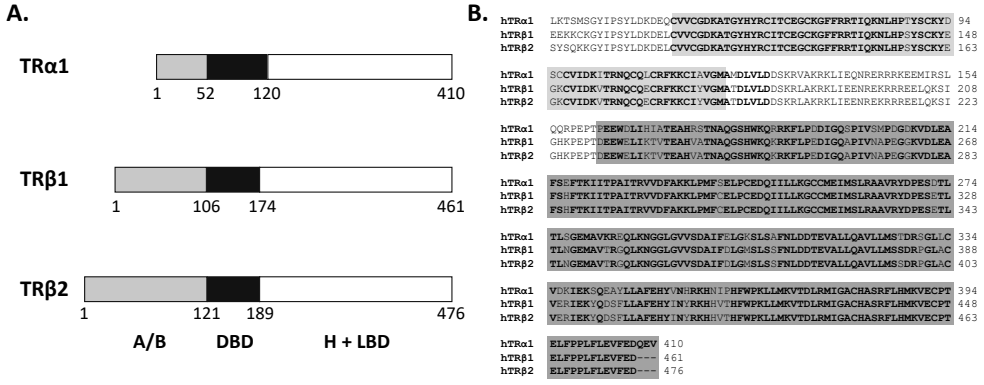

Figure 4. (A) Three TR isoforms that are capable of binding T3 and controlling gene transcription. TRα1 is encoded by *THRA* gene on chromosome 17. TRβ1 and TRβ2 are encoded by *THRB* gene on chromosome 3. (B) Comparison of the sequences shows a high sequence homology (bold) of the DBD (light grey) and LBD (dark grey) of the three TR isoforms. [A/B, A/B domain; DBD, DNA-binding domain; H, hinge region; LBD, ligand binding domain] (Adapted from Langlois MF et al. 1997, Hahm JB et al. 2013, and Wagner RL et al. 1995 (37-39))

The expression of TR isoforms varies among tissues. TRα1 is predominantly expressed in the central nervous system, bone, cardiac tissue, gastrointestinal tract, and skeletal muscle while the non-T3 binding isoform TRα2 is more wildly expressed throughout the whole body. TRβ1 is principally expressed in the liver, kidney and thyroid gland, whereas

TRβ2 is predominantly expressed in the retina, cochlea, as well as the hypothalamus and pituitary gland, where it plays a crucial role in the HPT axis regulation (34,35).

Isoform-dependent functions of TRs

To date, it is unclear whether the different TR isoforms have specific functions or share a similar role in gene transcriptional regulation. Although the properties of all TR isoforms are quite similar *in vitro*, *in vivo* studies show clear differences in the consequences of mutations in the different receptors (35,40). TRα gene knock-out mice ($TR\alpha^{0/0}$) have growth retardation, intestinal malformation, delayed bone maturation, bradycardia, abnormal cardiac contractility, and hypothermia (41). In contrast, TRβ gene knock-out mice ($TR\beta^{-/-}$), in which both TRβ1 and β2 are absent, have normal growth, but HPT axis dysfunction, hearing loss, and abnormal retinal development (42-44). These findings suggest differences in intrinsic properties and/or cell-specific effects of the receptor isoforms. In addition, the phenotypes of these knock-out mice are matched by the phenotypes of patients with resistance to thyroid hormone (RTH) due to mutations of *THRA* gene which is different from the phenotype of patients carrying mutations of the *THRB* gene.

It is generally assumed that differences in tissue distribution of the TRs predominantly dictate the isoform-specific functions. However, there is evidence suggesting that even in cell types where two TR isoforms are available, TRs regulate gene transcription in an isoform-specific manner. For instance, in brown adipose tissue (BAT) where both TRα1 and TRβ1 are expressed (45,46), TRα1 is responsible for norepinephrine-induced BAT thermogenesis whereas TRβ1 mediated expression of mitochondrial uncoupling protein 1 (UCP1), a mitochondrial membrane protein that plays a crucial role in BAT thermogenesis (47). Data from TR knock-out mice also showed that DIO1 expression have differences in tissue and isoform regulation. The expression is solely regulated by TRβ in the kidney but requires both TR isoforms in the liver (48). Furthermore, co-expression of both TRα1 and TRβ1 is also observed in Purkinje neurons, in which cell differentiation is T3-dependent. Only *Thra* knock-out, but not *Thrb* knock-out, altered *in vitro* differentiation of Purkinje neurons, suggesting an TRα1-specific effect (49). However, both *in vitro* studies performed in other cell types and *in vivo* studies are needed to confirm these findings.

Ligand of TRs: T3 and beyond

In 1952, it was recognized that T3 has a higher biological potency than T4 (50-53). This fundamental discovery led to the clinical concept that T3 is the biologically active hormone. Crystal structures showed that the LBD of TRs consists of 12 α-helices (H1-H12) that fold into a hydrophobic-core pocket. T3 can be tightly accommodated in this pocket and induce conformational changes of the TR, especially at the location of H12, to enclose the ligand-binding pocket (54,55). This conformational rearrangement induces corepressor protein dissociation and allows coactivator protein association, which is essential for gene transcriptional activation.

Follow up studies suggest that T4 can also bind to TRs with a lower binding affinity (10-30 fold) than that of T3 (56-58). The T4-bound WT TRβ1 crystal structure revealed that the ligand-binding pocket of TRβ1 could accommodate both T3 and T4, although the H11-H12 loop is more loosely packed in the presence of T4 than T3 (57). However, the molecular and structural mechanisms underlying the higher affinity of T3 than T4 have not been investigated in detail. In addition, the precise role of T4 as a prohormone and the possibility that T4 might function directly as an active hormone in at least specific cellular contexts remains inconclusive.

In addition to T3 and T4, there are naturally occurring TH metabolites that can also bind to TRs, such as 3,3',5-triiodothyroacitic acid (Triac), the T3-derivative containing an acetic acid group. Evidence indicates that Triac binds to TRα1 with a similar affinity as T3 and binds to TRβ1 and TRβ2 with a 3- to 6-fold higher affinity than T3 (59). Therefore, Triac is considered as a TRβ-selective agonist which can be used as a treatment option in a certain condition such as RTHβ and AHDS (60). However, since the concentration of Triac in human circulation is approximately 50-fold lower than that of T3, the physiological role of this TH derivative is yet unclear (60,61).

Over the past decades, numerous TH analogs have been synthesized in order to create novel therapeutic agents for certain conditions, for instance, hyperlipidemia, obesity, and non-alcoholic fatty liver diseases (NAFLD) (62-66). These analogs can bind to TRs with differences in isoform specificity. However, most of them are designed as more specific for the TRβ isoforms to minimize the TRα-dependent cardiac side effects. A list with examples of TH analogs is summarized in Table1.

Table 1. TH analogs

Compound	Isoform specificity	Potential benefit(s)
DITPA	Non-selective	↓ cholesterol and triglyceride levels, ↑ cardiac output (without significant increase in heart rate)
GC-1 (Sorbetirome)	TRβ	↓ cholesterol levels, ↓ hepatic steatosis, ↑ liver regeneration
GC24	TRβ	↓ triglyceride levels
KB-141	TRβ	↓ triglyceride levels, ↓ body weight
KB-2115 (Eprotirome)*	TRβ	↓ cholesterol and triglyceride levels, ↓ hepatic steatosis, ↑ hepatocyte proliferation
MB07811	TRβ	↓ cholesterol and triglyceride levels, ↓ hepatic steatosis
MGL3196	TRβ	↓ triglyceride levels, ↓ hepatic steatosis

*Evidence shows adverse effects on cartilage and drug-induced liver toxicity (elevated AST, ALT, and gamma glutamyltranspeptidase).

Multilevel regulation of TR transcriptional activation

Multiple configurations of thyroid hormone response elements

To regulate gene transcription, both unliganded and liganded TRs (in combination with other TR or RXRs) bind to the TREs using the DBD. The TREs consist of two consensus hexanucleotide half-sites [(A/G)GGT(C/A/G)A] that can be arranged as a direct repeat (DR), inverted repeat (IR), and everted repeat (ER) (Figure 5) (35). The space between the two half-sites varies, depending on the orientation of the half-site. There is evidence showing that the orientation of TREs determines the dimerization pattern of TRs (67,68). In addition, *in vitro* studies of TRβ1 mutations show a differential effect on different TREs of some mutants (69,70), suggesting a TRE-specific transcriptional impairment. However, ChIP-seq analyses show that the DR4-TRE is the most common TR binding site identified at the promoter regions of TH target genes (71-74). Therefore, the exact role of different TRE configurations on transcriptional gene regulation is still doubtful.

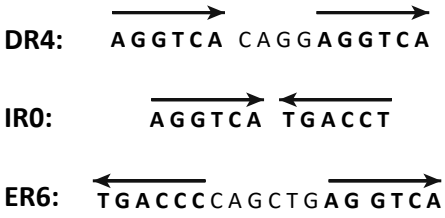

Figure 5. Consensus TRE half-site and three main TRE configurations. [DR4, direct repeat; IR0, inverted repeat; ER6, everted repeat] (Adapted from Cheng SY et al. 2010 (35))

TR-RXR heterodimerization

As mentioned previously, TRs either form homodimers or heterodimers with RXRs to regulate gene expression. However, heterodimerization with RXR is the primary form of TR-dimerization for both TRα1 and TRβ1 isoforms. The heterodimerization dramatically increases the binding of TRs to TREs, and the T3-induced transcriptional activation (35). TRs bind to RXRs via a highly conserved ninth heptad region in H11 of the TR LBD (Leu367-Leu374 of TRα1 and Leu421-Lue428 of TRβ1) (75). Mutations in this region concomitantly decrease heterodimerization and receptor transactivation (34) Although TRs mainly form heterodimers, previous studies indicate that TRβ1 may have a greater tendency than TRα1 to form homodimers on several TREs, suggesting that these two isoforms may have different dimerization potentials (34)

TR-coregulatory protein interactions

To control target gene expression, TRs associate with many coregulatory proteins. These proteins modify the histone core of nucleosomes by acetylation, methylation, and ubiquitination, all of which lead to a change of the chromatin structure (chromatin remodeling) and accessibility of target genes (73,76). In case of genes that are positively regulated by TH, unliganded TRs recruit corepressor proteins to repress gene transcription, while liganded TRs induce coactivator recruitment and consequently stimulate gene transcription. This process is called the “classic bimodal switch model” of TR action (Figure 6) (77).

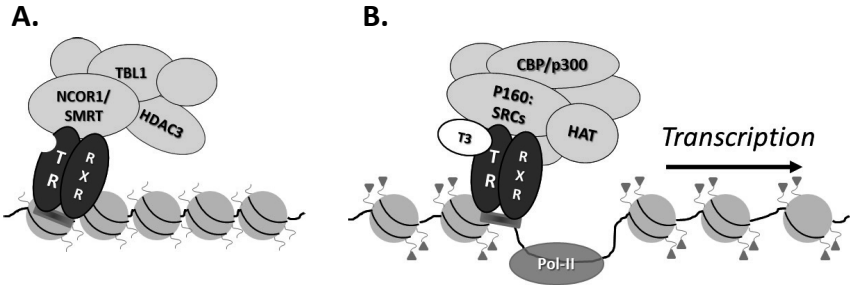

Figure 6. Classic bimodal switch model of TR action. (A) Unliganded-TR heterodimerizes with RXR and recruits corepressor proteins, leading to nucleosome packing. (B) Liganded-TR, in combination with RXR, recruits coactivator proteins, including histone acetyltransferase (HAT) that acetylate (triangles) neighboring histones. This process unpacks the nucleosomes and allows critical enzymes such as RNA-polymerase II (Pol-II) to approach the target gene and initiate gene transcription.

The most well-known TR corepressors are NCoR (nuclear receptor corepressor) and its homolog, SMRT (silencing mediator of retinoid and thyroid hormone receptors). These proteins bind to the corepressor interacting sites in the C-terminal region of TRs and recruit other nuclear proteins such as transducing-like protein (TBL1 or TBL1R) and histone deacetylase 3 (HDAC3) to form large corepressor complexes (78-80). By removing the acetyl group from histones, HDAC3 creates nucleosome compaction, thereby inhibiting the binding of RNA polymerase II which results in suppression of target gene transcription.

Binding of TH to TRs causes a conformational change in H12 of the TR-LBD, in a way that favors dissociation of the corepressors from and association of the coactivators with the TRs. The main TR-binding coactivators are steroid hormone receptor co-activator 1, 2, and 3 (SRC-1, -2, and -3) (81,82). SRCs interact with coactivator interaction sites of TRs by using the LXXLL motif (NR box) located in the central part of the SRC molecule. After binding to the TRs, two activating domains (ADs) located in the C-terminal region of SRC recruit chromatin-

modifying coregulatory complexes such as CBP/p300 processing histone acetyltransferase (HAT), which results in chromatin accessibility and activates gene transcription.

Apart from well-known corepressors and coactivators, other nuclear proteins have also been reported as coregulators for TRs. For instance, Hairless (83,84), Alien (85,86), RIP-140 (87), and Jab1 (88) were identified as corepressors, whereas nuclear receptor-interacting factor 3 (NRIF3), as known as integrin subunit beta 3 binding protein (ITG3BP), was identified as a coactivator for TRs (89,90). This evidence highlights the complexity of gene transcriptional regulation by TRs. In addition, the expression of many nuclear receptor coregulatory proteins could be tissue-dependent (40,91-93), and some patterns of coregulatory protein recruitment could be isoform-specific (38,91,94). These mechanisms could further explain the various transcriptional regulations of TR in different tissues.

Mutation of TRs: Resistance to thyroid hormone

Resistance to TH (RTH) is a syndrome of reduced sensitivity to TH of target tissues, which was firstly described in 1967 (95). Mutations of the gene encoding TRβ *(THRB)* were subsequently identified as a cause of this disease (96). Since then, the term RTH has become synonymous with this condition. In 2012, mutations of the gene encoding TRα *(THRA)* were identified (97,98), thereby extending the spectrum of RTH. Today, RTH includes all syndromes resulting from dysfunction in TH transport, deiodination and receptor dysfunction (99,100). However, in this thesis, we mainly focus on RTH caused by mutations of the TRs (RTHα and RTHβ respectively).

RTHβ

Mutations in the LBD of TRβ1 and TRβ2 lead to RTHβ. Common biochemical characteristic includes high serum T3 and T4 concentrations with normal or slightly increased TSH level. However, the clinical presentation varies between patients. This is partly dependent on the severity of hormonal resistance, but there is also large variation between different family members with the same mutation. Goiter is the main clinical finding that prompts patients to seek for medical investigations (100,101). Tachycardia, short stature, and attention deficit disorders can also be part of the clinical presentation in affected individuals because of the effect of high THs in TRα predominant tissues such as heart, brain, and bone. The incidence of RTHβ is approximately 1:40,000 live births (102,103).

RTHβ is usually inherited in an autosomal dominant fashion (100). Single nucleotide substitutions leading to amino acid replacement are more common than frameshift or nonsense mutations that result in premature protein truncations (104-106). To date, over 160 different mutations have been identified as a cause of RTHβ in more than 350 families (101,107). These mutations are located in three CpG rich hotspots (cluster 1; codon 426-461, cluster 2;

310-353, and cluster 3; codon 234-282) that are prone to mutate in the LBD and the hinge region of TRβ (100). Therefore, mutations commonly impair affinity for TH and consequently reduce transcriptional activity of the receptor. However, mutations that impair TR dimerization or interaction with nuclear co-regulatory proteins have also been reported (70,108-115).

RTHα

Because of a high degree homology between TRα and TRβ (overall 80% of amino acids in their LBD are identical), it was anticipated for many years that mutations in TRα would also be able to cause RTH. Therefore, many knock-in and knock-out mouse models were generated to predict the clinical phenotype of RTHα (116-119). All of the mutated mice showed impaired growth and bone development but near normal TFTs, complicating the easy identification of RTHα patients. As a consequence, mutations in *THRA* as a cause of RTHα had not been identified until 2012 (97,98), probably due to this lack of an obvious thyroid function abnormality.

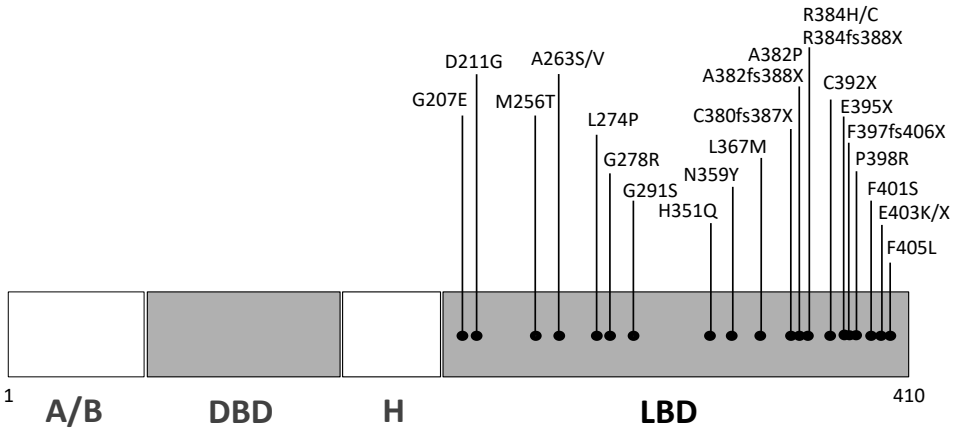

Figure 7. Localization of 25 TRα1 mutations identified in RTHα patients. [A/B, A/B domain; DBD, DNA-binding domain; H, hinge region; LBD, ligand binding domain]

The clinical phenotype of RTHα patients is distinct from RTHβ and includes growth retardation, macrocephaly, constipation, intellectual disability, autistic spectrum disorder, and anemia. Their TFTs are typically characterized by high to high-normal (F)T3, low to low-normal (F)T4, low rT3 and normal TSH concentrations, resulting in markedly increased (F)T3/(F)T4 and (F)T3/rT3 ratios. To date, 25 mutations (in a total of 40 patients) have been reported as a cause of RTHα, all of which are located in the LBD of TRα1 and impair T3 binding affinity (Figure 7). These mutations can be categorized into two groups based on the type of mutation.

The first group consists of truncating mutations caused by frameshift or nonsense mutations that lead to premature stop codons and shorten the length of the LBD (97,98,120-124). This structural alteration abolishes T3 affinity and T3-induced transcriptional activity of TRα1. The second group consists of missense mutations that result in single amino acid substitutions in the LBD (121,122,125-133). These mutant receptors can still bind T3 but with a lower affinity than the WT receptor.

Diverse functional impairment of TR mutants and phenotype variability

In RTHβ, patients who carry different mutations commonly have differences in phenotype severity as well as thyroid dysfunction. Interestingly, these differences are also found between individuals that express the same mutation (100,101). This same variety in clinical phenotype is also observed in RTHα patients. In general, patients with truncating mutations that completely abolish T3 binding affinity have a more severe phenotype than patients with missense mutations that have residual T3 binding (128). However, there are differences within each group and even between patients carrying the same mutation. For instance, in a large RTHα family carrying A263S mutation, the severity of constipation, macrocephaly, delay development, and anaemia, are diverse between affected members (121). So far, the underlying molecular mechanism to explain this observation has not been clearly revealed.

Since mutations in TRα and TRβ are mainly located in the LBD and affect T3 binding affinity of the receptors, it could be anticipated that the severity of T3 binding impairment by the different mutants correlates with the degree of transcriptional impairment and the severity of the clinical phenotype. However, it has been demonstrated in RTHβ that differences in T3 binding do not solely explain the diversely impaired transcriptional activation of the mutants. Some TRβ mutants have severe transcriptional impairment despite only mild disturbances in T3 binding affinity. *In vitro* studies showed that these mutants either impair dimerization (69,108,109,111,134) or TR-cofactor interaction (70,112-115,135). In addition, a small group of TRβ mutants impairs transcriptional activation only when associated with certain TRE configuration (70). These findings may partly explain the phenotype variability in RTHβ patients. Since RTHα has recently been identified, additional patients and studies to explore the differences in RTHα are needed.

Outline of the thesis

In this thesis, we focus on the complexity of the genomic actions of TH. In **chapter 2**, we describe a novel mutation, TRβ1-L341V, as a cause of RTHβ and emphasize the crucial role of the Leu341 in TRβ function. In **chapter 3**, we unravel the molecular and structural mechanism underlying the differences in biological activity of T3 and T4, prompted by the identification of a novel TRα1-M256T and previously reported TRβ1-M310T mutations in RTHα and β patients, respectively. In **chapter 4**, we investigate the factors that contribute to the differential impaired transcriptional activity of seven TRα missense mutations, four of which are derived from RTHα patients. In **chapter 5**, we study the difference in neurocognitive impairment of RTHα patients carrying various truncating mutations by evaluating the pattern of gene expression of stably expressed WT or mutant TRα1 in a human neuronal cell line (SH-SY5Y). In **chapter 6**, we explore the pattern of nuclear coregulatory protein recruitment of TRs using interactome analysis. **Chapter 6a** focuses on the cell-type specific coregulatory protein recruitment of TRα1 by performing the experiments in human liver and neuronal cell lines (HepG2 vs. SH-SY5Y). **Chapter 6b** focuses on the isoform-dependent (TRα1 vs. TRβ1) coregulatory protein recruitment. In **chapter 7**, we discuss the findings presented in this thesis combining with the currently available literature and the possible implications of these studies.

References

1. Klein AH, Meltzer S, Kenny FM. Improved prognosis in congenital hypothyroidism treated before age three months. *J Pediatr.* 1972;**81**(5):912-915.
2. Syed S. Iodine and the “near” eradication of cretinism. *Pediatrics.* 2015;**135**(4):594-596.
3. Grant DB, Smith I, Fuggle PW, Tokar S, Chapple J. Congenital hypothyroidism detected by neonatal screening: relationship between biochemical severity and early clinical features. *Arch Dis Child.* 1992;**67**(1):87-90.
4. Isichei UP, Das SC, Egbuta JO. Central cretinism in four successive siblings. *Postgrad Med J.* 1990;**66**(779):751-756.
5. Chaker L, Bianco AC, Jonklaas J, Peeters RP. Hypothyroidism. *Lancet.* 2017;**390**(10101):1550-1562.
6. Gilbert J. Thyrotoxicosis - investigation and management. *Clin Med (Lond).* 2017;**17**(3):274-277.
7. Smith TJ, Hegedus L. Graves’ Disease. *N Engl J Med.* 2016;**375**(16):1552-1565.
8. Hannoush ZC, Weiss RE. Defects of Thyroid Hormone Synthesis and Action. *Endocrinol Metab Clin North Am.* 2017;**46**(2):375-388.
9. Targovnik HM, Citterio CE, Rivolta CM. Iodide handling disorders (NIS, TPO, TG, IYD). *Best Pract Res Clin Endocrinol Metab.* 2017;**31**(2):195-212.
10. Persani L, Rurale G, de Filippis T, Galazzi E, Muzza M, Fugazzola L. Genetics and management of congenital hypothyroidism. *Best Pract Res Clin Endocrinol Metab.* 2018;**32**(4):387-396.
11. Wassner AJ, Brown RS. Congenital hypothyroidism: recent advances. *Current opinion in endocrinology, diabetes, and obesity.* 2015;**22**(5):407-412.
12. LaFranchi SH. Approach to the diagnosis and treatment of neonatal hypothyroidism. *J Clin Endocrinol Metab.* 2011;**96**(10):2959-2967.
13. Roelfsema F, Boelen A, Kalsbeek A, Fliers E. Regulatory aspects of the human hypothalamus-pituitary-thyroid axis. *Best Pract Res Clin Endocrinol Metab.* 2017;**31**(5):487-503.
14. Lechan RM, Fekete C. The TRH neuron: a hypothalamic integrator of energy metabolism. *Prog Brain Res.* 2006;**153**:209-235.
15. Fliers E, Alkemade A, Wiersinga WM, Swaab DF. Hypothalamic thyroid hormone feedback in health and disease. *Prog Brain Res.* 2006;**153**:189-207.
16. Alkemade A, Friesema EC, Kuiper GG, Wiersinga WM, Swaab DF, Visser TJ, Fliers E. Novel neuroanatomical pathways for thyroid hormone action in the human anterior pituitary. *Eur J Endocrinol.* 2006;**154**(3):491-500.
17. Fliers E, Unmehopa UA, Alkemade A. Functional neuroanatomy of thyroid hormone feedback in the human hypothalamus and pituitary gland. *Mol Cell Endocrinol.* 2006;**251**(1-2):1-8.
18. Groeneweg S, Visser WE, Visser TJ. Disorder of thyroid hormone transport into the tissues. *Best Pract Res Clin Endocrinol Metab.* 2017;**31**(2):241-253.
19. Friesema EC, Ganguly S, Abdalla A, Manning Fox JE, Halestrap AP, Visser TJ. Identification of monocarboxylate transporter 8 as a specific thyroid hormone transporter. *J Biol Chem.* 2003;**278**(41):40128-40135.
20. Friesema EC, Jansen J, Jachtenberg JW, Visser WE, Kester MH, Visser TJ. Effective cellular uptake and efflux of thyroid hormone by human monocarboxylate transporter 10. *Mol Endocrinol.* 2008;**22**(6):1357-1369.
21. Alkemade A, Friesema EC, Kalsbeek A, Swaab DF, Visser TJ, Fliers E. Expression of thyroid hormone transporters in the human hypothalamus. *J Clin Endocrinol Metab.* 2011;**96**(6):E967-971.
22. Friesema EC, Docter R, Moerings EP, Stieger B, Hagenbuch B, Meier PJ, Krenning EP, Hennemann G, Visser TJ. Identification of thyroid hormone transporters. *Biochem Biophys Res Commun.* 1999;**254**(2):497-501.
23. Zevenbergen C, Meima ME, Lima de Souza EC, Peeters RP, Kinne A, Krause G, Visser

WE, Visser TJ. Transport of Iodothyronines by Human L-Type Amino Acid Transporters. *Endocrinology.* 2015;**156**(11):4345-4355.

24. Allan W, Herndon CN, Dudley FC. Some examples of the inheritance of mental deficiency: Apparently sex-linked idiocy and microcephaly. *Am J Ment Defic.* 1944;**48**:325-334.
25. Friesema EC, Grueters A, Biebermann H, Krude H, von Moers A, Reeser M, Barrett TG, Mancilla EE, Svensson J, Kester MH, Kuiper GG, Balkassmi S, Uitterlinden AG, Koehrle J, Rodien P, Halestrap AP, Visser TJ. Association between mutations in a thyroid hormone transporter and severe X-linked psychomotor retardation. *Lancet.* 2004;**364**(9443):1435-1437.
26. Dumitrescu AM, Liao XH, Best TB, Brockmann K, Refetoff S. A novel syndrome combining thyroid and neurological abnormalities is associated with mutations in a monocarboxylate transporter gene. *Am J Hum Genet.* 2004;**74**(1):168-175.
27. Braun D, Schweizer U. Thyroid Hormone Transport and Transporters. *Vitam Horm.* 2018;**106**:19-44.
28. Stromme P, Groeneweg S, Lima de Souza EC, Zevenbergen C, Torgersbraten A, Holmgren A, Gurcan E, Meima ME, Peeters RP, Visser WE, Honeren Johansson L, Babovic A, Zetterberg H, Heuer H, Frengen E, Misceo D, Visser TJ. Mutated Thyroid Hormone Transporter OATP1C1 Associates with Severe Brain Hypometabolism and Juvenile Neurodegeneration. *Thyroid.* 2018;**28**(11):1406-1415.
29. Casula S, Bianco AC. Thyroid hormone deiodinases and cancer. *Front Endocrinol (Lausanne).* 2012;**3**:74.
30. Dentice M, Ambrosio R, Salvatore D. Role of type 3 deiodinase in cancer. *Expert Opin Ther Targets.* 2009;**13**(11):1363-1373.
31. Romitti M, Wajner SM, Zennig N, Goemann IM, Bueno AL, Meyer EL, Maia AL. Increased type 3 deiodinase expression in papillary thyroid carcinoma. *Thyroid.* 2012;**22**(9):897-904.
32. Romitti M, Wajner SM, Ceolin L, Ferreira CV, Ribeiro RV, Rohenkohl HC, Weber Sde S, Lopez PL, Fuziwara CS, Kimura ET, Maia AL. MAPK and SHH pathways modulate type 3 deiodinase expression in papillary thyroid carcinoma. *Endocr Relat Cancer.* 2016;**23**(3):135-146.
33. Bianco AC, da Conceicao RR. The Deiodinase Trio and Thyroid Hormone Signaling. *Methods Mol Biol.* 2018;**1801**:67-83.
34. Yen PM. Physiological and molecular basis of thyroid hormone action. *Physiol Rev.* 2001;**81**(3):1097-1142.
35. Cheng SY, Leonard JL, Davis PJ. Molecular aspects of thyroid hormone actions. *Endocr Rev.* 2010;**31**(2):139-170.
36. Flamant F, Cheng SY, Hollenberg AN, Moeller LC, Samarut J, Wondisford FE, Yen PM, Refetoff S. Thyroid Hormone Signaling Pathways: Time for a More Precise Nomenclature. *Endocrinology.* 2017;**158**(7):2052-2057.
37. Langlois MF, Zanger K, Monden T, Safer JD, Hollenberg AN, Wondisford FE. A unique role of the beta-2 thyroid hormone receptor isoform in negative regulation by thyroid hormone. Mapping of a novel amino-terminal domain important for ligand-independent activation. *J Biol Chem.* 1997;**272**(40):24927-24933.
38. Hahm JB, Privalsky ML. Research resource: identification of novel coregulators specific for thyroid hormone receptor-beta2. *Mol Endocrinol.* 2013;**27**(5):840-859.
39. Wagner RL, Apriletti JW, McGrath ME, West BL, Baxter JD, Fletterick RJ. A structural role for hormone in the thyroid hormone receptor. *Nature.* 1995;**378**(6558):690-697.
40. Flamant F, Gauthier K. Thyroid hormone receptors: the challenge of elucidating isotype-specific functions and cell-specific response. *Biochim Biophys Acta.* 2013;**1830**(7):3900-3907.
41. Gauthier K, Plateroti M, Harvey CB, Williams GR, Weiss RE, Refetoff S, Willott JF, Sundin V, Roux JP, Malaval L, Hara M, Samarut J, Chassande O. Genetic analysis reveals different functions for the products of the thyroid hormone receptor alpha locus. *Mol Cell Biol.* 2001;**21**(14):4748-4760.
42. Forrest D, Erway LC, Ng L, Altschuler R, Curran T. Thyroid hormone receptor beta is essential for development of auditory function. *Nat Genet.* 1996;**13**(3):354-357.

43. Weiss RE, Forrest D, Pohlenz J, Cua K, Curran T, Refetoff S. Thyrotropin regulation by thyroid hormone in thyroid hormone receptor beta-deficient mice. *Endocrinology.* 1997;**138**(9):3624-3629.

44. Shibusawa N, Hashimoto K, Nikrodhanond AA, Liberman MC, Applebury ML, Liao XH, Robbins JT, Refetoff S, Cohen RN, Wondisford FE. Thyroid hormone action in the absence of thyroid hormone receptor DNA-binding in vivo. *J Clin Invest.* 2003;**112**(4):588-597.

45. Hernandez A, Obregon MJ. Presence and mRNA expression of T3 receptors in differentiating rat brown adipocytes. *Mol Cell Endocrinol.* 1996;**121**(1):37-46.

46. Reyne Y, Nougues J, Cambon B, Viguerie-Bascands N, Casteilla L. Expression of c-erbA alpha, c-erbA beta and Rev-erbA alpha mRNA during the conversion of brown adipose tissue into white adipose tissue. *Mol Cell Endocrinol.* 1996;**116**(1):59-65.

47. Ribeiro MO, Carvalho SD, Schultz JJ, Chiellini G, Scanlan TS, Bianco AC, Brent GA. Thyroid hormone--sympathetic interaction and adaptive thermogenesis are thyroid hormone receptor isoform--specific. *J Clin Invest.* 2001;**108**(1):97-105.

48. Amma LL, Campos-Barros A, Wang Z, Vennstrom B, Forrest D. Distinct tissue-specific roles for thyroid hormone receptors beta and alpha1 in regulation of type 1 deiodinase expression. *Mol Endocrinol.* 2001;**15**(3):467-475.

49. Heuer H, Mason CA. Thyroid hormone induces cerebellar Purkinje cell dendritic development via the thyroid hormone receptor alpha1. *The Journal of neuroscience : the official journal of the Society for Neuroscience.* 2003;**23**(33):10604-10612.

50. Gross J, Pitt-Rivers R. Physiological activity of 3:5:3'-L-triiodothyronine. *Lancet.* 1952;**1**(6708):593-594.

51. Pitt-Rivers R. Metabolic effects of compounds structurally related to thyroxine in vivo: thyroxine derivatives. *J Clin Endocrinol Metab.* 1954;**14**(11):1444-1450.

52. Mussett MV, Pitt-Rivers R. The thyroid-like activity of triiodothyronine analogues. *Lancet.* 1954;**267**(6850):1212-1213.

53. Lerman J. The contribution of triiodothyronine to thyroid physiology. *J Clin Endocrinol Metab.* 1954;**14**(6):690-693.

54. Ribeiro RC, Apriletti JW, Wagner RL, Feng W, Kushner PJ, Nilsson S, Scanlan TS, West BL, Fletterick RJ, Baxter JD. X-ray crystallographic and functional studies of thyroid hormone receptor. *J Steroid Biochem Mol Biol.* 1998;**65**(1-6):133-141.

55. Nascimento AS, Dias SM, Nunes FM, Aparicio R, Ambrosio AL, Bleicher L, Figueira AC, Santos MA, de Oliveira Neto M, Fischer H, Togashi M, Craievich AF, Garratt RC, Baxter JD, Webb P, Polikarpov I. Structural rearrangements in the thyroid hormone receptor hinge domain and their putative role in the receptor function. *J Mol Biol.* 2006;**360**(3):586-598.

56. Apriletti JW, Eberhardt NL, Latham KR, Baxter JD. Affinity chromatography of thyroid hormone receptors. Biospecific elution from support matrices, characterization of the partially purified receptor. *J Biol Chem.* 1981;**256**(23):12094-12101.

57. Sandler B, Webb P, Apriletti JW, Huber BR, Togashi M, Cunha Lima ST, Juric S, Nilsson S, Wagner R, Fletterick RJ, Baxter JD. Thyroxine-thyroid hormone receptor interactions. *J Biol Chem.* 2004;**279**(53):55801-55808.

58. Schroeder A, Jimenez R, Young B, Privalsky ML. The ability of thyroid hormone receptors to sense t4 as an agonist depends on receptor isoform and on cellular cofactors. *Mol Endocrinol.* 2014;**28**(5):745-757.

59. Groeneweg S, Peeters RP, Visser TJ, Visser WE. Triiodothyroacetic acid in health and disease. *J Endocrinol.* 2017;**234**(2):R99-R121.

60. Groeneweg S, Peeters RP, Visser TJ, Visser WE. Therapeutic applications of thyroid hormone analogues in resistance to thyroid hormone (RTH) syndromes. *Mol Cell Endocrinol.* 2017;**458**:82-90.

61. Menegay C, Juge C, Burger AG. Pharmacokinetics of 3,5,3'-triiodothyroacetic acid and its effects on serum TSH levels. *Acta Endocrinol (Copenh).* 1989;**121**(5):651-658.

62. Brenta G, Danzi S, Klein I. Potential therapeutic applications of thyroid hormone analogs. *Nat Clin Pract Endocrinol Metab.* 2007;**3**(9):632-640.

63. Raparti G, Jain S, Ramteke K, Murthy M, Ghanghas R, Ramanand S, Ramanand J. Selective thyroid hormone receptor modulators. *Indian J Endocrinol Metab.* 2013;**17**(2):211-218.

64. Meruvu S, Ayers SD, Winnier G, Webb P. Thyroid hormone analogues: where do we stand in 2013? *Thyroid.* 2013;**23**(11):1333-1344.

65. Coppola M, Glinni D, Moreno M, Cioffi F, Silvestri E, Goglia F. Thyroid hormone analogues and derivatives: Actions in fatty liver. *World J Hepatol.* 2014;**6**(3):114-129.

66. Kowalik MA, Columbano A, Perra A. Thyroid Hormones, Thyromimetics and Their Metabolites in the Treatment of Liver Disease. *Front Endocrinol (Lausanne).* 2018;**9**:382.

67. Chen Y, Young MA. Structure of a thyroid hormone receptor DNA-binding domain homodimer bound to an inverted palindrome DNA response element. *Mol Endocrinol.* 2010;**24**(8):1650-1664.

68. Paquette MA, Atlas E, Wade MG, Yauk CL. Thyroid hormone response element half-site organization and its effect on thyroid hormone mediated transcription. *PLoS One.* 2014;**9**(6):e101155.

69. Collingwood TN, Adams M, Tone Y, Chatterjee VK. Spectrum of transcriptional, dimerization, and dominant negative properties of twenty different mutant thyroid hormone beta-receptors in thyroid hormone resistance syndrome. *Mol Endocrinol.* 1994;**8**(9):1262-1277.

70. Collingwood TN, Wagner R, Matthews CH, Clifton-Bligh RJ, Gurnell M, Rajanayagam O, Agostini M, Fletterick RJ, Beck-Peccoz P, Reinhardt W, Binder G, Ranke MB, Hermus A, Hesch RD, Lazarus J, Newrick P, Parfitt V, Raggatt P, de Zegher F, Chatterjee VK. A role for helix 3 of the TRbeta ligand-binding domain in coactivator recruitment identified by characterization of a third cluster of mutations in resistance to thyroid hormone. *EMBO J.* 1998;**17**(16):4760-4770.

71. Ayers S, Switnicki MP, Angajala A, Lammel J, Arumanayagam AS, Webb P. Genome-wide binding patterns of thyroid hormone receptor beta. *PLoS One.* 2014;**9**(2):e81186.

72. Chatonnet F, Guyot R, Benoit G, Flamant F. Genome-wide analysis of thyroid hormone receptors shared and specific functions in neural cells. *Proc Natl Acad Sci U S A.* 2013;**110**(8):E766-775.

73. Grontved L, Waterfall JJ, Kim DW, Baek S, Sung MH, Zhao L, Park JW, Nielsen R, Walker RL, Zhu YJ, Meltzer PS, Hager GL, Cheng SY. Transcriptional activation by the thyroid hormone receptor through ligand-dependent receptor recruitment and chromatin remodelling. *Nat Commun.* 2015;**6**:7048.

74. Ramadoss P, Abraham BJ, Tsai L, Zhou Y, Costa-e-Sousa RH, Ye F, Bilban M, Zhao K, Hollenberg AN. Novel mechanism of positive versus negative regulation by thyroid hormone receptor beta1 (TRbeta1) identified by genome-wide profiling of binding sites in mouse liver. *J Biol Chem.* 2014;**289**(3):1313-1328.

75. Au-Fliegner M, Helmer E, Casanova J, Raaka BM, Samuels HH. The conserved ninth C-terminal heptad in thyroid hormone and retinoic acid receptors mediates diverse responses by affecting heterodimer but not homodimer formation. *Mol Cell Biol.* 1993;**13**(9):5725-5737.

76. Zhang T, Cooper S, Brockdorff N. The interplay of histone modifications - writers that read. *EMBO Rep.* 2015;**16**(11):1467-1481.

77. Astapova I. Role of co-regulators in metabolic and transcriptional actions of thyroid hormone. *J Mol Endocrinol.* 2016;**56**(3):73-97.

78. Li J, Wang J, Wang J, Nawaz Z, Liu JM, Qin J, Wong J. Both corepressor proteins SMRT and N-CoR exist in large protein complexes containing HDAC3. *EMBO J.* 2000;**19**(16):4342-4350.

79. Yoon HG, Chan DW, Huang ZQ, Li J, Fondell JD, Qin J, Wong J. Purification and functional characterization of the human N-CoR complex: the roles of HDAC3, TBL1 and TBLR1. *EMBO J.* 2003;**22**(6):1336-1346.

80. Guenther MG, Barak O, Lazar MA. The SMRT and N-CoR corepressors are activating cofactors for histone deacetylase 3. *Mol Cell Biol.* 2001;**21**(18):6091-6101.

81. Onate SA, Tsai SY, Tsai MJ, O'Malley BW. Sequence and characterization of a coactivator for

the steroid hormone receptor superfamily. *Science.* 1995;**270**(5240):1354-1357.

82. McKenna NJ, Lanz RB, O'Malley BW. Nuclear receptor coregulators: cellular and molecular biology. *Endocr Rev.* 1999;**20**(3):321-344.
83. Potter GB, Beaudoin GM, 3rd, DeRenzo CL, Zarach JM, Chen SH, Thompson CC. The hairless gene mutated in congenital hair loss disorders encodes a novel nuclear receptor corepressor. *Genes Dev.* 2001;**15**(20):2687-2701.
84. Thompson CC. Hairless is a nuclear receptor corepressor essential for skin function. *Nucl Recept Signal.* 2009;**7**:e010.
85. Dressel U, Thormeyer D, Altincicek B, Paululat A, Eggert M, Schneider S, Tenbaum SP, Renkawitz R, Baniahmad A. Alien, a highly conserved protein with characteristics of a corepressor for members of the nuclear hormone receptor superfamily. *Mol Cell Biol.* 1999;**19**(5):3383-3394.
86. Papaioannou M, Melle C, Baniahmad A. The coregulator Alien. *Nucl Recept Signal.* 2007;**5**:e008.
87. L'Horset F, Dauvois S, Heery DM, Cavailles V, Parker MG. RIP-140 interacts with multiple nuclear receptors by means of two distinct sites. *Mol Cell Biol.* 1996;**16**(11):6029-6036.
88. Hernandez-Puga G, Mendoza A, Leon-Del-Rio A, Orozco A. Jab1 is a T2-dependent coactivator or a T3-dependent corepressor of TRB1-mediated gene regulation. *J Endocrinol.* 2017;**232**(3):451-459.
89. Li D, Desai-Yajnik V, Lo E, Schapira M, Abagyan R, Samuels HH. NRIF3 is a novel coactivator mediating functional specificity of nuclear hormone receptors. *Mol Cell Biol.* 1999;**19**(10):7191-7202.
90. Li D, Wang F, Samuels HH. Domain structure of the NRIF3 family of coregulators suggests potential dual roles in transcriptional regulation. *Mol Cell Biol.* 2001;**21**(24):8371-8384.
91. Fozzatti L, Lu C, Kim DW, Cheng SY. Differential recruitment of nuclear coregulators directs the isoform-dependent action of mutant thyroid hormone receptors. *Mol Endocrinol.* 2011;**25**(6):908-921.
92. Paul BD, Buchholz DR, Fu L, Shi YB. Tissue- and gene-specific recruitment of steroid receptor coactivator-3 by thyroid hormone receptor during development. *J Biol Chem.* 2005;**280**(29):27165-27172.
93. Bebermeier JH, Brooks JD, DePrimo SE, Werner R, Deppe U, Demeter J, Hiort O, Holterhus PM. Cell-line and tissue-specific signatures of androgen receptor-coregulator transcription. *J Mol Med (Berl).* 2006;**84**(11):919-931.
94. Hahm JB, Schroeder AC, Privalsky ML. The two major isoforms of thyroid hormone receptor, TRalpha1 and TRbeta1, preferentially partner with distinct panels of auxiliary proteins. *Mol Cell Endocrinol.* 2014;**383**(1-2):80-95.
95. Refetoff S, DeWind LT, DeGroot LJ. Familial syndrome combining deaf-mutism, stuppled epiphyses, goiter and abnormally high PBI: possible target organ refractoriness to thyroid hormone. *The Journal of clinical endocrinology and metabolism.* 1967;**27**(2):279-294.
96. Sakurai A, Takeda K, Ain K, Ceccarelli P, Nakai A, Seino S, Bell GI, Refetoff S, DeGroot LJ. Generalized resistance to thyroid hormone associated with a mutation in the ligand-binding domain of the human thyroid hormone receptor beta. *Proceedings of the National Academy of Sciences of the United States of America.* 1989;**86**(22):8977-8981.
97. Bochukova E, Schoenmakers N, Agostini M, Schoenmakers E, Rajanayagam O, Keogh JM, Henning E, Reinemund J, Gevers E, Sarri M, Downes K, Offiah A, Albanese A, Halsall D, Schwabe JW, Bain M, Lindley K, Muntoni F, Vargha-Khadem F, Dattani M, Farooqi IS, Gurnell M, Chatterjee K. A mutation in the thyroid hormone receptor alpha gene. *N Engl J Med.* 2012;**366**(3):243-249.
98. van Mullem A, van Heerebeek R, Chrysis D, Visser E, Medici M, Andrikoula M, Tsatsoulis A, Peeters R, Visser TJ. Clinical phenotype and mutant TRalpha1. *N Engl J Med.* 2012;**366**(15):1451-1453.
99. Visser WE, van Mullem AA, Visser TJ, Peeters RP. Different causes of reduced sensitivity to thyroid hormone: diagnosis and clinical management. *Clin Endocrinol (Oxf).* 2013;**79**(5):595-605.

100. Dumitrescu AM, Refetoff S. The syndromes of reduced sensitivity to thyroid hormone. *Biochim Biophys Acta.* 2013;**1830**(7):3987-4003.

101. Singh BK, Yen PM. A clinician's guide to understanding resistance to thyroid hormone due to receptor mutations in the TRalpha and TRbeta isoforms. *Clin Diabetes Endocrinol.* 2017;**3**:8.

102. Lafranchi SH, Snyder DB, Sesser DE, Skeels MR, Singh N, Brent GA, Nelson JC. Follow-up of newborns with elevated screening T4 concentrations. *J Pediatr.* 2003;**143**(3):296-301.

103. Tajima T, Jo W, Fujikura K, Fukushi M, Fujieda K. Elevated free thyroxine levels detected by a neonatal screening system. *Pediatr Res.* 2009;**66**(3):312-316.

104. Maruo Y, Mori A, Morioka Y, Sawai C, Mimura Y, Matui K, Takeuchi Y. Successful every-other-day liothyronine therapy for severe resistance to thyroid hormone beta with a novel THRB mutation; case report. *BMC Endocr Disord.* 2016;**16**:1.

105. Miyoshi Y, Nakamura H, Tagami T, Sasaki S, Dorin RI, Taniyama M, Nakao K. Comparison of the functional properties of three different truncated thyroid hormone receptors identified in subjects with resistance to thyroid hormone. *Mol Cell Endocrinol.* 1998;**137**(2):169-176.

106. Phillips SA, Rotman-Pikielny P, Lazar J, Ando S, Hauser P, Skarulis MC, Brucker-Davis F, Yen PM. Extreme thyroid hormone resistance in a patient with a novel truncated TR mutant. *J Clin Endocrinol Metab.* 2001;**86**(11):5142-5147.

107. Concolino P, Costella A, Paragliola RM. Mutational Landscape of Resistance to Thyroid Hormone Beta (RTHbeta). *Mol Diagn Ther.* 2019;**23**(3):353-368.

108. Flynn TR, Hollenberg AN, Cohen O, Menke JB, Usala SJ, Tollin S, Hegarty MK, Wondisford FE. A novel C-terminal domain in the thyroid hormone receptor selectively mediates thyroid hormone inhibition. *J Biol Chem.* 1994;**269**(52):32713-32716.

109. Kitajima K, Nagaya T, Jameson JL. Dominant negative and DNA-binding properties of mutant thyroid hormone receptors that are defective in homodimerization but not heterodimerization. *Thyroid.* 1995;**5**(5):343-353.

110. Nagaya T, Jameson JL. Thyroid hormone receptor dimerization is required for dominant negative inhibition by mutations that cause thyroid hormone resistance. *J Biol Chem.* 1993;**268**(21):15766-15771.

111. Sasaki S, Nakamura H, Tagami T, Miyoshi Y, Nakao K. Functional properties of a mutant T3 receptor beta (R338W) identified in a subject with pituitary resistance to thyroid hormone. *Mol Cell Endocrinol.* 1995;**113**(1):109-117.

112. Clifton-Bligh RJ, de Zegher F, Wagner RL, Collingwood TN, Francois I, Van Helvoirt M, Fletterick RJ, Chatterjee VK. A novel TR beta mutation (R383H) in resistance to thyroid hormone syndrome predominantly impairs corepressor release and negative transcriptional regulation. *Mol Endocrinol.* 1998;**12**(5):609-621.

113. Collingwood TN, Rajanayagam O, Adams M, Wagner R, Cavailles V, Kalkhoven E, Matthews C, Nystrom E, Stenlof K, Lindstedt G, Tisell L, Fletterick RJ, Parker MG, Chatterjee VK. A natural transactivation mutation in the thyroid hormone beta receptor: impaired interaction with putative transcriptional mediators. *Proc Natl Acad Sci U S A.* 1997;**94**(1):248-253.

114. Safer JD, Cohen RN, Hollenberg AN, Wondisford FE. Defective release of corepressor by hinge mutants of the thyroid hormone receptor found in patients with resistance to thyroid hormone. *J Biol Chem.* 1998;**273**(46):30175-30182.

115. Yoh SM, Chatterjee VK, Privalsky ML. Thyroid hormone resistance syndrome manifests as an aberrant interaction between mutant T3 receptors and transcriptional corepressors. *Mol Endocrinol.* 1997;**11**(4):470-480.

116. Kaneshige M, Suzuki H, Kaneshige K, Cheng J, Wimbrow H, Barlow C, Willingham MC, Cheng S. A targeted dominant negative mutation of the thyroid hormone alpha 1 receptor causes increased mortality, infertility, and dwarfism in mice. *Proc Natl Acad Sci U S A.* 2001;**98**(26):15095-15100.

117. Tinnikov A, Nordstrom K, Thoren P, Kindblom JM, Malin S, Rozell B, Adams M, Rajanayagam O, Pettersson S, Ohlsson C, Chatterjee K, Vennstrom B. Retardation of post-natal development caused by a negatively acting thyroid hormone receptor alpha1. *EMBO J.* 2002;**21**(19):5079-5087.

118. Liu YY, Schultz JJ, Brent GA. A thyroid hormone receptor alpha gene mutation (P398H) is associated with visceral adiposity and impaired catecholamine-stimulated lipolysis in mice. *J Biol Chem.* 2003;**278**(40):38913-38920.

119. Quignodon L, Vincent S, Winter H, Samarut J, Flamant F. A point mutation in the activation function 2 domain of thyroid hormone receptor alpha1 expressed after CRE-mediated recombination partially recapitulates hypothyroidism. *Mol Endocrinol.* 2007;**21**(10):2350-2360.

120. Moran C, Schoenmakers N, Agostini M, Schoenmakers E, Offiah A, Kydd A, Kahaly G, Mohr-Kahaly S, Rajanayagam O, Lyons G, Wareham N, Halsall D, Dattani M, Hughes S, Gurnell M, Park SM, Chatterjee K. An adult female with resistance to thyroid hormone mediated by defective thyroid hormone receptor alpha. *J Clin Endocrinol Metab.* 2013;**98**(11):4254-4261.

121. Demir K, van Gucht AL, Buyukinan M, Catli G, Ayhan Y, Bas VN, Dundar B, Ozkan B, Meima ME, Visser WE, Peeters RP, Visser TJ. Diverse Genotypes and Phenotypes of Three Novel Thyroid Hormone Receptor-alpha Mutations. *J Clin Endocrinol Metab.* 2016;**101**(8):2945-2954.

122. Tylki-Szymanska A, Acuna-Hidalgo R, Krajewska-Walasek M, Lecka-Ambroziak A, Steehouwer M, Gilissen C, Brunner HG, Jurecka A, Rozdzynska-Swiatkowska A, Hoischen A, Chrzanowska KH. Thyroid hormone resistance syndrome due to mutations in the thyroid hormone receptor alpha gene (THRA). *J Med Genet.* 2015;**52**(5):312-316.

123. Stampfer M, Beck-Wodl S, RieB A, Haack T. Most severe case of thyroid-alpha-receptor deficiency in a female patient with severe growth and mental retardation, macrocephaly, pubertas tarda and dysgerminoma. Poster presented at The European Society of Human Genetics 28 May, 2017;P08.65A (abstract).

124. Sun H, Wu H, Xie R, Wang F, Chen T, Chen X, Wang X, Flamant F, Chen L. New Case of Thyroid Hormone Resistance alpha Caused by a Mutation of THRA /TRalpha1. *J Endocr Soc.* 2019;**3**(3):665-669.

125. Moran C, Agostini M, McGowan A, Schoenmakers E, Fairall L, Lyons G, Rajanayagam O, Watson L, Offiah A, Barton J, Price S, Schwabe J, Chatterjee K. Contrasting Phenotypes in Resistance to Thyroid Hormone Alpha Correlate with Divergent Properties of Thyroid Hormone Receptor alpha1 Mutant Proteins. *Thyroid.* 2017;**27**(7):973-982.

126. Moran C, Agostini M, Visser WE, Schoenmakers E, Schoenmakers N, Offiah AC, Poole K, Rajanayagam O, Lyons G, Halsall D, Gurnell M, Chrysis D, Efthymiadou A, Buchanan C, Aylwin S, Chatterjee KK. Resistance to thyroid hormone caused by a mutation in thyroid hormone receptor (TR)alpha1 and TRalpha2: clinical, biochemical, and genetic analyses of three related patients. *Lancet Diabetes Endocrinol.* 2014;**2**(8):619-626.

127. van Gucht AL, Meima ME, Zwaveling-Soonawala N, Visser WE, Fliers E, Wennink JM, Henny C, Visser TJ, Peeters RP, van Trotsenburg AS. Resistance to Thyroid Hormone Alpha in an 18-Month-Old Girl: Clinical, Therapeutic, and Molecular Characteristics. *Thyroid.* 2016;**26**(3):338-346.

128. van Gucht ALM, Moran C, Meima ME, Visser WE, Chatterjee K, Visser TJ, Peeters RP. Resistance to Thyroid Hormone due to Heterozygous Mutations in Thyroid Hormone Receptor Alpha. *Curr Top Dev Biol.* 2017;**125**:337-355.

129. Wejaphikul K, Groeneweg S, Hilhorst-Hofstee Y, Chatterjee VK, Peeters RP, Meima ME, Visser WE. Insight into molecular determinants of T3 vs. T4 recognition from mutations in thyroid hormone receptor alpha and beta. *J Clin Endocrinol Metab.* 2019;**104**(8):3491-3500**.**

130. Espiard S, Savagner F, Flamant F, Vlaeminck-Guillem V, Guyot R, Munier M, d'Herbomez M, Bourguet W, Pinto G, Rose C, Rodien P, Wemeau JL. A Novel Mutation in THRA Gene Associated With an Atypical Phenotype of Resistance to Thyroid Hormone. *J Clin Endocrinol Metab.* 2015;**100**(8):2841-2848.

131. Korkmaz O, Ozen S, Ozdemir TR, Goksen D, Darcan S. A novel thyroid hormone receptor alpha gene mutation, clinic characteristics, and follow-up findings in a patient with thyroid hormone resistance. *Hormones (Athens).* 2019;**10.1007/s42000-019-00094-9**.

132. Kalikiri MK, Mamidala MP, Rao AN, Rajesh V. Analysis and functional characterization of sequence variations in ligand binding domain of thyroid hormone receptors in autism spectrum disorder (ASD) patients. *Autism Res.* 2017;**10**(12):1919-1928.

133. Yuen RK, Thiruvahindrapuram B, Merico D, Walker S, Tammimies K, Hoang N, Chrysler C, Nalpathamkalam T, Pellecchia G, Liu Y, Gazzellone MJ, D'Abate L, Deneault E, Howe JL, Liu RS, Thompson A, Zarrei M, Uddin M, Marshall CR, Ring RH, Zwaigenbaum L, Ray PN, Weksberg R, Carter MT, Fernandez BA, Roberts W, Szatmari P, Scherer SW. Whole-genome sequencing of quartet families with autism spectrum disorder. *Nat Med.* 2015;**21**(2):185-191.

134. Hao E, Menke JB, Smith AM, Jones C, Geffner ME, Hershman JM, Wuerth JP, Samuels HH, Ways DK, Usala SJ. Divergent dimerization properties of mutant beta 1 thyroid hormone receptors are associated with different dominant negative activities. *Mol Endocrinol.* 1994;**8**(7):841-851.

135. Huber BR, Desclozeaux M, West BL, Cunha-Lima ST, Nguyen HT, Baxter JD, Ingraham HA, Fletterick RJ. Thyroid hormone receptor-beta mutations conferring hormone resistance and reduced corepressor release exhibit decreased stability in the N-terminal ligand-binding domain. *Mol Endocrinol.* 2003;**17**(1):107-116.

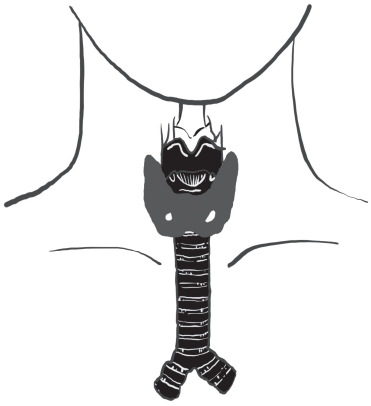

CHAPTER 2

Role of Leucine 341 in Thyroid Hormone Receptor Beta Revealed by a Novel Mutation Causing Thyroid Hormone Resistance

Karn Wejaphikul, Stefan Groeneweg, Prapai Dejkhamron, Kevalee Unachak, W. Edward Visser, V. Krishna Chatterjee, Theo J. Visser, Marcel E. Meima, Robin P. Peeters

*Extended version of **Thyroid.** 2018;28:1723-726.*

2

Abstract

Background: Leucine 341 has been predicted from crystal structure as an important residue for thyroid hormone receptor β (TRβ) function, but this has never been confirmed in functional studies. Here, we verify the role of Leu341, driven by the identification of a novel L341V mutation in a 12-year-old girl with resistance to thyroid hormone β (RTHβ).

Methods: Genomic DNA was sequenced for mutations in the *THRB* gene. A novel L341V mutation as well as three artificial mutations (L341A, L341I, and L341F) were modeled in the wild-type (WT) T3-bound TRβ1 crystal structure. T3 binding affinity and transcriptional activity of the mutants were determined and compared with WT TRβ1.

Results: A heterozygous missense mutation in *THRB* (c.1021C>G; p.L341V) was found in a patient presented with diffuse goiter, tachycardia, and high serum FT4 and FT3 with non-suppressed TSH, indicative of RTHβ. Structural modeling of this mutation showed altered side-chain orientation and interactions of T3 with receptor. This was confirmed by *in vitro* studies demonstrating reduced affinity for T3 and impaired transcriptional activity of TRβ1-L341V. In addition, substitution of Leu341 by an alanine (A), isoleucine (I), or phenylalanine (F) reduced receptor function to various degrees, depending on their side-chain size and orientation and thus ability to maintain important structural interaction.

Conclusion: Leu341 has a critical role in T3 binding and hence TRβ function, and its mutation results in the clinical phenotype of RTHβ.

Introduction

Thyroid hormone (TH) is crucial for normal growth, development and metabolism. It is widely accepted that TH predominantly mediates its effects via transcriptional regulation of genes by binding of the active hormone, triiodothyronine (T3), to nuclear thyroid hormone receptors (TRs). Three functional TR isoforms, i.e., TRα1, TRβ1 and, TRβ2, are encoded by two different genes, *THRA* on chromosome 17 and *THRB* on chromosome 3 (1). The expression of TRs varies among tissues. TRα1 is mainly expressed in the brain, bone, heart, intestine, and skeletal muscle, whereas TRβ1 is principally expressed in the liver, kidney, and thyroid gland. TRβ2 is predominantly expressed in the retina, cochlea, as well as the hypothalamus and pituitary, where it plays a crucial role in a negative feedback control of the hypothalamic-pituitary-thyroid (HPT) axis.

Mutations in the *THRB* gene cause resistance to thyroid hormone β (RTHβ), which was first described in 1967 (2) and the first mutation was subsequently identified in 1989 (3). The estimated incidence is approximately 1:40,000 live births (4,5). The biochemical characteristics are elevated T4 and T3 with non-suppressed TSH concentrations because of impaired TRβ2 function in hypothalamus and pituitary, which consequently alters negative feedback control. The clinical phenotype is variable and may include goiter, tachycardia, and learning disability with or without hyperactive behavior.

RTHβ is usually inherited in an autosomal dominant fashion (6,7). Single nucleotide substitutions resulting in amino acid replacement are more common than frameshift or nonsense mutations that lead to premature protein truncations (8-10). These mutations mainly locate in 3 CpG transition and CG rich cluster regions (cluster 1; codon 426-461, cluster 2; 310-353, and cluster 3; codon 234-282) which encode the ligand binding domain (LBD) and the hinge region of TRβ protein (6). Therefore, mutations commonly impair affinity for T3 and consequently reduce transcriptional activity of the receptor.

The affinity for T3 of TRβ is determined by the interactions between the T3 molecule and the amino acid residues that form the ligand-binding cavity (11,12). For instance, crystallization of the TRβ protein and subsequent *in vitro* studies revealed that Arg282 and His435 play a crucial role in hormone binding (13-17). Another residue that was found to line the ligand binding pocket is Leu341 (18,19). A proline substitution at this position (L341P) has previously been described in RTHβ patients, supporting the importance of this residue (20,21). However, functional studies on the role of this Leu341 for the function of TRβ1 have not yet been established.

In this study, we describe a 12-year-old girl with RTHβ caused by a novel L341V mutation in TRβ. *In silico* studies suggest altered T3 binding of TRβ1-L341V which is confirmed by reduced affinity for T3 and impaired transcriptional activity in *in vitro* studies. In addition, substituting Leu341 with other non-polar amino acids also impairs receptor function to various degrees, depending on their side-chain size and orientation and thus ability to maintain

important structural interactions. These findings emphasize the functional importance of Leu341 for TRβ activity.

Materials and methods

Clinical and genetic assessment

The index patient was referred to our institute because of poorly controlled Graves' disease. Thyroid function tests were evaluated after one month of methimazole (MMI) withdrawal using an electrochemiluminescence immunoassay kit (Roche Diagnostic, Mannheim, Germany). Informed consent was obtained from the parents of the index patient. The study was approved by the Medical Ethics Committee of the Faculty of Medicine, Chiang Mai University, Thailand.

Genomic DNA was extracted from peripheral blood leukocytes by QIAamp® DNA Mini Kit (Qiagen, Hilden, Germany). Exons 7-10 of the THRB gene [GeneBank: NM_000461.4], including exon-intron boundaries, were amplified (see Supplementary Table S1 for primers). Sequencing was performed as described previously (22). The exon carrying the mutation was re-amplified and sequenced to exclude a PCR error.

In silico prediction of mutant TRβ1 function

YASARA Structure Software (YASARA Bioscience GmbH, Vienna, Austria) (23) was used to model the TRβ1-L341V patient's mutation and three artificial mutants (L341A, L341I and L341F) into a T3-bound wild-type (WT) TRβ1 crystal structure (PDB-ID: 3GWS) (24) using the side-chain substitution tool. Side-chain orientations were optimized using SCWALL (Side-Chain conformations With ALL available methods) (25,26), after which the final models were minimized without further constraints. All images were created using YASARA Structure and Pov-Ray v3.6 software (www.povray.org).

DNA constructs and mutagenesis

The human TRβ1 cDNA was amplified and subcloned into the *EcoRI* and *XbaI* sites of the pcDNA3 expression vector fused at the 5'-end to the sequence encoding the FLAG-epitope tag and downstream of an optimized Kozak sequence (see Supplementary Table S1 for primers). The TRβ1-L341V patient's mutation (c.1021C>G) and three artificial mutants, including L341A, L341I and L341F, were introduced using the QuickChange II Mutagenesis kit (Agilent Technologies, Amstelveen, The Netherlands) according to manufacturers' protocol (see Supplementary Table S1 for primers). Sequences of mutant constructs were confirmed by Sanger sequencing.

[^{125}I]T3 competitive binding assay

Human FLAG-tagged TRβ1 WT and mutant (L341V, L341A, L341I and L341F) receptor proteins were synthesized in reticulocyte lysate using the TnT® T7 Quick Coupled Transcription/Translation System (Promega, Leiden, The Netherlands). The protein lysate was incubated with 0.02 nM of [^{125}I]T3 in 0.5 mL binding buffer (20 mM Tris, pH 8.0, 50 mM KCl, 1 mM $MgCl_2$, 10% glycerol, 5 mM DTT) and 0-10,000 nM unlabeled T3 for 2 hours at 30°C. Protein-bound [^{125}I]T3 was captured by filtering through a nitrocellulose filter membrane (Millipore HA filters, 0.45 µm) under vacuum. The data was corrected for non-specific binding (counts bound at 10,000 nM unlabeled T3) and expressed as percentage maximal [^{125}I]T3 binding (counts bound at 0 nM unlabeled T3). The [^{125}I]T3 displacement curve and the dissociation constant (Kd) were computed by GraphPad Prism program version 5.0 (GraphPad, La Jolla, CA) and shown as mean ± standard error of the mean (SEM) of three independent experiments performed in duplicate.

Cell culture and transfection

JEG-3 cells were cultured and transfected as previously described (27). In brief, 20 ng of FLAG-tagged WT or mutant TRβ1 expression vectors and 120 ng of luciferase reporter constructs containing either direct repeat (DR4), inverted repeat (IR0) or everted repeat (ER6) thyroid hormone response element (TRE) (28), as well as 60 ng pMaxGFP transfection control, were transiently transfected into cells in TH depleted medium using Xtreme Gene 9 transfection reagent (Roche Diagnostics, Almere, The Netherlands). To determine the effect of TRβ1-L341V on WT function (dominant-negative effect), we co-expressed WT and TRβ1-L341V receptors (1:1 equimolar ratio), or either WT or TRβ1-L341V with empty vector (EV) (as gene dose control). After 24 hours, cells used for luciferase assays were incubated in DMEM/F12 medium supplemented with 0.1% bovine serum albumin and containing 0-10,000 nM T3 for 24 hours.

Immunoblotting

To determine the expression of FLAG-tagged TRβ1 WT and mutants in JEG-3 cells, nuclear proteins were extracted as described previously with slight modifications (29). Briefly, cells were swollen on ice for 15 min in buffer A (10 mM Hepes, 10 mM KCl, 0.1 mM EDTA, 1 mM DTT, pH 7.9) supplemented with the Complete Protease Inhibitor cocktail (Roche Diagnostics) and were lysed by addition of 0.6% NP40. The nuclei were pelleted by centrifugation for 10 min at 2500 *g* and extracted for 45 min in buffer C (20 mM HEPES, 0.4 M NaCl, 1 mM EDTA, 1 mM DTT, Complete Protease Inhibitors, pH 7.9) at 4˚C. After centrifugation for 15 min at 20000 *g*, the supernatants containing nuclear proteins were collected and diluted in buffer D (20 mM HEPES, 1 mM EDTA, Complete Protease Inhibitors, pH 7.9). Immunoblotting was performed as previously described (27). The FLAG-tagged TRβ1 and Histone 3 (as loading control) were detected by FLAG-M2 antibody (#F1804 Sigma-Aldrich) and Histone 3 (H3; 1B1B2) antibody (#14269 Cell Signaling Technology), respectively, at a 1:1000 dilution and

visualized by Enhanced Chemiluminescence (Thermofisher Scientific) on the Alliance 4.0 Uvitec platform (Uvitec Ltd).

Luciferase assays

Luciferase activity of WT and mutant receptors was measured using the Dual Glo Luciferase kit (Promega, Leiden, The Netherlands) as previously described (22). The ratio between luciferase and GFP was calculated to adjust for transfection efficiency. Data were expressed as percentage maximal response of WT and half maximal effective T3 concentration (EC_{50}) and maximal response calculated using GraphPad Prism program version 5.0 (GraphPad, La Jolla, CA). The results are shown as mean ± SEM of at least three independent experiments performed in triplicate.

Statistical analysis

Statistical differences of logKd and logEC_{50} values between WT and mutants were analyzed by student's t-test. The percentage maximal response of mutants was compared to WT by one sample t-test. The statistical difference of logKd and logEC_{50} values between four mutants (L341V, L341A, L341I, and L341F) was determined by one-way ANOVA with Tukey's post-test. Statistical significance was considered when p-values < 0.05.

Results

Clinical and genetic assessment

A 12-year-old Thai girl (II.3) born to non-consanguineous parents presented with goiter and palpitations for four years. She had been diagnosed erroneously with Graves' disease and treated with methimazole for three years without remission. During treatment, she had fluctuating thyroid hormone and increased TSH concentrations. Physical examination showed a height of 134 cm (-3.17 SDS), a weight of 27.2 kg, a BMI of 15.1 kg/m^2 (-1.83 SDS), tachycardia (heart rate 144/min) and diffuse thyroid gland enlargement. Her thyroid function tests showed high FT4 and FT3 with non-suppressed TSH concentrations (Figure 1, Supplementary Table S2). Interestingly, an older sister (II.2) and her mother (I.2) also suffered from presumed Graves' disease, for which the mother had undergone a subtotal thyroidectomy and subsequently developed postoperative hypothyroidism, which required high doses of levothyroxine (300 µg/day). Because of the high TH with non-suppressed TSH concentrations of the index patient and affected family members, Graves' diagnosis was incorrect and RTHβ was suspected in this family.

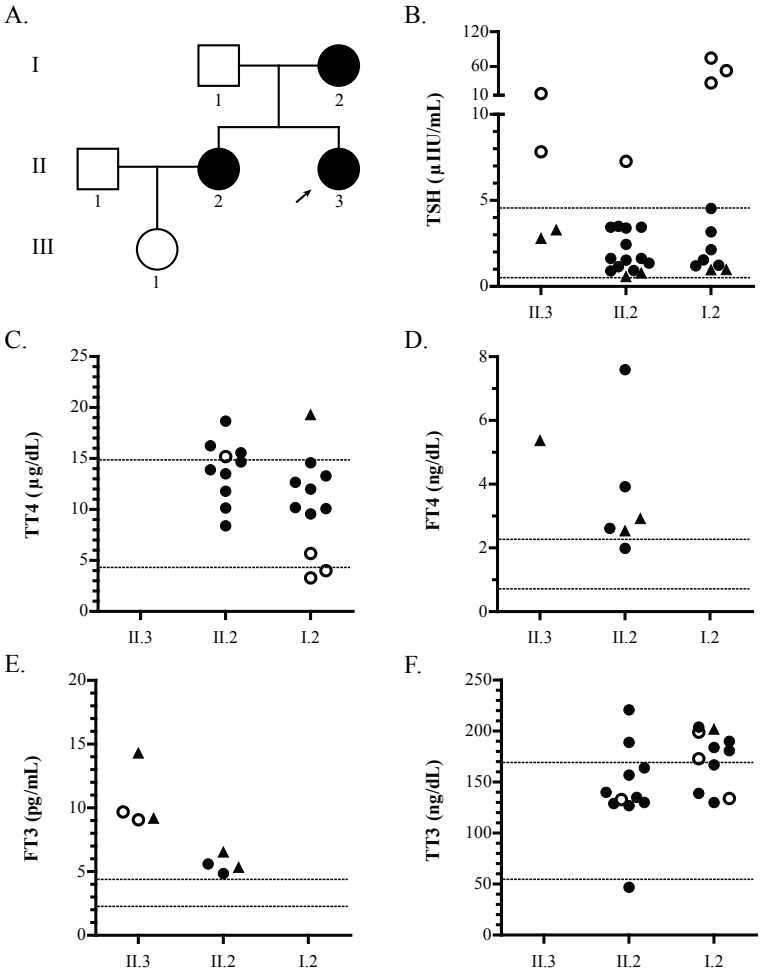

Figure 1. (A) The pedigree demonstrates three RTHβ patients in the family. (B-F) The graphs show thyroid function tests of affected family members (closed dot [●]: during antithyroid drug treatment and normal TSH; open dot [○]: during antithyroid drug treatment with high TSH; triangle [▲]: no treatment; [-----]: reference ranges).

After obtaining informed consent, genomic DNA of exons 7-10 of the *THRB* gene from the index patient and family members was sequenced and a novel heterozygous missense mutation at codon 341 leading to a leucine to valine substitution (c.1021C>G, p.L341V) was found in the index patient (II.3), the older sister (II.2) and the mother (I.2) (Supplementary Figure S1). This mutation was not found in the father (I.1) and is not present in public databases (dbSNP, 1000 Genomes, and Exome Aggregation Consortium [ExAC]).

In silico modeling of the TRβ1-L341V mutant

Inspection of the crystal structure of the T3-bound WT TRβ1 receptor (PDB-ID: 3GWS) revealed that Leu341 is located at the TRβ1 ligand-binding pocket (Figure 2A). Its aliphatic side-chain is predicted to form a direct hydrophobic interaction with the outer ring of the T3 molecule (Figure 2B). In addition, Leu341 interacts with several surrounding residues, amongst others the ligand-interacting residues Phe272, Leu330, and Leu346. In this way, Leu341 likely determines their orientation towards the T3 molecule and the overall shape and integrity of the ligand-binding pocket. Next, the L341V mutant was modeled into the T3-bound WT TRβ1 receptor crystal structure (Figure 4A). As a consequence of the shorter side-chain length of valine and an altered side-chain orientation as compared to the original leucine residue, it is not likely to form a direct interaction with ligand. Moreover, at least part of the hydrophobic interactions with surrounding residues, most importantly Leu330, is likely to be disturbed, which may impede the structural integrity of the ligand-binding pocket. All together, these observations suggest that the L341V mutant may reduce ligand-binding affinity and consequently receptor function.

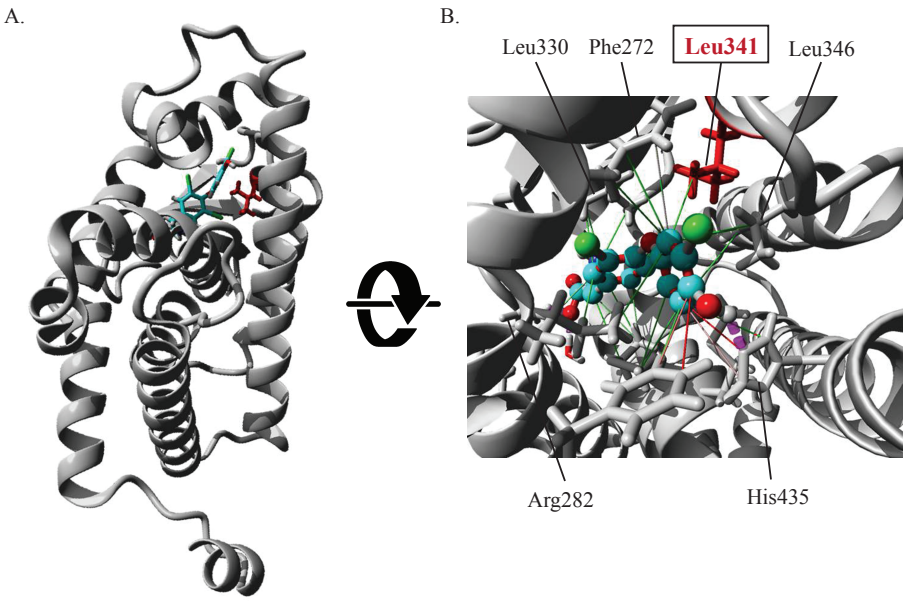

Figure 2. (A) Crystal structure of T3-bound WT TRβ1 (PDB-ID: 3GWS) in which the side chain of the affected Leu341 is depicted in red. (B) Close-up view of the ligand binding domain showing the side-chains of ligand-interacting residues. Arg282 and His435 form hydrogen bonds with the carboxyl group of the alanine side-chain and phenolhydroxyl group of T3, respectively (purple dashed lines). Together with Leu330, Phe272, and Leu346, Leu341 (in red) forms a hydrophobic pocket accommodating the two phenolic rings of the T3 molecule through hydrophobic (green lines) and pi-pi (pink-red lines) interactions.

In vitro functional analysis of TRβ1-L341V

To understand the effect of the L341V mutation on TRβ1 function, we performed [^{125}I]T3 competitive binding assays to determine the T3 binding affinity of the WT and mutant receptors. TRβ1-L341V showed a 16-fold higher dissociation constant (Kd) than WT TRβ1, indicating an impaired T3 binding affinity for the mutant (Figure 3A, Supplementary Table S3).

Next, we measured T3-dependent transcriptional activity of overexpressed WT or TRβ1-L341V receptors in JEG-3 cells using a luciferase reporter assay. The expression of receptor constructs was confirmed by immunoblotting (Figure 3B). The mutant receptor showed a significantly higher EC_{50} compared with WT TRβ1 on all TREs (60-fold on DR4, 40-fold on IR0, and 90-fold on ER6), reflecting an impaired T3-induced transcriptional activity of this mutation. However, the TRβ1-L341V showed similar maximal transcriptional activity with WT TRβ1, demonstrating that supra-physiological doses of T3 can rescue the transcriptional activity of the TRβ1-L341V (Figure 3C-E, Supplementary Table S3).

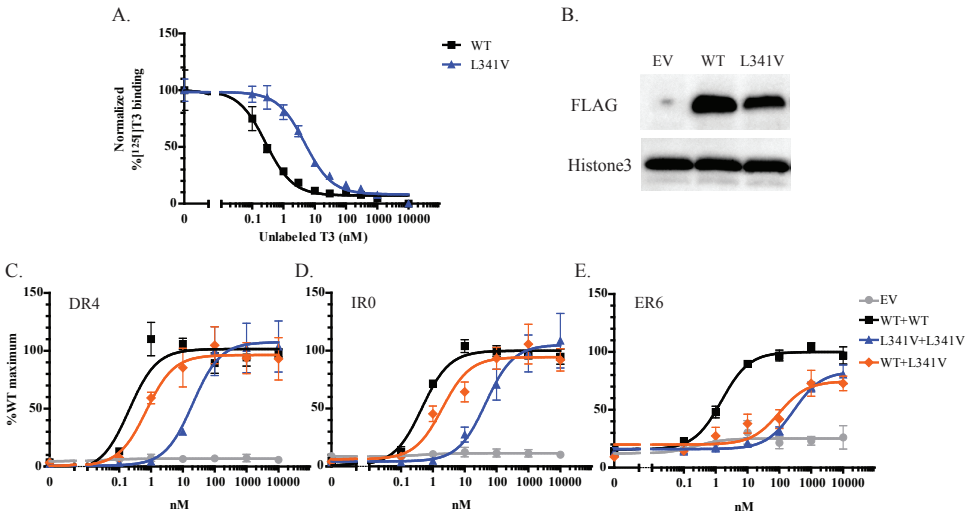

Figure 3. Functional analysis of TRβ1-L341V. (A) The [^{125}I]T3 dissociation curve of mutant shifts to the right suggesting an impaired affinity for T3 (data presented as mean ± SEM of three independent experiments performed in duplicate). (B) Immunoblotting confirms the expression of WT and TRβ1-L341V in JEG-3 cells. (C-E) The TRβ1-L341V shows impaired transcriptional activity on all TRE tested, as indicated by the right shift of the T3-induced dose-response curves. Co-transfection of WT with TRβ1-L341V alters transcriptional activity of WT in a dominant-negative manner (data presented as mean ± SEM of four independent experiments performed in triplicate).

The effect of TRβ1-L341V on WT TR function or its dominant-negative activity was tested by co-expressing WT and TRβ1-L341V. The EC_{50} of co-expressed WT and TRβ1-L341V was higher than that of WT only (3-fold on DR4, 5-fold on IR0, and 14-fold on ER6) suggesting a dominant-negative effect of the mutant receptor (Figure 3C-E, Supplementary Table S4). Together, these *in vitro* studies support an important role for Leu341 in substrate binding and receptor function.

In silico modeling and in vitro functional analysis of artificial mutations at 341 residue

To further delineate the function of Leu341, we generated expression constructs in which the Leu341 was substituted by an isoleucine (L341I), alanine (L341A), or phenylalanine (L341F). All of them have hydrophobic side-chains but of different sizes and structural properties (Figure 4A). In case of the isoleucine substitution, the branched chain character and the size of the side-chain are maintained, whereas the side-chain of an alanine is smaller. In contrast, the side-chain of phenylalanine is more bulky and rigid compared to the original isoleucine. Structural modeling of the L341I mutant suggested loss of direct contacts with ligand and slight alterations in the interactions with the surrounding residues. Obviously, these interactions were predicted to be even more extensively disturbed in case of the L341A mutant as a consequence of the size reduction of the side-chain. Although the bulky side-chain of phenylalanine was predicted to slightly alter the local architecture of the ligand-binding pocket, most of the essential interactions with the surrounding residues as well as the direct interaction(s) with the T3 molecule were preserved.

In vitro studies confirmed the functional impairment of these artificial mutants. The Kd of all three mutants indicating their affinity for T3, was significantly higher than WT. (Figure 4B, Supplementary Table S5). These results demonstrate that substitution of Leu341 by other non-polar amino acids with different side-chain size and orientation results in impaired T3 binding affinity of TRβ1. Interestingly, the shift in Kd was proportional to the size of the side-chain that was introduced and hence the distance to the substrate molecule and surrounding residues. Substitution by alanine and valine, which have a smaller size of the side-chain than isoleucine and phenylalanine, produced the higher shifts in Kd.

The shift of T3-induced transcriptional activity of the mutant receptors on the DR4 TRE showed a similar trend as the shift in affinity for T3. The EC_{50} of all mutants was significantly higher than that of WT TRβ1. In addition, the degree of the shift in EC_{50} also depended on the size and orientation of the side-chain (Figure 4C, Supplementary Table S5).

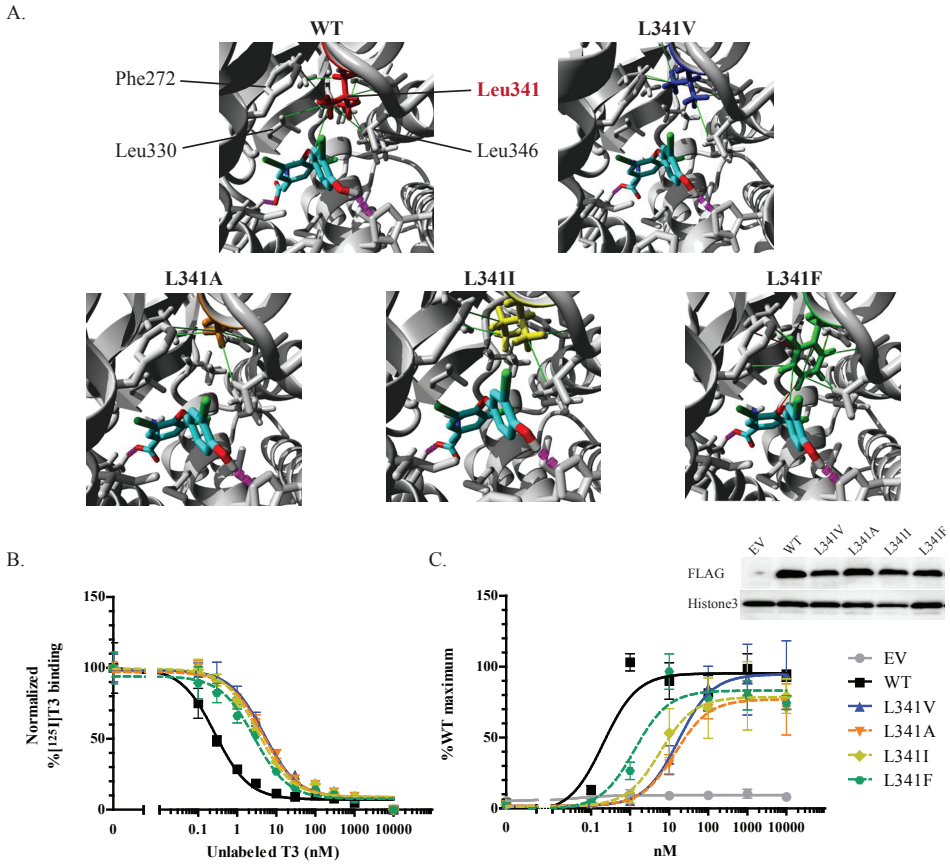

Figure 4. (A) Crystal structure of WT TRβ1 (PDB-ID: 3GWS) and structural models of the L341V and three artificial mutants (L341A, L341I and L341F) showing the side-chain size and orientation toward the T3 molecule and surrounding residues of the different residue side-chains. The WT Leu341 residue forms a direct interaction with ligand as well as extensive hydrophobic interactions (green lines) with its surrounding residues by which it stabilizes the hydrophobic pocket. All mutants were predicted to disturb these interactions to various degrees, with the L341F having the smallest impact. (B) The [^{125}I]T3 dissociation curve show the diverse severity of T3 binding impairment of the mutants (data presented as mean ± SEM of three independent experiments performed in duplicate). (C) Transcriptional activity of the mutant receptors is impaired, as indicated by the right-shifted of T3-induced dose-response curves tested on DR4 TRE (data presented as mean ± SEM of three independent experiments performed in triplicate). (Insert) Immunoblotting confirms the expression of all receptor constructs.

Discussion

In this study, we describe the role of Leu341 in TRβ function prompted by the identification of a novel TRβ1-L341V mutation in an RTHβ family. *In silico* modeling of TRβ1-L341V predicted interference with T3 binding, which was verified by [^{125}I]T3 competitive binding assays. Transcriptional impairment and dominant-negative ffect of this mutant was confirmed by *in vitro* studies. Additional artificial mutants (L341A, L341I, and L341F) were created based on the *in silico* predictions, showing different degrees of receptor impairment which depended on the side-chain size and exact orientation. With detrimental effects being observed even with subtle L341I and L341V mutations, illustrates the importance of Leu341 for TRβ1 function.

The novel L341V mutation reported in this study was identified in a patient and affected family members that had all been misdiagnosed with Graves' disease and treated with antithyroid drugs without remission. The mutation is located in a commonly mutated region (i.e., cluster 2) of TRβ1. Although the other mutation at this position, L341P, has been previously described (20,21), functional studies on the role of Leu341 in TRβ are lacking. Based on crystallographic analyses (24,30), Leu341 is predicted to be part of the TRβ1 ligand-binding surface.

Our *in silico* models suggest the presence of a direct hydrophobic interaction between Leu341 and the outer ring of the T3 molecule. Importantly, Leu341 also interacts with several other residues that line the ligand binding pocket, some of which (Phe272, Leu346) have been previously suggested to play an important role in ligand binding (15,31). Mutations in the latter have indeed been identified in RTHβ patients (20,32). Given its branched-chain character, Leu341 may therefore function as an important residue stabilizing the orientation of its surrounding residues. Shortening of its side-chain to valine would then affect the direct interaction with the T3 molecule, as well as the positioning and hence interactions of this residue with surrounding residues. The great impact of removing one side-chain methylene group in case of the TRβ1-L341V indeed suggests that the exact side-chain size and orientation at this position is of vital importance for substrate binding and hence receptor activity. We additionally confirmed this by studying three artificial mutations, L341A, L341I and L341F. The side-chains of these three amino acids all have similar hydrophobic properties but a different size and orientation, resulting in a variable distance to the T3 molecule.

The *in vitro* studies confirmed the results of the *in silico* modeling. The TRβ1-L341V has a reduced affinity for T3, as indicated by the higher Kd compared to WT TRβ1, and impaired T3-dependent transcriptional activity, as indicated by the increased EC_{50} on all TREs tested. These data illustrate the resistance of TRβ1-L341V to T3 stimulation, which can, however, be overcome in case of higher (supra-physiological) doses of T3. Such rescue of function at high T3 concentrations has also been described with other TRβ1 mutations (33-35) and is probably due to the fact that T3 binding affinity of these mutants is not completely

abolished. In addition to the *in vitro* studies of TRβ1-L341V, the three artificial mutants also showed significantly reduced affinity for T3 and impaired transcriptional activity. Interestingly, the degree of the shift in EC_{50} related to the distance between the side-chain and T3. These results further confirm that the interaction between T3 and TRβ1 receptor requires a proper distance between the amino acid at position 341 and inner ring iodine of T3.

TRβ1-L341V also showed a dominant-negative effect on transcriptional activity of co-expressed WT TRβ1 on all TREs tested, but strongest on the ER6 TRE. The strong dominant-negative effect on this TRE has also been observed in other TRβ1 mutants (34,36). In contrast to the DR4 and IR0 TREs, where TRβ1 engages predominantly as a heterodimer with RXR, TRβ1 acts on ER6 as a homodimer (37). This means that in the heterozygous situation, only 25% of homodimers are formed by WT receptors. If both receptors of the homodimer need to bind ligand in order to exert transcriptional activity, this may explain the stronger dominant-negative effects on ER6 TRE.

To our knowledge, this is the first study showing the role of the Leu341 residue in TRβ function, gaining more detailed insight into T3 and TRβ interaction. Taking into account the predictive nature of structural modelling, we managed to develop an *in silico* model that correctly predicts the degree of receptor impairment compared with *in vitro* studies. In addition, the creation of artificial mutations based on the *in silico* modeling proved to be a good approach to further explore the role and importance of affected amino acid residues.

In conclusion, we verify the importance of the Leu341 residue for TRβ function. The interactions between Leu341, its surrounding residues, and T3 are required for optimal affinity for T3 and transcriptional activity. Mutations at this amino acid residue can reduce affinity for T3 and impair transcriptional activity of TRβ.

Acknowledgements

We thank Dr. Dounghatai Pongpanat for her contribution to provide patients' information and help to contact family members. This work is supported by Zon-MWTOP Grant (91212044), an Erasmus MC Medical Research Advisory Committee (MRACE) grant (R.P.P., M.E.M.), Chiang Mai University (K.W.), and NIHR Cambridge Biomedical Centre (V.K.C.).

Author Disclosure Statement

The authors have nothing to disclose.

References

1. Cheng SY, Leonard JL, Davis PJ. Molecular aspects of thyroid hormone actions. *Endocr Rev.* 2010;**31**(2):139-170.
2. Refetoff S, DeWind LT, DeGroot LJ. Familial syndrome combining deaf-mutism, stuppled epiphyses, goiter and abnormally high PBI: possible target organ refractoriness to thyroid hormone. *J Clin Endocrinol Metab.* 1967;**27**(2):279-294.
3. Sakurai A, Takeda K, Ain K, Ceccarelli P, Nakai A, Seino S, Bell GI, Refetoff S, DeGroot LJ. Generalized resistance to thyroid hormone associated with a mutation in the ligand-binding domain of the human thyroid hormone receptor beta. *Proc Natl Acad Sci U S A.* 1989;**86**(22):8977-8981.
4. Lafranchi SH, Snyder DB, Sesser DE, Skeels MR, Singh N, Brent GA, Nelson JC. Follow-up of newborns with elevated screening T4 concentrations. *J Pediatr.* 2003;**143**(3):296-301.
5. Tajima T, Jo W, Fujikura K, Fukushi M, Fujieda K. Elevated free thyroxine levels detected by a neonatal screening system. *Pediatr Res.* 2009;**66**(3):312-316.
6. Dumitrescu AM, Refetoff S. The syndromes of reduced sensitivity to thyroid hormone. *Biochim Biophys Acta.* 2013;**1830**(7):3987-4003.
7. Singh BK, Yen PM. A clinician's guide to understanding resistance to thyroid hormone due to receptor mutations in the TRalpha and TRbeta isoforms. *Clin Diabetes Endocrinol.* 2017;**3**:8.
8. Maruo Y, Mori A, Morioka Y, Sawai C, Mimura Y, Matui K, Takeuchi Y. Successful every-other-day liothyronine therapy for severe resistance to thyroid hormone beta with a novel THRB mutation; case report. *BMC Endocr Disord.* 2016;**16**:1.
9. Phillips SA, Rotman-Pikielny P, Lazar J, Ando S, Hauser P, Skarulis MC, Brucker-Davis F, Yen PM. Extreme thyroid hormone resistance in a patient with a novel truncated TR mutant. *J Clin Endocrinol Metab.* 2001;**86**(11):5142-5147.
10. Miyoshi Y, Nakamura H, Tagami T, Sasaki S, Dorin RI, Taniyama M, Nakao K. Comparison of the functional properties of three different truncated thyroid hormone receptors identified in subjects with resistance to thyroid hormone. *Mol Cell Endocrinol.* 1998;**137**(2):169-176.
11. Ribeiro RC, Apriletti JW, Wagner RL, Feng W, Kushner PJ, Nilsson S, Scanlan TS, West BL, Fletterick RJ, Baxter JD. X-ray crystallographic and functional studies of thyroid hormone receptor. *J Steroid Biochem Mol Biol.* 1998;**65**(1-6):133-141.
12. Ye L, Li YL, Mellstrom K, Mellin C, Bladh LG, Koehler K, Garg N, Garcia Collazo AM, Litten C, Husman B, Persson K, Ljunggren J, Grover G, Sleph PG, George R, Malm J. Thyroid receptor ligands. 1. Agonist ligands selective for the thyroid receptor beta1. *J Med Chem.* 2003;**46**(9):1580-1588.
13. Wagner RL, Huber BR, Shiau AK, Kelly A, Cunha Lima ST, Scanlan TS, Apriletti JW, Baxter JD, West BL, Fletterick RJ. Hormone selectivity in thyroid hormone receptors. *Mol Endocrinol.* 2001;**15**(3):398-410.
14. Bleicher L, Aparicio R, Nunes FM, Martinez L, Gomes Dias SM, Figueira AC, Santos MA, Venturelli WH, da Silva R, Donate PM, Neves FA, Simeoni LA, Baxter JD, Webb P, Skaf MS, Polikarpov I. Structural basis of GC-1 selectivity for thyroid hormone receptor isoforms. *BMC Struct Biol.* 2008;**8**:8.
15. Martinez L, Nascimento AS, Nunes FM, Phillips K, Aparicio R, Dias SM, Figueira AC, Lin JH, Nguyen P, Apriletti JW, Neves FA, Baxter JD, Webb P, Skaf MS, Polikarpov I. Gaining ligand selectivity in thyroid hormone receptors via entropy. *Proc Natl Acad Sci U S A.* 2009;**106**(49):20717-20722.
16. Nomura Y, Nagaya T, Tsukaguchi H, Takamatsu J, Seo H. Amino acid substitutions of thyroid hormone receptor-beta at codon 435 with resistance to thyroid hormone selectively alter homodimer formation. *Endocrinology.* 1996;**137**(10):4082-4086.
17. Collingwood TN, Wagner R, Matthews CH, Clifton-Bligh RJ, Gurnell M, Rajanayagam O, Agostini M, Fletterick RJ, Beck-Peccoz P, Reinhardt W, Binder G, Ranke MB, Hermus A, Hesch RD, Lazarus J, Newrick P, Parfitt V, Raggatt P, de Zegher F, Chatterjee VK. A role for helix 3 of

the TRbeta ligand-binding domain in coactivator recruitment identified by characterization of a third cluster of mutations in resistance to thyroid hormone. *EMBO J.* 1998;**17**(16):4760-4770.

18. Li F, Xie Q, Li X, Li N, Chi P, Chen J, Wang Z, Hao C. Hormone activity of hydroxylated polybrominated diphenyl ethers on human thyroid receptor-beta: in vitro and in silico investigations. *Environ Health Perspect.* 2010;**118**(5):602-606.
19. Hangeland JJ, Friends TJ, Doweyko AM, Mellstrom K, Sandberg J, Grynfarb M, Ryono DE. A new class of high affinity thyromimetics containing a phenyl-naphthylene core. *Bioorg Med Chem Lett.* 2005;**15**(20):4579-4584.
20. Rivolta CM, Olcese MC, Belforte FS, Chiesa A, Gruneiro-Papendieck L, Iorcansky S, Herzovich V, Cassorla F, Gauna A, Gonzalez-Sarmiento R, Targovnik HM. Genotyping of resistance to thyroid hormone in South American population. Identification of seven novel missense mutations in the human thyroid hormone receptor beta gene. *Mol Cell Probes.* 2009;**23**(3-4):148-153.
21. Chiesa A, Olcese MC, Papendieck P, Martinez A, Vieites A, Bengolea S, Targovnik HM, Rivolta CM, Gruneiro-Papendieck L. Variable clinical presentation and outcome in pediatric patients with resistance to thyroid hormone (RTH). *Endocrine.* 2012;**41**(1):130-137.
22. van Mullem A, van Heerebeek R, Chrysis D, Visser E, Medici M, Andrikoula M, Tsatsoulis A, Peeters R, Visser TJ. Clinical phenotype and mutant TRalpha1. *N Engl J Med.* 2012;**366**(15):1451-1453.
23. Krieger E, Vriend G. YASARA View - molecular graphics for all devices - from smartphones to workstations. *Bioinformatics.* 2014;**30**(20):2981-2982.
24. Nascimento AS, Dias SM, Nunes FM, Aparicio R, Ambrosio AL, Bleicher L, Figueira AC, Santos MA, de Oliveira Neto M, Fischer H, Togashi M, Craievich AF, Garratt RC, Baxter JD, Webb P, Polikarpov I. Structural rearrangements in the thyroid hormone receptor hinge domain and their putative role in the receptor function. *J Mol Biol.* 2006;**360**(3):586-598.
25. Canutescu AA, Shelenkov AA, Dunbrack RL, Jr. A graph-theory algorithm for rapid protein side-chain prediction. *Protein Sci.* 2003;**12**(9):2001-2014.
26. Krieger E, Joo K, Lee J, Lee J, Raman S, Thompson J, Tyka M, Baker D, Karplus K. Improving physical realism, stereochemistry, and side-chain accuracy in homology modeling: Four approaches that performed well in CASP8. *Proteins.* 2009;**77 Suppl 9**:114-122.
27. van Gucht AL, Meima ME, Zwaveling-Soonawala N, Visser WE, Fliers E, Wennink JM, Henny C, Visser TJ, Peeters RP, van Trotsenburg AS. Resistance to Thyroid Hormone Alpha in an 18-Month-Old Girl: Clinical, Therapeutic, and Molecular Characteristics. *Thyroid.* 2016;**26**(3):338-346.
28. Collingwood TN, Adams M, Tone Y, Chatterjee VK. Spectrum of transcriptional, dimerization, and dominant negative properties of twenty different mutant thyroid hormone beta-receptors in thyroid hormone resistance syndrome. *Mol Endocrinol.* 1994;**8**(9):1262-1277.
29. Fozzatti L, Lu C, Kim DW, Cheng SY. Differential recruitment of nuclear coregulators directs the isoform-dependent action of mutant thyroid hormone receptors. *Mol Endocrinol.* 2011;**25**(6):908-921.
30. Wagner RL, Apriletti JW, McGrath ME, West BL, Baxter JD, Fletterick RJ. A structural role for hormone in the thyroid hormone receptor. *Nature.* 1995;**378**(6558):690-697.
31. Borngraeber S, Budny MJ, Chiellini G, Cunha-Lima ST, Togashi M, Webb P, Baxter JD, Scanlan TS, Fletterick RJ. Ligand selectivity by seeking hydrophobicity in thyroid hormone receptor. *Proc Natl Acad Sci U S A.* 2003;**100**(26):15358-15363.
32. Macchia E, Gurnell M, Agostini M, Giorgilli G, Marcocci C, Valenti TM, Martino E, Chatterjee KK, Pinchera A. Identification and characterization of a novel de novo mutation (L346V) in the thyroid hormone receptor beta gene in a family with generalized thyroid hormone resistance. *Eur J Endocrinol.* 1997;**137**(4):370-376.
33. Maraninchi M, Bourcigaux N, Dace A, El-Yazidi C, Malezet-Desmoulins C, Krempf M, Torresani J, Margotat A. A novel mutation (E333D) in the thyroid hormone beta receptor causing resistance to thyroid hormone syndrome. *Exp Clin Endocrinol Diabetes.* 2006;**114**(10):569-576.
34. Zavacki AM, Harney JW, Brent GA, Larsen PR. Dominant negative inhibition by mutant thyroid

hormone receptors is thyroid hormone response element and receptor isoform specific. *Mol Endocrinol.* 1993;**7**(10):1319-1330.

35. Chatterjee VK, Nagaya T, Madison LD, Datta S, Rentoumis A, Jameson JL. Thyroid hormone resistance syndrome. Inhibition of normal receptor function by mutant thyroid hormone receptors. *J Clin Invest.* 1991;**87**(6):1977-1984.

36. Zavacki AM, Harney JW, Brent GA, Larsen PR. Structural features of thyroid hormone response elements that increase susceptibility to inhibition by an RTH mutant thyroid hormone receptor. *Endocrinology.* 1996;**137**(7):2833-2841.

37. Chen Y, Young MA. Structure of a thyroid hormone receptor DNA-binding domain homodimer bound to an inverted palindrome DNA response element. *Mol Endocrinol.* 2010;**24**(8):1650-1664.

Supplementary Materials

Supplementary Table S1. Primers for *THRB* sequencing, FLAG-TRβ1 cloning, and FLAG-TRβ1 mutagenesis.

Condition	Primers (5'-3')
Exon 7 *THRA*	Forward: TGCAGCTTGCTGTGTATCTTG Reverse: CCCAAGGTGATGAGGACTG
Exon 8 *THRA*	Forward: CTTTCTGCAGCAACAGTCC Reverse: GTATTCCTGGAAACTGATGAAAC
Exon 9 *THRA*	Forward: GAAAACCATGGGCTCAAAG Reverse: TGAAGCTAAAGGGGGACTG
Exon 10 *THRA*	Forward: TAAAGGCCTGGAATTGGAC Reverse: TGCTTGGTGCTGGTGAG
FLAG-TRβ1 cloning	Forward: GTAGAATTCTGGCCGCAGAAATGGACTACAAAGACGATGACG ACAAGATGACTCCCAACAGTATGACAGAAAATG Reverse: CTATCTAGACTAATCCTCGAACACTTCCAAGAAC
L341V (CTG>GTG)	Forward: GACACGGGGCCAGGTGAAAAATGGGGG Reverse: CCCCCATTTTTCACCTGGCCCCGTGTC
L341A (CTG>GCG)	Forward: GTGACACGGGGCCAGGCGAAAAATGGGGGTCT Reverse: AGACCCCCATTTTTCGCCTGGCCCCGTGTCAC
L341I (CTG>ATC)	Forward: AGTGACACGGGGCCAGATCAAAAATGGGGGTCTTG Reverse: CAAGACCCCCATTTTTGATCTGGCCCCGTGTCACT
L341F (CTG>TTC)	Forward: AGTGACACGGGGCCAGTTCAAAAATGGGGGTCTTG Reverse: CAAGACCCCCATTTTTGAACTGGCCCCGTGTCACT

Supplementary Table S2. Clinical and biochemical characteristics of index patient and family members.

Parameter	Index case (II.3)	Sister (II.2)	Mother (I.2)
Age (year)	12	23	51
Clinical presentation	goiter, tachycardia	goiter, tachycardia	goiter
Thyroid function tests [normal range]			
- TSH (μIU/mL) [0.5-4.8]	3.29	2.45	1.2
- TT4 (μg/dL) [4.2-13.0]	N/A	13.5	12
- FT4 (ng/dL) [0.8-2.3]	5.37	N/A	N/A
- TT3 (ng/dL) [55-170]	N/A	221	190
- FT3 (pg/mL) [2.3-4.2]	14.31	N/A	N/A
- Anti-TPO (IU/mL) [<40]	5.0	N/A	N/A
- Anti-TG (IU/mL) [<125]	19.9	N/A	N/A
- TRAb (IU/L) [0.00-1.75]	<0.3	<0.3	N/A
Previous treatment	MMI 15 mg/day	MMI	MMI then subtotal thyroidectomy

TSH, thyroid-stimulating hormone; TT4, total thyroxine; FT4, free thyroxine; TT3, total triiodothyronine; FT3, free triiodothyronine; Anti-TPO, anti-thyroid peroxidase; Anti-TG, anti-thyroglobulin; TRAb, thyrotropin receptor autoantibody; MMI, methimazole; N/A, not available

Supplementary Table S3. Functional analysis of WT and TRβ1-L341V.

Parameter	TRE	WT TRβ1	TRβ1-L341V
LogKd [Kd(nM)]	-	-0.51±0.13 [0.31]	0.70±0.06** [5.01]
LogEC50 [EC_{50}(nM)]	DR4	-0.45±0.04 [0.35]	1.32±0.04*** [21.1]
	IR0	-0.17±0.04 [0.67]	1.69±0.16*** [49.5]
	ER6	0.31±0.09 [2.03]	2.43±0.16*** [269]
% WT maximal response	DR4	100	106±22.6
	IR0	100	107±22.5
	ER6	100	83.9±8.41

student's t-test compared to WT, *p<0.05, **p<0.01, ***p<0.001

Supplementary Table S4. The dominant-negative effect of TRβ1-L341V on transcriptional activity of WT receptor.

Parameter	TRE	WT+WT	WT+EV	L341V+ L341V	L341V+EV	WT+L341V	p-value (One way ANOVA)
$LogEC_{50}$ $[EC_{50}(nM)]$	DR4	-0.45±0.04 [0.35]	-0.47±0.04 [0.34]	1.32±0.04 [21.1]	1.36±0.02 [22.9]	$0.05±0.13^{***, ttt}$ [1.11]	<0.0001
	IR0	-0.17±0.04 [0.67]	-0.11±0.15 [0.77]	1.69±0.16 [49.5]	1.53±0.18 [33.7]	$0.52±0.13^{*,t}$ [3.29]	<0.0001
	ER6	0.31±0.09 [2.03]	0.32±0.30 [2.11]	2.43±0.16 [269]	2.43±0.19 [267]	1.46±0.45 [28.9]	<0.0001

Tukey's post-test compared to WT+WT, *p<0.05, **p<0.01, ***p<0.001, and WT+EV, †p<0.05, ††p<0.01, †††p<0.001

Supplementary Table S5. Functional analysis of artificial mutants at 341 amino acid residue.

Parameter	WT TRβ1	TRβ1-L341V	TRβ1-L341A	TRβ1-L341I	TRβ1-L341F	p-value (One way ANOVA)
LogKd [Kd(nM)]	-0.51±0.13 [0.31]	$0.70±0.06^{**}$ [5.01]	$0.66±0.06^{**}$ [4.54]	$0.47±0.10^{**}$ [2.94]	$0.53±0.11^{**}$ [3.42]	0.2606
$LogEC_{50}$ $[EC_{50}(nM)]$	-0.47±0.03 [0.34]	$1.33±0.04^{***}$ [21.38]	$1.37±0.04^{***}$ [23.12]	$1.19±0.35^{***}$ [15.35]	$0.33±0.06^{***}$ [2.14]	0.0113

student's t-test compared to WT, **p<0.01, ***p<0.001

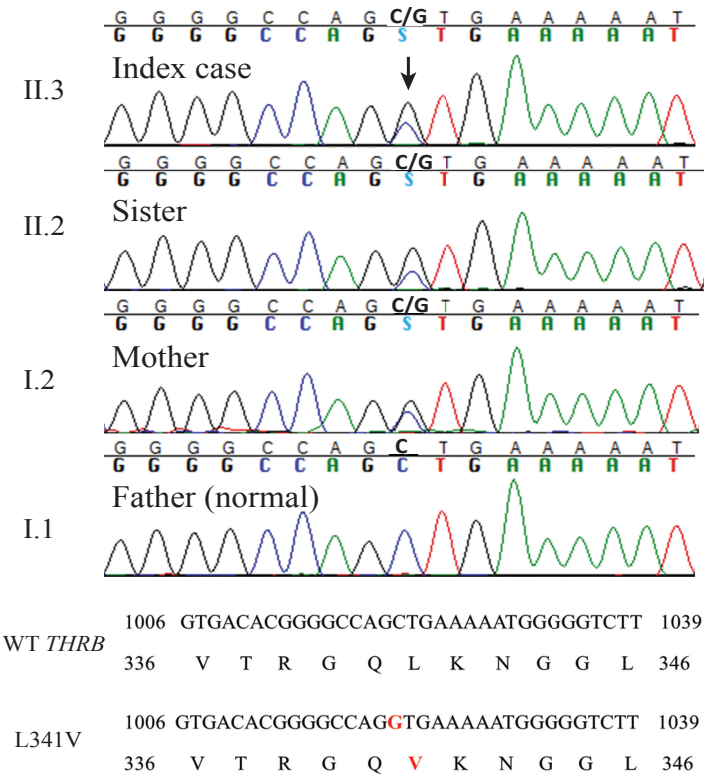

Supplementary Figure S1 Sequence analysis of exon 9 of *THRB* shows a heterozygous missense mutation (c.1021C>G) in index case (II.3), older sister (II.2) and mother (I.2), resulting in a valine substitution at codon 341 (p.L341V).

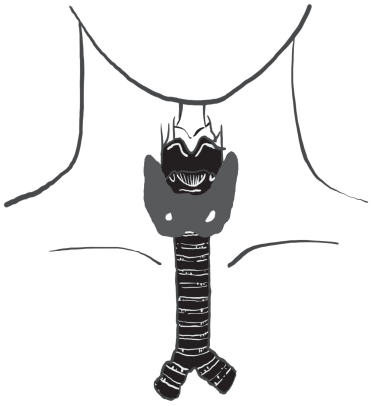

CHAPTER 3

Insight into Molecular Determinants of T3 vs T4 Recognition from Mutations in Thyroid Hormone Receptor *α* and *β*

Karn Wejaphikul, Stefan Groeneweg, Yvonne Hilhorst-Hofstee, V. Krishna Chatterjee, Robin P. Peeters, Marcel E. Meima, W. Edward Visser

J Clin Endocrinol Metab. *2019;104(8):3491-3500.*

3

Abstract

Context: The two major forms of circulating thyroid hormones (THs) are T3 and T4. T3 is regarded as the biologically active hormone because it binds to TH receptors (TRs) with greater affinity than T4. However, it is currently unclear what structural mechanisms underlie this difference in affinity.

Objective: Prompted by the identification of a novel M256T mutation in a resistance to TH (RTH)α patient, we investigated Met256 in TRα1 and the corresponding residue (Met310) in TRβ1, residues previously predicted by crystallographic studies in discrimination of T3 vs T4.

Methods: Clinical characterization of the RTHα patient and molecular studies (*in silico* protein modeling, radioligand binding, transactivation and receptor-cofactor studies) were performed.

Results: Structural modeling of the TRα1-M256T mutant showed that distortion of the hydrophobic niche to accommodate the outer ring of ligand was more pronounced for T3 than T4, suggesting that this substitution has little impact on the affinity for T4. In agreement with the model, TRα1-M256T selectively reduced the affinity for T3. Also, unlike other naturally occurring TRα mutations, TRα1-M256T had a differential impact on T3- vs T4-dependent transcriptional activation. TRα1-M256A and TRβ1-M310T mutants exhibited similar discordance for T3 vs T4.

Conclusions: Met256-TRα1/Met310-TRβ1 strongly potentiates the affinity of TRs for T3, thereby largely determining that T3 is the bioactive hormone rather than T4. These observations provide insight into the molecular basis for underlying the different affinity of TRs for T3 vs T4, delineating a fundamental principle of TH signaling.

Introduction

Thyroid hormones (THs) are indispensable for normal growth, development, and metabolism. T3 and T4 are the two major forms of TH. In 1952, it was recognized that T3 has greater biological potency than T4 (1-4). This fundamental discovery led to the clinical concept that T4, despite being the most abundant circulating iodothyronine, functions as a prohormone, with T3 being the biologically active hormone. Since then, this paradigm has remained unchanged, although the molecular and structural mechanisms underlying this have not been investigated in detail.

The genomic actions of THs are exerted through binding to the three functional isoforms of TH receptors (TRs), namely TRα1, TRβ1, and TRβ2, which are highly homologous but have distinctive expression patterns (5-7). Mutations in TRα and TRβ give rise to clinically distinct syndromes in humans, termed resistance to TH (RTH) α and β, respectively (8-14). RTHβ patients commonly present with goiter and tachycardia with abnormal thyroid function tests, including high serum (F)T3 and (F)T4 concentrations with normal or slightly increased TSH concentrations. The clinical phenotype of RTHα is distinct from RTHβ and includes growth retardation, macrocephaly, constipation, intellectual disability, and anemia. In RTHβ, thyroid function tests are typically characterized by high to high-normal (F)T3, low to low-normal (F)T4, low reverse T3 and normal TSH concentrations.

The greater biological activity of T3 vs T4 is explained by differences in affinity for the functional isoforms of TH receptors (TRs). The binding affinity of T4 to the TRs is 10- to 30-fold less compared with T3 (15-17). Previous crystallographic studies revealed that the ligand-binding pocket of TRβ1 is able to accommodate both T3 and T4, although the helix (H)11-H12 loop is more loosely packed in the presence of T4 than T3 (16). These structural adaptations of TRβ1, which are required to accommodate the larger T4 molecule, have been attributed to possible steric hindrance of its bulky 5'-iodine moiety with the surrounding amino acids, especially the methionine residue located at position 310 in TRβ1. Although no cocrystallization studies of TRα with T4 are available, a similar role for Met256 in TRα (equivalent position of Met310 in TRβ), has been suggested (18). However, no functional studies, to support the relevance of these residues for the differences in affinity for T3 and T4, have been performed.

Therefore, we combined structural modeling and *in vitro* approaches to determine the differential role of these methionine residues in T3 vs T4 binding by TRs and characterized a newly identified TRα1-M256T and previously published TRβ1-M310T mutations, which naturally occur in patients with RTH (19-21). We showed that these methionine residues are of particular importance for the binding of T3, and not T4. This observation provides the underlying molecular and structural basis for the role of T4 as prohormone and T3 as bioactive hormone in a paradigm for TH physiology and daily clinical practice.

Materials and Methods

TRα-M256T identification

The TRα-M256T mutation in an RTHα patient was identified by exome sequencing and was confirmed by Sanger sequencing as previously described (12) after obtaining an inform consent. This study was conducted following the Declaration of Helsinki principles and was approved by the Medical Ethical Committee of the Erasmus Medical Center, Rotterdam, Netherlands (MEC-2015-362).

In silico prediction of TRα1-M256T function

The TRα1-M256T mutation bound to T3 and T4 was modeled into the wild-type (WT) TRα1 crystal structure (PDB-ID: 2H77) (22), and the M256T and M256A mutations were introduced using the side-chain substitution tool of the YASARA Structure Software (YASARA Bioscience GmbH, Vienna, Austria) (23) and processed as previously described (24).

DNA constructs and mutagenesis

The pcDNA3 FLAG-TRα1 and TRβ1 expression vectors containing full-length human TRα1 and TRβ1 with 5' FLAG-tagged (11,24) and the pCMX VP16-TRα1 expression vector containing full-length human TRα1 fused with VP16 (25) have been described previously. The TRα1-M256T, TRβ1-M310T, as well as the other TRα1 mutations (M256A, A263S, D211G, and R384H) were introduced, using the QuickChange II Mutagenesis kit (Agilent Technologies, Amstelveen, Netherlands) according to the manufacturers' protocol. The introduced mutations were confirmed by Sanger sequencing.

Radioligand competitive binding assays

FLAG-TRα1 WT, M256T, and M256A receptor proteins were synthesized using the TnT® T7 Quick Coupled Transcription/Translation System (Promega, Leiden, Netherlands). The affinity for T3 and T4 of the receptors was determined by competitive binding assays as previously described (24) using [^{125}I]T3 and [^{125}I]T4, respectively. The dissociation constant (Kd) was analyzed by GraphPad Prism program version 5.0 (GraphPad, La Jolla, CA) and shown as a mean ± SEM of three independent experiments performed in duplicate.

Cell culture and transfection

JEG-3 cells (ECACC Cat# 92120308, RRID:CVCL_0363; Sigma-Aldrich, Munich Germany) were cultured and transfected as previously described (24,26). Given the absence of 5'-deiodinating activity in this cell-type (27), there is no intracellular deiodination of T4 to T3, which allowed us to study the direct effect of T3 and T4 on transactivation. For transcriptional activity assays, WT or mutant receptors were coexpressed with luciferase reporter constructs containing direct repeat thyroid hormone response elements (DR4-TRE) as well as pMaxGFP

as a transfection control. We also coexpressed WT and TRα1-M256T in 1:1 equimolar ratio to determine the effect of the mutant on WT function (i.e., the dominant-negative effect). For receptor-cofactor interaction (two-hybrid) assays, VP16-fused WT or TRα1-M256T were coexpressed with a luciferase reporter construct containing Gal4 binding site (UAStkLuc), together with pSG424 expression vectors containing the Gal4DBD fused to the interacting domains of NCoR1 or SRC1 (11). After transfection for 24 hours, cells were stimulated with 0 to 10,000 nM T3 (Cat. No. T2877; Sigma-Aldrich) or T4 (Cat. No. T2376; Sigma-Aldrich) in DMEM/F12 medium supplemented with 0.1% bovine serum albumin for 24 hours.

Immunoblotting

The expression of FLAG-tagged and VP16-fused receptors in JEG-3 cells was verified by immunoblotting nuclear extracts as previously described (24,26). FLAG-tagged TRα1 and VP16-TRα1 were detected with a 1:1000 dilution of FLAG-M2 (#F1804; Sigma-Aldrich) and VP16 (sc-7545; Santa Cruz Biotechnology, Heidelberg, Germany) antibodies. The Histone 3 protein was detected as loading control with a 1:1000 dilution of a Histone 3 antibody (H3; 1B1B2) (#14269; Cell Signaling Technology, Leiden, Netherlands).

Luciferase assays

Luciferase activity was measured as previously described (12,24). Data were expressed as percentage maximal response of WT stimulated by T3. Half-maximal effective concentration (EC_{50}), half-maximal inhibitory concentration (IC_{50}), and maximal response were calculated using GraphPad Prism program version 5.0 (GraphPad, La Jolla, CA). The results are shown as a mean ± SEM of at least three independent experiments performed in triplicate.

Statistical analysis

Statistical differences of logKd, logIC_{50}, and logEC_{50} values between groups were analyzed by student's t-test or one-way ANOVA with Tukey's post-test. The percentage maximal response of mutants was compared to WT by one sample t-test. Statistical significance was considered when p-values < 0.05.

Results

Clinical characterization

A *de novo* heterozygous missense mutation in the *THRA* gene (c.767T>C), resulting in substitution of threonine for methionine at codon 256 (p.M256T), was identified in a 19-year-old male presenting with features similar to previously reported RTHα patients, including disproportionate ischial leg length (sitting height to height ratio +2.5 SD score), mild neurodevelopmental delay, coarse facies, macrocephaly (head circumference 60 cm, +2.5

SD score), and high serum T3/T4 ratio with normal TSH concentrations [FT4, 10.6 pmol/L (normal range, 11 to 25 pmol/L); total T4, 67 nmol/L (normal range, 58 to 128 nmol/L); total T3, 2.9 nmol/L (normal range, 1.4 to 2.5 nmol/L); reverse T3, 0.18 nmol/L (normal range, 0.22 to 0.54 nmol/L); T3/T4 ratio, 0.043 (normal range, 0.01 to 0.03); and TSH, 1.83 mU/L (normal range, 0.4 to 4.3 mU/L)] (Figure 1). This mutation is not present in public databases (dbSNP, 1000Genome, and Exome Aggregation Consortium [ExAC]).

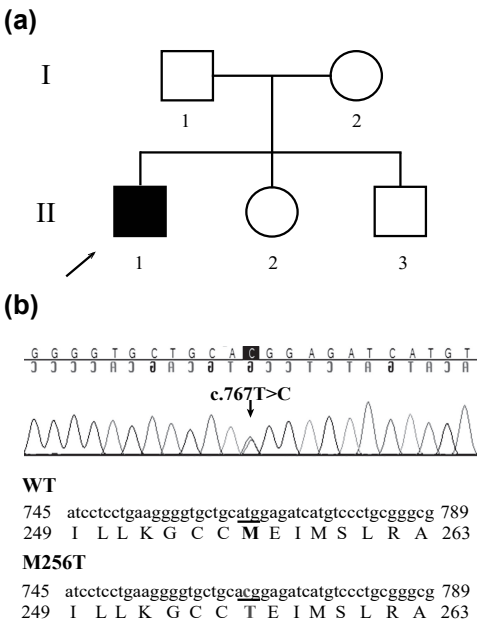

Figure 1. (a) Pedigree chart demonstrating that only the index patient (II.1) has the clinical phenotype of RTHα. (b) Sequence analysis of exon 8 of *THRA* gene shows a *de novo* heterozygous missense mutation (c.767T>C) in index patient, resulting in a methionine to threonine substitution at codon 256 (p.M256T).

Protein modeling

The role of the Met256 in TRα1 function and the potential effect of this mutation on the affinity of T3 and T4 were predicted by *in silico* modeling. Given the absence of a T4-bound TRα crystal structure, we studied the structural organization of the domains surrounding the outer ring of TH in the available T3- (PDB ID: 1xzx) and T4-liganded (PDB ID: 1y0x) crystal structures of TRβ1. In line with a previous report (16), we observed that the 5' position of the outer ring of both T3 and T4 is flanked by Ile276 (H3), Met310 and Met313 (H6), His435 (H11), Phe455 and Phe459 (H12) of TRβ1. Together, these residues form a niche that allows the accommodation of T4 despite the presence of its bulky 5'-iodine. The same niche is also present within the T3-liganded TRβ1 crystal but is considerably smaller in the absence of the

5'-iodine. Met310 (corresponding to Met256 of TRα1) is in closest structural proximity to the 5' carbon of the outer ring and forms an extensive network of (hydrophobic) interactions that link H6, H11 and H12.

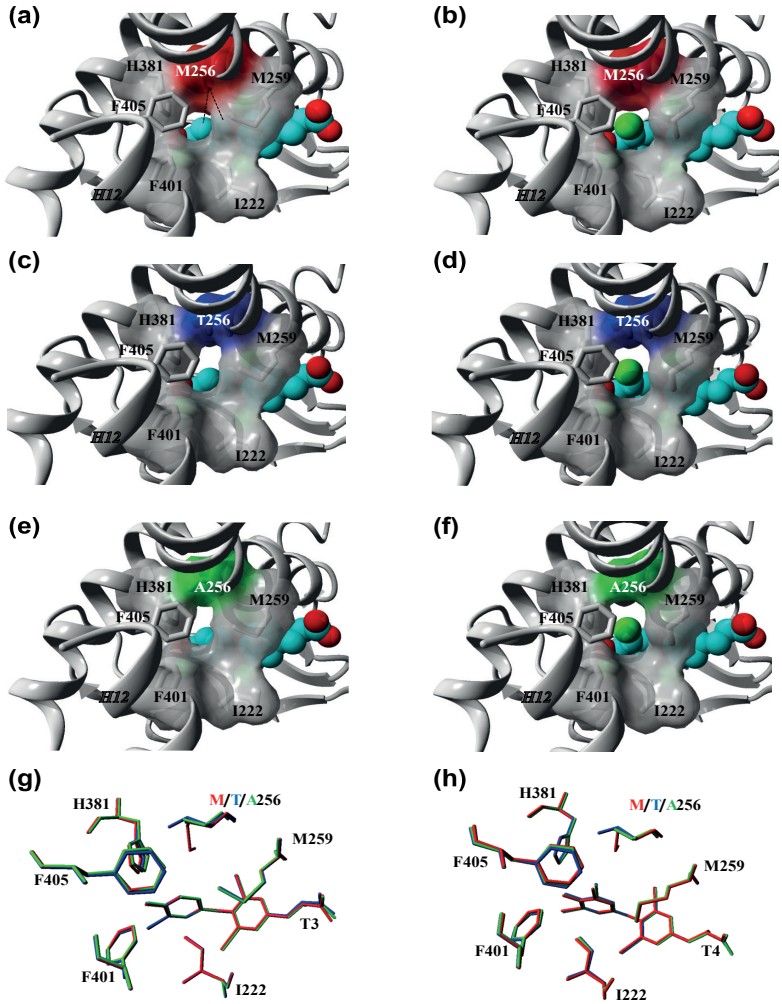

Figure 2. Comparison of the architecture of the TRα1 ligand binding pocket in the presence of T3 and T4. (a and b) Close-up view of the ligand-binding pocket of the TRα1 crystal structure in complex with (a) T3 (PDB ID: 2h77) and (b) T4. The residue side-chains lining the niche that accommodates the outer ring of T3 and T4 are highlighted, and their molecular surface is shown except for Phe405 for clarity. The 5' iodine group of T4 is represented by the green ball in T4-bound TRα1 model. The hydrophobic contacts between Met256 and the phenolic outer ring are depicted as dashed lines. (c and d) Structural models of the TRα1-M256T mutant in complex with (c) T3 and (d) T4. (e and f) Structural models of the TRα1-M256A mutant in complex with (e) T3 and (f) T4. (g and h) Overlay of the structural orientation of the residue side-chains that face the (g) T3 and (h) T4 ligands at the 5' position in WT (gray), M256T (blue) and M256A (red) mutant TRα1 models. All figures were created in YASARA Structure using PovRay imaging software.

We next modeled a T4 molecule into the ligand-binding pocket of the available T3-liganded TRα1 crystal structure (PDB-ID: 2H77) [Figure 2(b)]. Compared with the T3-liganded TRα1 structure [Figure 2(a)], a slight outward shift of H11 and H12 was observed in the T4-liganded model, which was accompanied by reorientation of side-chains of residues surrounding the 5' iodine. This resulted in a loss of the direct hydrophobic interactions between Met256 and the outer ring and a less tightly packed structural organization of the ligand binding pocket. These changes were similar to those observed in the corresponding TRβ1 crystal structures, validating the accuracy of the modeling procedure.

We subsequently modeled the M256T (shortening of side-chain, hydrophilic moiety) mutant in both T3- and T4-bound TRα1 structures and analyzed the impact on the conformation of the ligand binding domain and direct substrate interactions [Figure 2(c) and 2(d)]. The artificial M256A mutant was also modeled to reduce the side-chain length while maintaining the hydrophobic property of the residue [Figure 2(e) and 2(f)]. Due to shortening of side-chain length in both mutants, direct hydrophobic interaction with the outer ring of T3 was lost [Figure 2(c) and 2(e)]. Moreover, both mutants enlarged the niche surrounding the 5' position of T3 due to reorientation of various residue side-chains in H11 and H12 and the subsequent outward shift of these helices. As a result, the niche adopts a structural configuration that resembles the WT receptor in T4-bound state. These changes were more pronounced for the M256T than the M256A, exemplified by the degree of re-orientation of His381, which was previously implicated to interact with the phenolhydroxyl group of T3 (18) [Figure 2(g)]. In the case of T4, both mutations had little effect on structural organization [Figure 2(d), 2(f), and 2(h)]. Based on these *in silico* predictions, we hypothesized that both substitutions would have a greater impact on T3 than on T4 binding and action.

Functional studies

We performd *in vitro* studies to test this hypothesis. In line with previous literature (15-17), competitive binding assays showed that the affinity for T4 of WT TRα1 was approximately sevenfold lower than for T3, indicating by the higher Kd of T4 than T3 [Figure 3(a); Tabel 1]. The TRα1-M256T mutant showed a ~40-fold lower T3 binding affinity than WT, whereas T4 affinity was unchanged [Figure 3(c); Table 1]. Also, the binding affinity of the TRα1-M256A mutant for T3 was selectively reduced (approximately sixfold) [Figure 3(e); Table 1].

To evaluate the impact of both mutations on the transcriptional activity, WT and mutant receptors were cotransfected with a reporter construct in which luciferase expression is under control of a TH response element (TRE) into JEG-3 cells with increasing concentrations of T3 or T4. Equal expression of WT and both mutants was confirmed by immunoblotting nuclear extracts with anti-FLAG antibodies [Figure 3(b)]. In line with the binding assays and previous studies (16,17), the transcriptional activation assay showed that the EC_{50} of WT TRα1 induced by T4 was ~60-fold higher than that induced by T3 [Figure 3(b); Table 1]. The EC_{50} of TRα1-M256T was 100-fold higher for T3 but was unchanged for T4 compared with WT [Figure 3(d); Table 1]. The TRα1-M256A also selectively reduced transcriptional activity induced by T3

[Figure 3(f); Table 1]. The transcriptional activity was also reduced when WT and TRα1-M256T were coexpressed compared to WT expressed alone, suggesting a dominant-negative effect of this mutant (data not shown). In mammalian two-hybrid assays compared with WT, the TRα1-M256T mutant also affected ligand-dependent interactions with the corepressor NCoR1 (fold increase IC_{50}: ~80-fold for T3 and ~6-fold for T4) and the coactivator SRC1 (fold increase EC_{50}: ~90-fold for T3 and approximately sixfold for T4) [Figure 4(a)-4(d); Table1]. Together, our results indicate that the mutations located at the Met256 of TRα1 have a differential impact on the binding and activation of the receptor by T4 vs T3.

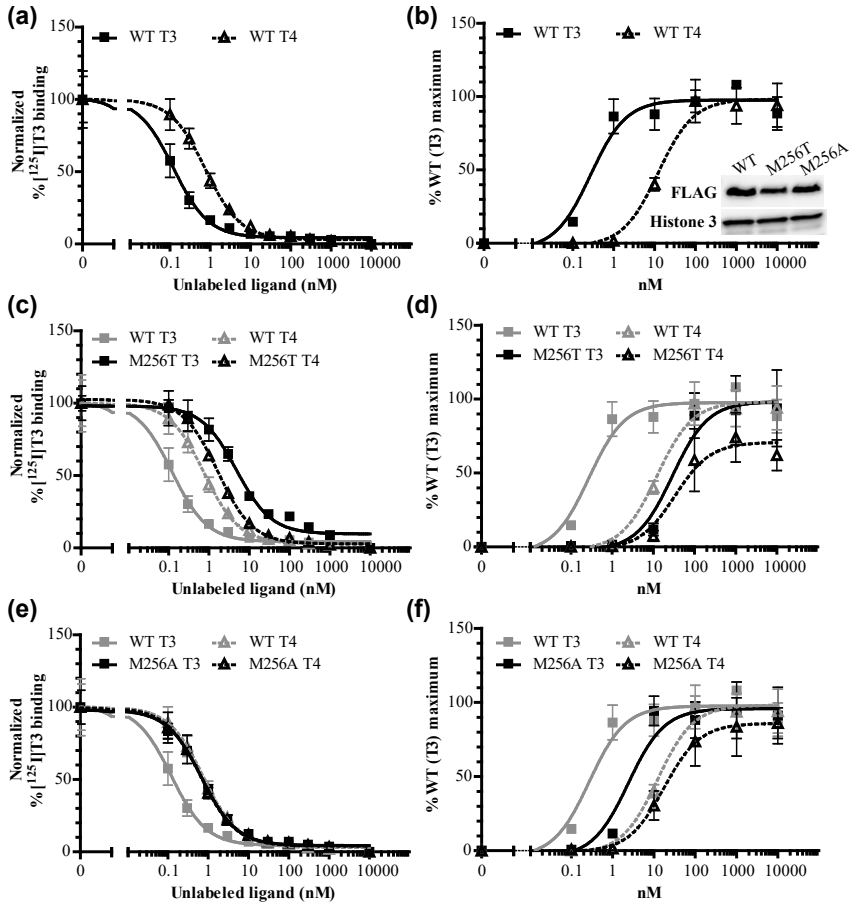

Figure 3. (a, c, e) [^{125}I]T3 dissociation curves showing that compared with (a) WT, (c) the TRα1-M256T mutation and (e) TRα1-M256A mutation reduces the affinity for T3 (solid line) more than for T4 (dashed line) (mean ± SEM of three experiments for WT and M256T and two experiments for M256A performed in duplicate). (b, d, f) The TRα1-M256T and TRα1-M256A mutations also had a larger effect on T3- than on T4-dependent transcriptional activation (mean ± SEM of three experiments performed in triplicate). The effect of the alanine substitution on the ligand binding affinity and the transcriptional activity of TRα1 was less than the effect of the threonine substitution. The insert in (b) shows Immunoblots confirming an equal expression of WT, M256T, and M256A FLAG-tagged TRα1 and Histone 3 as a loading control in the nuclear fraction of JEG-3 cells.

Table 1. Summary of the results of competitive binding, transcriptional activity, and protein-protein interaction assays of WT, TRα1-M256T and TRα1-M256A mutants.

	T3 stimulation			T4 stimulation		
	WT	**M256T**	**M256A**	**WT**	**M256T**	**M256A**
LogKd [Kd(nM)]	-0.91±0.08 [0.12]	0.71±0.10*** [5.14]	-0.16±0.34**,††† [0.69]	-0.09±0.10 [0.81]	0.22±0.05 [1.67]	-0.18±0.02 [0.66]
LogEC$_{50}$-DR4 [EC$_{50}$ (nM)]	-0.60±0.10 [0.25]	1.51±0.16*** [32.3]	0.51±0.08**,†† [3.26]	1.16±0.07 [14.5]	1.67±0.11 [46.6]	1.44±0.25 [27.2]
LogIC$_{50}$-NCoR1 [IC$_{50}$ (nM)]	-1.26±0.04 [0.06]	0.69±0.18*** [4.87]	-	0.02±0.06 [1.05]	0.82±0.14** [6.64]	-
LogEC$_{50}$-SRC1 [EC$_{50}$ (nM)]	-0.76±0.05 [0.17]	1.19±0.07*** [15.5]	-	0.42±0.07 [2.65]	1.16±0.08** [14.6]	-

Data are presented as mean ± SEM (one-way ANOVA with Tukey post test, *p<0.05, **p<0.01, ***p<0.001 for WT vs. mutant, and †p<0.05, ††p<0.01, †††p<0.001 for M256T vs. M256A).

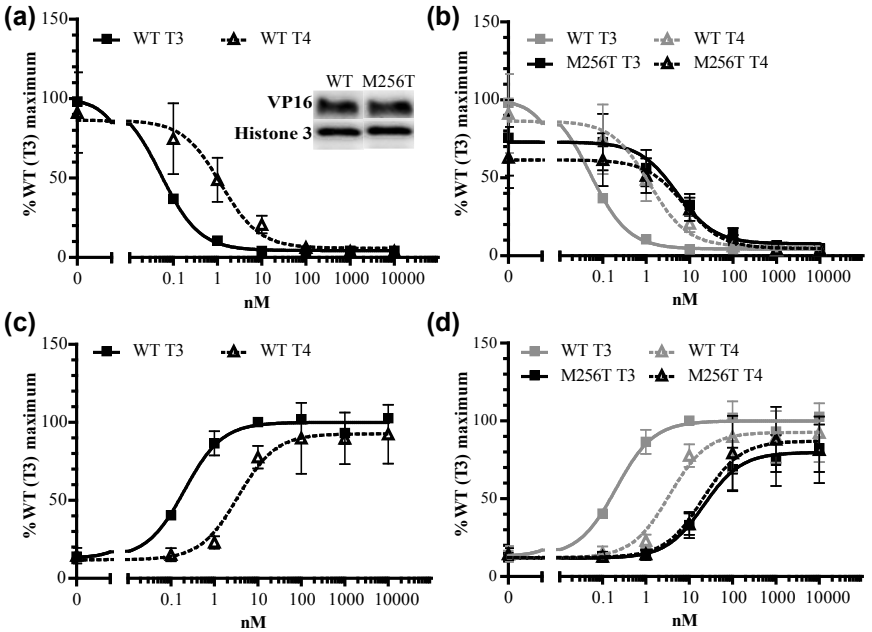

Figure 4. The TRα1-M256T mutation had a larger effect on T3- than on T4-dependent (a and b) GAL4-NCoR1 dissociation, and (c and d) GAL4-SRC1 association (mean ± SEM of at least three experiments performed in triplicate). The insert of (a) shows immunoblots confirming an equal expression of WT and M256T VP16 TRα1 fusion proteins and Histone 3 as loading control in the nuclear fraction of JEG-3 cells.

We next investigated if this T3 vs T4 difference is present in other TRα mutants located outside the niche surrounding the 5'-iodine position. However, these naturally occurring mutations (D211G, A263S, and R384H) had a similar impact on T3 and T4 induced transactivation, and, as for WT TRα, the EC_{50} values for T4 exceeded those for T3 by ~30- to 50-fold [Figure 5(a)-5(c)]. These transcriptional activation profiles were in contrast to the M256T mutant [Figure 5(d)], strongly indicating that only this mutant has a predominant impact on T3 affinity. To extend our findings to TRβ, we also studied the transcriptional activity of a corresponding mutation in TRβ1 (TRβ1-M310T). The EC_{50} of WT TRβ1 induced by T4 was ~70-fold higher than that induced by T3 [Figure 6(a)], which was similar to WT TRα1. The T3-induced transcriptional response of TRβ-M310T was greatly reduced, which contrasted with the T4-induced transcriptional activity (fold increase EC_{50}: ~350-fold for T3 and approximately threefold for T4) [Figure 6(b)].

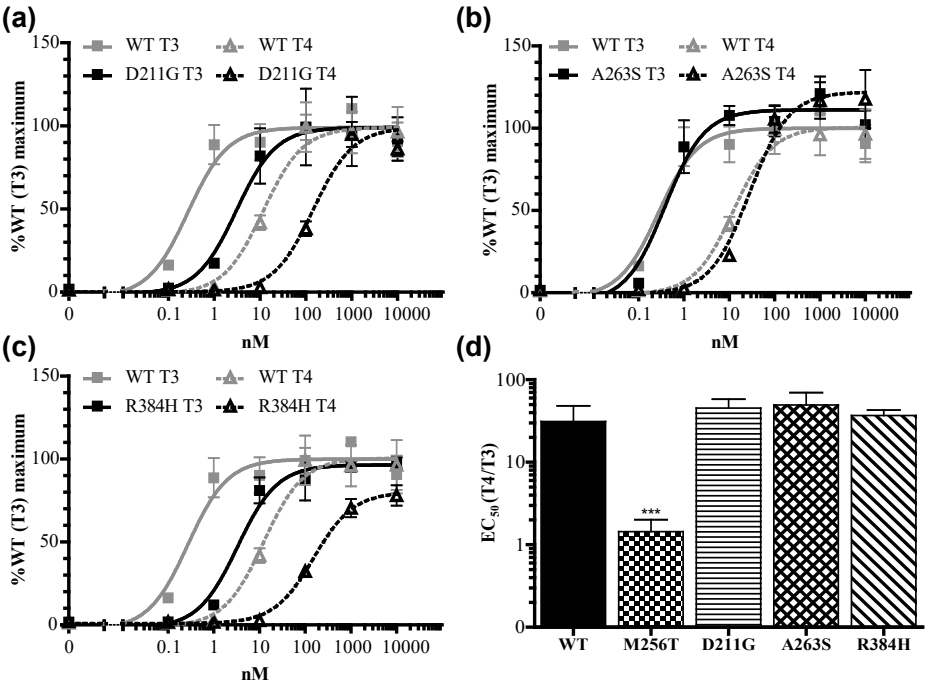

Figure 5. (a-c) The T4-induced transcriptional activity of three TRα1 mutations identified in RTHα patients is lower than that is induced by T3, which is similar to WT [Figure 3(d)] (mean ± SEM of three experiments performed in triplicate). (d) The EC_{50} of T4 is ~30- to 50-fold higher than the EC_{50} of T3, except for TRα1-M256T ***$P < 0.001$ (one-way ANOVA with Tukey post test).

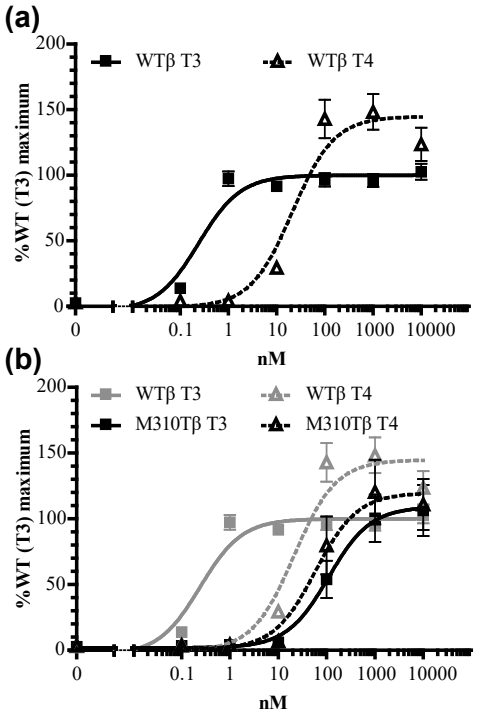

Figure 6. The T3- and T4-induced transcriptional activity of (a) WT and (b) TRβ1-M310T in JEG-3 cells shows that the TRβ1-M310T mutation affects T3- more than T4-dependent transcriptional activation (mean ± SEM of four experiments performed in triplicate), which is in line with the results of TRα1-M256T [Figure 3(d)].

Discussion

Although the notion of T4 and T3 being the precursor and active hormone, respectively, is widely recognized in both the clinical and scientific community, the molecular and structural basis of this dogma has received little attention. In this study, we highlight the crucial role of residue Met256 of TRα1 and Met310 of TRβ1 in determining the differential bioactivity of T3 vs T4, using a novel mutant (TRα1-M256T) identified in an RTHα patient and a mutant at the corresponding position (TRβ1-M310T) identified in RTHβ patients (19-21). In contrast to WT TRα or TRβ and mutations involving other residues, mutations at these methionine residues selectively affected binding and transactivation of TR by T3. These observations emphasize the key role of these residues in designating T4 as the prohormone and T3 as the major bioactive hormone.

In line with previous reports (15-17), our results showed that T3 has a higher binding affinity for WT TRα1 and stimulates receptor activity with a higher potency than T4. Previous structural studies in TRβ1 have suggested that the lower affinity for T4 is caused by decreased packing of the ligand binding domain in presence of T4 vs T3, which particularly allows oscillation of H12 between liganded and unliganded states, resulting in a higher ligand dissociation rate (16). Here, we extend these observations by showing that the ligand binding domain of T3-liganded TR has a similar decrease in packing as observed in T4-liganded WT receptors upon substitution of Met256 in TRα1 or Met310 in TRβ1 by threonine. In contrast, these substitutions hardly changed the predicted structure of T4-liganded mutant receptors. Based on these models, we postulated that the extensive (hydrophobic) interactions of methionine with surrounding residues are key in stabilizing interhelical interactions (e.g., between H6, H11, and H12), which facilitate the tight packing of the ligand binding domain as observed in T3-liganded receptors. Moreover, we observed a direct interaction between methionine and the 5' position of the outer ring of T3, which was not formed with T4. This suggests that Met256 in TRα1 and Met310 in TRβ1 have a critical role in achieving optimal folding and enthalpy in T3-liganded receptors, whereas their role in T4 binding is of less importance.

This *in silico* prediction was confirmed by *in vitro* studies indicating that TRα1-M256T selectively affected binding affinity for T3 as well as cofactor interactions and transcriptional activity of T3-stimulated receptor. These properties seemed specific for the M256T mutant because the transactivational potency of T3 and T4 with TRα mutants identified in other RTHα patients [D211G (26), A263S, and R384H (28)] was affected equally. Additional testing of the naturally occurring mutation at the corresponding residue in the TRβ1 (M310T) (19-21) further substantiated the specificity of the findings.

Threonine substitution at position 256 in TRα1 or 310 in TRβ1 not only alters the binding space but also affects the hydrophobicity of the ligand-binding pocket. Therefore, we tested the artificial TRα1-M256A mutant, which reduces the size of the side-chain but maintains the hydrophobic property of the ligand-binding pocket. Indeed, functional studies showed that TRα1-M256A also selectively impairs T3 binding affinity and T3-induced transcriptional activity, whereas T4 binding and activity are maintained. Although the effect of TRα1-M256T mutation in our functional and structural models was slightly greater than that of TRα1-M256A, these findings support the notion that loss of the specific properties of methionine, rather than the unfavorable impact of the hydrophilic moiety of threonine on the hydrophobic environment, are mainly responsible for the differential impact on T3 vs T4 signaling. Based on our studies and on a previous report (16), we propose that Met256 in TRα1 and Met310 in TRβ1 are crucial residues that determine specific affinity for T3 vs T4. Threonine and alanine substitution at these methionine positions significantly affected the hydrophobic interactions with T3 and altered the niche accommodating the outer ring of T3 to a "T4-bound" configuration, both resulting in a reduced binding affinity of the mutants for T3. In contrast, because the ligand binding domain of T4-liganded receptors already exhibit looser

packing without direct interaction(s) between methionine and the T4 molecule, mutations in the methionine residue are better tolerated.

No unique phenotype was discernible in the newly-identified M256T RTHα patient when compared to other cases of RTHα harbouring missense mutations in the *THRA* gene (25,26,28-30), or in patients carrying TRβ-M310T (19-21) when compared to other RTHβ cases reported in the literature. These findings indicate that although mutations at Met256-TRα1/Met310-TRβ1 residues preserve T4 binding to mutant receptor proteins, this property is not sufficient to prevent patients from developing features of RTH, implying that the phenotype of RTH is linked primarily to defective T3 rather than T4 binding by mutant TRs.

This study provides *in vitro* evidence for the importance of Met256 in TRα1 and Met310 in TRβ1 in ligand recognition. Our studies highlight the relevance of this methionine residue in TRs for discrimination between T3 and T4, providing the molecular basis for the role of T4 as prohormone and T3 as bioactive hormone.

Acknowledgements

In the early stage of writing this manuscript, professor Theo J. Visser suddenly and unexpectedly passed away. We highly value his contributions to the field and we miss a great scientist, mentor and friend. While deceased contributors are rightfully recognized and acknowledged, they cannot be added posthumously to an article's byline.

Financial Support: This work is supported by Zon-MWTOP Grant 91212044, by an Erasmus MC Medical Research Advisory Committee grant (to R.P.P., M.E.M., and W.E.V.), by a grant from Chiang Mai University (to K.W.), and by Wellcome Trust Grant 210755/Z/18/Z and an NIHR Cambridge Biomedical Centre grant (to V.K.C.).

Disclosure Summary: The authors have nothing to disclose.

References

1. Gross J, Pitt-Rivers R. Physiological activity of 3:5:3'-L-triiodothyronine. *Lancet.* 1952;**1**(6708):593-594.
2. Pitt-Rivers R. Metabolic effects of compounds structurally related to thyroxine in vivo: thyroxine derivatives. *J Clin Endocrinol Metab.* 1954;**14**(11):1444-1450.
3. Mussett MV, Pitt-Rivers R. The thyroid-like activity of triiodothyronine analogues. *Lancet.* 1954;**267**(6850):1212-1213.
4. Lerman J. The contribution of triiodothyronine to thyroid physiology. *J Clin Endocrinol Metab.* 1954;**14**(6):690-693.
5. Cheng SY, Leonard JL, Davis PJ. Molecular aspects of thyroid hormone actions. *Endocr Rev.* 2010;**31**(2):139-170.
6. Singh BK, Yen PM. A clinician's guide to understanding resistance to thyroid hormone due to receptor mutations in the TRalpha and TRbeta isoforms. *Clin Diabetes Endocrinol.* 2017;**3**:8.
7. Lazar MA. Thyroid hormone receptors: multiple forms, multiple possibilities. *Endocr Rev.* 1993;**14**(2):184-193.
8. Refetoff S, DeWind LT, DeGroot LJ. Familial syndrome combining deaf-mutism, stuppled epiphyses, goiter and abnormally high PBI: possible target organ refractoriness to thyroid hormone. *J Clin Endocrinol Metab.* 1967;**27**(2):279-294.
9. Sakurai A, Takeda K, Ain K, Ceccarelli P, Nakai A, Seino S, Bell GI, Refetoff S, DeGroot LJ. Generalized resistance to thyroid hormone associated with a mutation in the ligand-binding domain of the human thyroid hormone receptor beta. *Proc Natl Acad Sci U S A.* 1989;**86**(22):8977-8981.
10. Dumitrescu AM, Refetoff S. The syndromes of reduced sensitivity to thyroid hormone. *Biochim Biophys Acta.* 2013;**1830**(7):3987-4003.
11. Bochukova E, Schoenmakers N, Agostini M, Schoenmakers E, Rajanayagam O, Keogh JM, Henning E, Reinemund J, Gevers E, Sarri M, Downes K, Offiah A, Albanese A, Halsall D, Schwabe JW, Bain M, Lindley K, Muntoni F, Vargha-Khadem F, Dattani M, Farooqi IS, Gurnell M, Chatterjee K. A mutation in the thyroid hormone receptor alpha gene. *N Engl J Med.* 2012;**366**(3):243-249.
12. van Mullem A, van Heerebeek R, Chrysis D, Visser E, Medici M, Andrikoula M, Tsatsoulis A, Peeters R, Visser TJ. Clinical phenotype and mutant TRalpha1. *N Engl J Med.* 2012;**366**(15):1451-1453.
13. van Gucht ALM, Moran C, Meima ME, Visser WE, Chatterjee K, Visser TJ, Peeters RP. Resistance to Thyroid Hormone due to Heterozygous Mutations in Thyroid Hormone Receptor Alpha. *Curr Top Dev Biol.* 2017;**125**:337-355.
14. Moran C, Chatterjee K. Resistance to Thyroid Hormone alpha-Emerging Definition of a Disorder of Thyroid Hormone Action. *J Clin Endocrinol Metab.* 2016;**101**(7):2636-2639.
15. Apriletti JW, Eberhardt NL, Latham KR, Baxter JD. Affinity chromatography of thyroid hormone receptors. Biospecific elution from support matrices, characterization of the partially purified receptor. *J Biol Chem.* 1981;**256**(23):12094-12101.
16. Sandler B, Webb P, Apriletti JW, Huber BR, Togashi M, Cunha Lima ST, Juric S, Nilsson S, Wagner R, Fletterick RJ, Baxter JD. Thyroxine-thyroid hormone receptor interactions. *J Biol Chem.* 2004;**279**(53):55801-55808.
17. Schroeder A, Jimenez R, Young B, Privalsky ML. The ability of thyroid hormone receptors to sense t4 as an agonist depends on receptor isoform and on cellular cofactors. *Mol Endocrinol.* 2014;**28**(5):745-757.
18. Wagner RL, Apriletti JW, McGrath ME, West BL, Baxter JD, Fletterick RJ. A structural role for hormone in the thyroid hormone receptor. *Nature.* 1995;**378**(6558):690-697.
19. Kim HK, Kim D, Yoo EH, Lee JI, Jang HW, Tan AH, Hur KY, Kim JH, Kim KW, Chung JH, Kim SW. A case of resistance to thyroid hormone with thyroid cancer. *J Korean Med Sci.*

2010;**25**(9):1368-1371.

20. Mitchell CS, Savage DB, Dufour S, Schoenmakers N, Murgatroyd P, Befroy D, Halsall D, Northcott S, Raymond-Barker P, Curran S, Henning E, Keogh J, Owen P, Lazarus J, Rothman DL, Farooqi IS, Shulman GI, Chatterjee K, Petersen KF. Resistance to thyroid hormone is associated with raised energy expenditure, muscle mitochondrial uncoupling, and hyperphagia. *J Clin Invest.* 2010;**120**(4):1345-1354.
21. Takeda K, Weiss RE, Refetoff S. Rapid localization of mutations in the thyroid hormone receptor-beta gene by denaturing gradient gel electrophoresis in 18 families with thyroid hormone resistance. *J Clin Endocrinol Metab.* 1992;**74**(4):712-719.
22. Nascimento AS, Dias SM, Nunes FM, Aparicio R, Ambrosio AL, Bleicher L, Figueira AC, Santos MA, de Oliveira Neto M, Fischer H, Togashi M, Craievich AF, Garratt RC, Baxter JD, Webb P, Polikarpov I. Structural rearrangements in the thyroid hormone receptor hinge domain and their putative role in the receptor function. *J Mol Biol.* 2006;**360**(3):586-598.
23. Krieger E, Vriend G. YASARA View - molecular graphics for all devices - from smartphones to workstations. *Bioinformatics.* 2014;**30**(20):2981-2982.
24. Wejaphikul K, Groeneweg S, Dejkhamron P, Unachak K, Visser WE, Chatterjee K, Visser TJ, Meima ME, Peeters RP. Role of Leucine 341 in Thyroid Hormone Receptor Beta Revealed by a Novel Mutation Causing Thyroid Hormone Resistance. *Thyroid.* 2018;**28**(12):1723-1726.
25. Moran C, Agostini M, McGowan A, Schoenmakers E, Fairall L, Lyons G, Rajanayagam O, Watson L, Offiah A, Barton J, Price S, Schwabe J, Chatterjee K. Contrasting Phenotypes in Resistance to Thyroid Hormone Alpha Correlate with Divergent Properties of Thyroid Hormone Receptor alpha1 Mutant Proteins. *Thyroid.* 2017;**27**(7):973-982.
26. van Gucht AL, Meima ME, Zwaveling-Soonawala N, Visser WE, Fliers E, Wennink JM, Henny C, Visser TJ, Peeters RP, van Trotsenburg AS. Resistance to Thyroid Hormone Alpha in an 18-Month-Old Girl: Clinical, Therapeutic, and Molecular Characteristics. *Thyroid.* 2016;**26**(3):338-346.
27. Kester MH, Kuiper GG, Versteeg R, Visser TJ. Regulation of type III iodothyronine deiodinase expression in human cell lines. *Endocrinology.* 2006;**147**(12):5845-5854.
28. Demir K, van Gucht AL, Buyukinan M, Catli G, Ayhan Y, Bas VN, Dundar B, Ozkan B, Meima ME, Visser WE, Peeters RP, Visser TJ. Diverse Genotypes and Phenotypes of Three Novel Thyroid Hormone Receptor-alpha Mutations. *J Clin Endocrinol Metab.* 2016;**101**(8):2945-2954.
29. Tylki-Szymanska A, Acuna-Hidalgo R, Krajewska-Walasek M, Lecka-Ambroziak A, Steehouwer M, Gilissen C, Brunner HG, Jurecka A, Rozdzynska-Swiatkowska A, Hoischen A, Chrzanowska KH. Thyroid hormone resistance syndrome due to mutations in the thyroid hormone receptor alpha gene (THRA). *J Med Genet.* 2015;**52**(5):312-316.
30. Espiard S, Savagner F, Flamant F, Vlaeminck-Guillem V, Guyot R, Munier M, d'Herbomez M, Bourguet W, Pinto G, Rose C, Rodien P, Wemeau JL. A Novel Mutation in THRA Gene Associated With an Atypical Phenotype of Resistance to Thyroid Hormone. *J Clin Endocrinol Metab.* 2015;**100**(8):2841-2848.

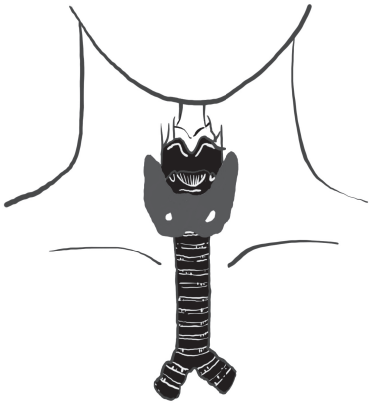

CHAPTER 4

The *in vitro* Functional Impairment of Thyroid Hormone Receptor Alpha 1 Isoform Mutants is Mainly Dictated by Reduced Ligand-Sensitivity

Karn Wejaphikul, Anja L.M. van Gucht, Stefan Groeneweg, W. Edward Visser, Theo J. Visser, Robin P. Peeters, Marcel E. Meima

Thyroid *(in press)*

4

Abstract

Background: Thyroid hormone (TH) acts on TH receptors (TRs) and regulates gene transcription by binding of TRs to TH response elements (TREs) in target gene promoters. The transcriptional activity of TRs is modulated by interactions with TR-coregulatory proteins. Mutations in TRα cause resistance to thyroid hormone alpha (RTHα). In this study, we analyzed if, beyond reduced T3 affinity, altered interactions with cofactors or different TREs could account for the differential impaired transcriptional activity of different mutants.

Methods: We evaluated four mutants derived from patients (D211G, M256T, A263S, and R384H) and three artificial mutants at equivalent positions in patients with RTHβ (T223A, L287V, and P398H). The *in vitro* transcriptional activity was evaluated on TRE-luciferase reporters (DR4, IR0, and ER6). The affinity for T3 and interaction with coregulatory proteins (NCoR1 and SRC1) were also determined.

Results: We found that the affinity for T3 was significantly reduced for all mutants, except for TRα1-T223A. The reduction in the T3 sensitivity of the transcriptional activity on three TREs, the dissociation of the corepressor NCoR1, and the association of the coactivator SRC1 recruitment for each mutant correlated with the reduced affinity for T3. We did not observe mutation-specific alterations in interactions with cofactors or TREs.

Conclusion: In summary, the degree of impaired transcriptional activity of mutants is mainly determined by their reduced affinity for T3.

Introduction

Genomic actions of thyroid hormone (TH) are regulated by binding of the active form of TH, tri-iodothyronine (T3), to its nuclear TH receptors (TRs), which act predominantly as heterodimers with retinoid X receptors (RXRs) on thyroid hormone response elements (TREs) in the promoter region of target genes (1,2). TREs usually consist of two-consensus half-sites that can be organized in direct repeats (DRs), inverted repeats (IRs), and everted repeats (ERs), separated by a stretch of random nucleotides of various lengths, of which the DR4-TRE is the predominant TR-binding form (3-6). In the absence of ligand, TRs repress target gene transcription by recruitment of corepressors such as nuclear receptor corepressor 1 (NCoR1). Binding of T3 causes dissociation of the corepressors and allows coactivators, such as steroid receptor coactivator 1 (SRC1), to bind to the TR, resulting in activation of gene transcription (1,7).

Mutations in the ligand binding domain (LBD) of TRα1 cause resistance to thyroid hormone alpha (RTHα) which was first described in 2012 (8,9). The phenotype of RTHα patients includes growth retardation, macrocephaly, constipation, intellectual disability, anemia, and a high (F)T3/(F)T4 ratio (10,11). To date, 22 mutations (in a total of 37 patients) have been reported as a cause of RTHα. These mutations can be categorized into two groups based on the type of mutation. The first group consists of truncating mutations caused by nonsense or frameshift mutations that create premature stop codons and shorten the length of the LBD (8,9,12-14). This structural alteration completely abolishes T3 affinity and T3-induced transcriptional activity of TRα1. The second group consists of missense mutations that result in single amino acid substitutions in the LBD (10,13-20). These mutant receptors can still bind T3 but with a lower affinity than wild-type (WT) receptors.

There is a variety in the clinical phenotype of RTHα patients. Patients with truncating mutations generally have a more severe phenotype than patients with missense mutations (9,12-14). Within the latter group, there are notable differences in the neurocognitive features (14,17,20). At present, it is unclear whether these differences are solely explained by differences in T3 binding. In RTHβ, mutation-specific effects on particular TREs and differences in interaction with coactivators versus corepressors have been described (21-24). Here, we studied if mutation-specific effects on TRE or cofactor binding are present in a selected series of seven specific TRα1 missense mutations.

Materials and methods

Plasmid constructs

The coding sequence (cDNA) of full-length TRα1 fused at the 5' end to the FLAG epitope or to VP16 were cloned into the pcDNA3 (9) and the pCMX expression vectors (18),

respectively, as previously described. Selected TRα1 missense mutations were introduced into pcDNA3-FLAG TRα1 and pCMX-VP16 TRα1 expression vectors using the QuickChange II Mutagenesis kit (Align Technologies, Amstelveen, The Netherlands) (see Supplementary Table S1 for primers) and confirmed by Sanger sequencing.

The luciferase reporter constructs containing either direct (DR4), inverted (IR0), or everted repeat (ER6) TRE configurations (TRE-tkLuc) (25), the luciferase reporter construct containing Gal4 binding site (UAStkLuc), and the pSG424 expression vector constructs containing the Gal4 DNA-binding domain (GAL4-DBD) fused to the interacting domains of NCoR1 or SRC1 (8) have all been described elsewhere.

[^{125}I]T3 competitive binding assays

[^{125}I]T3 competitive binding assays were performed as previously described (26). In brief, WT and mutant FLAG-TRα1 proteins were synthesized using the TnT® T7 Quick Coupled Transcription/Translation System (L1170, Promega, Leiden, The Netherlands). The proteins were incubated with 0.02 nM of [^{125}I]T3 (prepared in-house as previously described (27)) and 0-10,000 nM unlabeled T3 (Cat. No. T2877, Sigma-Aldrich) at 30°C for 2 hours. The input of WT and mutant FLAG-TRα1 proteins lysate was adjusted to obtain 10-20% maximal [^{125}I]T3 binding, in order to prevent ligand-depletion effect. TR bound [^{125}I]T3 was measured and calculated as a percentage [^{125}I]T3 input. The dissociation constant (Kd) was computed by GraphPad Prism 5.0 (GraphPad, La Jolla, CA)

In silico model prediction

The various TRα1 mutations were introduced into the WT T3-bound TRα1 crystal structure (PDB-ID: 2H77 (28)) using the side-chain substitution and optimization tools of the YASARA Structure Software (YASARA Bioscience GmbH, Vienna, Austria) (29). The structural models of the TRα1 mutants have been processed and compared to the WT TRα1 structure as previously described (20). Given their location outside the ligand-binding pocket, the D211G, T223A, R384H, and P398H mutant models were compared to WT after additional molecular dynamic simulations in an AMBER force field with water as a solvent to investigate their impact on the structural integrity of the receptor.

Ligand-binding energy was calculated using the BindEnergy command implemented in YASARA Structure Software, which calculates the in *vacuo* binding energy in a NOVA force field without considering solvation effects (30). As such, this approach is suitable for detecting changes in binding energy by mutations that affect substrate interactions directly, and not for those having indirect effects. A high value indicates a favorable T3 binding.

Cell culture and transfection

JEG-3 cells (ECACC Cat# 92120308, RRID:CVCL_0363, Sigma-Aldrich) were cultured in 24-well plates using the growth medium (DMEM/F12 supplemented with 9%FBS,

100 nM Na_2SeO_3, 100 U/mL penicillin, and 100 µg/mL streptomycin) and transfected as previously described (19,26). Briefly, 20 ng of FLAG-TRα1 plasmid was co-transfected with 120 ng TRE-tkLuc reporter construct for transcriptional activity assays. For protein-protein interaction (mammalian two-hybrid) assays, 20 ng of TRα1 fused to the transcriptional activator VP16 (VP16-TRα1) plasmid was co-transfected with 20 ng of NCoR1 or SRC1 fused to the DNA binding domain of Gal4 (GAL4-NCoR1 or GAL4-SRC1) and 120 ng of UAS-tkLuc. In both assays, 20 ng pMaxGFP plasmid was co-transfected to monitor the transfection efficiency. All of the transfection processes were performed in TH-depleted medium (DMEM/F12 supplemented with 9% charcoal-stripped FBS) using Xtreme Gene 9 transfection reagent (Roche Diagnostics, Almere, NL). After 24-hour transfection, cells were stimulated for 24 hours with 0-10,000 nM T3 in DMEM/F12 supplemented with 0.1% bovine serum albumin (BSA).

Immunoblotting

The expression of FLAG- and VP16-TRα1 proteins in cells was verified by immunoblotting nuclear extracts of JEG-3 cells transfected with WT or mutant TR expression constructs as previously described (19,26). The receptors were probed with 1:1000 dilution of FLAG-M2 antibody (#F1804 Sigma-Aldrich) or 1:1000 dilution of VP16 antibody (sc-7545, Santa Cruz Biotechnology). Histone 3 protein was detected with 1:1000 dilution of Histone 3 (H3; 1B1B2) antibody (#14269 Cell Signaling Technology) to verify comparable protein input. Bands were visualized on the Alliance 4.0 Uvitec platform (Uvitec Ltd) by Enhanced Chemiluminescence (Thermofisher Scientific).

Electrophoretic mobility shift assays (EMSA)

A double-stranded overlapping oligonucleotide probe containing DR4-TRE was obtained by annealing 25 ng of sense and antisense oligonucleotides 5'end labeling with fluorescence dye (5'IRDye®700) (Integrated DNA Technologies, Leuven, Belgium) at 80°C for 5 minutes (sense oligonucleotides: 5'-AGGACGTTGGGGTTAGGGGAGGACAGTGGAC-3', antisense oligonucleotides: 5'-GTCCACTGTCCTCCCCTAACCCCAACGTCCT-3'). The DR4-TRE probe was diluted to a final concentration of 1 ng/µL in 50 µL 1xTE buffer (10mM Tris HCl pH 8.0, 1 mM EDTA). FLAG-TRα1 and RXRα proteins were synthesized by the TnT® T7 Quick Coupled Transcription/Translation System (L1170, Promega, Leiden, The Netherlands). Since equal amounts of *in vitro* translated receptors were detected on an immunoblot (data not shown), we decided to use 1 µL of *in vitro* translated WT or mutant FLAG-TRα1 and 2 µL of *in vitro* translated RXRα. TR and RXRα were co-incubated in the dark with 0.5 µL of DR4-TRE probe, and 2 µg of poly(deoxyinosinic-deoxycytidylic) acid sodium salt (SC-286691, Santa Cruz Biotechnology) in a final 10 µL of binding buffer (10x binding buffer: 100mM Tris, 10 mM EDTA, 1M KCl, 1 mM DDT, 50% glycerol, 0.1 mg/mL BSA) for 30 minutes at room temperature. Gel electrophoresis was performed on 6%DNA retardation gel (EC6365BOX, Invitrogen). The TR-DNA complexes and residual unbound probe were visualized using an Odyssey® imaging system (LI-COR, Leusden, The Netherlands).

Luciferase assays

Luciferase activity was determined using the Dual Glo Luciferase kit (E2940, Promega, Leiden, The Netherlands). Luciferase and GFP activities were measured by a luminometer (Victor™ X4, PerkinElmer, Groningen, The Netherlands). Half-maximal effective T3 concentration (EC_{50}), half-maximal inhibitory T3 concentration (IC_{50}), and %WT maximal response were analyzed using GraphPad Prism 5.0 (GraphPad, La Jolla, CA)

Statistical analysis

The statistical differences between WT and mutants were analyzed by One sample T-tests. The statistical differences of fold changes of logKd, logEC_{50}, and logIC_{50} between WT and mutants were determined by one-way ANOVA with Tukey's post-test. Statistical significance was considered at p-values < 0.05.

Results

Selection of mutants

We tested seven TRα1 mutants, of which four were derived from RTHα patients (D211G (19), M256T (20), A263S, and R384H (14)). These mutations covered the three CpG-rich regions of the LBD of TRα1 that are equivalent to the mutation-prone hotspots of the TRβ1 receptor, namely R384H in cluster 1, M256T and A263S in cluster 2, and D211G in cluster 3. The other three mutations were derived from RTHβ patients. TRα1-P398H (cluster 1), the equivalent of TRβ1-P452H, gave rise to an unusual phenotype that included obesity and marked metabolic disturbances in a murine model for RTHα (31). TRα1-T223A (cluster 3) is the equivalent of TRβ1-T277A, which was previously shown to specifically impair transcriptional activity on an ER6-TRE and diminish affinity for SRC-1 (24). Finally, TRα1-L287V (cluster 2) is the equivalent of TRβ1-L341V, a recently identified mutation that causes a strong decrease in T3-binding affinity and a concomitant reduction in the T3-sensitivity of transcriptional activity and cofactor recruitment (26).

T3 binding affinity of the TRα1 mutants

We first determined the binding affinity of *in vitro* translated mutant receptors using a [^{125}I]T3 competitive binding assay. The [^{125}I]T3 binding curves were shifted to the right for most mutants (Figure 1A), which reflects a higher required dose of T3 to saturate binding and hence a lower binding affinity. The dissociation constant (Kd) which is the concentration of T3 at which half the binding sites are occupied, varied between mutants (Figure 1B and Supplementary Table S2). TRα1-M256T showed the lowest affinity, as is illustrated by the highest Kd of all mutants (160-fold higher than WT). Binding of T3 was similarly affected for

TRα1-D211G (Kd 25-fold higher than WT), -R384H (25-fold), -L287V (19-fold), and -P398H (17-fold), but significantly less impaired for TRα1-A263S (Kd 5-fold higher than WT) whereas the Kd of TRα1-T223A was not different from WT. These data indicate that the binding affinity is reduced to a different extent for the different mutants.

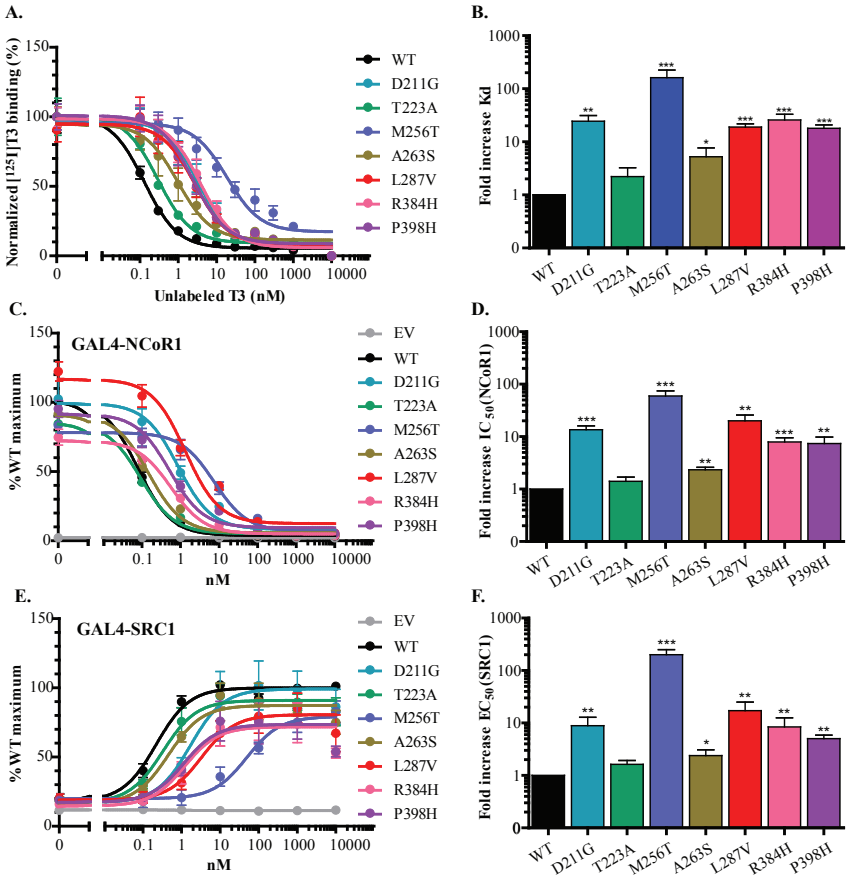

Figure 1. (A-B) [^{125}I]T3 competitive binding assays of the TRα1 WT and mutants. (A) The dissociation curves of all mutants are shifted to the right, indicative of a reduced T3 binding affinity. (B) The fold increase of the Kd are various between mutants (One-sample T-test, *P<0.05, **P<0.01, ***P<0.001). Data presented as mean ± SEM from four independent experiments performed in duplicate. (C-F) Mammalian two-hybrid assays demonstrating TRα1-cofactor interactions. (C) T3-induced GAL4-NCoR1 dissociation and (E) GAL4-SRC1 association curves show a various degree of reduced T3-dependent NCoR1 release and SRC1 recruitment of mutants, respectively. These are indicated by the right shift of the curves and higher IC_{50}-NCoR1 or EC_{50}-SRC1 than that of WT. (D) The fold increases in IC_{50} for the NCoR1 dissociation are similar to (E) the fold increase in EC_{50} for the SRC1 association for each mutation (the fold increases IC_{50}-NCoR1 and EC_{50}-SRC1 of the mutants were compared to WT by One-sample T-test; *P<0.05, **P<0.01, ***P<0.001). Data presented as mean ± SEM from at least four independent experiments performed in triplicate.

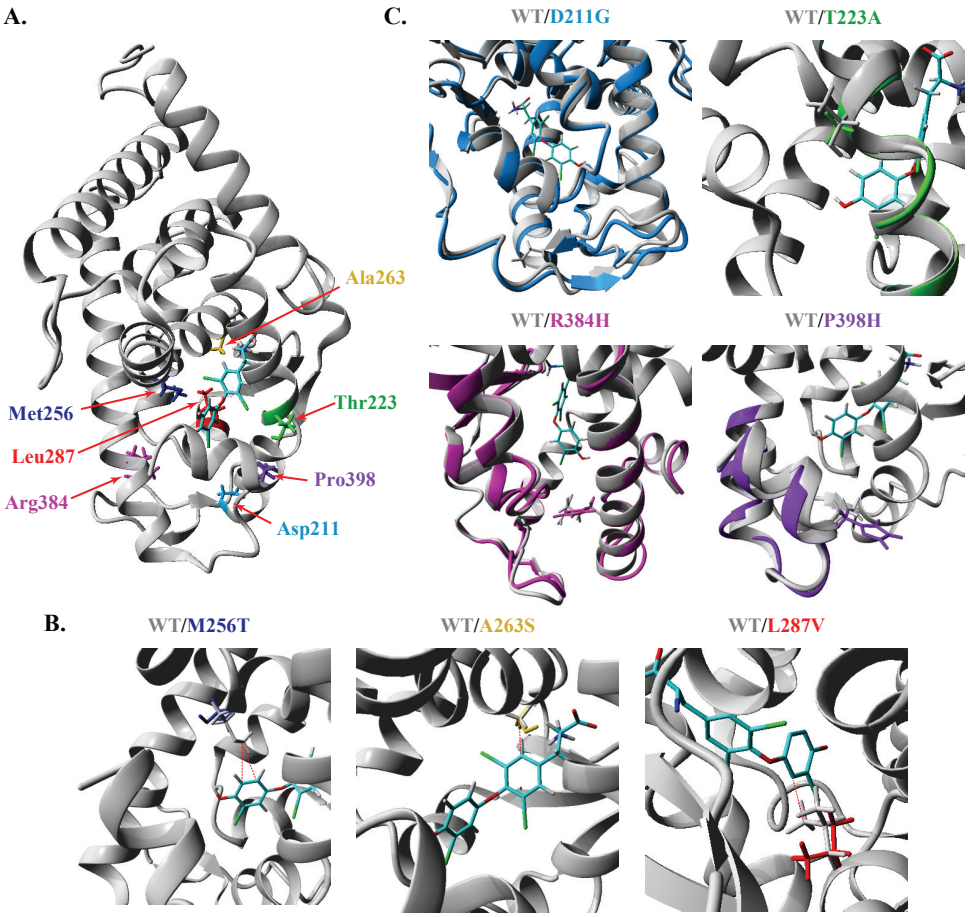

Figure 2. (A) The WT TRα1 crystal structure in complex with T3 (PDB ID: 2H77) in which the locations of the mutated residues studied are highlighted. (B) Close-up view of the TRα1 ligand-binding pocket, presented as an overlay of the WT crystal (grey) and indicated mutant models (colored). The side-chains of the mutant residues are displayed in blue (M256T, left panel), orange (A263S, middle panel), and red (L287V, right panel) and of the corresponding WT residues in grey. Hydrophobic interactions between WT residues and T3 are indicated with a red dashed line. The interaction between mutant residues and T3 are not observed. For clarity, the small deviations in the carbon-backbone structure are not displayed. (C) Close-up view of the overlay of the WT TRα1 structure and models with indicated mutations that affect residues outside the ligand-binding pocket. Mutant models are displayed in blue (D211G, left upper panel), green (T223A, right upper panel), pink (R384H, left lower panel), and purple (P398H, right lower panel), and WT TRα1 in grey. The T3 ligand is displayed in all panels in element color. All figures were created in YASARA Structure using PovRay imaging software.

In silico model of mutant TRα1

Structural modeling was used to validate our *in vitro* studies. The side-chains of Ala263, Met256, and Leu287 face to the ligand-binding pocket (Figure 2A and 2B) and are predicted to make direct interactions with T3 (Supplementary Figure S1). The hydrophobic interaction between the side-chain of Ala263 and the inner ring of T3 is lost in the A263S mutant. As previously reported (20), the M256T abrogates the direct interactions of Met256 with T3 and simultaneously disturbs the structural niche accommodating the outer ring of T3. In analogy to the predicted *in silico* effects of the L341V mutant in TRβ1 (26), the L287V mutant disrupts the direct hydrophobic interaction of Leu287 with T3. In agreement with our *in vitro* studies, all three mutations reduced the calculated T3-binding energy compared to WT TRα1 in the order M256T>L287V>A263S (Supplementary Figure 1D). Due to their location outside the binding pocket, the side-chains of Asp211, Arg384, Pro398 (facing other internal domains), and Thr223 (facing the external protein surface), do not make direct contact with T3 (Figure 2A and 2C), which prevents reliable *in silico* prediction of their impact on binding affinity. Structural modeling revealed extensive structural changes for the D211G (predominantly within the loop connecting H2 and H3), R384H and P398H (predominantly H11 and H12) mutants, whereas the T223A mutant displayed only minor local structural changes of the backbone configuration (Figure 2C). These observations may well explain the differential effects of these mutations on *in vitro* binding affinity.

Heterodimerization of TRα1 mutants with RXRα

To determine whether the dimerization of the mutants with RXR and binding of the dimer to DNA was affected, we performed electrophoretic mobility shift assays (EMSAs) with *in vitro* translated WT or mutant TRα1 and RXRα on a fluorescently labeled DR4-TRE (Supplementary Figure S2). The result showed that only a co-incubation of TRα1 and RXRα could shift the DR4-TRE oligonucleotide probe upward. The upward shift of the probe was not observed in an incubation of WT TRα1 or RXRα alone. These findings indicate that the WT receptors exclusively bound to the DR4-TRE as heterodimers with RXRα, which is in contrast to the TRβ1 isoform that can bind as both homo- and heterodimers (32,33). The intensity of the heterodimer band was similar to WT for all mutants. In addition, heterodimer binding to the DR4-TRE was independent of the presence of T3 for WT and mutants. These results show that heterodimerization with RXRα and binding to the DR4-TRE is not affected in any of the mutants.

Receptor-cofactor interaction of the TRα1 mutants

To determine whether cofactor recruitment of the mutants was impaired, we next evaluated the interaction of the mutants with the corepressor NCoR1 and the coactivator SRC1, which directly bind to TRs and play a crucial role in receptor function (1,7). In a mammalian two-hybrid assay, VP16-TRα1 activates a luciferase reporter (UAS-tkLuc) only when it interacts with GAL4-NCoR1 or -SRC1. As a measure for T3-dependence, we

determined the concentration that gave half-maximum dissociation of NCoR1 (IC_{50}) and half-maximum association of SRC1 (EC_{50}). Stimulation of WT TRα1 with low concentrations of T3 (0.1-1 nM) already resulted in dissociation of GAL4-NCoR1 (IC_{50} 0.08 nM) and association of GAL4-SRC1 (EC_{50} 0.28 nM). Most mutants required higher T3 concentrations to dissociate from NCoR1 (Figure 1C) and recruit SRC1 (Figure 1E). Consistent with the affinity for T3, TRα1-M256T showed the highest IC_{50} for NCoR1 dissociation (60-fold higher than WT) and EC_{50} for SRC1 association (200-fold) (Figure 1D, 1F, Supplementary Figure S3, and Supplementary Table S3). The TRα1-D211G, L287V, R384H, and P398H mutants showed higher IC_{50}-NCoR1 dissociation and EC_{50}-SRC1 association than WT but lower than TRα1-M256T. The fold increase IC_{50} and EC_{50} of these four mutations were similar. The IC_{50}-NCoR1 dissociation and EC_{50}-SRC1 association of A263S-TRα1 mutation were approximately two-fold higher than WT, corresponding to the changes of its Kd in competitive binding assays. For TRα1-T223A, the T3-induced NCoR1 dissociation and SRC1 association were similar to the WT receptor. We did not observe major differences in maximal binding of either NCoR1 or SRC1 to mutants compared to WT, indicating that the affinity of the mutants for these cofactors is not markedly disturbed.

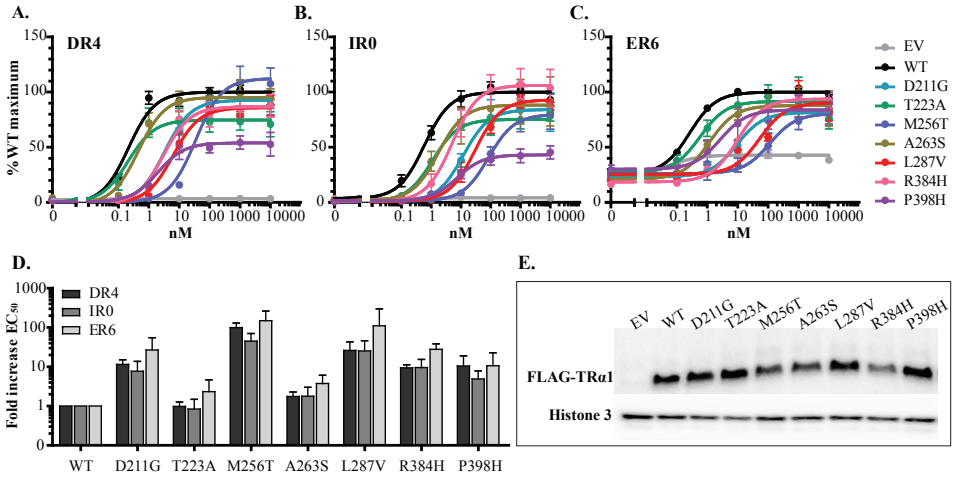

Figure 3. The T3-induced transcriptional activity of TRα1 WT and mutants tested on three different TRE-luciferase reporter constructs. (A-C) The dose-response curves show a various degree of impaired transcriptional activity of mutants, as indicated by the right shift of the curves and higher EC_{50} than WT. (D) The fold increases of mutants' EC_{50} are various between mutations. The shift of EC_{50} on three TREs generally follows a similar trend for each mutation. Data presented as mean ± SEM from at least three independent experiments performed in triplicate. (E) Immunoblot confirms the expression of WT and mutant FLAG-TRα1 in JEG-3 cells.

Transcriptional activity of the TRα1 mutants

We then tested the mutants for transcriptional activity using a reporter assay. For this, we co-transfected WT or mutant receptors into JEG-3 cells with constructs in which the coding sequence for firefly luciferase is under control of a DR4, IR0 or ER6-TRE.

The T3-induced transcriptional activity on the DR4-TRE was impaired for most mutant receptors, as indicated by a rightward shift of the dose-response curves as compared to WT and a concomitant increase in EC_{50}, representing the T3 dose that is needed to achieve a half-maximal response. (Figure 3A and Supplementary Table S4). TRα1-M256T had the highest EC_{50} (100-fold higher than WT). The EC_{50} of TRα1-D211G, L287V, R384H, and P398H was approximately 10 to 20-fold higher than that of WT. In contrast, the EC_{50} of TRα1-A263S and T223A was not significantly different from WT. The fold increase in EC_{50} tested on the IR0- and ER6-TREs of each mutant was not significantly different from that tested on the DR4-TRE (Figure 3B-D), suggesting that the effects of these mutations are not TRE-specific. Most of the mutants showed a similar maximal transcriptional activity as WT at supraphysiological T3 concentrations, with the exception of TRα1-T223A on DR4-TRE and TRα1-P398H on DR4- and IR0-TRE that were significantly lower than that of WT.

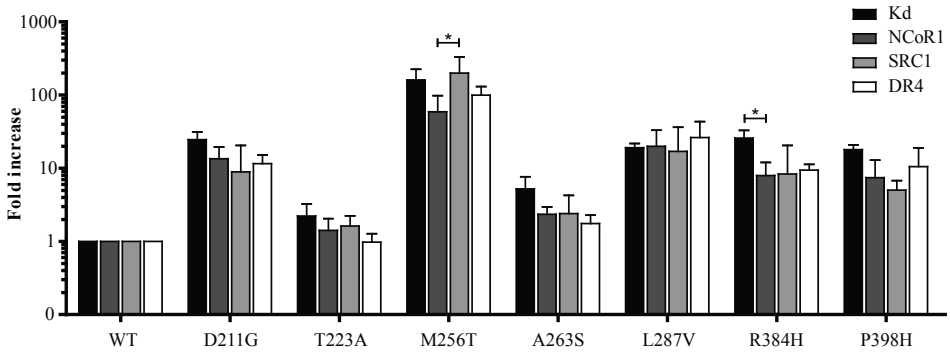

Figure 4. Fold increases of Kd, IC_{50}-NCoR1 dissociation, EC_{50}-SRC1 association and EC_{50} of T3-induced transcriptional activity on the DR4-TRE. These fold increases are various among mutants but generally follow a similar trend for each mutant, except for M256T and R384H (One-way ANOVA with Tukey's post-test *P<0.05).

Correlation between T3-affinity, cofactor binding, and transcriptional activity of TRα1 mutants

Finally, in order to determine whether certain aspects of receptor regulation were proportionally stronger affected than that would be expected from the effect of the mutation on T3-binding, we correlated the fold increase of parameters for binding affinity, and T3-dependent activity and cofactor recruitment (Figure 4). The fold increases in IC_{50}-NCoR1,

EC_{50}-SRC1, and EC_{50} on DR4-TRE generally followed the same trend as the fold increase in Kd of each mutant with two exceptions. First, the fold increase in EC_{50}-SRC1 of TRα1-M256T was slightly but significantly higher than its IC_{50}-NCoR1, which would suggest a marginally stronger effect of the mutation on T3-dependent SRC1 recruitment than NCoR1 release. Second, the fold increase in Kd of TRα1-R384H was slightly higher than its IC_{50}-NCoR1. In both cases, however, this did not result in a significant effect on the EC_{50}-DR4 TRE, indicating that these differences do not majorly contribute to the degree of functional impairment.

Discussion

In the current study, we report *in vitro* functional studies of seven TRα1 missense mutations. The main purpose was to investigate if other factors, beyond disturbed T3 binding, contribute to the functional impairment of TRα1 mutations. According to our results, the reduced affinity for T3 is the main factor that determines both the severity of impaired transcriptional activity as well as impaired TR-cofactor interaction of the mutants. In our series, we did not find evidence for mutation-specific effects on different TREs or coregulatory protein binding.

Our selection of mutants covered the equivalents of the three mutation-prone hotspots in TRβ1. We evaluated the effect of the mutations on the transcriptional activity by overexpressing WT or mutant receptors with a reporter gene under control of TREs. Since some TRβ1 mutants display TRE selective defects, we included all three reported half-site configurations (DR4, IR0, and ER6). As expected, the mutants had an impaired T3-dependent transcriptional activity, as illustrated by their dose-response curves with a clear shift to the right side of the WT curve and corresponding higher EC_{50} than WT. The degree of impaired transcriptional activity varied among the mutants and correlated with the reduced T3-binding energy of the mutants predicted by the *in silico* modeling and the reduction in T3-affinity from the *in vitro* binding assays. This finding is in line with previous reports of the other mutants derived from RTHα patients (8,12,15,25). In addition, the degree of impaired transcriptional activity seemed to be related to the severity of the phenotype of the RTHα patients, especially the delayed motor development which is much more prominent in the patients carrying TRα1-D211G and -R384H mutations than in the patient carrying a TRα1-A263S mutation. This is in agreement with a previous report by Moran et al. that showed that the functional properties of two TRα1 mutations (A263V and L274P) correlate with the clinical features of the patients (18).

There was no TRE-selective reduction in T3-dependent receptor activity since the fold increase in EC_{50} on all three TREs was similar for each mutant. Of note, the T223A-TRα1 mutant did not show any differential effect on different TREs, which is in contrast with its equivalent TRβ1-T277A, which is selectively affected on an ER6-TRE (24). However, the maximal response of T223A and P398H were lower than that of WT on the DR4- and

IR0-TRE. This TRE-specific submaximal response has been previously reported in TRβ1-T277A (24); however, in these studies the submaximal response was found on the DR4- and ER6-TRE. The TRE-specific transcriptional impairment may be caused by different patterns of dimer formation and cofactor recruitment among TREs (34,35). Nevertheless, since numerous chromatin occupation studies have suggested that the DR4-TRE is the most important TRE playing a role in the *in vivo* TR transcription (3-6), the pattern of TR-regulating gene transcription is more likely to follow the *in vitro* result of DR4-TRE rather than IR0- and ER6-TRE. Therefore, selective transcriptional impairment of the mutants on IR0- and ER6-TRE found *in vitro* may not have a large contribution in the severity of phenotypes in RTH patients.

It has been shown that submaximal response of mutant receptors can be caused by impaired TR-cofactor interactions. For instance, the reduced maximal response of TRβ1-T277A was due to a reduced affinity for SRC1, which could be rescued by overexpression of SRC1 (24). Mutations at the residues adjacent to the Pro452 of the TRβ1 (homologous to Pro398 of TRα1), Pro453 and Leu454, were also unable to reach WT maximal response and have been shown to have a defective TR-cofactor interaction that consequently affects transcriptional activity to a greater extent than what would be expected based on their reduced affinity for T3 (25,36,37). We, therefore, evaluated the interaction of selected TRα1 mutants with the NCoR1 corepressor and the SRC1 coactivator. Except for T223A, the mutants required higher T3 levels than WT to dissociate from NCoR1 and to associate with SRC1, illustrating the impaired T3-dependent TR-cofactor interaction of these mutants. However, the degree of impaired TR-cofactor interaction was similar to the reduced affinity for T3 for all selected mutants. In addition, the maximum binding of TRα1-T223A and -P398H was similar to WT. These findings suggest that these mutations alter the T3-dependent TRα1-cofactor recruitment via their reduced T3 affinity, but that the submaximal response is likely explained by another mechanism such as impaired interaction of the mutants with other nuclear cofactors. For this reason, we also studied the heterodimerization property of the selected TRα1 mutants and found that none of them disturbed heterodimer formation on the DR4-TRE, suggesting that the submaximal response of these mutant receptors is not explained by altered heterodimerization with RXR.

To our knowledge, our study reports the *in vitro* functional impairment at different levels of the largest series of TRα1 mutants to date, including four mutations derived from RTHα patients which cover all three CpG-rich clusters of TRα1 that correspond with the mutation-prone hotspots of TRβ1. However, the transcriptional activation of mutants in this study was only tested on the most abundant TRE configuration, DR4 (3-6), and the other two well-known TRE configurations, IR0 and ER6, which do not cover all natural TREs. Therefore, the results should be interpreted and applied cautiously. Our study also did not explore some issues that might complicate the phenotype of RTH patients, for instance, the negative transcriptional gene regulation by TRs and the effect of mutant TRs on WT receptor function, as known as a dominant-negative effect. In addition, our experiments were performed exclusively *in*

vitro and mainly by the overexpressing system in the JEG-3 cells which might not be entirely comparable to the *in vivo* situation. Although JEG-3 cells comprise a well-established model to study the impact of TRs mutations, the results of which correlating with the severity of the clinical phenotype, it may not represent the situation in other cell types or tissues. Therefore, studies in different TR-overexpressing cell lines, or in models that rely on endogenously expressed mutant TRs (such as CRISPR-Cas9 genome editing or primary cells derived from patients) may substantiate our findings.

RTHα patients are currently treated with levothyroxine (LT4) to normalize FT4 levels and reduce the hypothyroid state of tissues that predominantly express TRα1, which in some cases has been shown to ameliorate the developmental delay and chronic symptoms (15,18,19), however, the working mechanism is yet unclear. Since FT4 and T3 levels are only marginally increased, it seems unlikely that this treatment results in a significant occupation of receptors that have 10 to 100-fold reduction in ligand affinity, but rather increases the number of activated WT receptors. Given that the functional defects of TRα1 missense mutants are driven by their reduced ligand-affinity, agonists that provide a better fit to the altered ligand-binding pockets could, therefore, be a tailor-made treatment. Although such agonists are currently lacking, the finding that some TRβ1 mutants are more efficiently dissociated from NCoR1 by the natural T3 analogue triiodoacetic acid (TRIAC), which is sometimes used to suppress FT4 levels in RTHβ patients, and the TR antagonist NH-3 (38), shows that such an approach may be viable.

In summary, this study demonstrates that the severity of impaired transcriptional activity of mutant TRα1 receptors is mainly determined by the reduced affinity for T3. These mutations also alter TR-cofactor interactions to the same magnitude as the T3 binding defect. However, further studies are required to extensively evaluate the *in vivo* consequences of the TRα1 mutations.

Acknowledgements

We would like to thank Prof. V. Krishna Chatterjee (Wellcome-MRC Institute of Metabolic Science, University of Cambridge, United Kingdom) for kindly providing some of the plasmids used in this study. This work is supported by Zon-MWTOP Grant 91212044 and an Erasmus MC Medical Research Advisory Committee (MRACE) grant (RPP, MEM), and Chiang Mai University (KW).

Author Disclosure Statement

The authors have nothing to disclose.

References

1. Cheng SY, Leonard JL, Davis PJ. Molecular aspects of thyroid hormone actions. *Endocr Rev.* 2010;**31**(2):139-170.
2. Flamant F, Cheng SY, Hollenberg AN, Moeller LC, Samarut J, Wondisford FE, Yen PM, Refetoff S. Thyroid Hormone Signaling Pathways: Time for a More Precise Nomenclature. *Endocrinology.* 2017;**158**(7):2052-2057.
3. Chatonnet F, Guyot R, Benoit G, Flamant F. Genome-wide analysis of thyroid hormone receptors shared and specific functions in neural cells. *Proc Natl Acad Sci U S A.* 2013;**110**(8):E766-775.
4. Ayers S, Switnicki MP, Angajala A, Lammel J, Arumanayagam AS, Webb P. Genome-wide binding patterns of thyroid hormone receptor beta. *PLoS One.* 2014;**9**(2):e81186.
5. Grontved L, Waterfall JJ, Kim DW, Baek S, Sung MH, Zhao L, Park JW, Nielsen R, Walker RL, Zhu YJ, Meltzer PS, Hager GL, Cheng SY. Transcriptional activation by the thyroid hormone receptor through ligand-dependent receptor recruitment and chromatin remodelling. *Nat Commun.* 2015;**6**:7048.
6. Ramadoss P, Abraham BJ, Tsai L, Zhou Y, Costa-e-Sousa RH, Ye F, Bilban M, Zhao K, Hollenberg AN. Novel mechanism of positive versus negative regulation by thyroid hormone receptor beta1 (TRbeta1) identified by genome-wide profiling of binding sites in mouse liver. *J Biol Chem.* 2014;**289**(3):1313-1328.
7. Astapova I. Role of co-regulators in metabolic and transcriptional actions of thyroid hormone. *J Mol Endocrinol.* 2016;**56**(3):73-97.
8. Bochukova E, Schoenmakers N, Agostini M, Schoenmakers E, Rajanayagam O, Keogh JM, Henning E, Reinemund J, Gevers E, Sarri M, Downes K, Offiah A, Albanese A, Halsall D, Schwabe JW, Bain M, Lindley K, Muntoni F, Vargha-Khadem F, Dattani M, Farooqi IS, Gurnell M, Chatterjee K. A mutation in the thyroid hormone receptor alpha gene. *N Engl J Med.* 2012;**366**(3):243-249.
9. van Mullem A, van Heerebeek R, Chrysis D, Visser E, Medici M, Andrikoula M, Tsatsoulis A, Peeters R, Visser TJ. Clinical phenotype and mutant TRalpha1. *N Engl J Med.* 2012;**366**(15):1451-1453.
10. van Gucht ALM, Moran C, Meima ME, Visser WE, Chatterjee K, Visser TJ, Peeters RP. Resistance to Thyroid Hormone due to Heterozygous Mutations in Thyroid Hormone Receptor Alpha. *Curr Top Dev Biol.* 2017;**125**:337-355.
11. Moran C, Chatterjee K. Resistance to Thyroid Hormone alpha-Emerging Definition of a Disorder of Thyroid Hormone Action. *J Clin Endocrinol Metab.* 2016;**101**(7):2636-2639.
12. Moran C, Schoenmakers N, Agostini M, Schoenmakers E, Offiah A, Kydd A, Kahaly G, Mohr-Kahaly S, Rajanayagam O, Lyons G, Wareham N, Halsall D, Dattani M, Hughes S, Gurnell M, Park SM, Chatterjee K. An adult female with resistance to thyroid hormone mediated by defective thyroid hormone receptor alpha. *J Clin Endocrinol Metab.* 2013;**98**(11):4254-4261.
13. Tylki-Szymanska A, Acuna-Hidalgo R, Krajewska-Walasek M, Lecka-Ambroziak A, Steehouwer M, Gilissen C, Brunner HG, Jurecka A, Rozdzynska-Swiatkowska A, Hoischen A, Chrzanowska KH. Thyroid hormone resistance syndrome due to mutations in the thyroid hormone receptor alpha gene (THRA). *J Med Genet.* 2015;**52**(5):312-316.
14. Demir K, van Gucht AL, Buyukinan M, Catli G, Ayhan Y, Bas VN, Dundar B, Ozkan B, Meima ME, Visser WE, Peeters RP, Visser TJ. Diverse Genotypes and Phenotypes of Three Novel Thyroid Hormone Receptor-alpha Mutations. *J Clin Endocrinol Metab.* 2016;**101**(8):2945-2954.
15. Moran C, Agostini M, Visser WE, Schoenmakers E, Schoenmakers N, Offiah AC, Poole K, Rajanayagam O, Lyons G, Halsall D, Gurnell M, Chrysis D, Efthymiadou A, Buchanan C, Aylwin S, Chatterjee KK. Resistance to thyroid hormone caused by a mutation in thyroid hormone receptor (TR)alpha1 and TRalpha2: clinical, biochemical, and genetic analyses of three related patients. *Lancet Diabetes Endocrinol.* 2014;**2**(8):619-626.
16. Espiard S, Savagner F, Flamant F, Vlaeminck-Guillem V, Guyot R, Munier M, d'Herbomez M, Bourguet W, Pinto G, Rose C, Rodien P, Wemeau JL. A Novel Mutation in THRA Gene

Associated With an Atypical Phenotype of Resistance to Thyroid Hormone. *J Clin Endocrinol Metab.* 2015;**100**(8):2841-2848.

17. Kalikiri MK, Mamidala MP, Rao AN, Rajesh V. Analysis and functional characterization of sequence variations in ligand binding domain of thyroid hormone receptors in autism spectrum disorder (ASD) patients. *Autism Res.* 2017;**10**(12):1919-1928.
18. Moran C, Agostini M, McGowan A, Schoenmakers E, Fairall L, Lyons G, Rajanayagam O, Watson L, Offiah A, Barton J, Price S, Schwabe J, Chatterjee K. Contrasting Phenotypes in Resistance to Thyroid Hormone Alpha Correlate with Divergent Properties of Thyroid Hormone Receptor alpha1 Mutant Proteins. *Thyroid.* 2017;**27**(7):973-982.
19. van Gucht AL, Meima ME, Zwaveling-Soonawala N, Visser WE, Fliers E, Wennink JM, Henny C, Visser TJ, Peeters RP, van Trotsenburg AS. Resistance to Thyroid Hormone Alpha in an 18-Month-Old Girl: Clinical, Therapeutic, and Molecular Characteristics. *Thyroid.* 2016;**26**(3):338-346.
20. Wejaphikul K, Groeneweg S, Hilhorst-Hofstee Y, Chatterjee VK, Peeters RP, Meima ME, Visser WE. Insight into molecular determinants of T3 vs. T4 recognition from mutations in thyroid hormone receptor alpha and beta. *J Clin Endocrinol Metab.* 2019;**104**(8):3491-3500.
21. Clifton-Bligh RJ, de Zegher F, Wagner RL, Collingwood TN, Francois I, Van Helvoirt M, Fletterick RJ, Chatterjee VK. A novel TR beta mutation (R383H) in resistance to thyroid hormone syndrome predominantly impairs corepressor release and negative transcriptional regulation. *Mol Endocrinol.* 1998;**12**(5):609-621.
22. Safer JD, Cohen RN, Hollenberg AN, Wondisford FE. Defective release of corepressor by hinge mutants of the thyroid hormone receptor found in patients with resistance to thyroid hormone. *J Biol Chem.* 1998;**273**(46):30175-30182.
23. Huber BR, Desclozeaux M, West BL, Cunha-Lima ST, Nguyen HT, Baxter JD, Ingraham HA, Fletterick RJ. Thyroid hormone receptor-beta mutations conferring hormone resistance and reduced corepressor release exhibit decreased stability in the N-terminal ligand-binding domain. *Mol Endocrinol.* 2003;**17**(1):107-116.
24. Collingwood TN, Wagner R, Matthews CH, Clifton-Bligh RJ, Gurnell M, Rajanayagam O, Agostini M, Fletterick RJ, Beck-Peccoz P, Reinhardt W, Binder G, Ranke MB, Hermus A, Hesch RD, Lazarus J, Newrick P, Parfitt V, Raggatt P, de Zegher F, Chatterjee VK. A role for helix 3 of the TRbeta ligand-binding domain in coactivator recruitment identified by characterization of a third cluster of mutations in resistance to thyroid hormone. *EMBO J.* 1998;**17**(16):4760-4770.
25. Collingwood TN, Adams M, Tone Y, Chatterjee VK. Spectrum of transcriptional, dimerization, and dominant negative properties of twenty different mutant thyroid hormone beta-receptors in thyroid hormone resistance syndrome. *Mol Endocrinol.* 1994;**8**(9):1262-1277.
26. Wejaphikul K, Groeneweg S, Dejkhamron P, Unachak K, Visser WE, Chatterjee VK, Visser TJ, Meima ME, Peeters RP. Role of Leucine 341 in Thyroid Hormone Receptor Beta Revealed by a Novel Mutation Causing Thyroid Hormone Resistance. *Thyroid.* 2018;**28**(12):1723-1726.
27. Mol JA, Visser TJ. Synthesis and some properties of sulfate esters and sulfamates of iodothyronines. *Endocrinology.* 1985;**117**(1):1-7.
28. Nascimento AS, Dias SM, Nunes FM, Aparicio R, Ambrosio AL, Bleicher L, Figueira AC, Santos MA, de Oliveira Neto M, Fischer H, Togashi M, Craievich AF, Garratt RC, Baxter JD, Webb P, Polikarpov I. Structural rearrangements in the thyroid hormone receptor hinge domain and their putative role in the receptor function. *J Mol Biol.* 2006;**360**(3):586-598.
29. Krieger E, Vriend G. YASARA View - molecular graphics for all devices - from smartphones to workstations. *Bioinformatics.* 2014;**30**(20):2981-2982.
30. Krieger E, Koraimann G, Vriend G. Increasing the precision of comparative models with YASARA NOVA--a self-parameterizing force field. *Proteins.* 2002;**47**(3):393-402.
31. Liu YY, Schultz JJ, Brent GA. A thyroid hormone receptor alpha gene mutation (P398H) is associated with visceral adiposity and impaired catecholamine-stimulated lipolysis in mice. *J Biol Chem.* 2003;**278**(40):38913-38920.
32. Kitajima K, Nagaya T, Jameson JL. Dominant negative and DNA-binding properties of mutant

thyroid hormone receptors that are defective in homodimerization but not heterodimerization. *Thyroid.* 1995;**5**(5):343-353.

33. Yen PM, Wilcox EC, Hayashi Y, Refetoff S, Chin WW. Studies on the repression of basal transcription (silencing) by artificial and natural human thyroid hormone receptor-beta mutants. *Endocrinology.* 1995;**136**(7):2845-2851.
34. Paquette MA, Atlas E, Wade MG, Yauk CL. Thyroid hormone response element half-site organization and its effect on thyroid hormone mediated transcription. *PLoS One.* 2014;**9**(6):e101155.
35. Chen Y, Young MA. Structure of a thyroid hormone receptor DNA-binding domain homodimer bound to an inverted palindrome DNA response element. *Mol Endocrinol.* 2010;**24**(8):1650-1664.
36. Collingwood TN, Rajanayagam O, Adams M, Wagner R, Cavailles V, Kalkhoven E, Matthews C, Nystrom E, Stenlof K, Lindstedt G, Tisell L, Fletterick RJ, Parker MG, Chatterjee VK. A natural transactivation mutation in the thyroid hormone beta receptor: impaired interaction with putative transcriptional mediators. *Proc Natl Acad Sci U S A.* 1997;**94**(1):248-253.
37. Yoh SM, Chatterjee VK, Privalsky ML. Thyroid hormone resistance syndrome manifests as an aberrant interaction between mutant T3 receptors and transcriptional corepressors. *Mol Endocrinol.* 1997;**11**(4):470-480.
38. Harrus D, Demene H, Vasquez E, Boulahtouf A, Germain P, Figueira AC, Privalsky ML, Bourguet W, le Maire A. Pathological Interactions Between Mutant Thyroid Hormone Receptors and Corepressors and Their Modulation by a Thyroid Hormone Analogue with Therapeutic Potential. *Thyroid.* 2018;**28**(12):1708-1722.

Supplementary Materials

Supplementary Table S1. Primer used for TRα1 mutagenesis.

Mutations	Bases change	Primers (5'-3')
D211G	GAC>GGC	Forward: TGAAGGCTTCCAGGCCCACCTTGTCTCCG Reverse: CGGAGACAAGGTGGGCCTGGAAGCCTTCA
T233A	ACC>GCC	Forward: CGAGTTTACCAAGATCATCGCCCCGGCCATCAC Reverse: GTGATGGCCGGGGCGATGATCTTGGTAAACTCG
M256T	ATG>ACG	Forward: CTGAAGGGGTGCTGCACGGAGATCATGTCCC Reverse: GGGACATGATCTCCGTGCAGCACCCCTTCAG
A263S	GCG>TCG	Forward: GCGGACAGCCGACCGCAGGGACA Reverse: TGTCCCTGCGGTCGGCTGTCCGC
L287V	CTC>GTC	Forward: CAAGCGGGAGCAGGTCAAGAATGGCGG Reverse: CCGCCATTCTTGACCTGCTCCCGCTTG
R384H	CGC>CAC	Forward: CATGTGGAGGAAGTGGCTGGCGTGGCA Reverse: TGCCACGCCAGCCACTTCCTCCACATG
P398H	CCC>CAC	Forward: CACCGAACTCTTCCACCCACTCTTCCTCG Reverse: CGAGGAAGAGTGGGTGGAAGAGTTCGGTG

Supplementary Table S2. Affinity for T3 of TRα1 WT and mutants from the [^{125}I]T3 competitive binding assay.

TRα1	LogKd [Kd (nM)]	LogKd(MT/WT) [Fold Kd]
WT	-0.87±0.10 [0.1]	-
D211G	0.52±0.15 [3.3]	1.39±0.11** [24.5]
T223A	-0.52±0.15 [0.3]	0.35±0.17 [2.2]
M256T	1.34±0.22 [21.9]	2.21±0.15*** [161]
A263S	-0.15±0.24 [0.7]	0.72±0.17* [5.2]
L287V	0.41±0.09 [2.6]	1.28±0.06*** [19.0]
R384H	0.55±0.16 [3.5]	1.41±0.11*** [25.8]
P398H	0.39±0.07 [2.4]	1.25±0.07*** [17.9]
P value$^{\phi}$		<0.001

Data are means ± SEM from four independent experiments (duplicate). *P<0.05, **P<0.01, ***P<0.001 compared with WT=0, One-sample T-test. $^{\phi}$P value of One-way ANOVA compared between mutants.

Supplementary Table S3. T3-dependence of GAL4-NCoR1 dissociation and GAL4-SRC1 association of TRα1 WT and mutants.

TRα1	NCoR1			SRC1		
	$LogIC_{50}$ [IC_{50} (nM)]	$LogIC_{50}$(MT/WT) [Fold IC_{50}]	Max response (%)	$LogEC_{50}$ [EC_{50} (nM)]	$LogEC_{50}$(MT/WT) [Fold EC_{50}]	Max response (%)
WT	-1.09±0.07 [0.1]	-	100	-0.55±0.08 [0.3]	-	100
D211G	-0.02±0.09 [1.0]	1.13±0.07*** [13.6]	98.6±23.9	0.38±0.15 [2.4]	0.95±0.16** [8.9]	103±16.0
T223A	-0.99±0.04 [0.1]	0.15±0.08 [1.4]	84.0±9.2	-0.32±0.11 [0.5]	0.21±0.07 [1.6]	92.2±7.3
M256T	0.78±0.08 [6.0]	1.77±0.10*** [59.5]	77.7±12.3†	1.69±0.08 [48.6]	2.30±0.10*** [200]	79.3±7.3†
A263S	-0.79±0.07 [0.2]	0.37±0.05** [2.3]	89.9±3.6†	-0.19±0.10 [0.7]	0.38±0.11* [2.4]	89.1±9.8
L287V	0.16±0.07 [1.5]	1.30±0.11** [20.1]	115±5.2	0.70±0.08 [5.1]	1.23±0.16** [17.2]	83.4±10.5
R384H	-0.26±0.06 [0.6]	0.90±0.08*** [7.9]	71.7±11.4††	0.36±0.18 [2.3]	0.92±0.18** [8.4]	76.7±14.0
P398H	-0.27±0.11 [0.5]	0.87±0.12** [7.4]	91.7±3.3	0.17±0.10 [1.5]	0.70±0.06** [5.1]	77.3±13.9
*P value*ϕ		<0.001	<0.01		<0.001	NS

Data are means ± SEM from at least four independent experiments (triplicate). *P<0.05, **P<0.01, ***P<0.001 compared with WT=0, and †P<0.05, ††P<0.01, †††P<0.01 compared with WT=100, One-sample T-test. ϕP value of One-way ANOVA compared between mutants (NS=not significant).

Supplementary Table S4. Transcriptional activity of TRα1 WT and mutants tested on three TREs.

TRα1	TREs								
	DR4			IR0			ER6		
	$LogEC_{50}$ [EC_{50} (nM)]	$LogEC_{50}$(MT/WT) [Fold EC_{50}]	Max response (%)	$LogEC_{50}$ [EC_{50} (nM)]	$LogEC_{50}$(MT/WT) [Fold EC_{50}]	Max response (%)	$LogEC_{50}$ [EC_{50} (nM)]	$LogEC_{50}$(MT/WT) [Fold EC_{50}]	Max response (%)
WT	-0.46±0.09 [0.4]	-	100	-0.02±0.16 [1.0]	-	100	-0.40±0.07 [0.4]	-	100
D211G	0.63±0.11 [4.2]	1.06±0.12*** [11.5]	95.3±13.6	1.07±0.13 [11.7]	0.89±0.25* [7.7]	79.6±11.8	1.02±0.16 [10.5]	1.43±0.31* [26.8]	84.5±9.2
T223A	-0.52±0.15 [0.3]	-0.01±0.11 [1.0]	77.6±7.0†	0.10±0.07 [1.3]	-0.07±0.24 [0.8]	73.5±8.7	-0.05±0.17 [0.9]	0.37±0.30 [2.3]	92.6±10.8
M256T	1.57±0.04 [37.5]	2.00±0.12*** [99.7]	108±10.5	1.90±0.16 [78.5]	1.65±0.20* [45.0]	76.9±8.7	1.94±0.26 [87.2]	2.18±0.24* [150]	83.4±9.4
A263S	-0.19±0.06 [0.7]	0.24±0.11 [1.8]	98.2±10.2	0.43±0.16 [2.7]	0.25±0.23 [1.8]	84.9±14.2	0.17±0.08 [1.5]	0.58±0.21 [3.8]	87.4±11.3
L287V	0.91±0.15 [8.1]	1.42±0.22** [26.2]	91.8±9.0	1.58±0.09 [38.3]	1.41±0.26* [25.4]	93.3±6.0	1.64±0.30 [43.7]	2.05±0.43* [111]	94.9±10.6
R384H	0.55±0.09 [3.6]	0.97±0.08** [9.4]	86.3±11.0	0.78±0.07 [6.0]	0.98±0.20* [9.6]	110±13.4	1.04±0.06 [10.9]	1.45±0.14** [28.0]	93.6±2.0†
P398H	0.51±0.16 [3.3]	1.02±0.25* [10.5]	59.2±9.8†	0.87±0.10 [7.4]	0.69±0.20* [4.9]	41.8±6.1†	0.62±0.20 [4.2]	1.03±0.32 [10.7]	83.8±10.2
*P value*ϕ		<0.001	NS		<0.001	<0.01		<0.01	NS

Data are means ± SEM from at least three independent experiments (triplicate). *P<0.05, **P<0.01, ***P<0.001 compared with WT=0, and †P<0.05, ††P<0.01, †††P<0.01 compared with WT=100, One-sample T-test. ϕP value of One-way ANOVA compared between mutants (NS=not significant).

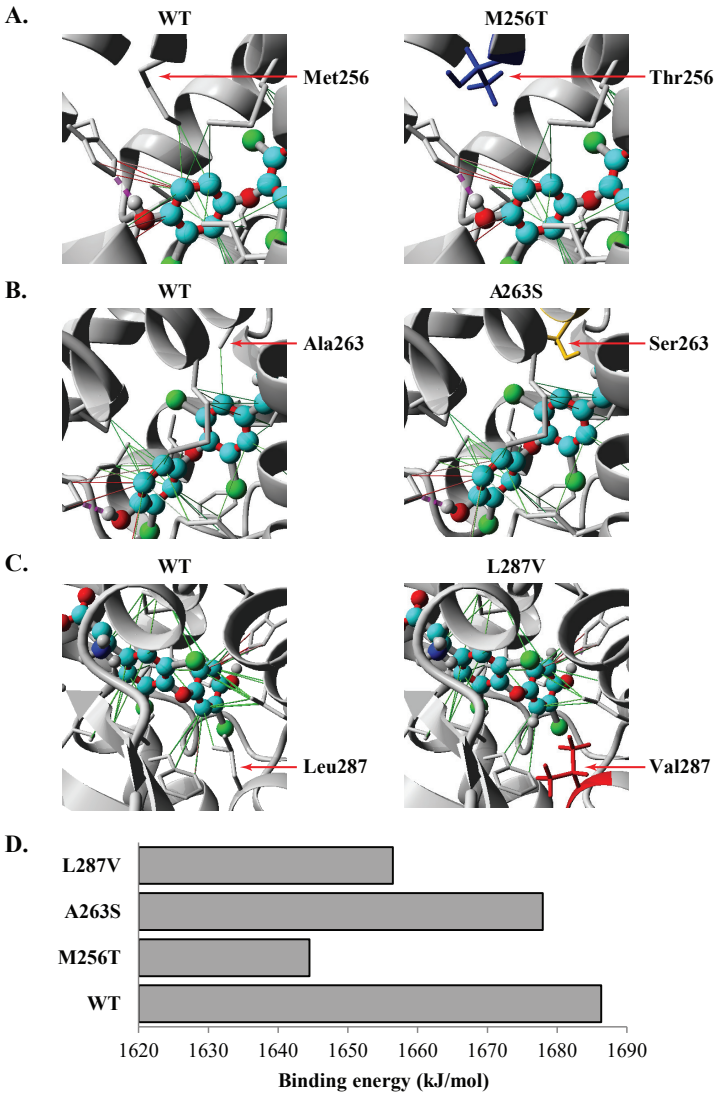

Supplementary Figure S1. (A-C) Close-up views of the wild-type (WT) TRα1 structure (left) and indicated mutant (right) structural models in which the side-chains of all ligand-interacting residues are displayed. The side-chains of the affected residues are indicated with an arrow. WT residues are shown in grey, and mutant residues are highlighted in color. H-bonds are indicated with a purple dashed line, pi-pi interactions with a solid pink line, and hydrophobic interactions with a solid green line. The T3 ligand is displayed in ball-stick style in element colors. All figures were created in YASARA Structure using PovRay imaging software. (D) The bar chart shows reduced T3-binding energy of the mutants predicted by the *in silico* modeling.

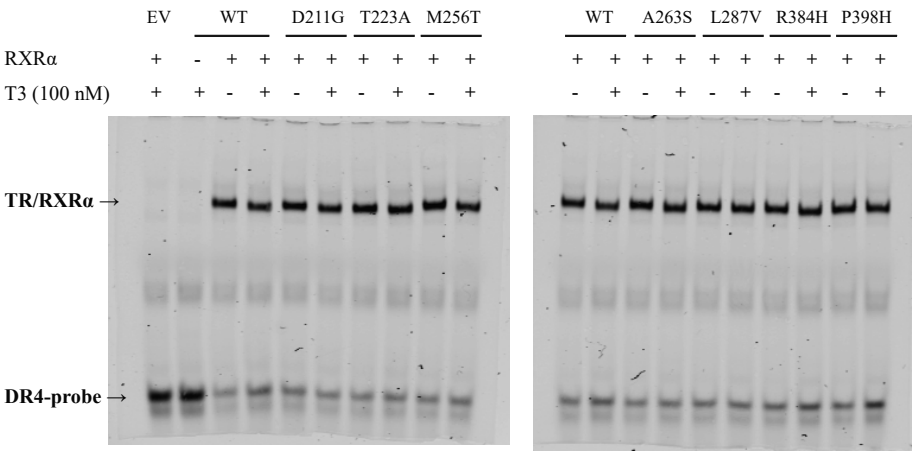

Supplementary Figure S2. Electrophoretic mobility shift assay (EMSA) showing the TR/RXRα heterodimer complex on the DR4-TRE. The heterodimer formation of all mutants is similar to WT and independent of T3 stimulation.

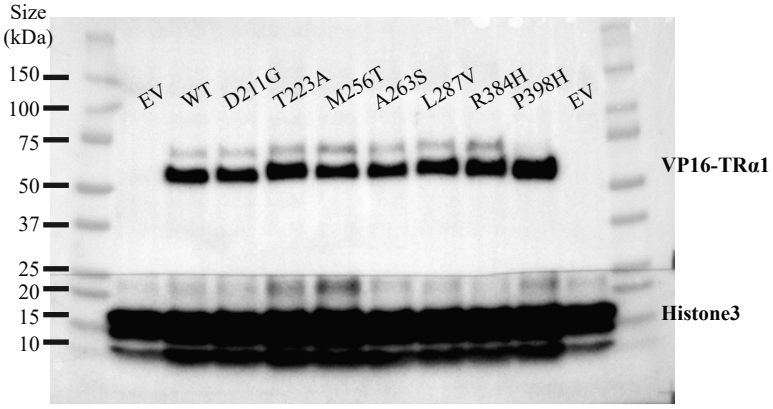

Supplementary Figure S3. Immunoblot confirms the expression of VP16-TRα1 WT and mutants in JEG-3 cells.

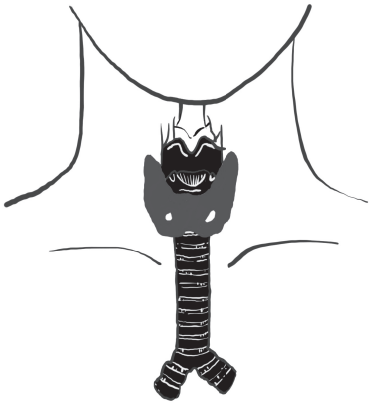

CHAPTER 5

The Effect of Thyroid Hormone Receptor Truncating Mutants on Gene Transcription in Neuronal Cells

Karn Wejaphikul, W. Edward Visser, Selmar Leeuwenburgh, Wilfred F.J. van IJcken, Robin P. Peeters, Marcel E. Meima

Manuscript in preparation

5

Abstract

Thyroid hormone receptor (TR) α1 is the predominant TR isoform in the brain and plays a vital role in neurodevelopment. Mutations in TRα1 that reduce or abolish T3 binding to the receptor are the cause of the syndrome of resistance to thyroid hormone alpha (RTHα), which is characterized among others by motor and cognitive impairment in RTHα patients. Although a genotype-phenotype relation has been reported, it is clear that the severity of the neurological phenotype does not always correlate with the degree of T3 binding impairment of mutant receptors. However, the mechanism underlying this phenotypic difference is unclear. To understand the differences of the neurological phenotype in RTHα patients, we analyzed gene regulation by two TRα1 truncating mutations, C380fsx387 and F397fsx406, both of which exhibited negligible T3 binding but create a different degree of cognitive impairment in patients. RNA was extracted from human-derived neuronal (SH-SY5Y) cells stably expressing FLAG-HA-tagged (FH) wild-type (WT) or mutant TRα1 after stimulation with vehicle or 10 nM T3. Transcriptomes were analyzed by RNA sequencing. The results showed that, in contrast to WT, cells expressing the mutant receptors lacked any T3-induced gene expression. Unstimulated gene expression was also different in cell expressing mutant versus WT receptors. This difference was more pronounced in FHTRα1-C380fsx387 than in -F397fsx406 expressing cells, indicating a differential effect of these mutants on baseline gene expression. Many genes that are specifically dysregulated by FHTRα1-C380fsx387 but not -F397fsx406 compared to both WT are involved in the nervous system development and neuronal migration. These findings may explain the more severe neurological phenotype found in the patient carrying the C380fsx387-TRα1 mutation.

Introduction

Thyroid hormone (TH) is indispensable for proper neurodevelopment. Impaired TH action during brain development can lead to various degrees of psychomotor retardation and neurological impairment (1-3). The genomic actions of TH are regulated by thyroid hormone receptors (TRs). The TR isoform α1 (TRα1) is broadly expressed in the brain and is considered the major isoform to be involved in brain development (4-7).

Mutations in the ligand binding domain (LBD) of TRα1 cause resistance to thyroid hormone alpha (RTHα). The clinical phenotype of RTHα patients includes growth retardation, macrocephaly, constipation, and anemia (8-10). Patients also present with neurodevelopmental defects, including cognitive and motor impairment, autistic spectrum disorder (ASD), and epilepsy (8,11), confirming the importance of TRα1 for a proper brain development. To date, 25 mutations (in a total of 40 patients) have been identified as a cause of RTHα. These mutations can be categorized into two groups. The first group consists of truncating mutations that create premature stop codons and shorten the length of the LBD. These mutations abolish the T3 binding affinity and T3-induced transcriptional activity of TRα1 (12-19). The second group consists of missense mutations that result in single amino acid substitutions in the LBD. These mutants bind T3 but with a lower affinity than wild-type (WT) receptors (8,15,17,20-27).

The neurological phenotype of patients with truncating mutations is generally more severe than that of patients with missense mutations (8). Interestingly, there is also a striking diversity in the severity of the neurological phenotype within the group of patients carrying truncating mutations. For instance, patients with a TRα1-F397fsx406 mutation have a relative mild neurological phenotype with borderline cognitive and motor impairment (IQ score 90) (13,14), whereas the patients with a TRα1-C380fsx387 and -A382fsx388 mutations have severe mental retardation (TRα1-C380fsx387 patient was unable to walk and communicate at 12 years of age and TRα1-A382fsx388 patient has IQ score 52) (16,17). Since all TRα1 truncating mutants exhibited negligible T3 binding (13,17), other mechanisms than impaired T3-affinity must be involved that are causing this differences in the neurocognitive phenotype.

In order to better understand the diversity of neurocognitive impairment of RTHα patients carrying truncating mutations, we studied the pattern of neuronal gene expression regulated by WT TRα1 and two truncating TRα1 mutants (C380fsx387 and F397fsx406) of patients with two very distinct neurocognitive phenotypes.

Materials and Methods

Plasmid constructs

A lentiviral bicistronic vector to drive expression of N-terminal FLAG and Hemagglutinin (HA) tagged (FH) WT human TRα1 together with the puromycin resistance marker, and green fluorescent protein (GFP) (pLentiFHTRα1 WT) was created as previously described (Chapter 6a). The TRα1-C380fsx387 (pLentiFHTRα1-C380fsx387) or -F397fsx406 (pLentiFHTRα1-F397fsx406) mutations were generated using the Quik Change II kit according to the manufacturer's protocol (Agilent Technologies, Amstelveen, The Netherlands). An empty vector (EV; pLentiMCS) expressing only the puromycin resistance marker and GFP was used to create an EV control cell line. The pMD2.G and psPAX2 packaging vectors (Chapter 6a) were used to produce lentiviruses in 293FT cells. The pdV-L1 luciferase-renilla reporter construct containing the luciferase reporter gene under control of a thyroid hormone response element (TRE) (22) was used to study the T3-induced transcriptional activity of TRs in TR-expressing cell lines.

Stable expression of TRs in SH-SY5Y cells

Lentivirus production and viral transduction have been previously described (Chapter 6a). Briefly, lentiviruses containing pLentiFHTRα1 WT, pLentiFHTRα1-C380fsx387, pLentiFHTRα1-F397fsx406, and pLentiMCS were produced in 293FT cells seeded in 10 cm tissue culture dishes by co-transfecting 4 µg of lentiviral constructs with 4 µg of psPAX2 and pMD2.G plasmids using Xtreme Gene 9 transfection reagent according to the manufacturer's protocol (Roche Diagnostics, Almere, NL). SH-SY5Y cells were grown in 6-well plate using growth medium (DMEM/F12 supplemented with 9%FBS, 100 U/mL penicillin, 100 µg/mL streptomycin, 100 nM Na_2SeO_3) and infected with lentivirus at 25% confluency. After 48 hours, infected cells were selected with 2 µg/mL of puromycin. Puromycin-resistant SH-SY5Y cells (SH-SY5Y/FHTRα1 WT, -C380fsx387, -F397fsx406, and MCS) were expanded in selection medium (growth medium supplemented with 2 µg/mL puromycin). After two passages, cells were subcultured at a 1:10,000 dilution ratio into 10 cm culture dishes in order to growth of separate clones. The clones were selected and screened for TR expression by immunoblotting before expanding for subsequent experiments.

Immunoblotting

The expression of FH-TRα1 WT and mutants in monoclonal SH-SY5Y cells was verified by immunoblotting of nuclear extracts (NEs) as previously described (22,28), using 1:1,000 dilution of a HA-Tag antibody (C29F4) Rabbit mAb (#3724, Cell Signaling Technology, Leiden, NL). Histone 3 protein was detected as a loading control using a 1:1,000 dilution of a Histone 3 (H3; 1B1B2) antibody (#14269, Cell Signaling Technology, Leiden, NL).

Transfection and luciferase assays

T3-induced transcriptional activity of FH-TRα1 WT and mutants in monoclonal SH-SY5Y cells was determined by transfecting 200 ng of the pdV-L1 luciferase-renilla reporter construct into cells at 80% confluency in 24-wells tissue culture plates in TH-depleted medium (DMEM/F12 supplemented 9% charcoal-treated FBS) using Xtreme Gene 9 transfection reagent (Roche Diagnostics, Almere, NL) according to the manufacturer's protocol. After 24 hours transfection, cells were stimulated with 0-1,000 nM T3 for 24 hours in DMEM/F12 supplemented with 0.1% bovine serum albumin (BSA). Luciferase and renilla activities in cell lysates were measured as previously described (13) using the Dual Glo Luciferase kit (Promega, Leiden, NL). The luciferase to renilla ratio was calculated to adjust for transfection efficiency and was shown as mean ± standard error of the mean (SEM) of four independent experiments performed in triplicate.

T3 stimulation and RNA isolation for transcriptome analysis and qRT-PCR

The monoclonal transduced SH-SY5Y cells were plated in 6-well culture plates in selection medium. At 80% confluency, the cells were cultured for 24 hours in DMEM/F12 supplemented with 9% charcoal-stripped FBS to deplete TH and subsequently stimulated for 6 hours with 0 or 10 nM T3 in DMEM/F12 supplemented with 0.1% BSA. RNA was then isolated from the cells using Trizol reagent (TRI Reagent®, Sigma-Aldrich, Zwijndrecht, NL) and further purified with EchoCLEAN RNA CleanUp kit (020-002-050-050, BioEcho, Cologne, Germany), according to the manufacturer's protocol. RNA samples of three independent experiments performed in triplicate for each receptor and T3 concentration were collected. One sample of each triplicate was sent for RNA sequencing, and the other two samples were used for qRT-PCR.

Next-generation RNA sequencing (RNA-seq)

Purity and quality of isolated RNA were assessed by Agilent 2100 Bioanalyzer (Agilent Technologies, Santa Clara, CA). The RNA was prepped with the Illumina TruSeq Stranded mRNA Library Prep Kit (Illumina, Eindhoven, NL). The resulting DNA libraries were sequenced according to the Illumina TruSeq Rapid v2 protocol on an Illumina HiSeq2500 sequencer. Reads were generated of 50 base-pairs in length. Subsequently, adapter sequences were trimmed off, and the trimmed reads were matched against the requested reference (GRCh38 version of the human reference genome) using HiSat2 (version 2.1.0). Gene expression values were called using HTseq-count (version 0.9.1).

Differential gene expression analysis

Gene expression values from HTseq-count were analyzed using the R program. Read counts were first normalized with the DEseq2 package from R (29) and filtered for genes that had a false discovery rate (FDR) above 0.05 and low normalized count (<10 reads in

more than 21 samples). Principle component analysis (PCA) and pairwise distance heat map were performed to visualize the clustering of the samples. Pairwise comparisons of differential expression were determined using the DEseq2 package from R (29). A p-value adjusted for multiple comparisons < 0.05 was considered significant. Subset of genes that have at least a 4-fold difference in expression (log2 fold change ≥ ±2) for each pairwise comparison was defined as highly differentially expressed genes (H-DE genes). Gene Ontology terms (molecular function, MF; biological process, BP; cellular component, CC) enrichment analysis was performed by DAVID functional annotation chart (DAVID Bioinformatics Resources 6.8, NIAID/NIH: https://david.ncifcrf.gov/) using default setting (count 2, ease 0.1). Statistical significance was considered when p-values of modified Fisher's exact test (EASE score) with Benjamini post-test < 0.05.

Quantitative real-time polymerase chain reaction (qRT-PCR)

RNA was reverse transcribed using the transcriptor high fidelity cDNA synthesis kit (05091248001, Roche Diagnostics, Almere, NL) according to the manufacturer's protocols. qRT-PCR was performed on 25 ng cDNA using TaqMan probes for KLF9 (Hs00230918_m1), HR (Hairless) (Hs00218222_m1), and Cyclophilin A (Cat. No. 4310883E, ThermoFisher Scientific, Landsmeer, NL), and qPCR Core kit for SYBR® Green (Eurogentec, Maastrich, NL) with *GAPDH* (forward primer: 5'-GAGTCCTTCCACGATACCAAAG-3', reverse primer: 5'-GGTGTGAACCATGAGAAGTATGA-3') and *THRA* (forward primer: 5'-AGACCAGATCATCCTCCTGAA-3', reverse primer: 5'-CCGCTTGACAGCCATCTC-3') primers. The expression of *KLF9*, *HR* and *THRA* were quantified by the ddCt method using the geometric means of two house-keeping genes (Cyclophilin A and GAPDH) expression for normalization. Data are presented as mean ± SEM of three independent experiments performed in duplicate.

Results

Expression and transcriptional activity of FH-TRα1 WT and mutants in SH-SY5Y cells

To study the effect of TRα1 truncating mutations on gene expression in neuronal cells, we introduced WT TRα1 and two truncating mutants, C380fsx387 and F397fsx406, into SH-SY5Y cells using lentiviral transduction. Monoclonal cell strains were selected to get a genetically homogenous and clonal population. The mRNA expression of *THRA* in all three TRα1 expressing cell lines was substantially higher than the MCS control cells (approximately 100-fold for SH-SY5Y/FHTRα1 WT, 60-fold for -C380fsx387, and 90-fold for -F397fsx406 cells), confirming a low level of endogenous TRα1 expression in SH-SY5Y cells and the success of FH-TRα1 transduction (Supplementary Figure S1A). Immunoblots of NEs

from SH-SY5Y cells confirmed that all three FHTRα1 are efficiently expressed in the cells, albeit with slightly lower expression levels for FHTRα1-C380fsx387 than for FHTRα1 WT and FHTRα1-F397fsx406 (Supplementary Figure S1B). WT TRα1 showed normal T3-induced transcriptional activity in luciferase assays (Supplementary Figure S1C). In contrast, the two truncating mutants showed no response to T3-stimulation at any of the concentrations tested, indicating a complete loss of T3-induced transcriptional activity for these mutants.

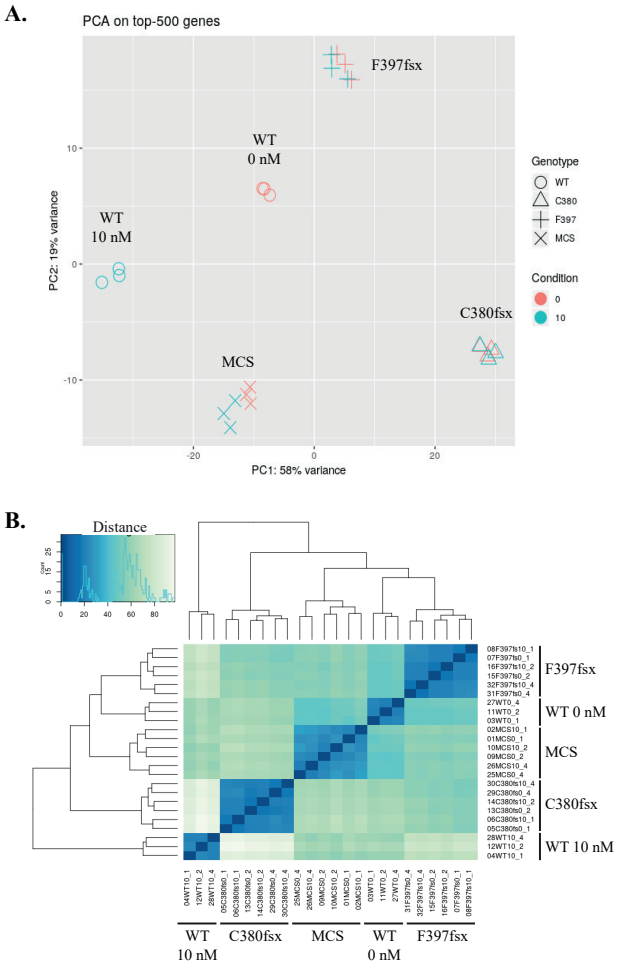

Figure 1. (A) Principal component analysis (PCA) of the top 500 genes of RNA sequencing data from SH-SY5Y/FHTRα1 WT, -C380fsx387, -F397fsx406, and MCS control cells (after 6 hours 0 or 10 nM T3 stimulation) clearly demonstrates the clustering of biological replicates from a similar TR and T3 condition. The samples from cells expressing WT receptor are separated into two clusters, depending on the T3 concentration. In contrast, samples from cells stimulated by 0 and 10 nM T3 are clustered together in MCS control and the two mutants, suggesting a small effect of T3 on their transcriptomes. (B) The heatmap illustrates the pairwise distance between samples clustered by hierarchical clustering analysis. The key color on the top left indicates the distances between samples. In agreement with the PCA plot, samples from the same cell type and T3 condition are clustered together.

Overall gene expression

RNA sequencing was performed to evaluate the different patterns of gene expression elicited by WT and the two TRα1 truncating mutants in SH-SY5Y cells. At least 23 million reads were generated for each sample, and more than 95% of these reads were aligned with the reference sequence. After normalization and filtering, 17,788 genes remained for analysis. The PCA plot and pairwise distance heat map showed a high degree of clustering of the three biological replicates for each TR and T3 condition (Figure 1). The cluster of T3-stimulated SH-SY5Y/FHTRα1 WT was separated from unstimulated WT (0 nM T3), indicating global changes in the pattern of gene expression elicited by the liganded WT TRα1. In contrast, the six biological replicates of the SH-SY5Y/FHTRα1-C380fsx387 and -F397fsx406 were clustered together, regardless of T3, indicating that these two mutants did not respond to T3. The fold increase in RNA reads of two known TH responsive genes, *KLF9* and *HR*, were similar to the results of qPCR (independent samples) (Supplementary Figure S2), confirming the reliability of the RNA sequencing.

We then analyzed the effect of 10 nM T3 stimulation on gene expression of each cell line. The relatively short 6-hour T3 incubation was chosen to minimize the chance that differentially expressed genes were not directly controlled by T3-TRα1 but rather secondarily via a T3-induced transcription factor (30-32). The results showed that, in the presence of WT TRα1, the expression of 5,688 genes was significantly changed by 10 nM T3 (2,999 T3-upregulated genes and 2,689 T3-downregulated genes) (Figure 2). In contrast, only 43 genes were differentially expressed between unstimulated and 10 nM T3 stimulated in the MCS control group. In SH-SY5Y/FHTRα1-C380fsx387 or -F397fsx406 cells, T3 did not significantly alter the expression of any gene.

Since T3 did not affect the pattern of gene expression in SH-SY5Y/FHTRα1-C380fsx387 and -F397fsx406 cells, we from here on only focused on unstimulated gene expression to study the difference between the two mutants. The expression heat map showed that the overall pattern of unstimulated gene expression of the SH-SY5Y/FHTRα1-F397fsx406 cells was more similar to WT than to -C380fsx387 cells (Figure 2). We set stringent criteria of a minimal 4-fold difference in gene expression levels, designated highly differentially expressed (H-DE) genes, to ensure that the differences are likely to have a biological impact. The number of H-DE genes between unstimulated SH-SY5Y/FHTRα1-F397fsx406 and WT cells was also much smaller than between unstimulated SH-SY5Y/FHTRα1-C380fsx387 and WT cells (Figure 3), confirming that the C380fsx387 mutant creates a more distinct pattern of baseline gene expression compared to WT than the F397fsx406 mutant.

Differential gene expression of FHTRα1-C380fsx387 versus -F397fsx406

We performed pairwise comparison to determine which genes are differentially expressed between unstimulated SH-SY5Y/FHTRα1-C380fsx387 and -F397fsx406 cells. Overall, 4,629 genes were differentially expressed between the two cell lines, of which 721

were H-DE genes. Of those, 342 genes were T3 responsive genes, i.e., genes that had a significantly different expression level after 10 nM T3 stimulation in the WT cells (Figure 4A).

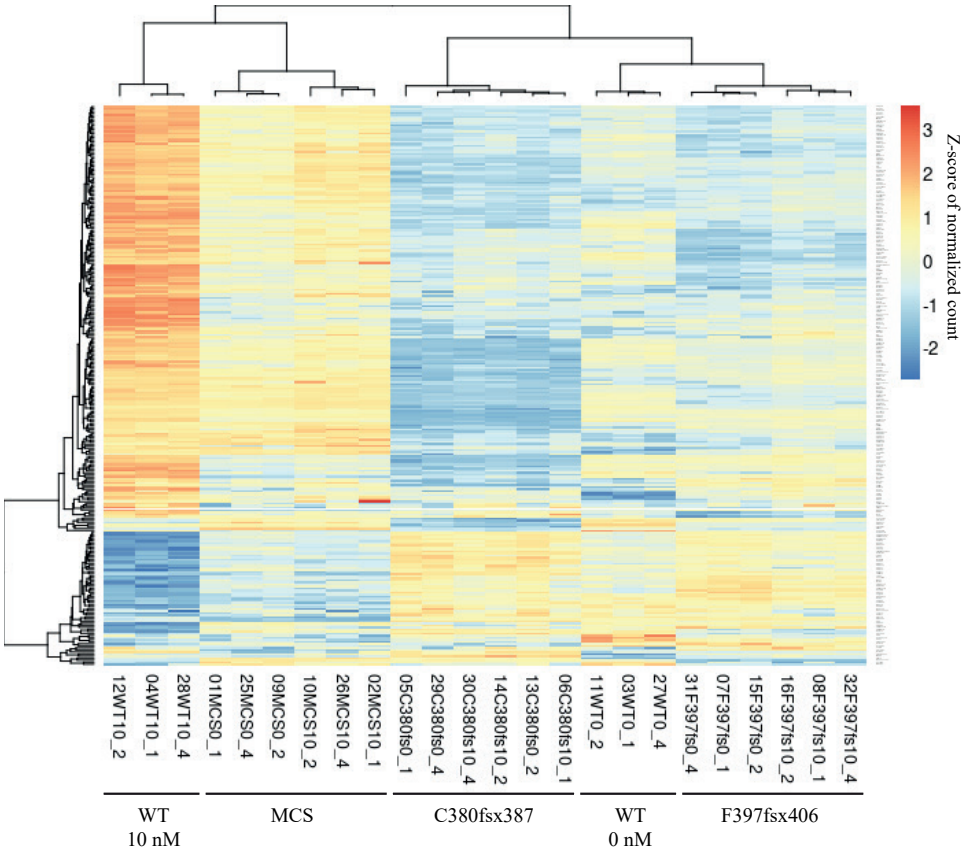

Figure 2. The expression heat map of the normalized RNA sequencing data illustrates the pattern of gene expression of all samples. Data are shown as a Z-score of normalized counts per gene (key color on the right). The dendrogram shows hierarchical clustering of genes (row) and samples (column) (analyzed by average linkage clustering and Pearson distance measurement methods). The heat map is clearly different between unstimulated and 10 nM T3 stimulation in WT cells. In contrast, there is no clear difference in the heat map of SH-SY5Y/FHTRα1-C380fsx387 and -F397fsx406 cells after 10 nM T3 stimulation (all samples are clustered together). In addition, the heat map of SH-SY5Y/FHTRα1-F397fsx406 cells is more similar to unstimulated WT than that of -C380fsx387 cells, suggesting a stronger effect of the C380fsx387 mutation than the F397fsx406 mutation on gene expression of unstimulated cells.

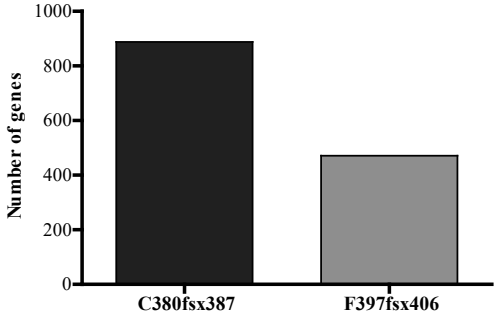

Figure 3. The bar chart shows number of H-DE genes between unstimulated SH-SY5Y/FHTRα1-C380fsx387 and WT cells (888 genes, black bar) and between SH-SY5Y/FHTRα1-F397fsx406 and WT cells (471 genes, grey bar).

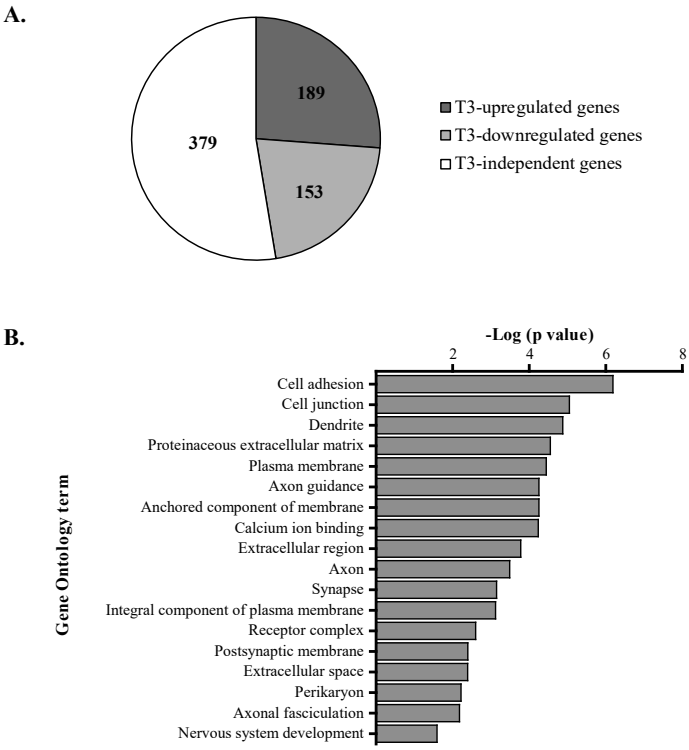

Figure 4. 721 H-DE genes between unstimulated SH-SY5Y/FHTRα1-C380fsx387 and -F397fsx406 cells. (A) Pie chart shows that 342 genes (47%) are T3-responsive genes, i.e., genes that had a significantly different expression level after 10 nM T3 stimulation in the WT cells (189 genes are T3-upregulated and 153 genes are T3-downregulated), whereas 379 genes (53%) are T3-independent (the expression level does not change after 10 nM T3 stimulation). (B) The result of the gene ontology (GO) enrichment analysis showed that the genes were significantly enriched (Benjamini p value < 0.05) with 18 GO terms, most of which are related to the physiology of neurons.

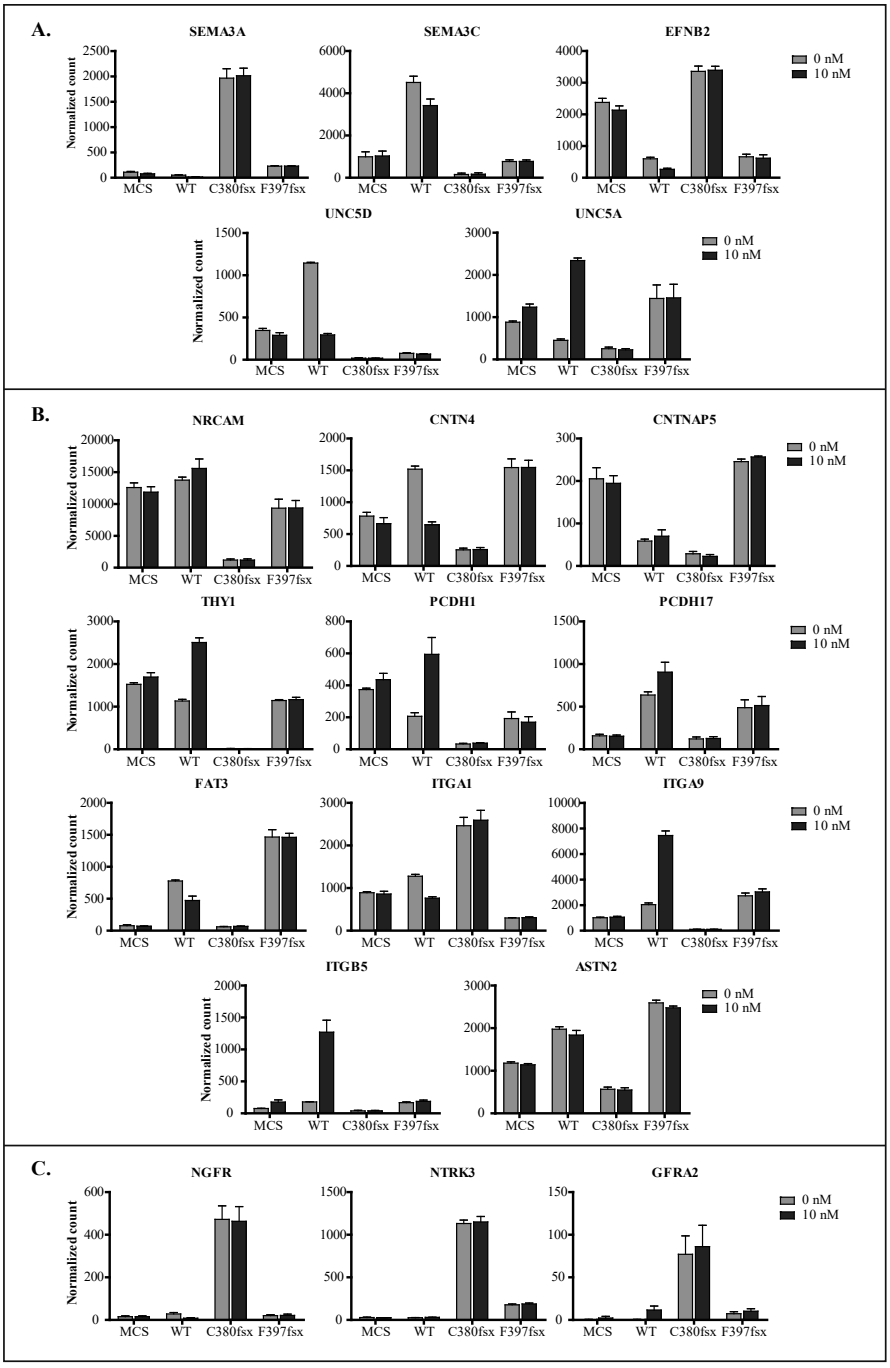

Figure 5. Expression of selected individual genes that are significantly enriched for at least one GO term. These genes encode (A) neuronal guidance molecules, (B) cell adhesion molecules, and (C) neurotrophic factors, which play an important role in nervous system development and neuronal growth and migration. (Data are shown as mean ± SEM of three biological replicates of normalized count from RNA sequencing.)

Gene ontology (GO) enrichment analysis of FHTRα1-C380fsx387 highly differential genes

Next, we analyzed whether the H-DE genes between unstimulated SH-SY5Y/FHTRα1-C380fsx387 and -F397fsx406 cells were associated with specific GO terms. The result showed that 328 genes were significantly enriched for at least one GO term. The genes were enriched for 18 terms, including one molecular function, four biological processes, and thirteen cellular components, most of which are related to the physiology of neurons (Figure 4B and Table 1). Many genes that significantly enriched with these GO terms encode neuronal guidance molecules, cell adhesion molecules, and neurotrophic factors, which play important roles in nervous system development and neuronal growth and migration (Figure 5 and Table 2). Interestingly, in addition to the genes that were enriched, the expression of two genes that are vital for neuronal differentiation, *ASCL1* and *NEUROG2*, was also remarkably different between SH-SY5Y/FHTRα1-C380fsx387 and SH-SY5Y/FHTRα1 WT or -F397fsx406 (Figure 6 and Table 2).

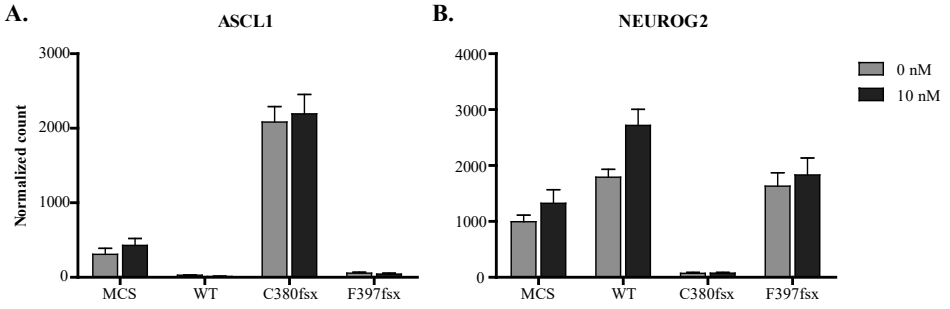

Figure 6. The disparate expression of (A) *ASCL1* and (B) *NEUROG2* in SH-SY5Y/FHTRα1-C380fsx387 cells compared to the SH-SY5Y/FHTRα1 WT and -F397fsx406 cells. (Data are shown as mean ± SEM of three biological replicates of normalized count from RNA sequencing.)

Table 1. Significant Gene Ontology enrichment analysis by DAVID Bioinformatics Resources 6.8, NIAID/NIH (https://david.ncifcrf.gov/).

GO term	Gene list	Fold enrichment	FDR	Benjamini p value
Biological Process (BP)				
Axonal fasciculation (GO:0007413)	CNR1, CNTN2, CNTN4, CRTAC1, NDN, NRCAM, SEMA3A	13.1	0.015	0.007
Axon guidance (GO:0007411)	ANOS1, CNTN2, CNTN4, EFNB2, EPHA8, FEZ1, GFRA3, LGI1, NGFR, NR4A3, NTN4, RELN, SEMA3A, SEMA3C, SLIT1, SLIT2, TENM2, TGFB2, TNR, UNC5A, UNC5D	4.46	<0.001	<0.001
Cell adhesion (GO:0007155)	ADAM12, ADGRE2, ADGRE5, AJAP1, ANOS1, AZGP1, CD9, CNTN2, CNTN4,CNTN6, CNTNAP4, CNTNAP5, COL6A3, EDIL3, EFNB2, ENG, EPHA8, FEZ1, FREM2, ISLR, ITGA8, ITGA9, ITGB5, JCAD, KITLG, LPP, MYBPC2, NLGN4X, NTM, PCDH17, PRKCA, PTPRK, PTPRT, RELN, SIRPA, SORBS2, SPOCK1, SPON1, SSPO, THY1, TNFAIP6, TNR	3.09	<0.001	<0.001
Nervous system development (GO:000739)	CNTN4, CSGAL, NACT1, ENC1, FEZ1, FOS, FUT9, GFRA1, GFRA2, GFRA3, HES4, ITM2A, JAG1, LGI1, MAB21L2, MAFB, MPPED2, NDN, PCDH1, RGS9, SOX14, SPOCK1, ST8SIA4, ZIC5	2.71	0.080	0.025
Molecular Function (MF)				
Calcium ion binding (GO:0005509)	ADGRE2, ADGRE5, ASTN2, CACNA1E, CAPN13, CCBE1, CPS1, CRTAC1, DGKB, DGKG, EDIL3, EYS, FAT3, FBLN2, FSTL4, GUCA1A, HPCAL4, JAG1, KCNIP1, LRP1B, LRP4, MATN3, MCTP1, MCTP2, ME1, MMP17, NID1, PCDH1, PCDH17, PCDHGB7, PHF24, PLA2G4A, PRRG1, RPH3A, S100A10, S100A11, SCGN, SLIT1, SLIT2, SMOC1, SNCB, SPOCK1, SPOCK3, SYT17, SYT2, SYT4, TENM2, TLL2	2.35	<0.001	<0.001
Cellular Component (CC)				
Anchored component of membrane (GO:0031225)	ART4, CD177, CNTN2, CNTN4, CNTN6, GFRA1, GFRA2, GFRA3, GPC5, LYPD1, LYPD6B, MMP17, NT5E, NTM, PRNP, TFPI	4.92	0.001	<0.001
Axon (GO:0030424)	CNR1, CNTN4, COBL, FEZ1, GRIK3, HTR2A, IGF2BP1, IRX3, KCNA2, KCNA3, KCNB1, KIF21B, MME, NEFL, NEFM, PRSS12, PTPRK, SEMA3A, STMN4, SYT4, TGFB2	3.29	0.009	<0.001
Cell junction (GO:0030054)	CADPS, CAMK2N1, CBLN4, CNTNAP4, CXCR4, DACT1, FAIM2, GABRA5, GABRB1, GABRB3, GABRG3, GCOM1, GRIA2, GRIA3, GRIK3, GRIK4, GRIK5, KCNA2, KCNB1, LGI1, LRRC7, LRRTM3, MYZAP, NLGN4X, PRIMA1, RIMS3, RPH3A, SDK2, SIPA1L1, STXBP5, SV2B, SYN3, SYNPR, SYT2, SYT4, TENM2, TMEM163, TRIM9	2.80	<0.001	<0.001

GO term	Gene list	Fold enrichment	FDR	Benjamini p value
Dendrite (GO:0030425)	BRINP2, BRINP3, CAMK2N1, CNTNAP4, COBL, FEZ1, GABRA5, GABRB1, GNG3, GRIK3, GRIK5, HTR2A, KCNA2, KCNB1, KCNIP1, KIF21B, LRP4, MME, NLGN4X, P2RY1, PRSS12, PSD2, PTPRK, RELN, SEMA3A, SLC32A1, SYT4, TENM2, THY1, TRIM9, ZNF385A	3.22	<0.001	<0.001
Extracellular region (GO:0005576)	A2M, ADAM12, ADAMTS3, ADAMTS5, ALKAL2, ANOS1, AOAH, APLN, APOL4, AZGP1, BCHE, BRINP2, BRINP3, C1orf54, C1QTNF1, C6, C7, CLUL1, CNTN4, COL14A1, COL24A1, COL2A1, COL6A3, COLEC11, DBH, DMBT1, FAM19A5, FBLN2, FGF22, FGF7, FSTL4, GPC5, GREM2, IGFBP3, IL13RA2, INHBE, ISLR, JAG1, KITLG, KNG1, LGI1, LYPD1, MATN3, MR1, NGFR, NID1, NPY, NRCAM, NRG3, NTN4, NTS, NXPH1, OAS1, OTOR, PRRG1, PTX3, RBP3, RSPO4, SCGN, SEMA3A, SERPINA5, SLIT1, SLIT2, SUSD4, TAC3, TFPI, TGFB2, TIMP3, TLL2, TNFRSF1A, TNR, TUBA4A, TULP2, VEGFD, VIP, VSTM2A, WNT11, WNT16, XYLT1	1.71	0.004	<0.001
Extracellular space (GO:0005615)	ADAMTS3, ADAMTS5, ADGRE5, ANGPTL2, ANOS1, APLN, APOL4, AZGP1, C1QTNF1 ,CBLN4, CCBE1, CD9, COL14A1, COL2A1, COL6A3, CPB1, CPNE9, DBH, DMBT1, ENG, FGF22, GLDN, GPC5, GREM2, GSDMD, HIST1H2BF, IGFBP3, IL13RA2, INHBE, KIT, KITLG, KNG1, LGI1, NLGN4X, NPY, NRG3, PTGIS, PTX3, RBP3, RELN, S100A11, SEMA3A, SEMA3C, SERPINA5, SERPINB6, SEZ6, SLIT1, SLIT2, SPINK13, SPOCK1, SPOCK3, SPON1, SSPO, TAC3, TFPI, TGFA, TGFB2, TIMP3, TNFAIP6, TNFRSF1A, VEGFD, WNT11, WNT16	1.63	0.196	0.004
Integral component of plasma membrane (GO:0005887)	ABCB4, ABCG1, ADGRE5, AGTR1, APCDD1, AQP10, AQP3, ASIC1, C1QTNF1, CACNB2, CALCRL, CALY, CD9, CNR1, CNTN2, EFNB2, EPHA8, ESYT3, GABRA5, GABRB1, GABRB3, GPC5, GPR1, GRIA2, GRIK3, GRIK4, HAS2, HTR2A, INSRR, JAG1, KCNA2, KCNJ9, KCNK3, KCNK9, LIFR, MME, MMP17, NGFR, NLGN4X, NRCAM, NRG3, NTRK3, P2RX3, P2RY1, PCDH1, PLPPR4, PLPPR5, PLXNA2, PRKD1, PROKR2, PRRG1, PTGER2, PTH1R, PTPRK, RHBG, SLC18B1, SLC6A16, SLC7A14, SLITRK6, SSTR1, TENM2, TGFA, THY1, TLR1, TNFRSF1A, TRHDE, TSPAN2, TSPAN8, VIPR1	1.70	0.024	<0.001
Perikaryon (GO:0043204)	ASS1, ASTN1, ASTN2, GRIK3, GRIK5, ITGA1, ITGA8, KCNA2, KCNAB1, KCNB1, NDN, TMEM100	3.94	0.316	0.006
Proteinaceous extracellular matrix (GO:0005578)	ADAMTS16, ADAMTS3, ADAMTS5, ANOS1, CCBE1, COL14A1, COL24A1, COL6A3, CRTAC1, FBLN2, GLDN, GPC5, MATN3, MMP17, RELN, SLIT1, SLIT2, SMOC1, SPOCK1, SPOCK3, SPON1, TFPI2, TIMP3, TNR, WNT11, WNT16	3.37	<0.001	<0.001

GO term	Gene list	Fold enrichment	FDR	Benjamini p value
Postsynaptic membrane (GO:0045211)	CAMK2N1, FAIM2, GABRA5, GABRB1, GABRB3, GABRG3, GRIA2, GRIA3, GRIK3, GRIK4, GRIK5, KCNB1, LRRC7, LRRTM3, NLGN4X, P2RY1, SIPA1L1, TENM2	2.97	0.177	0.004
Plasma membrane (GO:0005886)	ABCB1, ABCB4, ABCG1, ABCG4, ADAM12, ADCY8, ADGRE2, ADGRE5, AGTR1, ANO3, ANOS1, AQP10, AQP3, ARHGEF28, ART4, ASIC1, ATP10A, AZGP1, BAMBI, CA14, CACNA1E, CACNA1G, CACNB2, CACNG2, CALCRL, CARD11, CD177, CD9, CERK, CNR1, CNTN2, CNTN4, CNTN6, COBL, COLEC12, CSMD2, CXCR4, DGKB, DGKG, DGKK, DOCK5, EFNB2, ELMO1, EPHA8, FAM155B, FAM84B, FAT3, FEZ1, FGFRL1, FREM2, GABRA5, GABRB1, GABRB3, GABRG3, GFRA1, GFRA2, GFRA3, GLDN, GLP1R, GNG3, GPBAR1, GPC5, GPR160, GPR37L1, GRIA2, GRIA3, GRIK3, GRIK4, GRIK5, GSDMD, GUCA1A, HEPH, HTR2A, IFNLR1, ITGA1, ITGA8, ITGA9, ITGB5, ITM2A, JAG1, KCNA2, KCNA3, KCNAB1, KCNB1, KCNIP1, KCNJ3, KCNJ9, KCNK3, KCNK9, KCNN3, KCNQ3, KIRREL1, KIT, KITLG, KNG1, LIFR, LPP, LYPD1, LYPD6B, ME1, MME, MR1, MYOF, NFATC2, NGFR, NLGN4X, NRCAM, NT5E, NTM, NTN4, P2RX3, P2RY1, PANX2, PCDH1, PCDH17, PCDHGB7, PHACTR2, PIK3AP1, PLCE1, PLPPR4, PLPPR5, PLXNA2, PRIMA1, PRKCA, PRKD1, PRNP, PROKR2, PRSS12, PTGER2, PTH1R, PTPRT, PYGL, RAP1GAP2, RELN, RGS9, RHBG, RPH3A, SCN1A, SDK2, SEZ6, SGK1, SHB, SIRPA, SLC27A6, SLC32A1, SLIT2, SSTR1, STXBP5, SV2B, SYT17, SYT2, SYT4, TBC1D30, TENM2, TFPI, TGFA, THY1, TLR1, TMEM100, TMEM119, TMEM204, TNFRSF19, TNFRSF1A, UNC5A, UNC5D, VIM, VIPR1, VSTM2A	1.42	<0.001	<0.001
Receptor complex (GO:0043235)	ENG, GPR160, GPR37L1, INSRR, ITGB5, LIFR, LRP1B, NTRK3, P2RX3, PEX5L, PTH1R, TNFRSF1A, VDR, VIPR1	3.83	0.101	0.003
Synapse (GO:0045202)	ASIC1, CBLN4, CNTN2, DACT1, GABRA5, GABRB3, LGI1, MME, MYO7A, NLGN4X, NRCAM, PPFIA2, PRIMA1, RPH3A, SCGN, SDK2, SNCB, TENM2	3.46	0.026	<0.001

FDR, false discovery rate

Table 2. Selected genes with different expression levels in the FHTRα1-C380fsx387 regulated compared to FHTRα1 WT and -F397fsx406, and with known functions in neuronal growth and migration (the gene descriptions are extracted from GeneCards: www.genecards.org).

Gene symbol	Protein	Description
Guidance molecules		
SEMA3A	Semaphorin 3A	Protein can function as either a chemorepulsive (inhibiting outgrowth of axon), or a chemoattractive agent (stimulating the growth of axon)
SEMA3C	Semaphorin 3C	Functions as attractant for growing axons, and thereby plays an important role in axon growth and axon guidance
SLIT1	Slit guidance ligand 1	SLIT1 and SLIT2 together seem to be essential for midline guidance in the forebrain by acting as repulsive signal preventing inappropriate midline crossing by axons projecting from the olfactory bulb
EFNB2	Ephrin B2	Cell surface transmembrane ligand for Eph receptors which are crucial for migration, repulsion and adhesion during neuronal development
UNC5A	UNC-5 netrin receptor A	Protein belongs to a family of netrin-1 receptors thought to mediate the chemorepulsive effect of netrin-1 on specific axons
UNC5D	UNC-5 netrin receptor D	Receptor for the netrin NTN4. Plays a role in axon guidance by inhibit axon growth cones in the nervous system development upon ligand binding
Cell adhesion molecules		
NRCAM	Neuronal cell adhesion (Immunoglobulin superfamily, IgSF)	Involved in neuron-neuron adhesion and directional signal during axonal growth
CNTN4	Contactin 4 (Contactin family of immunoglobulin)	Function in neuronal network formation and plasticity
CNTNAP5	Contactin associated protein like 5 (Neurexin family)	Function as cell adhesion molecules in the vertebrate nervous system
THY1	Thy-1 cell surface antigen (IgSF superfamily)	Involved in cellular adhesion of the immune and nervous systems
PCDH1	Protocadherin 1 (Cadherin superfamily)	Involved in neural cell adhesion, suggesting a possible role in neuronal development
PCDH17	Protocadherin 17 (Cadherin superfamily)	Protein may involve in the cellular connections in the brain
FAT3	FAT atypical cadherin 3	May play a role in the interactions between neurites derived from specific subsets of neurons during development
ITGA1	Integrin subunit alpha 1 (integrin superfamily)	The protein heterodimerizes with the beta 1 subunit and involved in cell-cell adhesion
ITGA9	Integrin subunit alpha 9 (Integrin superfamily)	The protein heterodimerizes with the beta chain and mediates cell-cell and cell-matrix adhesion
ITGB5	Integrin subunit beta 5 (Integrin superfamily)	Combines with different alpha chains to form a variety of integrin heterodimers and participates in cell adhesion and cell surface mediates signaling
ASTN2	Astrotactin 2	Protein is expressed in the brain and may function in neuronal migration

Gene symbol	Protein	Description
Neurotrophic factors		
NGFR	Nerve growth factor receptor	Low affinity receptor which binds to multiple neurotrophic factors and regulates neuronal cell survival and cell death
NTRK3	Neurotrophic receptor tyrosine kinase 3	Binds to its ligand neurotropin 3 (NT-3) and involved in nervous system development
GFRA2	Glial-derived neurotrophic factor (GDNF) family receptor alpha 2	Encoded protein acts preferentially as a receptor for neurturin (NTN), potent neurotrophic factors for neuron survival and differentiation
Neuronal differentiation		
ASCL1	Achaete-Scute family bHLH transcription factor 1	Protein plays a role in the neuronal cell commitment and differentiation
NEUROG2	Neurogenin 2	Protein is expressed in neural progenitor cells within the developing central and peripheral nervous systems to specify a neuronal fate

Discussion

In this study, we evaluated the differences in the transcriptomes controlled by two TRα1 truncating mutants (C380fsx387 and F397fsx406) and WT TRα1 in a neuronal cell model (SH-SY5Y) in order to gain a better understanding of the differential effects of these mutations on the neurological phenotype of RTHα patients. The results showed that the transcriptomes of SH-SY5Y cells overexpressing FHTRα1-C380fsx387 and -F397fsx406 mutants were very different from the T3-stimulated but also the unstimulated transcriptome of WT TRα1. This suggests that the presence of these two mutants alters both baseline and T3-induced gene transcription. In addition, the transcriptomes of the two mutants were very different from each other, suggesting a differential effect of these two different mutations on gene transcription.

Previous studies showed that the phenotype of RTHα patients is mainly caused by the reduced T3 binding affinity of TRα1 mutants. However, patients that carry different TRα1 truncating mutations, all of which exhibited negligible T3 binding, display a striking variation in the cognitive phenotype. For instance, the patient who carries TRα1-C380fsx387 mutation was severely handicapped and unable to communicate at 12 years of age, suggesting severe cognitive impairment (17). Patients who carry TRα1-A382fsx388 and C392X mutations also had a low IQ score (IQ score 52 and 22, respectively) (15,16). In contrast, patients who carry TRα1-F397fsx406 and E403X mutations had borderline cognitive impairment (IQ score 90 and 70, respectively) (13-15). This suggests that other effects of the mutation that are independent from T3-binding can contribute to the phenotype as well (8,12,13,15-17,33). TRα1-C380fsx387 and -F397fsx406 were selected because of the marked differences in the

severity of the cognitive impairment in the patients harboring these mutations. In agreement with previous reports (13,17), both mutants had no response to T3 in luciferase experiments, confirming that T3 could not stimulate transcriptional activity for these mutants.

In SH-SY5Y/FHTRα1 WT cells, the expression of a substantial number of genes (5,688 genes) was regulated by T3 in contrast to SH-SY5Y/MCS controls cells (43 genes). The T3-induced response of WT receptor can be divided into two groups. The first group is a positive regulation in which the level of gene expression is increased in the presence of T3 (2,999 genes, 53%). The second group is a negative regulation in which the level of gene expression is decreased in the presence of T3 (2,689 genes, 47%). Interestingly, the number of genes in both groups is similar. The number of T3 negatively regulated genes in the brain varies (15-60%) between reports, depending on the cellular context and experimental technique (34-38). So far, the molecular mechanisms underlying the negative regulation by T3 have not yet been clearly established.

In contrast to the WT receptor, the transcriptomes regulated by FHTRα1-C380fsx387 and -F397fsx406 were not significantly altered by 10 nM T3 stimulation for any gene, which is in line with negligible T3 binding of these two mutants. Since we were interested in the differential effect of these two mutants on gene transcription, we then studied whether these mutants alter unstimulated gene expression compared to the WT receptor in a different way. The results indicate that the number of H-DE genes between SH-SY5Y/FHTRα1-C380fsx387 and WT cells was higher than that between -F397fsx406 and WT cells (888 vs. 471 genes). This finding suggests that the effect of these two mutants on gene expression is beyond their loss of affinity for T3. In addition, the much larger impact of the C380fsx387 mutant on unstimulated gene transcription compared to the F397fsx406 mutant likely contributes to the difference in the neurological phenotype of the patients.

We performed gene ontology (GO) term enrichment analysis to understand the functions of the genes that are differentially expressed between unstimulated SH-SY5Y/FHTRα1-C380fsx387 vs. -F397fsx406 cells. We only selected the H-DE genes that had at least a 4-fold difference in expression between the two mutants for the analysis since a difference in expression of these genes is likely to have an impact on the difference in phenotype of patients. The results showed that approximately 50% of the selected genes were significantly enriched for at least one GO term. Most of the significant terms were related to neurons (axon, dendrite, synapse) and physiology of the neurons (axon guidance, axon fasciculation, cell adhesion, calcium ion binding, and cell junction). These findings further support the hypothesis that a differential effect of the C380fsx387 and F397fsx406 mutants on gene expression may disturb the pathways that are critical for the brain and neurons.

One of the most significant terms in our GO analysis is axon guidance. Genes enriched for this term encode proteins that act as extracellular guidance cues for neuronal growth and migration. These cues can either attract or repulse axon growth. *SEMA3A* and *SEMA3C* encode Semaphorin 3A and 3C that bind to the plexin and neuropillin receptor and

inhibit axon growth (39-42). *SLIT1* encodes Slit1 that signals through Roundabout (Robo) family receptors and controls midline guidance of axons (42-45). *EFNB2* encodes Ephrin B2, which is a membrane-bound ligand that binds to EphB tyrosine kinase receptors, and mediates cell to cell communication and neuronal development (42,46-48). *UNC5A* and *UNC5D* encode UNC-5 homolog proteins A and D which function as receptors for axonal attractive molecule, Netrin (42,49,50). In addition to the axonal growth, these cues are involved in dendrite development (51,52) and cortical migration of the neurons (53). By responding to appropriate signals, the neurons grow into the correct paths, which leads to proper neurodevelopment. Since the expression of these genes in SH-SY5Y/ FHTRα1-C380fsx387 cells was significantly different from both SH-SY5Y/ FHTRα1 WT and -F397fsx406 cells, it is likely that these genes may have contributed to the more severe neurodevelopmental impairment found in the patient carrying the C380fsx387 mutation.

Apart from the genes that were enriched for GO terms, the expression of *ASCL1* and *NEUROG2* was also markedly different in SH-SY5Y/FHTRα1-C380fsx387 cells compared to SH-SY5Y/FHTRα1 WT and -FHTRα1-F397fsx406 cells (Figure 6). These genes encode Achaete-scute homolog 1 (ASCL1) and Neurogenin 2 (NEUROG2), respectively, which are master regulators of neuronal differentiation. Many studies using murine models suggest that in cortical brain development, Neurog2 expression commits progenitor cells to become excitatory (glutamatergic) neurons, whereas Ascl1 expression commits cells to become inhibitory (GABAergic) neurons (54-58). In addition, highly expressed Ascl1 keeps neuron progenitor cells in the proliferative phase rather than enter the differentiation process (55). Therefore, the relatively high expression of the *ASCL1* and low expression of the *NEUROG2* in SH-SY5Y/ FHTRα1-C380fsx387 cells (Figure 6) are likely to affect progenitor cell differentiation and the balance between excitatory and inhibitory neurons, which may relate to the severe cognitive impairment found in the TRα1-C380fsx387 patient.

Although our study showed that TRα1-C380fsx387 and TRα1-F397fsx406 have a differential effect on gene transcription, the underlying mechanism explaining this differential effect remains unclear. It has been shown that the C-terminal region of TRα1 protein is important for the interaction with corepressor and coactivator proteins (59-62). Since the location of the frameshift and premature stop codon of TRα1-C380fsx387 is proximal to that of TRα1-F397fsx406 mutant, the C-terminal region of the TRα1-C380fsx387 mutant is likely more distorted. The C380fsx387 mutation alters both Helix [H] 11 and 12, whereas the F397fsx406 mutation only alters H12. The more prominent structural changes in the TRα1-C380fsx387 mutant might result in more exposure to the corepressor docking surface than in case of the TRα1-F397fsx406 mutant. This would allow corepressor proteins to bind stronger to the TRα1-C380fsx387 mutant than to the TRα1-F397fsx406 mutant and lead to stronger gene repression. Alternatively, since TRs can associate with and be regulated by multiple coregulatory proteins, different binding surfaces of the mutants may result in the recruitment of a different repertoire of proteins that ultimately affects the expression of target genes.

It is important to emphasize that our experiments were performed by overexpressing WT or mutant TRα1 in SH-SY5Y cells, which creates a non-physiologic level of TRα1 expression. A high level of mutant TRα1 in the cells against a background of low levels of endogenous WT TRα1 expression may not mimic the actual situation in which both WT and mutant *THRA* alleles are expressed at equal levels. Therefore, the effect of the mutants may be under or overestimated in our system. Although the lentiviral transduction with subsequent clonal selection is widely used to create a stable cell line of interest, it has a (tiny) chance that viral DNA that integrates into the cell genome disrupts a vital region of the genome, which may have complicated the result. Therefore, experiments in more physiologic systems such as CRISPR-Cas9 genome editing, primary cells derived from patients, or knock-in animals are needed to independently confirm our findings. Last, since neuronal development is a highly dynamic process, data from one snap-shot in a neuroblastoma cell line may represent only a small part of the whole neurodevelopmental process.

In summary, the transcriptome regulated by the two TRα1 truncating mutants, TRα1-C380fsx387 and -F397fsx406, in SH-SY5Y cells are widely different. Unstimulated gene expression controlled by the TRα1-C380fsx387 mutant is more different from WT than that controlled by the TRα1-F397fsx406 mutant. Interestingly, this involves many genes that have a vital role in neuronal development. These findings may, at least in part, explain the more severe neurological phenotype found in the patient carrying the TRα1-C380fsx387 mutation.

Acknowledgement

This work is supported by Zon-MWTOP Grant 91212044 and an Erasmus MC Medical Research Advisory Committee (MRACE) grant (RPP, MEM), and Chiang Mai University (KW).

Disclosure

The authors have nothing to disclose.

References

1. Bernal J. Thyroid hormone regulated genes in cerebral cortex development. *J Endocrinol.* 2017;**232**(2):R83-R97.
2. Bernal J. Thyroid hormone receptors in brain development and function. *Nat Clin Pract Endocrinol Metab.* 2007;**3**(3):249-259.
3. Gothie JD, Demeneix B, Remaud S. Comparative approaches to understanding thyroid hormone regulation of neurogenesis. *Mol Cell Endocrinol.* 2017;**459**:104-115.
4. Wallis K, Dudazy S, van Hogerlinden M, Nordstrom K, Mittag J, Vennstrom B. The thyroid hormone receptor alpha1 protein is expressed in embryonic postmitotic neurons and persists in most adult neurons. *Mol Endocrinol.* 2010;**24**(10):1904-1916.
5. Mellstrom B, Naranjo JR, Santos A, Gonzalez AM, Bernal J. Independent expression of the alpha and beta c-erbA genes in developing rat brain. *Mol Endocrinol.* 1991;**5**(9):1339-1350.
6. Bradley DJ, Towle HC, Young WS, 3rd. Spatial and temporal expression of alpha- and beta-thyroid hormone receptor mRNAs, including the beta 2-subtype, in the developing mammalian nervous system. *The Journal of neuroscience : the official journal of the Society for Neuroscience.* 1992;**12**(6):2288-2302.
7. Flamant F, Gauthier K, Richard S. Genetic Investigation of Thyroid Hormone Receptor Function in the Developing and Adult Brain. *Curr Top Dev Biol.* 2017;**125**:303-335.
8. van Gucht ALM, Moran C, Meima ME, Visser WE, Chatterjee K, Visser TJ, Peeters RP. Resistance to Thyroid Hormone due to Heterozygous Mutations in Thyroid Hormone Receptor Alpha. *Curr Top Dev Biol.* 2017;**125**:337-355.
9. Singh BK, Yen PM. A clinician's guide to understanding resistance to thyroid hormone due to receptor mutations in the TRalpha and TRbeta isoforms. *Clin Diabetes Endocrinol.* 2017;**3**:8.
10. Moran C, Chatterjee K. Resistance to Thyroid Hormone alpha-Emerging Definition of a Disorder of Thyroid Hormone Action. *J Clin Endocrinol Metab.* 2016;**101**(7):2636-2639.
11. Moran C, Chatterjee K. Resistance to thyroid hormone due to defective thyroid receptor alpha. *Best Pract Res Clin Endocrinol Metab.* 2015;**29**(4):647-657.
12. Bochukova E, Schoenmakers N, Agostini M, Schoenmakers E, Rajanayagam O, Keogh JM, Henning E, Reinemund J, Gevers E, Sarri M, Downes K, Offiah A, Albanese A, Halsall D, Schwabe JW, Bain M, Lindley K, Muntoni F, Vargha-Khadem F, Dattani M, Farooqi IS, Gurnell M, Chatterjee K. A mutation in the thyroid hormone receptor alpha gene. *N Engl J Med.* 2012;**366**(3):243-249.
13. van Mullem A, van Heerebeek R, Chrysis D, Visser E, Medici M, Andrikoula M, Tsatsoulis A, Peeters R, Visser TJ. Clinical phenotype and mutant TRalpha1. *N Engl J Med.* 2012;**366**(15):1451-1453.
14. van Mullem AA, Chrysis D, Eythimiadou A, Chroni E, Tsatsoulis A, de Rijke YB, Visser WE, Visser TJ, Peeters RP. Clinical phenotype of a new type of thyroid hormone resistance caused by a mutation of the TRalpha1 receptor: consequences of LT4 treatment. *The Journal of clinical endocrinology and metabolism.* 2013;**98**(7):3029-3038.
15. Tylki-Szymanska A, Acuna-Hidalgo R, Krajewska-Walasek M, Lecka-Ambroziak A, Steehouwer M, Gilissen C, Brunner HG, Jurecka A, Rozdzynska-Swiatkowska A, Hoischen A, Chrzanowska KH. Thyroid hormone resistance syndrome due to mutations in the thyroid hormone receptor alpha gene (THRA). *J Med Genet.* 2015;**52**(5):312-316.
16. Moran C, Schoenmakers N, Agostini M, Schoenmakers E, Offiah A, Kydd A, Kahaly G, Mohr-Kahaly S, Rajanayagam O, Lyons G, Wareham N, Halsall D, Dattani M, Hughes S, Gurnell M, Park SM, Chatterjee K. An adult female with resistance to thyroid hormone mediated by defective thyroid hormone receptor alpha. *J Clin Endocrinol Metab.* 2013;**98**(11):4254-4261.
17. Demir K, van Gucht AL, Buyukinan M, Catli G, Ayhan Y, Bas VN, Dundar B, Ozkan B, Meima ME, Visser WE, Peeters RP, Visser TJ. Diverse Genotypes and Phenotypes of Three Novel Thyroid Hormone Receptor-alpha Mutations. *The Journal of clinical endocrinology and metabolism.* 2016;**101**(8):2945-2954.

18. Stampfer M, Beck-Wodl S, RieB A, Haack T. Most severe case of thyroid-alpha-receptor deficiency in a female patient with severe growth and mental retardation, macrocephaly, pubertas tarda and dysgerminoma. Poster presented at The European Society of Human Genetics 28 May, 2017;P08.65A (abstract).

19. Sun H, Wu H, Xie R, Wang F, Chen T, Chen X, Wang X, Flamant F, Chen L. New Case of Thyroid Hormone Resistance alpha Caused by a Mutation of THRA /TRalpha1. *J Endocr Soc.* 2019;**3**(3):665-669.

20. Moran C, Agostini M, Visser WE, Schoenmakers E, Schoenmakers N, Offiah AC, Poole K, Rajanayagam O, Lyons G, Halsall D, Gurnell M, Chrysis D, Efthymiadou A, Buchanan C, Aylwin S, Chatterjee KK. Resistance to thyroid hormone caused by a mutation in thyroid hormone receptor (TR)alpha1 and TRalpha2: clinical, biochemical, and genetic analyses of three related patients. *Lancet Diabetes Endocrinol.* 2014;**2**(8):619-626.

21. Espiard S, Savagner F, Flamant F, Vlaeminck-Guillem V, Guyot R, Munier M, d'Herbomez M, Bourguet W, Pinto G, Rose C, Rodien P, Wemeau JL. A Novel Mutation in THRA Gene Associated With an Atypical Phenotype of Resistance to Thyroid Hormone. *J Clin Endocrinol Metab.* 2015;**100**(8):2841-2848.

22. van Gucht AL, Meima ME, Zwaveling-Soonawala N, Visser WE, Fliers E, Wennink JM, Henny C, Visser TJ, Peeters RP, van Trotsenburg AS. Resistance to Thyroid Hormone Alpha in an 18-Month-Old Girl: Clinical, Therapeutic, and Molecular Characteristics. *Thyroid.* 2016;**26**(3):338-346.

23. Moran C, Agostini M, McGowan A, Schoenmakers E, Fairall L, Lyons G, Rajanayagam O, Watson L, Offiah A, Barton J, Price S, Schwabe J, Chatterjee K. Contrasting Phenotypes in Resistance to Thyroid Hormone Alpha Correlate with Divergent Properties of Thyroid Hormone Receptor alpha1 Mutant Proteins. *Thyroid.* 2017;**27**(7):973-982.

24. Kalikiri MK, Mamidala MP, Rao AN, Rajesh V. Analysis and functional characterization of sequence variations in ligand binding domain of thyroid hormone receptors in autism spectrum disorder (ASD) patients. *Autism Res.* 2017;**10**(12):1919-1928.

25. Wejaphikul K, Groeneweg S, Hilhorst-Hofstee Y, Chatterjee VK, Peeters RP, Meima ME, Visser WE. Insight into molecular determinants of T3 vs. T4 recognition from mutations in thyroid hormone receptor alpha and beta. *J Clin Endocrinol Metab.* 2019;**104**(8):3491-3500.

26. Korkmaz O, Ozen S, Ozdemir TR, Goksen D, Darcan S. A novel thyroid hormone receptor alpha gene mutation, clinic characteristics, and follow-up findings in a patient with thyroid hormone resistance. *Hormones (Athens).* 2019;**10.1007/s42000-019-00094-9**.

27. Yuen RK, Thiruvahindrapuram B, Merico D, Walker S, Tammimies K, Hoang N, Chrysler C, Nalpathamkalam T, Pellecchia G, Liu Y, Gazzellone MJ, D'Abate L, Deneault E, Howe JL, Liu RS, Thompson A, Zarrei M, Uddin M, Marshall CR, Ring RH, Zwaigenbaum L, Ray PN, Weksberg R, Carter MT, Fernandez BA, Roberts W, Szatmari P, Scherer SW. Whole-genome sequencing of quartet families with autism spectrum disorder. *Nat Med.* 2015;**21**(2):185-191.

28. Wejaphikul K, Groeneweg S, Dejkhamron P, Unachak K, Visser WE, Chatterjee VK, Visser TJ, Meima ME, Peeters RP. Role of Leucine 341 in Thyroid Hormone Receptor Beta Revealed by a Novel Mutation Causing Thyroid Hormone Resistance. *Thyroid.* 2018;**28**(12):1723-1726.

29. Love MI, Huber W, Anders S. Moderated estimation of fold change and dispersion for RNA-seq data with DESeq2. *Genome Biol.* 2014;**15**(12):550.

30. Bernal J, Morte B. Expression Analysis of Genes Regulated by Thyroid Hormone in Neural Cells. *Methods Mol Biol.* 2018;**1801**:17-28.

31. Chatonnet F, Flamant F, Morte B. A temporary compendium of thyroid hormone target genes in brain. *Biochim Biophys Acta.* 2015;**1849**(2):122-129.

32. Gil-Ibanez P, Bernal J, Morte B. Thyroid hormone regulation of gene expression in primary cerebrocortical cells: role of thyroid hormone receptor subtypes and interactions with retinoic acid and glucocorticoids. *PLoS One.* 2014;**9**(3):e91692.

33. Huang T, Wang T, Heianza Y, Zheng Y, Sun D, Kang JH, Pasquale LR, Rimm EB, Manson JE, Hu FB, Qi L. Habitual consumption of long-chain n-3 PUFAs and fish attenuates genetically

associated long-term weight gain. *The American journal of clinical nutrition.* 2019;**109**(3):665-673.

34. Chatonnet F, Guyot R, Benoit G, Flamant F. Genome-wide analysis of thyroid hormone receptors shared and specific functions in neural cells. *Proceedings of the National Academy of Sciences of the United States of America.* 2013;**110**(8):E766-775.
35. Diez D, Grijota-Martinez C, Agretti P, De Marco G, Tonacchera M, Pinchera A, de Escobar GM, Bernal J, Morte B. Thyroid hormone action in the adult brain: gene expression profiling of the effects of single and multiple doses of triiodo-L-thyronine in the rat striatum. *Endocrinology.* 2008;**149**(8):3989-4000.
36. Miller LD, McPhie P, Suzuki H, Kato Y, Liu ET, Cheng SY. Multi-tissue gene-expression analysis in a mouse model of thyroid hormone resistance. *Genome Biol.* 2004;**5**(5):R31.
37. Morte B, Diez D, Auso E, Belinchon MM, Gil-Ibanez P, Grijota-Martinez C, Navarro D, de Escobar GM, Berbel P, Bernal J. Thyroid hormone regulation of gene expression in the developing rat fetal cerebral cortex: prominent role of the Ca2+/calmodulin-dependent protein kinase IV pathway. *Endocrinology.* 2010;**151**(2):810-820.
38. Gil-Ibanez P, Garcia-Garcia F, Dopazo J, Bernal J, Morte B. Global Transcriptome Analysis of Primary Cerebrocortical Cells: Identification of Genes Regulated by Triiodothyronine in Specific Cell Types. *Cereb Cortex.* 2017;**27**(1):706-717.
39. Jongbloets BC, Pasterkamp RJ. Semaphorin signalling during development. *Development.* 2014;**141**(17):3292-3297.
40. Mann F, Chauvet S, Rougon G. Semaphorins in development and adult brain: Implication for neurological diseases. *Prog Neurobiol.* 2007;**82**(2):57-79.
41. Masuda T, Taniguchi M. Contribution of semaphorins to the formation of the peripheral nervous system in higher vertebrates. *Cell Adh Migr.* 2016;**10**(6):593-603.
42. Dickson BJ. Molecular mechanisms of axon guidance. *Science.* 2002;**298**(5600):1959-1964.
43. Blockus H, Chedotal A. Slit-Robo signaling. *Development.* 2016;**143**(17):3037-3044.
44. Andrews WD, Barber M, Parnavelas JG. Slit-Robo interactions during cortical development. *J Anat.* 2007;**211**(2):188-198.
45. Bagri A, Marin O, Plump AS, Mak J, Pleasure SJ, Rubenstein JL, Tessier-Lavigne M. Slit proteins prevent midline crossing and determine the dorsoventral position of major axonal pathways in the mammalian forebrain. *Neuron.* 2002;**33**(2):233-248.
46. Kania A, Klein R. Mechanisms of ephrin-Eph signalling in development, physiology and disease. *Nat Rev Mol Cell Biol.* 2016;**17**(4):240-256.
47. Singhal J, Nagaprashantha LD, Vatsyayan R, Ashutosh, Awasthi S, Singhal SS. Didymin induces apoptosis by inhibiting N-Myc and upregulating RKIP in neuroblastoma. *Cancer Prev Res (Phila).* 2012;**5**(3):473-483.
48. Niethamer TK, Bush JO. Getting direction(s): The Eph/ephrin signaling system in cell positioning. *Dev Biol.* 2019;**447**(1):42-57.
49. Rajasekharan S, Kennedy TE. The netrin protein family. *Genome Biol.* 2009;**10**(9):239.
50. Boyer NP, Gupton SL. Revisiting Netrin-1: One Who Guides (Axons). *Front Cell Neurosci.* 2018;**12**:221.
51. Lanoue V, Cooper HM. Branching mechanisms shaping dendrite architecture. *Dev Biol.* 2019;**451**(1):16-24.
52. Goshima Y, Yamashita N, Nakamura F, Sasaki Y. Regulation of dendritic development by semaphorin 3A through novel intracellular remote signaling. *Cell Adh Migr.* 2016;**10**(6):627-640.
53. Ayala R, Shu T, Tsai LH. Trekking across the brain: the journey of neuronal migration. *Cell.* 2007;**128**(1):29-43.
54. Chouchane M, Costa MR. Instructing neuronal identity during CNS development and astroglial-lineage reprogramming: Roles of NEUROG2 and ASCL1. *Brain Res.* 2019;**1705**:66-74.
55. Wilkinson G, Dennis D, Schuurmans C. Proneural genes in neocortical development.

Neuroscience. 2013;**253**:256-273.

56. Guillemot F, Hassan BA. Beyond proneural: emerging functions and regulations of proneural proteins. *Curr Opin Neurobiol.* 2017;**42**:93-101.
57. Schuurmans C, Armant O, Nieto M, Stenman JM, Britz O, Klenin N, Brown C, Langevin LM, Seibt J, Tang H, Cunningham JM, Dyck R, Walsh C, Campbell K, Polleux F, Guillemot F. Sequential phases of cortical specification involve Neurogenin-dependent and -independent pathways. *EMBO J.* 2004;**23**(14):2892-2902.
58. Berninger B, Guillemot F, Gotz M. Directing neurotransmitter identity of neurones derived from expanded adult neural stem cells. *Eur J Neurosci.* 2007;**25**(9):2581-2590.
59. Tagami T, Gu WX, Peairs PT, West BL, Jameson JL. A novel natural mutation in the thyroid hormone receptor defines a dual functional domain that exchanges nuclear receptor corepressors and coactivators. *Mol Endocrinol.* 1998;**12**(12):1888-1902.
60. Rosen MD, Privalsky ML. Thyroid hormone receptor mutations found in renal clear cell carcinomas alter corepressor release and reveal helix 12 as key determinant of corepressor specificity. *Mol Endocrinol.* 2009;**23**(8):1183-1192.
61. Marimuthu A, Feng W, Tagami T, Nguyen H, Jameson JL, Fletterick RJ, Baxter JD, West BL. TR surfaces and conformations required to bind nuclear receptor corepressor. *Mol Endocrinol.* 2002;**16**(2):271-286.
62. Wu SY, Cohen RN, Simsek E, Senses DA, Yar NE, Grasberger H, Noel J, Refetoff S, Weiss RE. A novel thyroid hormone receptor-beta mutation that fails to bind nuclear receptor corepressor in a patient as an apparent cause of severe, predominantly pituitary resistance to thyroid hormone. *J Clin Endocrinol Metab.* 2006;**91**(5):1887-1895.

Supplementary Materials

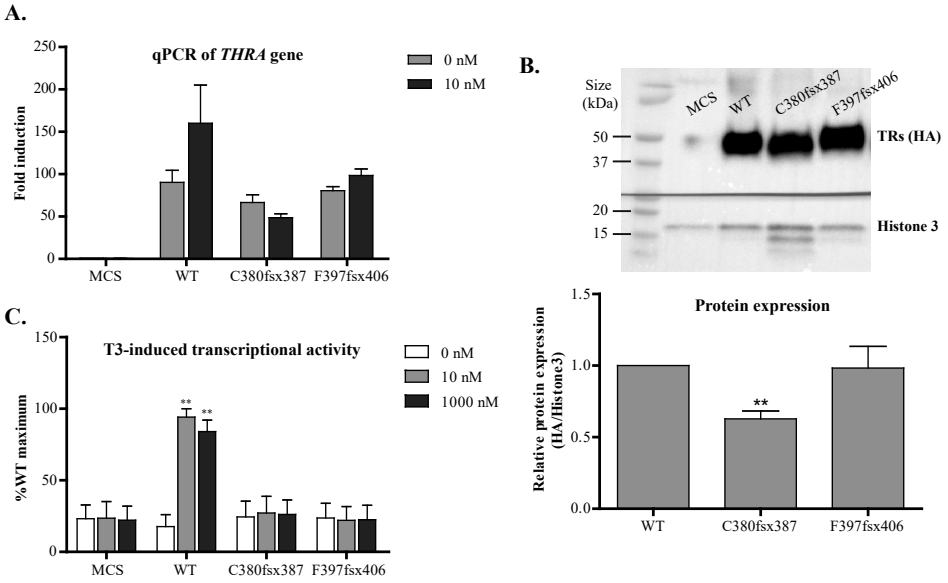

Supplementary Figure S1. (A) The qPCR analysis shows a high expression of the *THRA* in all three FHTRα1 expressing cell lines (SH-SY5Y/FHTRα1 WT, -C380fsx387, and -F397fsx406), confirming the success of FHTRα1 transduction. (B) The FHTRα1 protein expression (detected by 1:1,000 dilution of a HA antibody) showed that all three FHTRα1 are expressed in the cells with a slightly lower expression level for FHTRα1-C380fsx387 than for WT and -F397fsx406. (Relative protein expression (band intensity) of three independent blots is quantified by ImageJ program and showed as mean ± SEM, One-sample t-test compared to WT **p<0.01.) (C) The T3-induced transcriptional activity of FHTRα1 WT is increased in the presence of T3. In contrast, the two truncating mutants showed no response to T3-stimulation, indicating a complete loss of T3-induced transcriptional activity (data are shown as mean ± SEM of three independent luciferase assay experiments performed in triplicates, Student's t-test compared to 0 nM T3 **p<0.01).

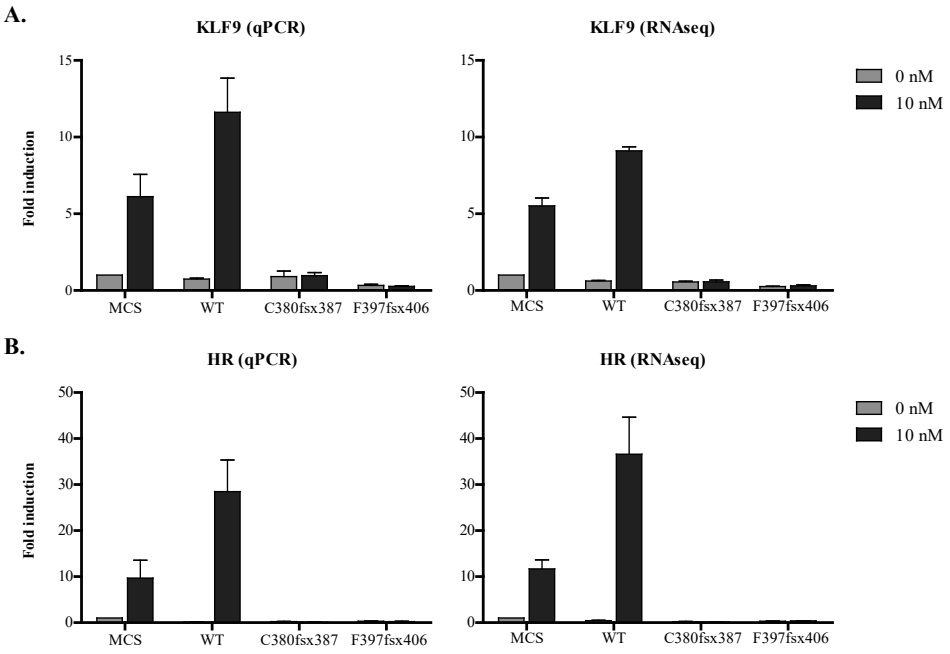

Supplementary Figure S2. qRT-PCR analysis (left panel) and RNA sequencing (right panel) of the (A) *KLF9* and (B) *HR* (Hairless) show a similar pattern between the two methods. The data are shown as mean ± SEM of the fold induction (adjusted MCS 0 nM T3 = 1).

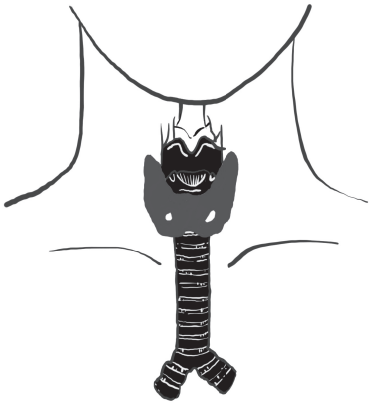

CHAPTER 6a

Human Liver and Neuronal Interactomes Reveal Novel Binding Partners for the T3 Receptor Isoform α1

Marcel E. Meima, **Karn Wejaphikul**, Selmar Leeuwenburgh, Anja L.M. van Gucht, Lona Zeneyedpour, Lennard J.M. Dekker, W. Edward Visser, Theo M. Luider, Robin P. Peeters

Submitted

6

Abstract

Thyroid hormone receptors (TRs) recruit cofactor complexes to regulate their transcriptional activity. Mutations in the TRα1 isoform result in a syndrome of resistance to thyroid hormone α (RTHα) that is characterized amongst others by growth retardation, and intellectual and motor disabilities. However, the severity of the phenotype differs widely between patients. To fully understand the impact of mutations in the RTHα syndrome beyond the effect on binding of T3 to TRα1, a comprehensive elucidation of the profiles of TRα1-associated cofactors in different tissues is required. In this study, we used a tandem-affinity purification method to identify TRα1-interactomes from a liver cell model and a neuronal cell model in the presence or absence of the ligand T3. The interactomes differed extensively between liganded and unliganded receptors. However, they mostly overlapped between the different cell types, suggesting that the general regulatory mechanisms are rather conserved in different cells. The presence of known cofactors, such as NCoR1, SRC1 and the mediator complex confirmed the validity of the approach. In addition, we identified novel putative binding partners including transcription factors and chromatin remodelling proteins. We confirmed the findings by co-immunoprecipitations. The identification of these novel binding partners of TRα1 expands the understanding of the molecular regulation of TRα1 and allows subsequent studies on the mechanisms how specific TRα1 mutations contribute to the RTHα phenotype.

Introduction

Thyroid hormone receptors (TRs) are ligand-dependent transcriptional regulators that are pivotal for the control of development, metabolism and tissue homeostasis (1,2). TRs are encoded by two genes (*THRA* and *THRB*) that yield three nuclear hormone-binding isoforms, TRα1, TRβ1, and TRβ2, which have high homology but differ in their tissue-specific distribution. TRs predominantly bind as heterodimers with Retinoid X Receptors (RXR) to thyroid hormone response elements (TREs) to regulate the expression of target genes.

Mutations in TRs can cause syndromes of resistance to thyroid hormone (RTH) with distinct clinical outcomes. RTHα, caused by mutations in *THRA,* was recently identified and is characterized by intellectual disability, growth and psychomotor retardation, and developmental delay (3). The severity of the phenotype and the panel of traits differ widely between patients. Apart from ligand binding affinity, this may be explained by impaired recruitment of specific cofactors, some of which may be expressed or associated in a tissue-specific pattern. A thorough identification of tissue-specific interactomes of liganded and unliganded TRα1 will therefore contribute to better understanding the molecular regulation of TRα1 action in health and disease.

Similar to other nuclear receptors (NRs), TR activity is regulated via recruited cofactors that determine the local chromatin structure and thereby facilitate the accessibility to the promoter region of target genes (4). In the absence of triiodothyronine (T3), the biologically active form of thyroid hormone (TH), TRs are bound to members of the nuclear corepressor/silencing mediator for retinoid and thyroid hormone receptors (NCoR/SMRT) proteins that recruit a complex of proteins that favour histone deacetylation, which renders the local chromatin in a closed confirmation. Binding of T3 induces conformational changes of the TRs that cause the NCoR/SMRT complex to dissociate and results in the recruitment of members of the Nuclear Coactivator (NCoA) family, also known as steroid receptor coactivators (SRCs), which are complexed with histone acetyl transferases (HATs). This results in acetylation of histones, which turns the local chromatin in an open and accessible state allowing the subsequent recruitment of the Mediator complex, which recruits general transcription factors (GTFs) and the RNA polymerase II complex to initiate gene transcription (5-7). Apart from these classical cofactors, numerous proteins have been identified that can directly bind to TRs and modulate their transcriptional activity, including other scaffolding and chromatin remodeling proteins, transcription factors, signaling proteins, and structural proteins (8-11). Some of these non-classical cofactors exhibit isoform preference, (11,12), adding to the complexity of TH action.

Previous studies that identified TR-interacting proteins and protein complexes used two-hybrid (8), GST-pull downs (11), and affinity purification methods (5,12). Fozzatti and coworkers developed a tandem-affinity purification (TAP) method to purify isoform-specific interacting proteins from HeLa cells (12). However, their study was limited to proteins associated

with TR mutants deficient in T3-binding and returned only a limited number of proteins that were isolated from SDS-PAGE gels. In the current study, we optimized their method to purify TRα1-interactomes from models for liver cells and neuronal cells in the presence or absence of ligand, and subsequently to co-purify proteins of the intact complexes that were identified by LC-MS/MS without prior separation. The interactomes mostly overlapped between the two cell types, but differed strongly between liganded and unliganded receptors. Importantly, we identified novel interacting proteins and multisubunit complexes with yet to be identified regulatory functions in TH action.

Materials and methods

Cell culture

293FT (Thermofisher, #R70007), human HepG2 (ATCC® HB-8065™) hepatocellular carcinoma and human SH-SY5Y (ATCC® CRL-2266™) neuroblastoma cells were grown in DMEM/F12 medium (Lonza), supplemented with 9% FBS (Lonza), 100 U/ml penicillin, 100 µg/ml streptomycin (Lonza), and 100 nM Na_2SeO_3 at 37 °C and 5% CO_2. Cells were routinely passaged and medium refreshed twice a week. Before transfections, the medium was first replaced with hypothyroid Ct-medium (DMEM/F12, 9% charcoal-treated FBS without penicillin/streptomycin).

Constructs

The plasmid pCDNA3-FLAGTRα1 was used to transiently express FLAG-tagged human TRα1 as described previously (13). A lentiviral construct was used to stably express N-terminal FLAG and hemagglutinin (HA) double-epitope tagged human TRα1 (from hereon called FHTRα1). To select cells, we used a construct that produces a bicistronic messenger from which FHTRα1 is translated together with the puromycin selection marker coupled to GFP by a cleavable 2A peptide (Supplementary Figure S1). The entry vectors pENTL1-MCS-R5, pENTL5-IRESPuro2AGFP-R2, the lentiviral vector pWCAGpCasC, and the packaging vectors pMD2.G and psPAX2 were all kindly gifted by Dr. Lammert Dorssers (Department of Pathology, Erasmus MC, Rotterdam). Please see the supplemental methods for the generation of the plasmids pWCAGpCasC-MCS-IRESPuro2AGFP and pWCAGpCasC-FHTRα1-IRESPuro2AGFP (from hereon called pLentiMCS or pLentiFHTRα1) (14).

Lentivirus production and transduction

To generate lentiviral particles, 293FT cells were seeded into 10 cm dishes and transfected with 4 µg of pLentiMCS or pLentiFHTRα1, 4 µg psPAX2, and 4 µg pMD2.G at ~90% confluency in growth medium without antibiotics, using Xtreme Gene. Supernatants were harvested at 48 and 72 hour after transfection and subsequently, filtered through 0.45 µm

PES filters to obtain cell-free lentiviral stocks. For infections, HepG2 and SH-SY5Y cells were seeded in growth medium in 6-wells dishes and infected at ~25% confluency with different amounts of viral stocks. After 2 days, infected cells were selected with 2 µg/ml puromycin. The medium was refreshed every 2-3 day and wells with similar number of puromycin resistant cells were expanded and used for further analysis.

Luciferase assay

HepG2 and SH-SY5Y cells stably expressing FHTRα1 were seeded in 24 wells plates and grown in growth medium to 70-80% confluency. The cells were transfected with Xtreme Gene (Roche) using the manufacturer's protocol in Ct medium with 200 ng of the plasmid pdV-L1 that contains firefly luciferase under control of a direct and inverted repeat TRE, and renilla luciferase as described previously (15). Results are presented as the means ± SEM of three experiments performed in triplicate.

Tandem-affinity purification (TAP)

FHTRα1 expressing or MCS control cells were seeded in growth medium in 10 (HepG2) or 20 (SH-SY5Y) 145 mm dishes per cell line per condition. At 80-90% confluency, the cells were incubated overnight with DMEM/F12 supplemented with 0.1% BSA and subsequently incubated for 4 hours with vehicle or 100 nM T3. FHTRα1-containing protein complexes in nuclear extracts were sequentially purified on anti-FLAG and anti-HA resins as described previously with adaptations (12). A detailed protocol of the purification and LC-MS/MS analysis of the enriched proteins is provided in the supplementary material section (14).

Co-immunoprecipitations

HepG2 or SH-SY5Y cells were transfected with the plasmids pCDNA3-FLAGTRα1 or pCDNA3 as empty vector control in Ct medium with Xtreme Gene (Roche) according to the manufacturer's protocol. After overnight incubation in DMEM/F12 supplemented with 0.1% BSA, the cells were stimulated with vehicle or 100 nM T3 for 4 hours. Cells were collected in buffer A (10 mM Hepes.NaOH, 10 mM KCl, 0.1 mM EDTA, 1 mM DTT, cOmplete™ protease inhibitors (Roche), pH 7.9) and lysed by adding 0.6% NP40. Nuclei were extracted in buffer C (20 mM HEPES.NaOH, 400 mM NaCl, 1 mM EDTA, 1 mM DTT, cOmplete™ protease inhibitors, pH 7.9) and diluted in buffer D (20 mM HEPES.NaOH, 1 mM EDTA, cOmplete™ protease inhibitors, pH 7.9) to restore NaCl concentrations to 150 mM. Nuclear extracts were incubated overnight with 10 µl bed volume of FLAG-agarose beads (clone M2; Sigma). The beads were washed 4 times with 1 ml wash buffer (20 mM HEPES.NaOH, 150 mM NaCl, 1 mM EDTA, 1 mM DTT, pH 7.9) and eluted with 200 µg/ml FLAG peptide in wash buffer. Nuclear extracts and immunocomplexes were denatured in 1x NuPAGE LDS sample buffer supplemented with 10 mM DTT at 70 °C for 10 minutes.

Immunoblotting

Nuclear extracts and immunocomplexes were separated on 4-15% Mini-Protean TGX gels (Bio-rad) and transferred to Immobilon PDVF membranes (Whatmann). Membranes were probed with 1:1000 dilutions (unless stated otherwise) of the following antibodies: FLAG M2 clone (F1804, RRID:AB_262044), Prox1 (1:2000) (P7124, RRID:AB_1079691) (both Sigma Aldrich), HA (clone C29F4, #3724, RRID:AB_10693385), CHD4 (clone D8B12, #11912, RRID:AB_2751014), NCoR1 (#5948, RRID:AB_10834809), RXRα (clone D6H10, #3085, RRID:AB_11140620), SRC-1 (clone 128E7, #2191, RRID:AB_2196189), HDAC3 (clone 7G6C5, #3949, RRID:AB_10986336), MED26 (clone D4B1X, #14950, RRID:AB_2798656), Histone 3(clone 1B1B2, #14269, RRID:AB_2756816), Brg1 (clone D1Q7F, #49360, RRID:AB_2728743), KIF11/Eg5 (#7625, RRID:AB_10860412) (all Cell Signaling Technology). Blots were then probed with 1:3000 dilutions of horse radish peroxidase (HRP)-conjugated goat anti-mouse or goat anti-rabbit (Biorad) and proteins were visualized by Enhanced Chemiluminescence (ECL).

Results

Stable expression of FHTRα1 in HepG2 and SH-SY5Y cells

HepG2 and SH-SY5Y cell lines that stably expressed FHTRα1 transcribed from a bicistronic messenger RNA that also encodes the puromycin selection marker and GFP for selection of transduced cells (Supplementary Figure S1 (14)) were successfully generated. Cells transduced with the empty vector (MCS) that only expresses the puromycin selection marker and GFP were also generated as a control. Equal amounts of nuclear extracts prepared from all stable cell lines were analysed by immunoblotting. By probing with HA antibodies, specific bands at the predicted size of ~49 kD were visualized for both HepG2 and SH-SY5Y cells (Figure 1A). A dose-dependent increase in luciferase activity was found in both HepG2 and SH-SY5Y cells expressing FHTRα1 after 24 hours T3 incubation, confirming that the FH-tag did not interfere with receptor activation (Figure 1B).

Tandem-affinity purifications (TAP)

To confirm the effectiveness of our TAP protocol, we first purified FHTRα1 from HepG2 cells that had been stimulated for 4 hours with 100 nM T3 or vehicle. A third of the final eluate was separated by SDS-PAGE. After visualization by Colloidal Coomassie Blue staining, the bait as well as additional bands were shown in lanes with eluates from HepG2/FHTRα1 but not control (MCS) cells, confirming that our method is effective to purify TRα1 and associated proteins (Supplementary Figure S2 (14)). In addition, the staining pattern differed between cells incubated in the presence or absence of T3, indicating that the association of many proteins depended on the occupation state of the receptor.

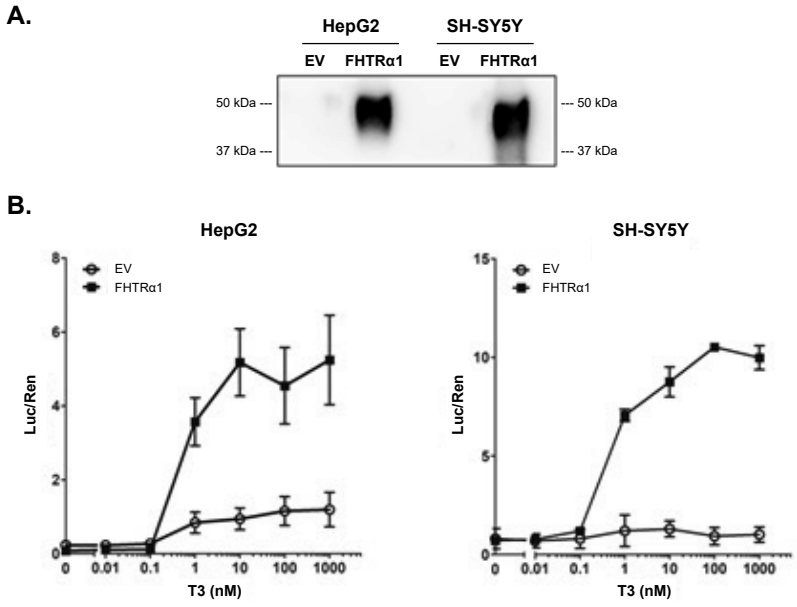

Figure 1. *FHTRα1 has T3-stimulated activity.* (A) Western blot showing expression of FHTRα1 in HepG2 and SH-SY5Y cells. Equal amounts of nuclear proteins extracted from HepG2 and SH-SY5Y cells with stable integration of FHTRα1 or empty vector (MCS) as control were immunoblotted with an HA antibody. (B) Luciferase reporter assay showing T3-dependent transcriptional activity of FHTRα1. HepG2 and SH-SY5Y cells with stable integration of FHTRα1 or empty vector (MCS) as control were transfected with a reporter construct in which the gene encoding firefly luciferase is under control of a TRE and constitutively expresses renilla luciferase as transfection control, incubated with increasing concentrations of T3 and lysates measured for luciferase and renilla activity. Data represent mean ± SEM of three independent experiments performed in triplicate.

General composition of the interactomes

An additional purification from HepG2 cells, and two independent purifications from SH-SY5Y cells were performed, and all eluates were subjected to LC-MS/MS analysis. Proteins that were identified with an FDR of 1% in any of the control purifications were excluded. A total number of 252 proteins were identified in all purifications combined (Supplementary Table 1 (14)). Gene enrichment analysis for cellular compartments using DAVID showed that 148 were nuclear proteins (Benjamini corrected p value for enrichment $2.0x10^{-20}$, Supplementary Figure S3 (14)). Proteins generally overlapped between purifications for the same cell type and condition (Table 1), although the second HepG2 purification returned a larger number of hits many of which were not present in the first purification. This may be due to impurity of the enriched complex, which is underscored by the relatively large number of ribosomal and ribonuclear proteins (Table 2, Supplementary Table 1 (14)).

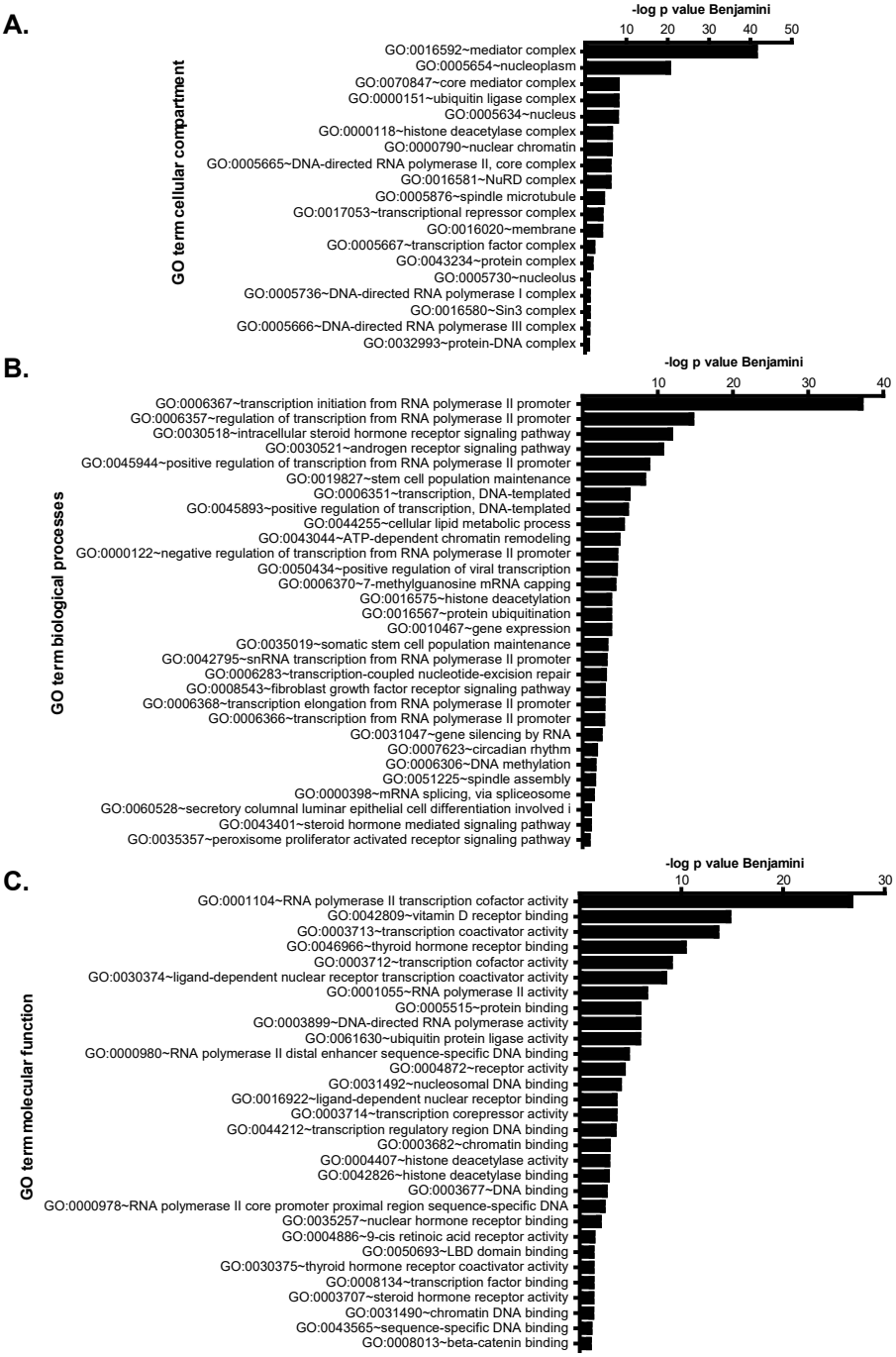

Figure 2. *Enrichment of GO terms in the profile.* Proteins that were replicated in for at least one cell line and condition (see Table 2) were analysed for enrichment of (A) cellular compartments, (B) biological processes or (C) molecular function using DAVID (minimum count 2, ease 0.1). The top 30 most significant GO terms are displayed. P values were adjusted for false discovery rates using the Benjamini correction.

Table 1: Total number of hits and replication between purifications

Cell/condition	Purification 1	Purification 2	Overlap
HepG2 vehicle	22	130	11
HepG2 T3	58	76	37
SH-SY5Y vehicle	21	21	9
SH-SY5Y T3	20	65	14

Proteins and peptides were compared with Scaffold version 4.8.3. FDR was set at 1% for proteins and peptides. Probability scores that met criteria were 5% for proteins and 78% for peptides and 2 peptides minimum for HepG2 purification and 99% and 91% with 1 peptide for the other purifications. Proteins found in control purifications were excluded.

Many copurifying proteins belong to protein complexes and are involved in gene regulation

Of the total number of proteins, 55 were replicated for at least one cell type plus condition, and are listed with probability scores and coverage (exclusive unique peptides and percentage coverage) in Table 2. For global analysis of the functional relevance of these proteins, we used DAVID for gene enrichment analysis (Figure 2). For biological processes and molecular functions, we found enrichment of transcriptional regulation via the RNA polymerase II complex, nuclear receptor signalling and regulation, histone modification, chromatin remodelling and cofactor binding, all confirming a strong association of the profile with gene regulation. Enrichment for cellular components showed that the profile is strongly enriched for nuclear chromatin binding proteins and/or proteins associated with complexes that are involved in gene regulation, such as Mediator complex, histone deacetylation complexes, RNA polymerase II complex, and the nuclear remodelling and deacetylase (NuRD) complex. Screening of the entire profile of 252 proteins for cellular components identified enrichment of additional chromatin remodelling complexes with lower coverage and significance, including the strongly overlapping SWItch/Sucrose Non-Fermentable (SWI/SNF), neuron-specific BRG1 or HBRM-associated factor (nBAF) and neural progenitor BAF (npBAF) complex, and the mixed-lineage leukemia 4 (MLL4) complex (Supplementary Figure S3 (14)).

Dependence of ligand state and cell lineage on composition of TRα1-interactomes

To characterize the protein complexes in our profiles and the effect of T3-binding, we built an interaction network based on experimentally proven interactions using the STRING database where we separated between proteins found in the presence or absence of T3 (Figure 3). In addition, we listed proteins by complexes and/or function by cell-type and ligand

state (Table 3). Since there were differences in recovery between HepG2 and SH-SY5Y cells and because distant interactions of some members of the complexes may have been so weak that they were close to the limit of detection, we included here proteins that were found in a single purification, when they belonged to a specific protein complex. As expected, TRα1 is associated with RXRs in the presence or absence of T3. In the absence of T3, the receptor is associated with the NCoR1-complex that further contains HDAC3 and the F-Box/WD40 repeat-containing proteins TBL1X and TBL1XR1. Both the corepressor nuclear receptor interacting protein 1 (NRIP1) and the Mediator complex were found under both conditions but strongly upregulated by T3, as indicated by the higher number of peptides and number of subunits for Mediator in the presence of T3, whereas the RNA polymerase II complex was only found in the presence of T3 (Figure 3 and Table 2). Surprisingly, we only found NCoAs in a single purification in the presence of T3 from HepG2, namely NCoA1/SRC1 and NCoA3/SRC3 (Supplementary Table 1 (14)), and no HATs. The NuRD complex was also present under both conditions, but slightly enriched by T3 (Table 3). Like NRIP1, the association of prospero homeobox 1 (Prox1) was increased by T3, whereas the phosphoserine/threonine phosphatase PPM1G was only found in the absence of T3.

The profiles extensively overlapped between cell lines. Both HepG2 and SH-SY5Y cells yielded the NCoR/SMRT, Mediator, and NuRD complexes (Tables 2 and 3). A number of hits appeared specific for a single cell line. NRIP1 was abundantly present in purifications from T3-treated HepG2 cells only (Table 2). In SH-SY5Y cells, we found a higher number of SWI/SNF complex members and specific association of transcription factor 4 (TCF4), and the protein encoded by the open reading frame C11orf84 (Table 3). In addition, the structural proteins KIF11 (also known as thyroid hormone receptor interacting protein 5 (TRIP5) and Eg5) and CLASP2 were only found in from SH-SY5Y cells. Other proteins that copurified with FHTRα1 in a cell-type specific manner appear less relevant for gene regulation, such as extracellular proteins, mitochondrial enzymes or membrane transport.

Co-immunoprecipitations confirm LC-MS/MS profiles

To validate selected hits from our profiles, we immunoprecipitated FLAG-TRα1 from transiently transfected HepG2 and SH-SY5Y cells using FLAG antibodies and immunoblotted the immunocomplexes (Figure 4). In both cell types, NCoR1 and HDAC3 were only detected in cells treated with vehicle, and SRC1 and MED26 (as representative of the Mediator complex) in T3-treated cells, whereas the association of RXRα was modestly increased by T3. Chromodomain helicase 4 (CHD4) was chosen as representative of the NuRD complex and specifically copurified with FLAG-TRα1 from both cell types. The transcription Prox1 copurified with FLAG-TRα1 from both cell types as well, and the association was strongly increased by T3, consistent with the increased coverage of Prox1 with T3 in the LC-MS/MS profiles (Table 2). Only BRG1 (also known as SMARCA4 and belonging to SWI/SNF and BAF complexes) and KIF11 were also present in immunoprecipitations from cells transfected with the empty vector and thus are likely false positives (results not shown).

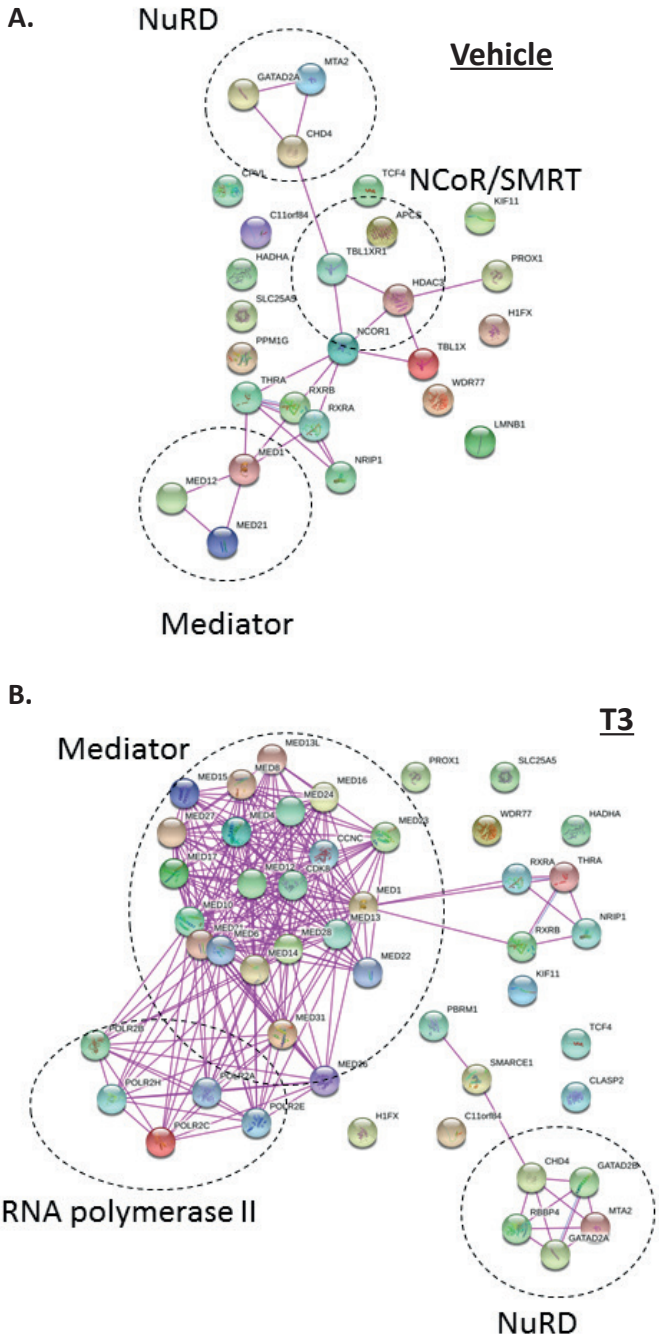

Figure 3. *Protein networks in the protein profile and the effect of ligand state.* Proteins that were replicated in at least one cell line and condition (see Table 2) were mined for existing experiment-based protein interactions, using STRINGS with minimum required interaction scores set at medium (0.400). Profiles found for the (A) absence or (B) presence of T3 were analysed separately. Dashed circles indicate protein complexes.

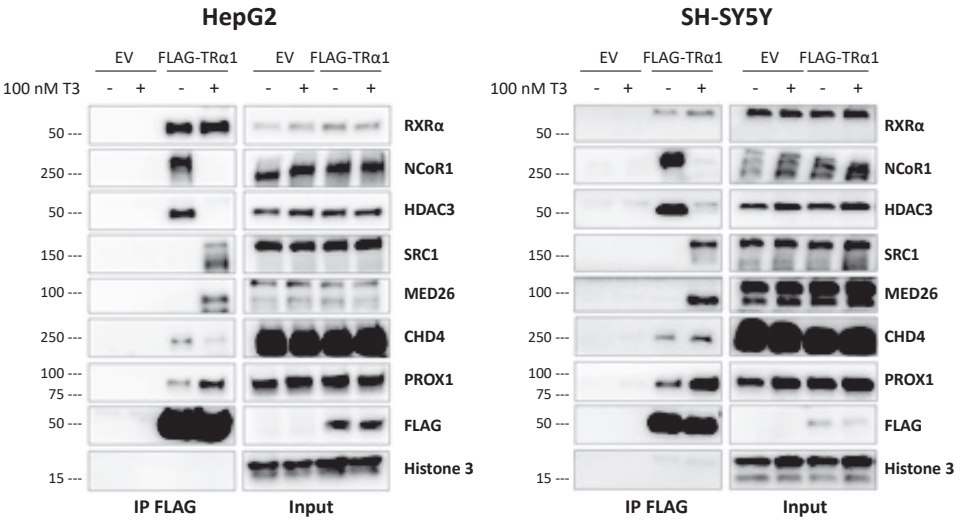

Figure 4. *Immunoprecipitation confirms association of selected proteins from the profiles with FHTRα1.* Representative immunoblots showing co-immunoprecipitation of selected hits with FHTRα1 from HepG2 and SH-SY5Y cells. Nuclear extracts from HepG2 and SH-SY5Y cells transfected with FLAG-TRα1 or empty vector (EV) as control were subjected to immunoprecipitation with anti-FLAG resin, proteins eluted with the FLAG peptide and the immunocomplexes or 10% of the nuclear extracts as input control subjected to western blotting. Segments of the blot around the expected molecular weight of the targeted proteins were immunoblotted with the indicated antibodies. Histone 3 was used as control for equal input.

Table 2. Protein replicated for at least one cell type and condition (**MW**, molecular weight; **Prob**, probability; **EUP**, exclusive unique peptides; **Cov**, coverage)

Protein name	Gene ID	MW (kDa)	HepG2												SH-SY5Y											
			Vehicle						100 nM T3						Vehicle						100 nM T3					
			Purification 1			Purification 2			Purification 1			Purification 2			Purification 1			Purification 2			Purification 1			Purification 2		
			Prob (%)	# EUP	Cov (%)	Prob (%)	# EUP	Cov (%)	Prob (%)	# EUP	Cov (%)	Prob (%)	# EUP	Cov (%)	Prob (%)	# EUP	Cov (%)	Prob (%)	# EUP	Cov (%)	Prob (%)	# EUP	Cov (%)	Prob (%)	# EUP	Cov (%)
Serum amyloid P-component	APCS	25.4													99.7	1	5.4	99.6	1	5.4						
Uncharacterized protein C11orf84	C11orf84	41.0													99.3	1	2.4	100	1	2.4	100	2	5.3	100	2	5.3
Cyclin-C	CCNC	33.2							100	3	9.9	100	1	3.5												
Cyclin-dependent kinase 8	CDK8	53.3							100	5	10.1	100	2	4.5												
Chromodomain-helicase-DNA-binding protein 4	CHD4	218.0				100	2	1.2	100	1	3.1	100	1	0.7												
CLIP-associating protein 2	CLASP2	141.1																			100	2	2.2	100	4	3.7
Probable serine carboxypeptidase CPVL	CPVL	54.2	100	2	3.8	99.9	1	2.1										99.5	1	2.9						
Transcriptional repressor p66-alpha	GATAD2A	68.1							100	2	5.7	99.9	1	1.9												
Transcriptional repressor p66-beta	GATAD2B	65.3							100	2	6.8	100	3	10.0										100	2	5.7
Histone H1x	H1FX	22.5																100	2	10.8	100	2	9.9	100	2	12.2
Trifunctional enzyme subunit alpha, mitrochondrial	HADHA	83.0	100	2	3.9	100	4	6.2				98.6	1	1.8												
Histone deacetylase 3	HDAC3	48.8	100	7	23.6	100	4	9.6																		
Kinesin-like protein KIF11	KIF11	119.2													99.0	1	1.3	99.9	2	2.7	100	2	2.7	100	3	3.6
Lamin-B1	LMNB1	66.4	91.6	1	3.2	99.8	1	4.1																		
Mediator of RNA polymerase II transcription subunit 1	MED1	168.5				99.9	1	0.9	100	21	16.3	100	17	13.4							100	2	1.5	100	5	3.9

Protein name	Gene ID	MW (kDa)	HepG2												SH-SY5Y											
			Vehicle						100 nM T3						Vehicle						100 nM T3					
			Purification 1			Purification 2			Purification 1			Purification 2			Purification 1			Purification 2			Purification 1			Purification 2		
			Prob (%)	# EUP	Cov (%)	Prob (%)	# EUP	Cov (%)	Prob (%)	# EUP	Cov (%)	Prob (%)	# EUP	Cov (%)	Prob (%)	# EUP	Cov (%)	Prob (%)	# EUP	Cov (%)	Prob (%)	# EUP	Cov (%)	Prob (%)	# EUP	Cov (%)
Mediator of RNA polymerase II transcription subunit 10	MED10	15.7							100	4	36.3	100	1	6.7												
Mediator of RNA polymerase II transcription subunit 12	MED12	243.1				99.7	1	0.6	100	19	11.8	100	8	4.9										100	3	1.8
Mediator of RNA polymerase II transcription subunit 13	MED13	239.3							100	17	10.2	100	6	3.9												
Mediator of RNA polymerase II transcription subunit 13-like	MED13L	242.6							100	5	2.9	100	3	2.5												
Mediator of RNA polymerase II transcription subunit 14	MED14	160.6							100	16	12.7	100	7	5.2										100	3	2.4
Mediator of RNA polymerase II transcription subunit 15	MED15	86.8							100	5	8.3	100	2	3.1										99.6	1	1.4
Mediator of RNA polymerase II transcription subunit 16	MED16	96.8							100	8	10.4	100	2	2.4										99.8	1	1.3
Mediator of RNA polymerase II transcription subunit 17	MED17	72.9							100	14	19.7	100	7	10.6										100	2	3.7
Mediator of RNA polymerase II transcription subunit 21	MED21	15.6	100	2	22.2				100	3	27.1	100	2	22.2												
Mediator of RNA polymerase II transcription subunit 22	MED22	22.2							100	6	21.0	100	3	13.5												
Mediator of RNA polymerase II transcription subunit 23	MED23	156.5							100	6	4.5	99.9	1	1.2												
Mediator of RNA polymerase II transcription subunit 24	MED24	110.3							100	9	13.1	100	4	5.3										100	1	1.8

Protein name	Gene ID	MW (kDa)	HepG2												SH-SY5Y											
			Vehicle						100 nM T3						Vehicle						100 nM T3					
			Purification 1			Purification 2			Purification 1			Purification 2			Purification 1			Purification 2			Purification 1			Purification 2		
			Prob (%)	# EUP	Cov (%)	Prob (%)	# EUP	Cov (%)	Prob (%)	# EUP	Cov (%)	Prob (%)	# EUP	Cov (%)	Prob (%)	# EUP	Cov (%)	Prob (%)	# EUP	Cov (%)	Prob (%)	# EUP	Cov (%)	Prob (%)	# EUP	Cov (%)
Mediator of RNA polymerase II transcription subunit 26	MED26	65.4							100	5	8.2	100	4	7.0												
Mediator of RNA polymerase II transcription subunit 27	MED27	35.4							100	7	25.1	100	2	6.4												
Mediator of RNA polymerase II transcription subunit 28	MED28	19.5							100	4	20.8	100	1	7.3										99.6	1	7.3
Mediator of RNA polymerase II transcription subunit 31	MED31	15.8							100	3	19.1	100	1	13.0												
Mediator of RNA polymerase II transcription subunit 4	MED4	29.7							100	8	37.8	100	5	22.2												
Mediator of RNA polymerase II transcription subunit 6	MED6	28.4							100	8	24.0	100	5	24.4							98.9	1	4.5	100	1	5.7
Mediator of RNA polymerase II transcription subunit 8	MED8	29.1							100	5	22.8	100	4	16.8												
Metastasis-associated protein MTA2	MTA2	75.0				100	3	5.1	100	3	6.1	100	4	7.2							99.9	1	2.3	100	2	5.4
Nuclear receptor corepressor 1	NCOR1	270.2	100	37	19.5	100	36	15.9							100	4	2	100	4	1.9						
Nuclear receptor-interacting protein 1	NRIP1	126.9	100	5	5.8				100	22	22.9	100	8	8.2												
Protein polybromo-1	PBRM1	193.0																			100	2	1.4	100	3	1.9
DNA-directed RNA polymerase II subunit RPB1	POLR2A	217.2							100	22	13.3	100	7	4.7												
DNA-directed RNA polymerase II subunit RPB2	POLR2B	133.9							100	12	12.2	100	2	2.1												

Protein name	Gene ID	MW (kDa)	HepG2												SH-SY5Y											
			Vehicle						100 nM T3						Vehicle						100 nM T3					
			Purification 1			Purification 2			Purification 1			Purification 2			Purification 1			Purification 2			Purification 1			Purification 2		
			Prob (%)	# EUP	Cov (%)	Prob (%)	# EUP	Cov (%)	Prob (%)	# EUP	Cov (%)	Prob (%)	# EUP	Cov (%)	Prob (%)	# EUP	Cov (%)	Prob (%)	# EUP	Cov (%)	Prob (%)	# EUP	Cov (%)	Prob (%)	# EUP	Cov (%)
DNA-directed RNA polymerase II subunit RPB3	POLR2C	31.4							100	6	36	100	2	6.6												
DNA-directed RNA polymerase I, II, III subunit RPABC1	POLR2E	24.6							100	4	23.8	100	2	8.6												
DNA-directed RNA polymerase I, II, III subunit RPABC3	POLR2H	17.1							100	2	10.7	100	3	25.3												
Protein phosphatase 1G	PPM1G	59.3				100	4	10.8							100	4	6.2	100	4	10.8						
Prospero homeobox protein 1	PROX1	83.2				100	6	9.8	100	11	15.6	100	13	19.0	100	2	4.5	100	3	6.1	100	7	11.1	100	14	19.1
Histone-binding protein RBBP4	RBBP4	47.7							100	1	7.5	100	2	4.7										99.5	1	2.1
Retinoic acid receptor RXR-alpha	RXRA	50.8	100	5	18.6	100	4	22.9	100	5	22.5	99.9	1	10.6												
Retinoic acid receptor RXR-beta	RXRB	56.9	100	10	30.0	100	6	23.5	100	12	41.7	100	7	26.1	100	1	4.9				100	3	9.2	100	4	9.2
ADP/ATP translocase 2	SLC25A5	32.9	100	2	7.4	100	2	7.1				99.7	1	3.7										100	2	10.4
SWI/SNF-related regulator of chromatin subfamily E member 1	SMARCE1	46.6																			100	2	6.3	100	3	9.3
F-box-like/WD repeat-containing protein TBL1X	TBL1X	62.5	100	8	28.9	100	3	14.2																		
F-box-like/WD repeat-containing protein TBL1XR1	TBL1XR1	55.6	100	13	48.4	100	6	19.8							100	3	9.7	100	4	12.5						
Transcription factor 4	TCF4	71.3																100	1	1.4	100	2	3.8	100	2	3.8

Table 3: Proteins by complexes and/or molecular function

Complex	HepG2		SH-SY5Y	
	vehicle	T3	vehicle	T3
Nuclear receptors	**THRA, RXRA, RXRB**	**THRA, RXRA, RXRB**	**THRA,** RXRB	**THRA, RXRB**
NCoR/SMRT	**NCoR1**, NCoR2, **HDAC3**,**TBL1X, TBL1XR1**, TBL1Y		NCoR1, TBL1XR1	
Other corepressors	NRIP1	**NRIP1**	**C11orf84**	**C11orf84**
Mediator	MED1, MED12, MED21	**MED1**, **MED4**, **MED6,** MED7, **MED8,** MED9**, MED10,** MED11, **MED12-17, MED13L,** MED19-20**, MED21-24, MED26-28,** MED29, **MED31, CCNC**, **CDK8**		**MED1, MED6,** MED12, MED14-17, MED24, MED28
RNA polymerase II		**POLR2A-C,** POLR2D, **POLR2E, POLR2H**, POLR2I, PAF1, RECQL5, RPAP2		
NuRD	CHD4, MTA1, MTA2	**CHD4, GATAD2A, GATAD2B,** HDAC2, MBD3, MTA1, **MTA2**, MTA3, **RBBP4,** RBBP7		GATAD2B**,** HDAC2, MTA1, **MTA2,** RBBP4
SWI/SNF nBAF npBAF	SMARCC2	SMARCB1		ACTL6A, **PBRM1**, SMARCA4/ BRG1, SMARCB1, **SMARCE1**
Histones			H1FX	**H1FX**
Transcription factor	PROX1	**PROX1**	PROX1, TCF4	**PROX1, TCF4**
Phosphatases	PPM1G		PPM1G	
Methylosome complex	WDR77		WDR77	WDR77
Membrane transport	**SLC25A5**	SLC25A5		
Enzyme	**HADHA, CPVL**	HADHA	CPVL	
Structural	LMNB1		KIF11	CLASP2, KIF11
Extracellular			APCS	

Proteins that were replicated for a cell line and condition are in bold. Proteins that were not replicated were included when they were replicated for another cell line and condition or when they belong to a protein complex (normal font).

Discussion

In this study, we purified TRα1 from two cell models in the presence and absence of the natural ligand T3 and identified several unknown binding partners of TRα1 by LC-MS/MS. Our approach revealed that the composition of TRα1-interactomes mostly overlaps between the two studied cell-types and strongly depends on ligand-state. In addition, we found novel putative binding partners, most notably transcription factors and proteins belonging to chromatin remodelling complexes.

Two important aims of our approach were to determine the effect of ligand and cell background on the composition of TRα1-interactomes. As expected, the interactomes varied clearly between unliganded and liganded receptors. This was confirmed by co-immunoprecipitations for members of the NCoR1, NCoA/SRCs and Mediator complexes, but also for potentially novel candidates such as the transcription factor Prox1. Whether these novel partners act as global regulators of T3-dependent TR activity or are involved in the regulation of a subset of genes at the cross-road of TH and other signalling pathways remains to be elucidated. The analysis of cell specificity dependence was complicated by the fact that recoveries of the bait and number of co-purifying proteins were consistently lower from SH-SY5Y cells than from HepG2 cells. As a result, interactions that are weakly preserved or are only incorporated in a subset of transcriptional complexes could have fallen below the detection limit in purifications from SH-SY5Y cells. This is underscored by the recovery of substantially less members of conserved protein complexes like Mediator from SH-SY5Y cells than from HepG2 cells. The lower recovery is likely due to the lower amount of input from SH-SY5Y cultures, even though we used twice the amount of tissue culture plates. Despite this, a number of hits were replicated in a single type, for example NRIP1 in HepG2 cells and TCF4 in SH-SY5Y cells, suggesting a cell-type specific association with TRα1 which could contribute to cell-type specific gene regulation. However, since according to the human protein atlas (https://proteinatlas.org) both proteins are expressed in liver and brain, but NRIP1 only in HepG2 and TCF4 only in SH-SY5Y cells, it cannot be proven whether the association is specific for the cellular context or merely a consequence of expression in the cell models.

Several proteins in our profiles belong to multisubunit chromatin remodelling complexes. Chromatin remodelling complexes combine different enzymatic activities that alter the local chromatin architecture by affecting the state of histone acetylation and methylation and repositioning nucleosomes. Most notably, we found many members of the NuRD complex, including CHD4, GATA zinc finger domain containing 2A and 2B (GATAD2A/GATAD2B), metastasis-associated factors (MTA1/MAT2/MTA3), histone binding proteins (RBBP4 and weakly RBBP7) and methyl-CpG domain binding protein (MBD3). The NuRD complex is a chromatin remodelling complex that facilitates predominantly transcriptional repression by combining helicase and histone deacetylase activities (16) and has been shown to repress TR activity in a *Xenopus* oocyte model (17). CHD4 was previously shown to co-purify with mutant TRs (12), and here co-immunoprecipitated with WT TRα1 in HepG2 and SH-SY5Y

cells (Figure 4). Interestingly, CHD4 directly binds to the nuclear receptor Retinoid Orphan Receptor gamma (RORγ) and inhibits its transcriptional activity (18).

Members of SWI/SNF complexes, also known as the BAF (BRG1/BRM-associated factors) complex, were weakly present in our profiles. BAF complexes are ATP-dependent chromatin remodelling complexes that confer epigenetic regulation of gene expression by altering the positioning of nucleosomes, and altered activity is associated with developmental disorders and cancer (19,20). Studies using TRβ1 and reporter construct injected *Xenopus* oocytes showed T3-stimulated recruitment of BRG1/SMARCA4 to chromatin (21). BAF proteins were predominantly found in SH-SY5Y cells treated with T3, but also in HepG2 cells treated with vehicle. However, immunoblotting against BRG1/SMARCA4 showed the presence of BRG1 in immunocomplexes of both control and FLAG-TRα1 transfected HepG2 and SH-SY5Y cells, leaving a TRα1-specific interaction questionable (results not shown). A third chromatin remodelling complex, the mixed-lineage leukemia 4 (MLL4) complex, was found in a single purification from HepG2 cells, and represented by the methylosome protein 50 (WDR5) in vehicle and T3-treated cells, and the histone lysine N-methyltransferase MLL4/KMT2D (sometimes also addressed as MLL2) and the lysine-specific histone demethylase UTX/KDM6A in T3-treated cells only. Mutations in MLL4/KMT2D and UTX/KDM6A cause the Kabuki syndrome, which is characterized by intellectual disability and distinct facial characteristics (22).

One of the strongest hits in our profiles was Prospero homeobox 1 (Prox1). Prox1 was associated with TRα1 in both HepG2 and SH-SY5Y cells and binding was enhanced by the presence of T3, as indicated by the higher coverage and confirmed by co-immunoprecipitation (Figure 4). Prox1 is a transcription factor that has important functions in cell fate specification and metabolism (23-25). Prox1 interacts with several other NRs, such as COUP-TFII in lymphatic endothelial cells, and hepatic nuclear factor 4 (HNF4α), liver receptor homologue-1 (LRH-1) and Retinoid Orphan Receptor (ROR) α and γ in liver (26-29). A recent systematic study of *in vitro* binding of peptides from coregulators to NRs showed that the Prox1 peptide bound to nearly all of the 24 NRs tested, including both TRs, which indicates that Prox1 may well be a general cofactor for NRs (30). In liver, Prox1 inhibits reverse cholesterol transport and represses HNF4α and LRH-1 mediated expression of CYP7A1, an important enzyme for the conversion of cholesterol into bile acid (25,27,28,31), processes that are also regulated by TH (32).

The advantage of the TAP-purification method used is that the bait is incorporated into the protein complexes in the intact cell and purified under native condition. This approach therefore preserves the natural composition of the complexes. In addition, the two consecutive purification steps ensured recovery of highly pure complexes with limited background. We adopted a TAP-method that was previously used to isolate proteins associated with ligand-binding defective TRα1 and TRβ1 mutants form HeLa cells (33), and improved on the method by i. using wt TRα1 as bait, which allowed us to compare interactomes of liganded

and unliganded receptors, ii. instead of first separating proteins by SDS-PAGE and proteins subjecting the final eluate directly to LC-MS/MS to identify all proteins irrespective of their visualization on an SDS-PAGE gel, and iii. replicating the purifications for each condition to minimize the number of false positive hits. Our profiles partially overlap with the study of Fozzatti and coworkers, but returned a larger number of proteins that associate with TRα1. For example, their study only returned CHD4, but we also found several additional proteins of the NuRD complex.

Our method was further validated by the recovery and co-immunoprecipitation of several known transcriptional co-regulators of TRs, such as RXR isoforms, the NCoR/SMRT corepressor complex in the absence of T3 and the Mediator and RNA polymerase II complexes in the presence of T3 (Table 3). Furthermore, the fact that we found many if not most subunits for these complexes shows that our method not only finds binary binding partners, but is mild and sensitive enough to preserve the complexes and identify indirect binding partners of TRα1. This is for example demonstrated by the fact that from the RNA polymerase complex II, which only associates with TRα1 via the large multisubunit Mediator complex, we also identified the regulatory kinase CDK9 (34) and phosphatase RPAP2 (35). One exception were the NCoA/SRC coactivator complexes, which were underrepresented in our purifications. We found NCoA1/SRC1 and NCoA3/SRC3 only in one HepG2 purification in the presence of T3 (Supplementary Table 1 (14)) and did not detect any HAT proteins. Co-immunoprecipitations, however, showed T3-dependent binding of SRC1 in both HepG2 and SH-SY5Y cells (Figure 4). Most likely, the SRC1 binding is sensitive to the prolonged purification procedure of the tandem versus the single affinity purification method.

In conclusion, we successfully and efficiently purified cell-type and ligand state specific TRα1-interactomes using a simple tandem-affinity purification method and identified potentially novel interactions with signalling proteins, transcriptional regulators and chromatin remodelling complexes. Future studies will need to elucidate how these novel binding partners contribute to TRα1-mediated gene regulation by TH and how specific mutations in TRα1 affect the repertoire of recruited cofactors and downstream gene regulation, and ultimately the RTHα phenotype in patients.

Acknowledgements

During the course of this work, our mentor and friend professor Theo J. Visser sadly passed away and has therefore not been able to approve the final version of this manuscript. We thank Theo deeply for his contributions.

Grants and funding

This work was supported by ZonMW TOP Grant 91212044 and an Erasmus MC Medical Research Advisory Committee (MRACE) grant (RPP, MEM, WEV), Chiang Mai University (KW), and ZonMW Grant 91113020 for financial support for the MS infrastructure and the research programme Open Technology from the Netherlands Organisation for Scientific Research (NWO), project number 12778 (TML, LJMD, LZ).

Disclosure statement

The authors have nothing to disclose

References

1. Cheng SY, Leonard JL, Davis PJ. Molecular aspects of thyroid hormone actions. *Endocr Rev.* 2010;**31**(2):139-170.
2. Brent GA. Mechanisms of thyroid hormone action. *J Clin Invest.* 2012;**122**(9):3035-3043.
3. van Gucht ALM, Moran C, Meima ME, Visser WE, Chatterjee K, Visser TJ, Peeters RP. Resistance to Thyroid Hormone due to Heterozygous Mutations in Thyroid Hormone Receptor Alpha. *Curr Top Dev Biol.* 2017;**125**:337-355.
4. Nagy L, Schwabe JW. Mechanism of the nuclear receptor molecular switch. *Trends Biochem Sci.* 2004;**29**(6):317-324.
5. Fondell JD, Ge H, Roeder RG. Ligand induction of a transcriptionally active thyroid hormone receptor coactivator complex. *Proc Natl Acad Sci U S A.* 1996;**93**(16):8329-8333.
6. Fondell JD. The Mediator complex in thyroid hormone receptor action. *Biochim Biophys Acta.* 2013;**1830**(7):3867-3875.
7. Allen BL, Taatjes DJ. The Mediator complex: a central integrator of transcription. *Nat Rev Mol Cell Biol.* 2015;**16**(3):155-166.
8. Lee JW, Choi HS, Gyuris J, Brent R, Moore DD. Two classes of proteins dependent on either the presence or absence of thyroid hormone for interaction with the thyroid hormone receptor. *Mol Endocrinol.* 1995;**9**(2):243-254.
9. Yap N, Yu CL, Cheng SY. Modulation of the transcriptional activity of thyroid hormone receptors by the tumor suppressor p53. *Proc Natl Acad Sci U S A.* 1996;**93**(9):4273-4277.
10. Wei LN, Hu X. Receptor interacting protein 140 as a thyroid hormone-dependent, negative co-regulator for the induction of cellular retinoic acid binding protein I gene. *Mol Cell Endocrinol.* 2004;**218**(1-2):39-48.
11. Hahm JB, Schroeder AC, Privalsky ML. The two major isoforms of thyroid hormone receptor, TRalpha1 and TRbeta1, preferentially partner with distinct panels of auxiliary proteins. *Mol Cell Endocrinol.* 2014;**383**(1-2):80-95.
12. Fozzatti L, Lu C, Kim DW, Cheng SY. Differential recruitment of nuclear coregulators directs the isoform-dependent action of mutant thyroid hormone receptors. *Mol Endocrinol.* 2011;**25**(6):908-921.
13. van Gucht AL, Meima ME, Zwaveling-Soonawala N, Visser WE, Fliers E, Wennink JM, Henny C, Visser TJ, Peeters RP, van Trotsenburg AS. Resistance to Thyroid Hormone Alpha in an 18-Month-Old Girl: Clinical, Therapeutic, and Molecular Characteristics. *Thyroid.* 2016;**26**(3):338-346.
14. Meima ME, Wejaphikul K, Leeuwenburgh S, Van Gucht ALM, Zeneyedpour L, Dekker LJM, Visser WE, Luider TM, Peeters RP. HUMAN LIVER AND NEURONAL INTERACTOMES REVEAL NOVEL BINDING PARTNERS FOR THE T3-RECEPTOR ISOFORM α1. *Erasmus MC Digital Repository 2019.* 2019;**Deposited 2 May 2019**(http://hdl.handle.net/1765/116349).
15. van Mullem AA, Chrysis D, Eythimiadou A, Chroni E, Tsatsoulis A, de Rijke YB, Visser WE, Visser TJ, Peeters RP. Clinical phenotype of a new type of thyroid hormone resistance caused by a mutation of the TRalpha1 receptor: consequences of LT4 treatment. *J Clin Endocrinol Metab.* 2013;**98**(7):3029-3038.
16. Denslow SA, Wade PA. The human Mi-2/NuRD complex and gene regulation. *Oncogene.* 2007;**26**(37):5433-5438.
17. Xue Y, Wong J, Moreno GT, Young MK, Cote J, Wang W. NURD, a novel complex with both ATP-dependent chromatin-remodeling and histone deacetylase activities. *Mol Cell.* 1998;**2**(6):851-861.
18. Johnson DR, Lovett JM, Hirsch M, Xia F, Chen JD. NuRD complex component Mi-2beta binds to and represses RORgamma-mediated transcriptional activation. *Biochem Biophys Res Commun.* 2004;**318**(3):714-718.
19. Sokpor G, Xie Y, Rosenbusch J, Tuoc T. Chromatin Remodeling BAF (SWI/SNF) Complexes in

Neural Development and Disorders. *Front Mol Neurosci.* 2017;**10**:243.

20. Wilson BG, Roberts CW. SWI/SNF nucleosome remodellers and cancer. *Nat Rev Cancer.* 2011;**11**(7):481-492.
21. Huang ZQ, Li J, Sachs LM, Cole PA, Wong J. A role for cofactor-cofactor and cofactor-histone interactions in targeting p300, SWI/SNF and Mediator for transcription. *EMBO J.* 2003;**22**(9):2146-2155.
22. Miyake N, Koshimizu E, Okamoto N, Mizuno S, Ogata T, Nagai T, Kosho T, Ohashi H, Kato M, Sasaki G, Mabe H, Watanabe Y, Yoshino M, Matsuishi T, Takanashi J, Shotelersuk V, Tekin M, Ochi N, Kubota M, Ito N, Ihara K, Hara T, Tonoki H, Ohta T, Saito K, Matsuo M, Urano M, Enokizono T, Sato A, Tanaka H, Ogawa A, Fujita T, Hiraki Y, Kitanaka S, Matsubara Y, Makita T, Taguri M, Nakashima M, Tsurusaki Y, Saitsu H, Yoshiura K, Matsumoto N, Niikawa N. MLL2 and KDM6A mutations in patients with Kabuki syndrome. *Am J Med Genet A.* 2013;**161A**(9):2234-2243.
23. Hong YK, Detmar M. Prox1, master regulator of the lymphatic vasculature phenotype. *Cell Tissue Res.* 2003;**314**(1):85-92.
24. Stergiopoulos A, Elkouris M, Politis PK. Prospero-related homeobox 1 (Prox1) at the crossroads of diverse pathways during adult neural fate specification. *Front Cell Neurosci.* 2014;**8**:454.
25. Stein S, Oosterveer MH, Mataki C, Xu P, Lemos V, Havinga R, Dittner C, Ryu D, Menzies KJ, Wang X, Perino A, Houten SM, Melchior F, Schoonjans K. SUMOylation-dependent LRH-1/PROX1 interaction promotes atherosclerosis by decreasing hepatic reverse cholesterol transport. *Cell Metab.* 2014;**20**(4):603-613.
26. Lee S, Kang J, Yoo J, Ganesan SK, Cook SC, Aguilar B, Ramu S, Lee J, Hong YK. Prox1 physically and functionally interacts with COUP-TFII to specify lymphatic endothelial cell fate. *Blood.* 2009;**113**(8):1856-1859.
27. Song KH, Li T, Chiang JY. A Prospero-related homeodomain protein is a novel co-regulator of hepatocyte nuclear factor 4alpha that regulates the cholesterol 7alpha-hydroxylase gene. *J Biol Chem.* 2006;**281**(15):10081-10088.
28. Qin J, Gao DM, Jiang QF, Zhou Q, Kong YY, Wang Y, Xie YH. Prospero-related homeobox (Prox1) is a corepressor of human liver receptor homolog-1 and suppresses the transcription of the cholesterol 7-alpha-hydroxylase gene. *Mol Endocrinol.* 2004;**18**(10):2424-2439.
29. Takeda Y, Jetten AM. Prospero-related homeobox 1 (Prox1) functions as a novel modulator of retinoic acid-related orphan receptors alpha- and gamma-mediated transactivation. *Nucleic Acids Res.* 2013;**41**(14):6992-7008.
30. Broekema MF, Hollman DAA, Koppen A, van den Ham HJ, Melchers D, Pijnenburg D, Ruijtenbeek R, van Mil SWC, Houtman R, Kalkhoven E. Profiling of 3696 Nuclear Receptor-Coregulator Interactions: A Resource for Biological and Clinical Discovery. *Endocrinology.* 2018;**159**(6):2397-2407.
31. Kamiya A, Kakinuma S, Onodera M, Miyajima A, Nakauchi H. Prospero-related homeobox 1 and liver receptor homolog 1 coordinately regulate long-term proliferation of murine fetal hepatoblasts. *Hepatology.* 2008;**48**(1):252-264.
32. Sinha RA, Singh BK, Yen PM. Direct effects of thyroid hormones on hepatic lipid metabolism. *Nat Rev Endocrinol.* 2018;**14**(5):259-269.
33. Fozzatti L, Kim DW, Park JW, Willingham MC, Hollenberg AN, Cheng SY. Nuclear receptor corepressor (NCOR1) regulates in vivo actions of a mutated thyroid hormone receptor alpha. *Proc Natl Acad Sci U S A.* 2013;**110**(19):7850-7855.
34. Ramanathan Y, Rajpara SM, Reza SM, Lees E, Shuman S, Mathews MB, Pe'ery T. Three RNA polymerase II carboxyl-terminal domain kinases display distinct substrate preferences. *J Biol Chem.* 2001;**276**(14):10913-10920.
35. Egloff S, Zaborowska J, Laitem C, Kiss T, Murphy S. Ser7 phosphorylation of the CTD recruits the RPAP2 Ser5 phosphatase to snRNA genes. *Mol Cell.* 2012;**45**(1):111-122.

Supplementary Materials

Supplementary Figures

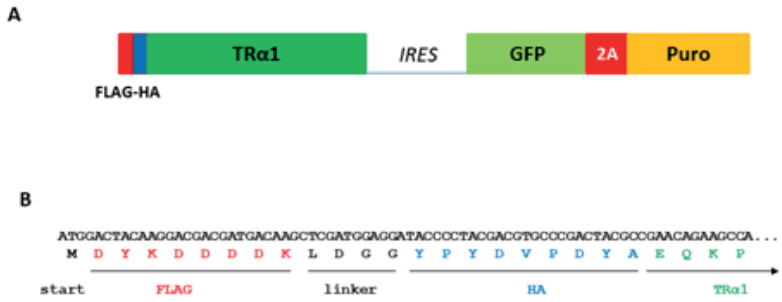

Supplementary Figure S1. Structure of expression cassette of the FLAG-HA tagged TRα1 (FHTRα1) construct. The second codon of the full length coding sequence of TRα1 is fused at the 5'-end to consecutive sequences encoding the FLAG and hemagglutinin (HA) epitope tags (B). To select cells expressing FHTRα1, the construct is expressed from a bicistronic messenger RNA, due to the inclusion of an internal ribosome entry site (IRES) sequence, together with a selection marker consisting of the sequences encoding the puromycine resistrance gene (PURO) and green fluorescent protein (GFP), fused by the sequence encoding the 2A self-cleaving peptide (A).

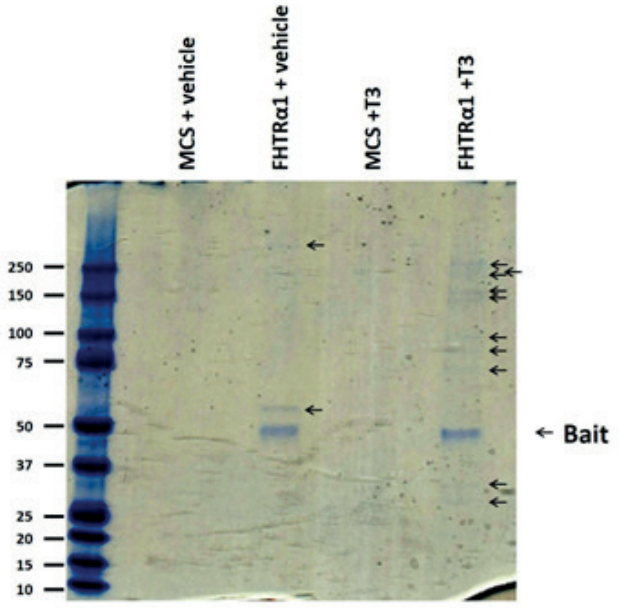

Supplementary Figure S2. SDS-PAGE of FHTRα1-containing protein complexes from HepG2 cells. HepG2 cells expressing FHTRα1 or empty vector (MCS) as control were stimulated for 4 hrs with vehicle or 100 nM T3 and subjected to TAP purifications. One third of the final eluates were separated on a 4-12% Bis-Tris gel and protein bands visualized by Colloidal Coomassie staining.

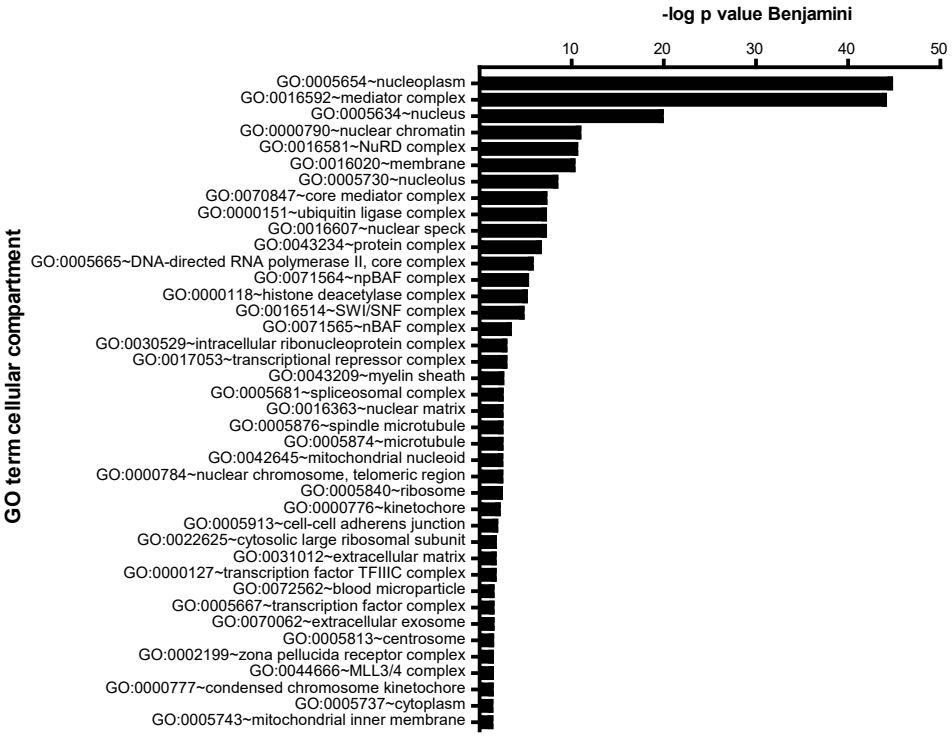

Supplementary Figure S3. Enrichment for cellular compartments of the total profile. Proteins that specifically co-purified with FHTRα1 in any purification (Supplementary Table 1) were analysed for enrichment of cellular compartment using DAVID (minimum count 2, ease 0.1). The top 40 most significant GO terms are displayed. P values were adjusted for false discovery rates using the Benjamini correction.

Supplementary Methods

Construction of lentiviral vectors pWCAGpCasC-MCS-IRESPuro2AGFP and pWCAGpCasC-FHTRα1-IRESPuro2AGFP

To add the sequence encoding the FLAG and HA epitope to the 5'-side of TRα1, the full length coding sequence for TRα1 was amplified using Pfu polymerase (Thermofisher) by which the start codon was replaced with consecutive sequences for the FLAG and HA epitope tag (Supplementary Figure S1). The resulting fragments was cloned into the pCR2.1TOPO vector (Invitrogen) and subsequently excised and ligated into the HindIII and BamHI sites of pENTL1-MCS-R5 to yield the plasmid pENTL1-FHTRα1-R5. The correct sequence was confirmed by Sanger sequencing. The MCS (multiple cloning site) or FHTRα1 fragments were next fused to the IRESPuro2AGFP-fragment from pENTL5-IRESPuro2AGFP-R2 and inserted into pWCAGpCasC by multiple gateway cloning using the LR II Clonase Plus (Invitrogen) according to the manufacturers protocol.

Tandem affinity purification

Throughout the procedure, buffers were supplemented with 100 nM T3 or vehicle, and cOmpleteTM protease inhibitors cocktail (Roche). Cells were washed twice with ice-cold DPBS, scraped into 2 ml DPBS per plate, pelleted in a table-top centrifuge at 1200 round per minute (rpm) for 5 minutes at 4 °C and resuspended in 5 ml buffer A (10 mM Hepes.NaOH, 10 mM KCl, 0.1 mM EDTA, 1 mM DTT, pH 7.9). After 15 min on ice, 0.6% NP40 was added and the cells were vortexed for 30 seconds to lyse the cells. Phosphatase inhibitors (5 mM NaF and 1 mM NaPPi) were added and nuclei pelleted by centrifugation at 2000 rpm for 10 minutes at 4 °C. Nuclear proteins were extracted by nutating the nuclei in 1.88 ml buffer C (20 mM HEPES.NaOH, 400 mM NaCl, 1 mM EDTA, 1 mM DTT, 5 mM NaF, 1 mM NaPPi, pH 7.9) for 20 minutes at 4 °C. The nuclei were spun down in a microfuge at 15000 rpm. The supernatant was transferred to a 15 ml conical tube, the salt concentration reduced by addition of 3.12 ml buffer D (20 mM HEPES.NaOH, 1 mM EDTA, 5 mM NaF, 1 mM NaPPi, pH 7.9) and NP40 added to a final concentration of 0.1%. Next, FHTRα1-containing protein complexes were bound overnight at 4 °C to 20 µl bedvolume of anti-FLAG agarose (clone M2; Sigma), washed 1 time with 10 ml and 4 times with 1 ml of ice-cold washbuffer (20 mM HEPES.NaOH, 150 mM NaCl, 1 mM EDTA, 5 mM NaF, 1 mM NaPPi, 0.1% NP40, pH 7.9) and eluted twice with 50 µl of 200 µg/ml FLAG peptide (Sigma) in washbuffer for 30' at 4 °C in spin columns (Biorad). Eluates were combined, 500 µl of washbuffer was added to the eluates and FHTRα1-containing protein complexes were bound overnight at 4 °C to 20 µl bedvolume of anti-HA agarose (Sigma), after which the resin was washed 4 times with 1 ml ice-cold washbuffer. For the first purification from HepG2 cells, the resin was subsequently washed 1 time with 1 ml washbuffer without NP40, transferred into a spin column and protein complexes eluted once at 4 °C and once at room temperature with 25 µl 400 µg/ml HA peptide (Sigma), after which the eluates were pooled. For the other purifications, 0.1% RapiFest SF (Waters)

was added to the final washbuffer and elution buffer, to improve bead handling. Elutes were pooled and subjected to LC-MS/MS for protein identification. For the first purification from HepG2 cells, 1/3 part of the eluate was denatured in 1x NuPAGE LDS sample buffer (Thermo Fisher Scientific) supplemented with 10 mM DTT at 70 °C for 10 minutes, separated by SDS-PAGE on a 4-12% Bis-Tris gel (Novex, Invitrogen) and bands visualized with a Colloidail Blue Staining Kit (Invitrogen).

In-solution digestion

Eluates from two independent purifications from each cell line were precipitated using acetone and then resuspended in 0.1% Rapigest in 50 mM NH_4HCO_3. The solution was reduced with 100 mM dithiothreitol (DTT) at 60 °C for 30 minutes. After the mixture was cooled down to room temperature, it was alkylated in the dark with 300 mM iodoacetamide at ambient temperature for 30 minutes, and digested overnight with 0.4 µg trypsin (Promega, Madison, WI). Five percent trifluoroacetic acid was added, to obtain a final concentration of 0.5% trifluoroacetic acid (pH < 2). After 45 minutes of incubation at 37 °C, the samples were centrifuged at 13,000 x g for 10 minutes.

NanoLC data dependent mass spectrometry measurements

Digested samples were subjected to LC-MS/MS analysis. Samples were analyzed by nano-LC (Ultimate 3000RS, Thermo Fisher Scientific, Germering, Germany). After pre-concentration and washing of the samples on a C18 trap column (1 mm × 300 µm i.d., Thermo Fisher Scientific), they were loaded onto a C18 column (PepMap C18, 75 mm ID × 150 mm, 2 µm particle and 100 Å pore size, Thermo Fisher Scientific) using a linear 15 minutes gradient (4-38% ACN/H20; 0.1% formic acid) at a flow rate of 250 nL/min. The separation of the peptides was monitored by a UV detector (absorption at 214 nm). The integrated area of the UV chromatogram is used to determine the maximum injection volumes for the LC-MS analyses. For the LC-MS the same type of LC system is used connected to a nanospray source. The LC system was equipped with a PepMap C18 column (75 mm ID × 250 mm, 2 µm particle and 100 Å pore size, Thermo Fisher Scientific) and a 30 or 90 minutes gradient (4-38% ACN/H20; 0.1% formic acid) at a flow rate of 300 nL/min coupled to either an Orbitrap Fusion or to a Orbitrap Fusion Lumos (Thermo Fisher Scientific, San Jose, CA, USA). The Orbitrap Fusion Lumos was operated in the data dependent acquisition (DDA) mode. Full scan MS spectra (m/z 375-1,500) in profile mode were acquired in the orbitrap with a resolution of 120,000 after accumulation of an AGC target of 400,000. A top speed method with a maximum duty cycle of 3 seconds was used. In these 3 seconds, the most intense peptide ions from the full scan in the orbitrap were fragmented by HCD (normalized collision energy 28%) and measured in the iontrap with a AGC target of 10,000. Maximum fill times were 50 ms for the full scans and 50 ms for the MS/MS scans. Precursor ion charge state screening was enabled and only charge states from 2-7 were selected for fragmentation. The dynamic exclusion was activated after the first time a precursor was selected for fragmentation and excluded for a

period of 60 seconds using a relative mass window of 10 ppm. Lock mass correction was activated to improve mass accuracy of the survey scan. In the Orbitrap Fusion the following settings were used; DDA mode, Full scan MS spectra (m/z 400-1,600) in profile mode with a resolution of 120,000 and an AGC target of 400,000. A top speed method with a maximum duty cycle of 3 seconds was used. In these 3 seconds, the most intense peptide ions from the full scan in the orbitrap were fragmented by CID (normalized collision energy 30%) and measured in the iontrap with a AGC target of 10,000. Maximum fill times were 100 ms for the full scans and 40 ms for the MS/MS scans. The rest of settings were the same as for the measurements on the Orbitrap Fusion Lumos. From the data files of both systems the MS/MS spectra were extracted and converted into mgf files by using MSConvert of ProteoWizard (version 3.0.06245). All mgf files were analyzed using Mascot (version 2.3.02; Matrix Science, London, UK). Mascot was used to perform database searches against the human subset of either uniprot_sprot download November 2015 (20194 entries) or download September 2014 (20196 entries), using Mascot version 2.3.02. Monoisotopic fragment tolerance was set to 0.50 Da and parental tolerance at 10 ppm. Carbamidomethylation of cysteine was specified as fixed modification and oxidation of methionine as variable modification for all, and n-terminal acetylation for the first HepG2 purification.

Version 4.8.3 of the Scaffold platform was used to validate proteins and peptides. Stringency settings allowed FDRs of 1% for proteins and peptides when screened against a decoy database. This allowed probability scores of 5% and 78% for proteins and peptides respectively with a minimum of 2 peptides for the first purification from HepG2, and 99% and 91% for proteins and peptides with a minimum of 1 peptide for the other purification. Proteins that were present in any of the control purifications were excluded from our final profile. The uniprot_sprot database contains the TRα isoform 2 (P10827-1) instead of our bait TRα1 (P10827-2). These isoforms differ in their C-terminal domain (371-410 in TRα1), which has high homology between TRα1 and TRβ. Therefore, a peptide (sequence MIGACHASR; position 376-384 in TRα1, position 440-448 in TRβ1) that is conserved between TRα1 and TRβ was scored as an exclusive unique peptide for the C-terminus of TRβ. Apart from one peptide with a probability score of 85% (sequence KLIEENR; position 190-196 in TRβ1), in HepG2 purification 1 from vehicle treated cells, we did not find any peptides that are unique for TRβ as well as TRα2. As such, we decided that all peptides are derived from TRa1 and assigned the C-terminal peptide and spectra to TRα1 in Table 2 and Supplementary Table 1. Gene enrichment analysis was performed using the Database for Annotation, Visualization and Integrated Discovery (DAVID), version 6.8 (https://david.ncifcrf.gov/) using default settings (count 2, ease 0.1) and p-values adjusted using the Benjamini correction. Existing protein interaction networks were searched using STRINGS (https://strings-db.org) with minimum required interaction scores set at medium confidence (0.400).

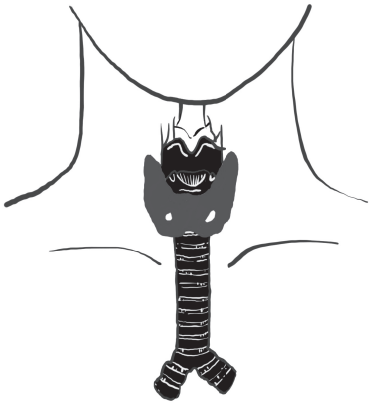

CHAPTER 6b

Coregulatory Protein Recruitment by Thyroid Hormone Receptors in Neuronal Cells

Karn Wejaphikul, Lona Zeneyedpour, W. Edward Visser, Selmar Leeuwenburgh, Theo M. Luider, Robin P. Peeters, Marcel E. Meima

Manuscript in preparation

6

Abstract

Thyroid hormone (TH) binding to its nuclear TH receptors (TRs) alters coregulatory protein recruitment of the TRs to regulate gene transcription. Considering the crucial role of TH in brain development and function, we aimed to identify the coregulatory proteins that are involved in neuronal TR activity by elucidating the interactomes for wild-type TRα1 and TRβ1 in a human-derived neuronal cell line (SH-SY5Y). TR-interacting proteins were purified from nuclear extracts of SH-SY5Y cells stably expressing epitope-tagged TRα1 and TRβ1 (FH-TRα1 and -TRβ1) by tandem-affinity purification and analyzed by LC-MS/MS. One hundred one proteins were co-purified with TRs, including the known TR-interacting proteins, such as retinoid X receptors (RXRs) (regardless of T3, the presence or absence of T3), NCoR1/SMRT/HDAC3 repressor complex (in the absence of T3), and SRCs and the Mediator complex (in the presence of T3). Several chromatin remodeling complexes that have not previously been described as coregulators of TRs were identified, for instance the nucleosome remodeling deacetylase (NuRD) and the Spt-Ada-Gcn5-Acetyltransferase (SAGA) complexes. Most of the proteins were shared between the two TR isoforms. However, we identified nine proteins that only associated with FH-TRα1 and two proteins with FH-TRβ1. These findings suggest that TRs not only interact with classical coregulatory proteins in SH-SY5Y cells but also with several potential novel binding partners. In addition, we identified a subset of distinct nuclear proteins that seem to interact with TRs in an isoform-specific manner.

Introduction

Thyroid hormone (TH) is indispensable for proper neurodevelopment (1). TH regulates gene transcription by binding of the bioactive TH form, triiodothyronine (T3), to thyroid hormone receptors (TRs). Impaired action of TH in the brain is associated with intellectual disability and psychomotor retardation in many conditions, including prolonged untreated congenital hypothyroidism patients (2,3), impaired TH transport to the brain in monocarboxylase transporter 8 (MCT8) deficiency (due to a mutation in MCT8) (4,5), and impaired function of TRα due to a mutation in this receptor leading to resistance to TH alpha (RTHα) (6,7).

Three TR isoforms, TRα1, β1, and β2 that have extensive structural similarity are capable of binding to T3. TRα1 is encoded by *THRA* gene on chromosome 17 whereas TRβ1 and TRβ2 are encoded by *THRB* gene on chromosome 3 (8). It has been shown that TRα1 is the most abundantly expressed in the brain and plays a crucial role in brain development (9-13). TRβ1 is also expressed in many regions of the brain but the distribution is more restricted compared to TRα1 (9,11). TRβ2 is predominantly expressed in the hypothalamus, pituitary, retina, and cochlea (11,14,15). These differential expression patterns suggests that TR isoforms could play different functional roles during development.

TRs mainly form heterodimers with retinoid X receptors (RXRs) on thyroid hormone response elements (TREs) and interact with many nuclear coregulatory proteins to regulate local chromatin structure and gene transcription. In the absence of T3, TRs recruit corepressor proteins, including nuclear receptor corepressor 1 (NCoR1), silencing mediator for retinoid or thyroid hormone receptors (SMRT), and histone deacetylases (HDACs), to modify the histone core of nucleosomes and create a closed chromatin conformation. Binding of T3 induces conformational changes in TRs, which favor recruitment of coactivator proteins, including steroid receptor coactivators (SRCs) and histone acetyltransferases (HATs), to create an open chromatin configuration and accessibility of target genes for general transcription factors (GTFs) and the RNA polymerase II complex (8,16). In addition to the classical TR coregulators, other nuclear proteins have been described that can have a direct or indirect interaction with TRs (17,18) and are involved in transcriptional regulation.

There is evidence indicating that the coregulatory protein recruitment by nuclear receptors is tissue-dependent, which may lead to diverging receptor functions in the different tissues (14,17,19,20). In addition, some studies showed that TRs recruit a subset of coregulatory proteins in an isoform-specific manner (17,18), adding to the complexity of transcriptional gene regulation by TRs. In order to gain more insight into the transcriptional gene regulation by TRs in the brain, we identified the coregulatory proteins that are involved in neuronal TR activity by interactome analysis for wild-type (WT) TRα1 and TRβ1 in a human-derived neuronal cell line (SH-SY5Y). We found that TRs interact with several nuclear proteins, some of which have not previously been described as TR interacting partners. In general, both

TR isoforms shared the same coregulatory proteins; however, a subset of proteins seemed to interact in an isoform-specific manner.

Materials and Methods

Plasmid constructs

Lentiviral constructs containing N-terminal FLAG and Hemagglutinin (HA) double-epitope tagged human WT TRα1 and TRβ1 and a bicistronic messenger RNA that allows the simultaneous expression of TRs, puromycin resistance marker, and green fluorescent protein (GFP) (pLentiFH-TRα1 and pLentiFH-TRβ1) were created as previously described (Chapter 6a). An empty vector construct (pLentiMCS) expressing only the puromycin resistance marker and GFP was also used to generate an empty vector control cell line. The packaging vectors, pMD2.G and psPAX2 (Chapter 6a), were used to produce TR containing lentiviruses as described below.

Stable expression of TRs in SH-SY5Y cells

FH-TRα1, -TRβ1 and empty vector (MCS) were stably expressed in SH-SY5Y human-derived neuroblastoma cells using lentiviral transduction as previously described (Chapter 6a). In brief, lentiviruses containing pLentiFH-TRα1, pLentiFH-TRβ1, and pLentiMCS were produced in HEK293FT cells by co-transfecting 4 µg of pLenti-CMV-FH-TRα1, -TRβ1, or -MCS constructs with 4 µg of psPAX2 and pMD2.G plasmids using Xtreme Gene 9 transfection reagent (Roche Diagnostics, Almere, NL). SH-SY5Y cells were transduced with lentiviruses for 48 hours in 6-well plates (at 25% confluency) and subsequently selected with 2 µg/mL of puromycin. Puromycin-resistant SH-SY5Y cells were expanded in growth medium (DMEM/F12 supplemented with 9%FBS, 100 U/mL penicillin, 100 µg/mL streptomycin, 100 nM Na_2SeO_3) and 2 µg/mL puromycin for subsequent experiments. SH-SY5Y cells stably expressing FH-TRα1, -TRβ1 or -MCS were designated as FH-TRα1, FH-TRβ1, or MCS cells, respectively.

Luciferase assays

To determine T3-induced transcriptional activity of stably expressed receptors, FH-TRα1, FH-TRβ1, and MCS cells were cultured in 24-well plates. At 80% confluency, cells were transfected for 24 hours with 200 ng pdV-L1 luciferase-renilla reporter construct (21) in TH depleted medium (DMEM/F12 supplemented with 9% charcoal-stripped FBS) using Xtreme Gene 9 transfection reagent (Roche Diagnostics, Almere, NL). After that, cells were stimulated with 0-10,000 nM T3 for 24 hours in DMEM/F12 medium supplemented with 0.1% bovine serum albumin (BSA). Luciferase and renilla activities were determined using the Dual Glo Luciferase kit (Promega, Leiden, NL) as previously described (7). The ratio between luciferase

and renilla was calculated to adjust for transfection efficiency. The results were shown as mean ± SEM of three independent experiments performed in triplicate. Dose-response curves were created by GraphPad Prism version 5.0 (GraphPad, La Jolla, CA).

Tandem-affinity purification

The FH-TRs and TR-interacting proteins were purified from SH-SY5Y cells as previously described (Chapter 6a). Briefly, the FH-TRα1, FH-TRβ1, and MCS cells were cultured until near confluency. Then, the cells were starved of TH for 24 hours in TH depleted medium and incubated for 4 hours with 0 (vehicle) or 100 nM T3 in DMEM/F12 supplemented with 0.1% BSA. After that, the cells were harvested, and nuclear proteins were extracted as previously described (22) (Chapter 6a). Nuclear extracts were incubated overnight with anti-Flag M2 affinity gel (#A2220, Sigma Aldrich) at 4°C to purify the TRs. The bound proteins were eluted with 200 µg/mL Flag peptide (#F3290, Sigma Aldrich) and subsequently incubated for 4 hours with EZview red anti-HA affinity gel (#E6779, Sigma Aldrich) at 4°C for the second purification. The proteins were eluted from HA-resin with 400 µg/mL HA peptide. The purified products (final HA eluates) of two independent tandem-affinity purifications per conditions were subjected for analysis by LC-MS/MS.

Immunoblotting

The expression of TRs in nuclear extracts prepared from FH-TRα1, FH-TRβ1, and MCS cells and FLAG and HA eluates from two tandem-affinity purification were verified by immunoblotting as previous described (21,22) using 1:1000 dilution HA-Tag (C29F4) Rabbit mAb (#3724, Cell Signaling Technology, Leiden, NL).

Proteomic analysis (Orbitrap LC-MS/MS)

Isolated proteins in the purified products were identified by Orbitrap LC-MS/MS as previously described (Chapter 6a). The peptide sequences identified by LC-MS/MS were mapped onto the reference amino acid sequences to determine individual proteins using Scaffold Viewer version 4.8.9 (Proteomic Software Inc., Oregon, USA). Proteins with at least two unique peptides assigned to them with 1% false detection rate (FDR) protein and peptide threshold were accepted as true identifications. Only proteins that were present in the two replicates of at least one TR and T3 conditions but absent in MCS control eluates were selected for further analysis. Individual proteins were clustered and presented as an expressing heat map using the Heatmapper online software (http://www.heatmapper.ca) (23). Pathway enrichment analysis was performed by DAVID functional annotation chart (DAVID Bioinformatics Resources 6.8, NIAID/NIH: https://david.ncifcrf.gov/) using default setting (count 2, ease 0.1). The gene-term enrichment was analyzed based on molecular function Gene Ontology terms. Statistical significance was considered when p-values of modified Fisher's exact test (EASE score) with Benjamini post-test < 0.05. The known protein-protein interactions (from curated databased and experimentally determined) between individual

proteins were analyzed by STRING database version 11.0 (http://string-db.org) with minimum required interaction scores set at medium confidence (0.400).

Results

The expression and transcriptional activation of FH-TRα1 and FH-TRβ1 in SH-SY5Y cells were evaluated before using the cells in TR purification. Both TR isoforms were detected with equal intensity on immunoblots of nuclear extracts (NEs) from FH-TRα1 and FH-TRβ1 expressing cells, showing similar expression levels of the TR isoforms in the cells (Figure 1A). FH-TRα1 and -TRβ1 cells also showed T3-dependent transactivation of the reporter gene in luciferase assays (Figure 1B), confirming that the stably expressed TRs have normal transcriptional activity, and the FH-tag did not interfere with receptor activity.

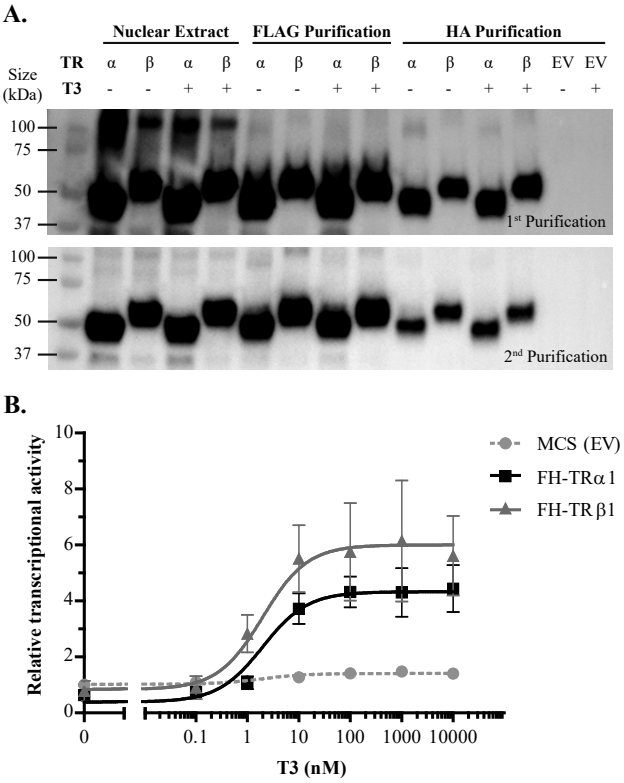

Figure 1. (A) Immunoblots show an equal amount of FH-TRα1 and FH-TRβ1 in nuclear extracts and purification products from SH-SY5Y cells of two tandem-affinity TR purifications (TR, thyroid hormone receptor; EV, empty vector control). (B) The T3-induced transcriptional activity of FH-TRα1, FH-TRβ1, and MCS (EV) confirms a normal function of stably expressing TRs in SH-SY5Y cells (data are presented as mean ± SEM of three independent experiments performed in triplicate).

To identify the nuclear coregulatory proteins that interact with TRs in SH-SY5Y cells, we performed two independent tandem-affinity TR purification using NEs of the FH-TRα1, FH-TRβ1, and MCS cells after 4 hours stimulation with 0 or 100 nM T3. TRs and associated proteins were sequentially co-immunoprecipitated using anti-FLAG and anti-HA resins. To estimate the recovery of the FH-TRs, proportional amounts of NEs and eluates from both FLAG- and HA-purification steps were analyzed by immunoblotting with HA antibodies. The amount of FH-TRα1 and -TRβ1 in the final (HA) eluates after tandem-affinity purification was slightly less than in the NE input but equal between conditions (Figure 1A), ensuring similar amounts of complexes in final eluates. These eluates were then subjected to LC-MS/MS analysis to identify distinct nuclear proteins associated with FH-TRs.

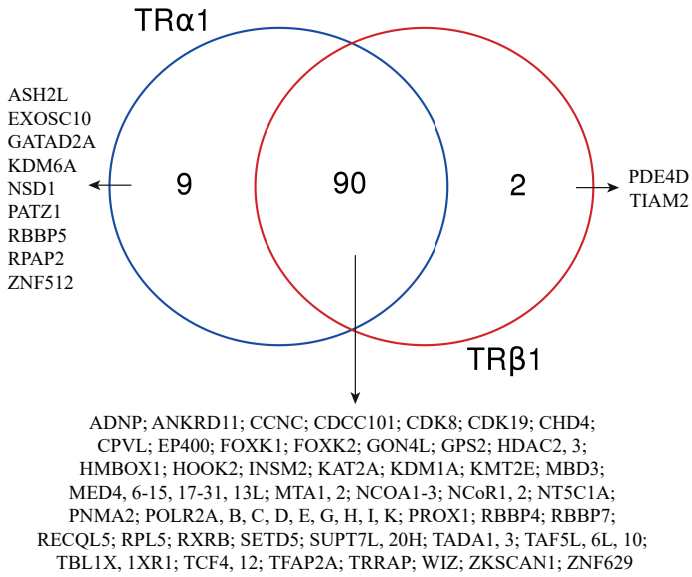

Figure 2. Venn diagram showing the number of distinct nuclear proteins that co-purified with FH-TRs. Most of the proteins are associated with both TR isoforms, indicating that TR action in SH-SY5Y cells is mainly regulated by common coregulatory proteins. However, eleven proteins were found to be exclusively associated with only one TR isoform (nine proteins for TRα1 and two proteins for TRβ1), suggesting an isoform-specific coregulatory protein recruitment.

One hundred and one different proteins were present in the two replicates of at least one TR (FH-TRα1 or -TRβ1) and T3 (0 or 100 nM) condition, but absent in MCS control eluates (Figure 2, Supplementary Table S1). Our strategy was validated by the identification of known TR-interacting proteins, such as RXRβ, the NCoR1/SMRT/HDAC3 corepressor complex, SRC coactivators, the Mediator complex, and the RNA polymerase II complex with a high percent coverage. Approximately 90% of the proteins overlapped between FH-TRα1

and FH-TRβ1, indicating that both TR isoforms mainly interact with the same coregulatory proteins to regulate gene transcription. However, nine proteins (8.9%) were only associated with FH-TRα1 (such as ASH2L, KDM6A (as known as UTX), and RBBP5) and two (2.0%) only with FH-TRβ1 (PDE4D and TIAM2) (Figure 2), suggesting that TRs could also be partly regulated by an isoform-specific subset of coregulatory proteins.

All identified proteins were then categorized by heat map analysis into two clusters (Figure 3). Cluster 1 consists of proteins that are predominantly identified in the absence of T3 (vehicle enriched group), and cluster 2 consists of proteins that are mainly identified in the presence of T3 (T3-enriched group). The molecular functions of proteins in these two clusters were explored by gene ontology (GO) enrichment analysis. The results showed that the proteins in the cluster 1 or vehicle enriched group (total N = 21) were significantly associated with transcriptional gene repression GO terms, such as transcription corepressor activity (N = 7, p-value <0.001) and histone deacetylase activity (N = 3, p-value <0.05) (Figure 4A). The proteins in the cluster 2 or T3-enriched group (total N = 80) were significantly associated with transcriptional gene activation GO terms, for instance, RNA polymerase II transcriptional cofactor activity (N = 22, p-value <0.01), transcriptional coactivator activity (N = 24, p-value <0.01), and histone acetyltransferase activity (N = 11, p-value <0.01) (Figure 4B).

Each cluster was subsequently analyzed for known interactions based on experimental data using the STRING online database (Figure 5). The analysis showed that the NCoR/SMRT complex was enriched in the absence of T3 for both isoforms. Apart from the direct TR-binding proteins NCoR1 and NCoR2/SMRT, the profiles included other members of the complex, such as HDAC3, transducin beta like 1 X-linked (TBL1X), transducing beta like 1 X-linked receptor 1 (TBL1XR1), and G-protein pathway suppressor 2 (GPS2). Many other proteins in this cluster have never been described to be associated with TRs, including the Forkhead box (FOX) transcription factor K1 and K2 (FOXK1 and FOXK2) proteins that are known to be part of Wnt/β-catenin signaling complex (Supplementary Table S2), ankyrin repeat domain-containing protein 11 (ANKRD11), and activity-dependent neuroprotector homeobox protein (ADNP).

The majority (77%) of the identified proteins co-purified with TRs in the presence of T3 (Figure 5B). The nuclear receptor coactivator (NCoA, also known as SRC) isoforms 1, 2, and 3, the Mediator complex, and RNA polymerase II complex that are known to associate with liganded TRs were all present in the T3-enriched cluster (Figure 5B, Supplementary Table S2). We also identified proteins belonging to chromatin remodeling complexes, including the nucleosome remodeling deacetylase (NuRD), the Spt-Ada-Gcn5-Acetyltransferase (SAGA), and the MLL/SET methyltransferase complexes (Figure 5B, Supplementary Table S2), all of which have not previously been reported to interact with TRs. The T3-enriched also contained other proteins which are unknown to interact with TRs and could not be categorized into any known complex, such as the transcription factors Prospero homeobox protein 1 (PROX1) and transcription factor 4 and 12 (TCF4 and TCF12).

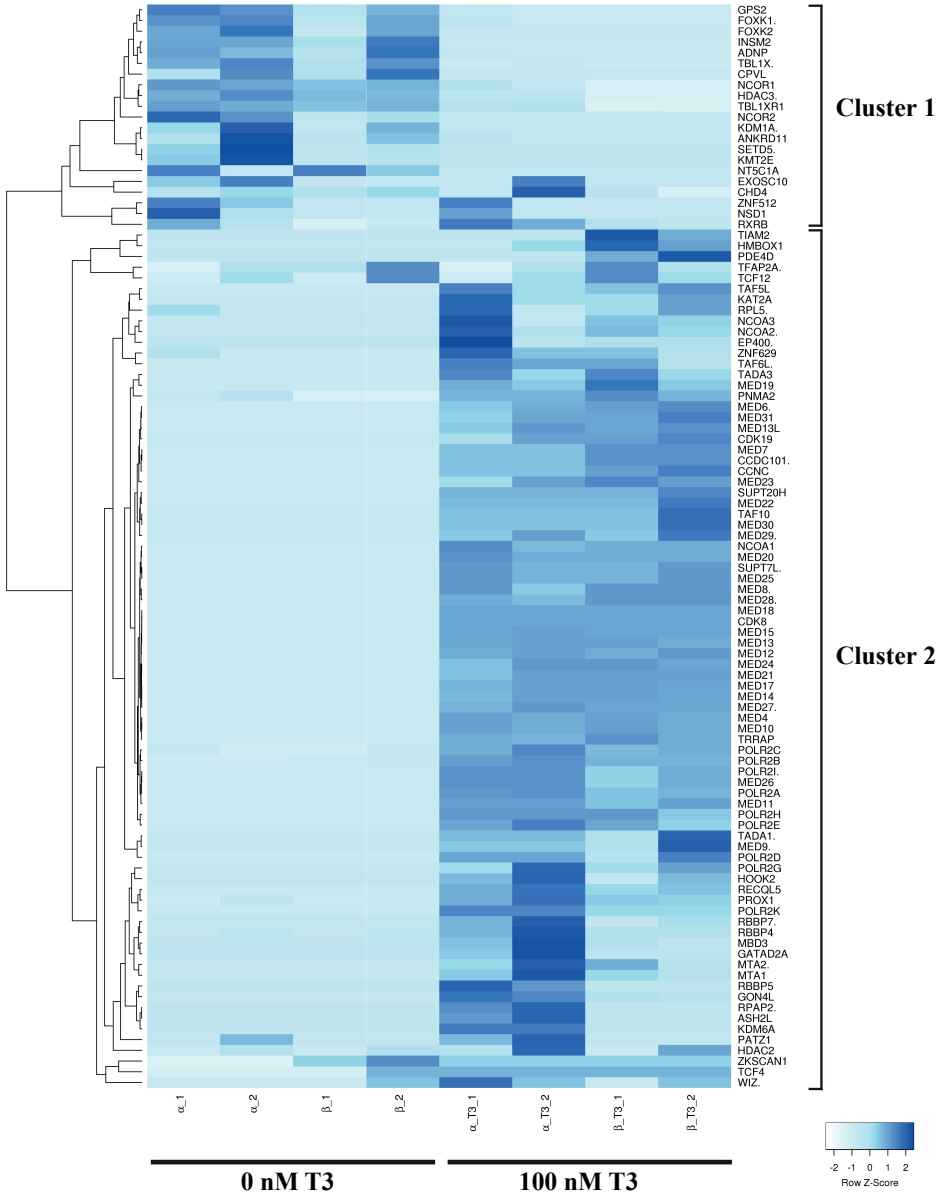

Figure 3. Heat map showing the profile of distinct nuclear proteins co-purified with FH-TRα1 and FH-TRβ1 after stimulating with 0 or 100 nM T3. The color intensity correlates with the Z-score of exclusive unique peptides identified by LC-MS/MS (white, low or undetectable level; blue, high level). According to hierarchical clustering (demonstrated by dendrogram on the left), the proteins are divided into two main clusters. The cluster 1 consists of proteins that are predominantly identified in the absence of T3 (vehicle enriched group), and the cluster 2 consists of proteins that are mainly identified in the presence of T3 (T3-enriched group). (Proteins are clustered by average linkage clustering and Pearson distance measurement methods using Heatmapper online software.)

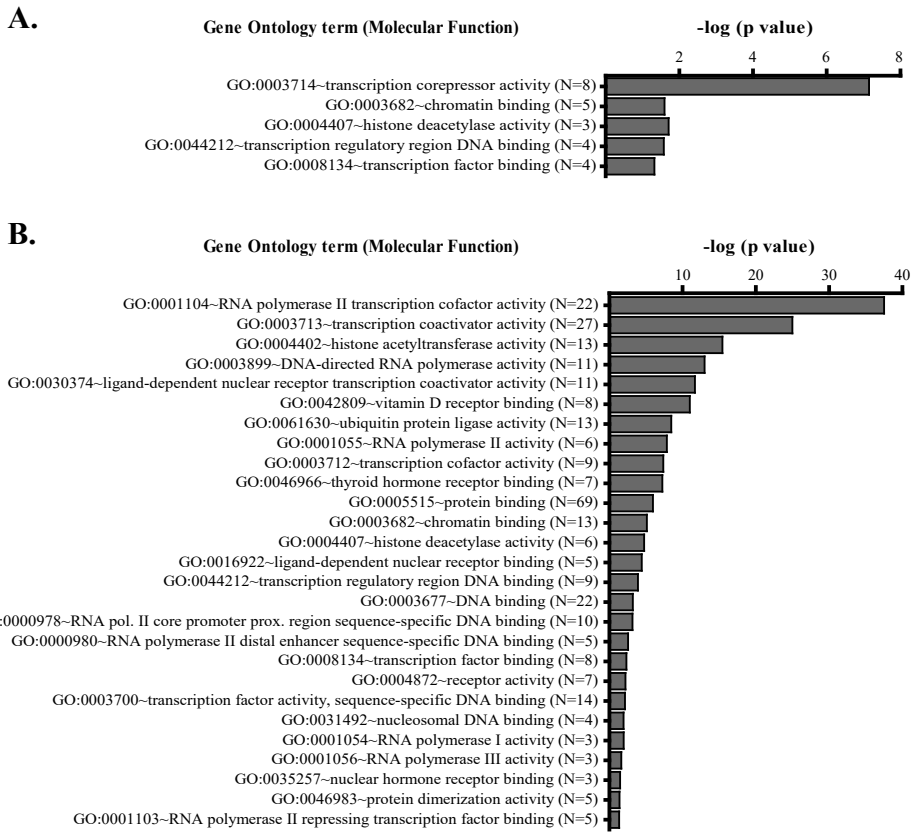

Figure 4. Gene Ontology term (molecular function) enrichment analysis. (A) The proteins found in the absence of T3 (cluster 1) are significantly related to transcriptional corepressor activity and histone deacetylase activity whereas (B) the proteins found in the presence of T3 (cluster 2) are related to transcriptional coactivator activity, histone acetyltransferase activity, and RNA polymerase II activity. Data are presented as –log (p value) of modified Fisher's exact test (EASE score) with Benjamini post-test from DAVID functional annotation chart [DAVID Bioinformatics Resources 6.8, NIAID/NIH]. (N = number of proteins associated to GO term)

Figure 5 (right page). Protein-protein interaction (PPI) network demonstrating known interactions (pink line) between identified proteins in the (A) absence and (B) presence of T3. Known TR-interacting proteins, such as the NCoR1, NCoR2 (SMRT), HDAC3, TBL1X, and TBL1XR1, in the absence of T3, and the SRC 1-3 coactivators, the Mediator complex, and RNA polymerase II complex, in the presence of T3, were identified, validating our strategy and suggesting a role for these proteins in neuronal TR activity. Strikingly, many other identified proteins are members of protein complexes that are involved in chromatin remodeling but have never been described as TR coregulators, for instance, ADNP, ANKRD11, FOXK1, and FOXK2, all of which were co-purified with TRs in the absence of T3, and the nucleosome remodeling deacetylase (NuRD), the Spt-Ada-Gcn5-Acetyltransferase (SAGA) complexes, and the MLL/SET methyltransferase complex, all of which were co-purified with TRs in the presence of T3. (Data are analyzed by STRING version 11.0)

A.

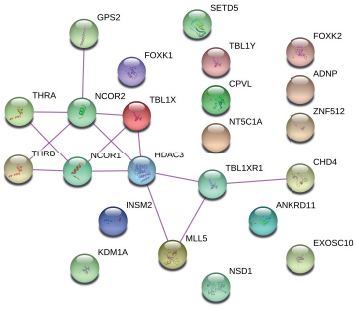
SETD5
GPS2
FOXK2
TBL1Y
FOXK1
ADNP
CPVL
THRA
NCOR2
TBL1X
ZNF512
NT5C1A
THRB
NCOR1
HDAC3
CHD4
TBL1XR1
INSM2
ANKRD11
MLL5
EXOSC10
KDM1A
NSD1

B.

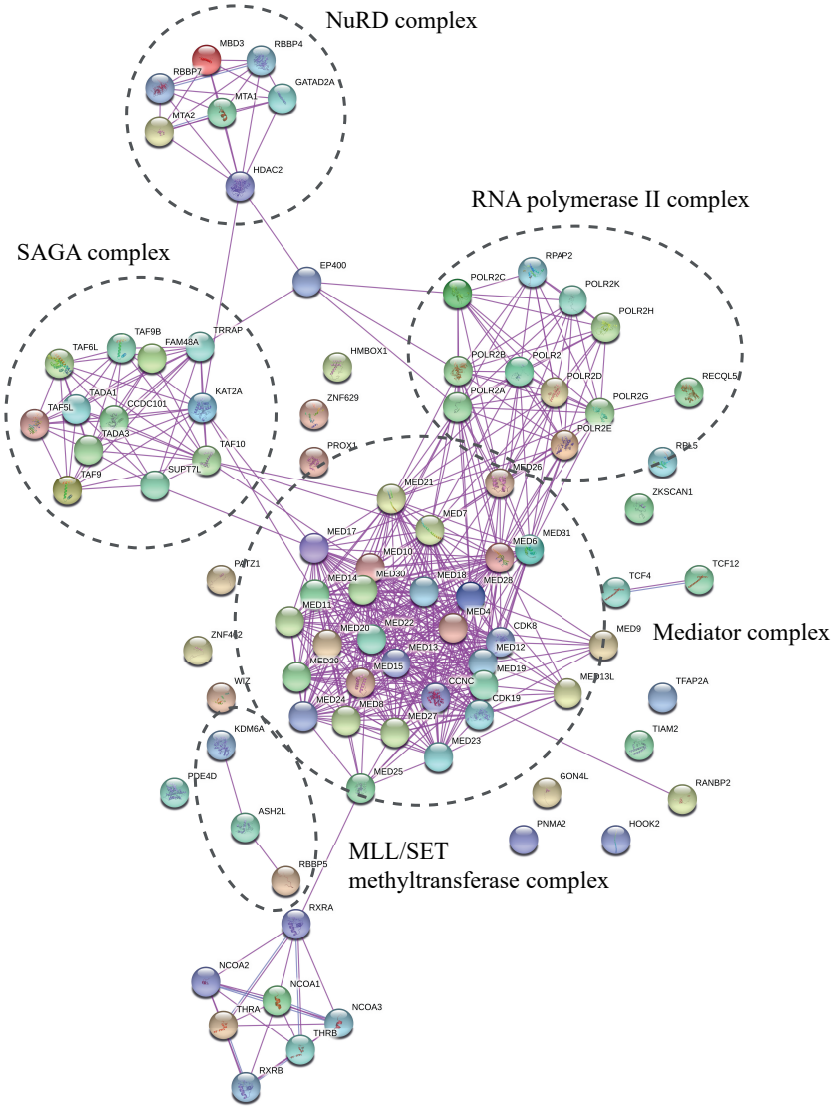
NuRD complex
MBD3
RBBP4
RBBP7
GATAD2A
MTA1
MTA2
HDAC2
RNA polymerase II complex
SAGA complex
EP400
RPAP2
POLR2C
POLR2K
POLR2H
TAF6L
TAF9B
FAM48A
TRRAP
HMBOX1
POLR2B
POLR2
POLR2D
RECQL5
TADA1
KAT2A
POLR2A
POLR2G
TAF5L
CCDC101
ZNF629
POLR2E
TADA3
TAF10
PROX1
RPA5
TAF9
SUPT7L
MED26
MED21
ZKSCAN1
MED7
MED17
MED31
MED10
MED6
PATZ1
MED30
MED14
MED18
MED28
TCF4
TCF12
MED11
MED4
MED22
CDK8
ZNF462
MED20
MED9
Mediator complex
MED13
MED12
MED15
MED19
CCNC
MED13L
WIZ
TFAP2A
MED24
MED8
CDK19
MED27
KDM6A
TIAM2
MED23
PDE4D
MED25
6ON4L
RANBP2
ASH2L
PNMA2
HOOK2
RBBP5
MLL/SET
methyltransferase complex
RXRA
NCOA2
NCOA1
NCOA3
THRA
THRB
RXRB

Discussion

In this study, we identified known and potentially novel binding partners for TRs in a human neuronal cell model. The majority of identified proteins associated with both TRα1 and TRβ1, suggesting that these two TR isoforms interact with common coregulatory proteins to regulate gene transcription. However, a subset of distinct nuclear proteins seems to interact with TRs in an isoform-specific manner.

We successfully identified a large number of TR associated proteins in this study. The yield of our study is higher than previous reports (17,18). Although the tandem-affinity TR purification technique we used was adopted from Fozzatti et al. (17), we performed direct LC-MS/MS analysis of the eluates rather than separated proteins by SDS-PAGE gel and subjected only proteins that are visualized on gel to LC-MS/MS analysis, which may lead to a higher yield. Therefore, we suggest that the methods we used is an optimal and effective technique for the interactome analysis of TRs. We also replicated the purifications for each condition and found some previously reported TR specific proteins in our controls. We, therefore, suggest to replicate the purifications as well, in order to increase the reliability of the results.

The nuclear proteins associated with TRs were categorized by heat map and hierarchical clustering into two groups. A vehicle enriched group is a group of proteins identified in the absence of T3, and a T3-enriched group is a group of proteins identified in the presence of T3. Gene ontology enrichment analyses confirmed this separation since the proteins from the two groups were significantly enriched with transcriptional gene repression and activation terms, respectively.

In the vehicle enriched group, we identified two well-known TR corepressors, NCoR1 and SMRT (NCoR2), showing the effectiveness of our approach. We also identified other members of the NCoR/SMRT complex that do not directly interact with TRs, namely HDAC3, TBL1X, TBL1XR1, and GPS2 (24-27), which shows that our method preserves protein complexes and can find distant binding partners for TRs. HDAC3 is responsible for remodeling of the chromatin by deacetylating histone tails, which promotes transcriptional repression of the TRs (24,27). TBL1X and its homolog TBL1XR1 stabilize the NCoR/SMRT complexes on the chromatin and promote efficient histone deacetylation by HDAC3 (26). GPS2 associates with the NCoR/SMRT complex to regulate gene repression of estrogen receptor (ER) α (28) and peroxisome proliferator-activated receptor (PPAR) γ (29). Although Guo et al. showed that the transcriptional activity of TRα1 is not affected in embryonic fibroblast cells derived from GPS2 knock-out mice (29), this does not necessarily rule out a role for GPS2 in neuronal T3-regulated gene expression.

Another protein that was identified in the absence of T3 is MLL5. This protein has been grouped into the lysine N-methyltransferase (KMTs) family because of its structural homology; however, it lacks intrinsic histone methyltransferase (HMT) activity (30). An orthologue protein, SETD5, was also found in the absence of T3 but with a lower peptide count than MLL5.

Osipovich et al. showed that SETD5 associates with NCoR repressor complexes (NCoR1, TBL1X, and HDAC3) and regulates histone deacetylation in HEK 293T cells (31). Evidence in yeast shows that Set3 (orthologue of human MLL5) interacts with Snt1 and Sif2 (i.e. Hif2) proteins (orthologues of human SMRT and TBL1X, respectively) to regulate gene transcription (32,33). Recently, MLL5 was found to interact with SMRT and also TBL1X and TBL1XR1 in nuclear extracts of HeLa cells (34)(www.nursa.org/10.1621/datasets.01002), indicating the role of this protein in corepressor complex. Therefore, the identification of MLL5 and SETD5 in our profiles suggests that they may play a role in transcriptional gene repression by TRs in neuronal cells as well.

Two closely related Forkhead box (FOX) transcription factors, FOXK1 and FOXK2, were also identified in the absence of T3 and have previously been shown to regulate gene repression. FOXK1/2, in combination with Sin3A-HDAC transcriptional repression complexes (Sin3A, SIN3 transcription regulator family member A), inhibit expression of cell autophagy genes in muscle cells and fibroblast (35). FOXK1 also interacts with Ten-eleven translocation 1 (TET1), a tumor suppressor protein, in breast cancer cell line and repress vascular endothelial growth factor VEGF gene expression (36). Wang et al. reported that FOXK1 and 2 positively regulate Wnt/β-catenin pathway by promoting the nuclear localization of phosphorylated Dishevelled (DVL) protein which helps to stabilize β-catenin/T-cell factor (TCF) transcriptional complex at the promoter region of Wnt target genes (37). Although the interaction between TRs and FOXK1/2 is unknown, both physical and functional interactions between TRs and Wnt/β-catenin signaling have been established (38-40).

In the T3-enriched group, we found many know TR-coactivator proteins, including SRC 1, 2, and 3, the RNA polymerase II complex, and the Mediator complex, together with both TR isoforms. In addition, several proteins belonging to the NuRD complex were co-purified with both TR isoforms in the presence of T3. Although originally identified as a gene repressing complex, subsequent studies have shown that the NuRD complex is involved in both transcriptional repression (41-43) and activation (44) by forming direct interactions with many nuclear receptors (45-47). The identification of the NuRD complex in the presence of T3 was similar to our previous TRα1 interactomes (Chapter 6a), suggesting that this complex may take part in T3-induced transcriptional activation. However, we and others (17) identified CHD4, one of the core components of the NuRD complex, also with TRs in the absence of T3. Ostapcuk et al. showed that apart from the NuRD complex, CHD4 can also form a complex with ADNP and HP1β and γ (heterochromatin protein 1 β and γ), called ChAHP, to represses gene transcription, which seems to be essential for neuronal cells differentiation (48). Since we and others (17) identified both CHD4 and ADNP with TRs in the absence of T3, TRs may interact with the ChAHP complex to facilitate T3-dependent gene repression as well.

The SAGA complex is one of the known coactivator complex which consists of a core structural module, a histone deubiquitinase module (DUB), a histone acetyltransferase module (HAT), and an activator-biding module (49,50). In this study, we co-purified many

nuclear proteins that belong to the SAGA complex with the TRs in the presence of T3, including members of core structural module (TAF5L, TAF6L, TAF10, SUPT7L, and SUPT20H), HAT module (KAT2A, TADA3, and CCDC101), and activator-binding module (TRRAP). A recent study showed that SAGA is recruited to upstream activating sequences (UASs) of most RNA polymerase II-transcribed genes (51,52), indicating that SAGA may act as a cofactor to modify chromatin structure and recruit the preinitiation complex (PIC) for transcriptional activation. To our knowledge, this is the first study showing an interaction between the SAGA complex and TRs.

Although the majority of identified proteins were associated with both TR isoforms, we identified a subset of nuclear proteins interacts with TRs in an isoform-specific manner, which is in line with previous reports (17,18). The confidence of these hits being isoform-specific is strengthened by the fact that they were explicitly identified with certain TR isoform in two independent purifications. Interestingly, we identified that lysine-specific demethylase 6A (KDM6A or UTX), set1/Ash2 histone methyltransferase complex subunit ASH2 (ASH2L), and retinoblastoma-binding protein 5 (RBBP5) are specific for TRα1. KDM6A removes repressive histone marks (H3K27me), and ASH2L and RBBP5, in combination with MLL1-4 (KMT2A-D) and WDR5 proteins, subsequently add active histone marks (H3K4me) to establish transcriptionally permissive chromatin for many key developmental genes such as HOX genes (53-56). The importance of these proteins in neurodevelopment was postulated because mutations in genes encoding KDM6A and MLL4 lead to a similar phenotype, including growth retardation, intellectual disability, and characteristic facial features (long palpebral fissures and ectropion of the lateral 1/3 of lower eyelids), as known as Kabuki syndrome (55,57,58). However, further studies are needed to explore the specificity for TRα1 and the role in transcriptional regulation of these proteins.

In summary, we identified known and potential novel binding partners of TRs in SH-SY5Y cells. In addition, a subset of distinct nuclear proteins seems to interact with TRs in an isoform-specific manner. These findings enable us to gain more understanding of the transcriptional gene regulation by TRs in the brain. However, additional experiments are needed to confirm the interaction between these proteins and TRs and to elucidate a functional relevance of these proteins in TR actions.

Acknowledgement

This work is supported by Zon-MWTOP Grant 91212044 and an Erasmus MC Medical Research Advisory Committee (MRACE) grant (RPP, MEM), and Chiang Mai University (KW).

Author Disclosure Statement

The authors have nothing to disclose.

References

1. Prezioso G, Giannini C, Chiarelli F. Effect of Thyroid Hormones on Neurons and Neurodevelopment. *Horm Res Paediatr.* 2018;**90**(2):73-81.
2. Rovet JF. Congenital hypothyroidism: an analysis of persisting deficits and associated factors. *Child Neuropsychol.* 2002;**8**(3):150-162.
3. Salazar P, Cisternas P, Martinez M, Inestrosa NC. Hypothyroidism and Cognitive Disorders during Development and Adulthood: Implications in the Central Nervous System. *Mol Neurobiol.* 2019;**56**(4):2952-2963.
4. Friesema EC, Grueters A, Biebermann H, Krude H, von Moers A, Reeser M, Barrett TG, Mancilla EE, Svensson J, Kester MH, Kuiper GG, Balkassmi S, Uitterlinden AG, Koehrle J, Rodien P, Halestrap AP, Visser TJ. Association between mutations in a thyroid hormone transporter and severe X-linked psychomotor retardation. *Lancet.* 2004;**364**(9443):1435-1437.
5. Dumitrescu AM, Liao XH, Best TB, Brockmann K, Refetoff S. A novel syndrome combining thyroid and neurological abnormalities is associated with mutations in a monocarboxylate transporter gene. *Am J Hum Genet.* 2004;**74**(1):168-175.
6. Bochukova E, Schoenmakers N, Agostini M, Schoenmakers E, Rajanayagam O, Keogh JM, Henning E, Reinemund J, Gevers E, Sarri M, Downes K, Offiah A, Albanese A, Halsall D, Schwabe JW, Bain M, Lindley K, Muntoni F, Vargha-Khadem F, Dattani M, Farooqi IS, Gurnell M, Chatterjee K. A mutation in the thyroid hormone receptor alpha gene. *N Engl J Med.* 2012;**366**(3):243-249.
7. van Mullem A, van Heerebeek R, Chrysis D, Visser E, Medici M, Andrikoula M, Tsatsoulis A, Peeters R, Visser TJ. Clinical phenotype and mutant TRalpha1. *N Engl J Med.* 2012;**366**(15):1451-1453.
8. Cheng SY, Leonard JL, Davis PJ. Molecular aspects of thyroid hormone actions. *Endocr Rev.* 2010;**31**(2):139-170.
9. Mellstrom B, Naranjo JR, Santos A, Gonzalez AM, Bernal J. Independent expression of the alpha and beta c-erbA genes in developing rat brain. *Mol Endocrinol.* 1991;**5**(9):1339-1350.
10. Schwartz HL, Strait KA, Ling NC, Oppenheimer JH. Quantitation of rat tissue thyroid hormone binding receptor isoforms by immunoprecipitation of nuclear triiodothyronine binding capacity. *J Biol Chem.* 1992;**267**(17):11794-11799.
11. Bradley DJ, Towle HC, Young WS, 3rd. Spatial and temporal expression of alpha- and beta-thyroid hormone receptor mRNAs, including the beta 2-subtype, in the developing mammalian nervous system. *The Journal of neuroscience : the official journal of the Society for Neuroscience.* 1992;**12**(6):2288-2302.
12. Wallis K, Dudazy S, van Hogerlinden M, Nordstrom K, Mittag J, Vennstrom B. The thyroid hormone receptor alpha1 protein is expressed in embryonic postmitotic neurons and persists in most adult neurons. *Mol Endocrinol.* 2010;**24**(10):1904-1916.
13. Ercan-Fang S, Schwartz HL, Oppenheimer JH. Isoform-specific 3,5,3'-triiodothyronine receptor binding capacity and messenger ribonucleic acid content in rat adenohypophysis: effect of thyroidal state and comparison with extrapituitary tissues. *Endocrinology.* 1996;**137**(8):3228-3233.
14. Flamant F, Gauthier K. Thyroid hormone receptors: the challenge of elucidating isotype-specific functions and cell-specific response. *Biochim Biophys Acta.* 2013;**1830**(7):3900-3907.
15. Harvey CB, Williams GR. Mechanism of thyroid hormone action. *Thyroid.* 2002;**12**(6):441-446.
16. Astapova I. Role of co-regulators in metabolic and transcriptional actions of thyroid hormone. *J Mol Endocrinol.* 2016;**56**(3):73-97.
17. Fozzatti L, Lu C, Kim DW, Cheng SY. Differential recruitment of nuclear coregulators directs the isoform-dependent action of mutant thyroid hormone receptors. *Mol Endocrinol.* 2011;**25**(6):908-921.
18. Hahm JB, Schroeder AC, Privalsky ML. The two major isoforms of thyroid hormone receptor,

TRalpha1 and TRbeta1, preferentially partner with distinct panels of auxiliary proteins. *Mol Cell Endocrinol.* 2014;**383**(1-2):80-95.

19. Paul BD, Buchholz DR, Fu L, Shi YB. Tissue- and gene-specific recruitment of steroid receptor coactivator-3 by thyroid hormone receptor during development. *J Biol Chem.* 2005;**280**(29):27165-27172.
20. Bebermeier JH, Brooks JD, DePrimo SE, Werner R, Deppe U, Demeter J, Hiort O, Holterhus PM. Cell-line and tissue-specific signatures of androgen receptor-coregulator transcription. *J Mol Med (Berl).* 2006;**84**(11):919-931.
21. van Gucht AL, Meima ME, Zwaveling-Soonawala N, Visser WE, Fliers E, Wennink JM, Henny C, Visser TJ, Peeters RP, van Trotsenburg AS. Resistance to Thyroid Hormone Alpha in an 18-Month-Old Girl: Clinical, Therapeutic, and Molecular Characteristics. *Thyroid.* 2016;**26**(3):338-346.
22. Wejaphikul K, Groeneweg S, Dejkhamron P, Unachak K, Visser WE, Chatterjee K, Visser TJ, Meima ME, Peeters RP. Role of Leucine 341 in Thyroid Hormone Receptor Beta Revealed by a Novel Mutation Causing Thyroid Hormone Resistance. *Thyroid.* 2018;**28**(12):1723-1726.
23. Babicki S, Arndt D, Marcu A, Liang Y, Grant JR, Maciejewski A, Wishart DS. Heatmapper: web-enabled heat mapping for all. *Nucleic Acids Res.* 2016;**44**(W1):W147-153.
24. Li J, Wang J, Wang J, Nawaz Z, Liu JM, Qin J, Wong J. Both corepressor proteins SMRT and N-CoR exist in large protein complexes containing HDAC3. *EMBO J.* 2000;**19**(16):4342-4350.
25. Zhang J, Kalkum M, Chait BT, Roeder RG. The N-CoR-HDAC3 nuclear receptor corepressor complex inhibits the JNK pathway through the integral subunit GPS2. *Mol Cell.* 2002;**9**(3):611-623.
26. Yoon HG, Chan DW, Huang ZQ, Li J, Fondell JD, Qin J, Wong J. Purification and functional characterization of the human N-CoR complex: the roles of HDAC3, TBL1 and TBLR1. *EMBO J.* 2003;**22**(6):1336-1346.
27. Guenther MG, Barak O, Lazar MA. The SMRT and N-CoR corepressors are activating cofactors for histone deacetylase 3. *Mol Cell Biol.* 2001;**21**(18):6091-6101.
28. Cheng X, Kao HY. G protein pathway suppressor 2 (GPS2) is a transcriptional corepressor important for estrogen receptor alpha-mediated transcriptional regulation. *J Biol Chem.* 2009;**284**(52):36395-36404.
29. Guo C, Li Y, Gow CH, Wong M, Zha J, Yan C, Liu H, Wang Y, Burris TP, Zhang J. The optimal corepressor function of nuclear receptor corepressor (NCoR) for peroxisome proliferator-activated receptor gamma requires G protein pathway suppressor 2. *J Biol Chem.* 2015;**290**(6):3666-3679.
30. Zhang X, Novera W, Zhang Y, Deng LW. MLL5 (KMT2E): structure, function, and clinical relevance. *Cell Mol Life Sci.* 2017;**74**(13):2333-2344.
31. Osipovich AB, Gangula R, Vianna PG, Magnuson MA. Setd5 is essential for mammalian development and the co-transcriptional regulation of histone acetylation. *Development.* 2016;**143**(24):4595-4607.
32. Rentas S, Saberianfar R, Grewal C, Kanippayoor R, Mishra M, McCollum D, Karagiannis J. The SET domain protein, Set3p, promotes the reliable execution of cytokinesis in Schizosaccharomyces pombe. *PLoS One.* 2012;**7**(2):e31224.
33. Pijnappel WW, Schaft D, Roguev A, Shevchenko A, Tekotte H, Wilm M, Rigaut G, Seraphin B, Aasland R, Stewart AF. The S. cerevisiae SET3 complex includes two histone deacetylases, Hos2 and Hst1, and is a meiotic-specific repressor of the sporulation gene program. *Genes Dev.* 2001;**15**(22):2991-3004.
34. Kittler R, Pelletier L, Heninger AK, Slabicki M, Theis M, Miroslaw L, Poser I, Lawo S, Grabner H, Kozak K, Wagner J, Surendranath V, Richter C, Bowen W, Jackson AL, Habermann B, Hyman AA, Buchholz F. Genome-scale RNAi profiling of cell division in human tissue culture cells. *Nat Cell Biol.* 2007;**9**(12):1401-1412.
35. Bowman CJ, Ayer DE, Dynlacht BD. Foxk proteins repress the initiation of starvation-induced atrophy and autophagy programs. *Nat Cell Biol.* 2014;**16**(12):1202-1214.

36. Sun T, Wang H, Li Q, Qian Z, Shen C. Forkhead box protein k1 recruits TET1 to act as a tumor suppressor and is associated with MRI detection. *Jpn J Clin Oncol.* 2016;**46**(3):209-221.

37. Wang W, Li X, Lee M, Jun S, Aziz KE, Feng L, Tran MK, Li N, McCrea PD, Park JI, Chen J. FOXKs promote Wnt/beta-catenin signaling by translocating DVL into the nucleus. *Dev Cell.* 2015;**32**(6):707-718.

38. Guigon CJ, Zhao L, Lu C, Willingham MC, Cheng SY. Regulation of beta-catenin by a novel nongenomic action of thyroid hormone beta receptor. *Mol Cell Biol.* 2008;**28**(14):4598-4608.

39. Ely KA, Bischoff LA, Weiss VL. Wnt Signaling in Thyroid Homeostasis and Carcinogenesis. *Genes (Basel).* 2018;**9**(4).

40. Skah S, Uchuya-Castillo J, Sirakov M, Plateroti M. The thyroid hormone nuclear receptors and the Wnt/beta-catenin pathway: An intriguing liaison. *Dev Biol.* 2017;**422**(2):71-82.

41. Xue Y, Wong J, Moreno GT, Young MK, Cote J, Wang W. NURD, a novel complex with both ATP-dependent chromatin-remodeling and histone deacetylase activities. *Mol Cell.* 1998;**2**(6):851-861.

42. Tong JK, Hassig CA, Schnitzler GR, Kingston RE, Schreiber SL. Chromatin deacetylation by an ATP-dependent nucleosome remodelling complex. *Nature.* 1998;**395**(6705):917-921.

43. Zhang Y, LeRoy G, Seelig HP, Lane WS, Reinberg D. The dermatomyositis-specific autoantigen Mi2 is a component of a complex containing histone deacetylase and nucleosome remodeling activities. *Cell.* 1998;**95**(2):279-289.

44. Bornelov S, Reynolds N, Xenophontos M, Gharbi S, Johnstone E, Floyd R, Ralser M, Signolet J, Loos R, Dietmann S, Bertone P, Hendrich B. The Nucleosome Remodeling and Deacetylation Complex Modulates Chromatin Structure at Sites of Active Transcription to Fine-Tune Gene Expression. *Mol Cell.* 2018;**71**(1):56-72 e54.

45. Cui Y, Niu A, Pestell R, Kumar R, Curran EM, Liu Y, Fuqua SA. Metastasis-associated protein 2 is a repressor of estrogen receptor alpha whose overexpression leads to estrogen-independent growth of human breast cancer cells. *Mol Endocrinol.* 2006;**20**(9):2020-2035.

46. Johnson DR, Lovett JM, Hirsch M, Xia F, Chen JD. NuRD complex component Mi-2beta binds to and represses RORgamma-mediated transcriptional activation. *Biochem Biophys Res Commun.* 2004;**318**(3):714-718.

47. Mazumdar A, Wang RA, Mishra SK, Adam L, Bagheri-Yarmand R, Mandal M, Vadlamudi RK, Kumar R. Transcriptional repression of oestrogen receptor by metastasis-associated protein 1 corepressor. *Nat Cell Biol.* 2001;**3**(1):30-37.

48. Ostapcuk V, Mohn F, Carl SH, Basters A, Hess D, Iesmantavicius V, Lampersberger L, Flemr M, Pandey A, Thoma NH, Betschinger J, Buhler M. Activity-dependent neuroprotective protein recruits HP1 and CHD4 to control lineage-specifying genes. *Nature.* 2018;**557**(7707):739-743.

49. Samara NL, Wolberger C. A new chapter in the transcription SAGA. *Curr Opin Struct Biol.* 2011;**21**(6):767-774.

50. Helmlinger D, Tora L. Sharing the SAGA. *Trends Biochem Sci.* 2017;**42**(11):850-861.

51. Baptista T, Grunberg S, Minoungou N, Koster MJE, Timmers HTM, Hahn S, Devys D, Tora L. SAGA Is a General Cofactor for RNA Polymerase II Transcription. *Mol Cell.* 2017;**68**(1):130-143 e135.

52. Taatjes DJ. The Continuing SAGA of TFIID and RNA Polymerase II Transcription. *Mol Cell.* 2017;**68**(1):1-2.

53. Sengoku T, Yokoyama S. Structural basis for histone H3 Lys 27 demethylation by UTX/KDM6A. *Genes Dev.* 2011;**25**(21):2266-2277.

54. Shpargel KB, Starmer J, Wang C, Ge K, Magnuson T. UTX-guided neural crest function underlies craniofacial features of Kabuki syndrome. *Proc Natl Acad Sci U S A.* 2017;**114**(43):E9046-E9055.

55. Steward MM, Lee JS, O'Donovan A, Wyatt M, Bernstein BE, Shilatifard A. Molecular regulation of H3K4 trimethylation by ASH2L, a shared subunit of MLL complexes. *Nat Struct Mol Biol.* 2006;**13**(9):852-854.

56. Froimchuk E, Jang Y, Ge K. Histone H3 lysine 4 methyltransferase KMT2D. *Gene.* 2017;**627**:337-

342.

57. Van Laarhoven PM, Neitzel LR, Quintana AM, Geiger EA, Zackai EH, Clouthier DE, Artinger KB, Ming JE, Shaikh TH. Kabuki syndrome genes KMT2D and KDM6A: functional analyses demonstrate critical roles in craniofacial, heart and brain development. *Human molecular genetics.* 2015;**24**(15):4443-4453.

58. Miyake N, Koshimizu E, Okamoto N, Mizuno S, Ogata T, Nagai T, Kosho T, Ohashi H, Kato M, Sasaki G, Mabe H, Watanabe Y, Yoshino M, Matsuishi T, Takanashi J, Shotelersuk V, Tekin M, Ochi N, Kubota M, Ito N, Ihara K, Hara T, Tonoki H, Ohta T, Saito K, Matsuo M, Urano M, Enokizono T, Sato A, Tanaka H, Ogawa A, Fujita T, Hiraki Y, Kitanaka S, Matsubara Y, Makita T, Taguri M, Nakashima M, Tsurusaki Y, Saitsu H, Yoshiura K, Matsumoto N, Niikawa N. MLL2 and KDM6A mutations in patients with Kabuki syndrome. *Am J Med Genet A.* 2013;**161A**(9):2234-2243.

Supplementary Table S1. List of proteins identified by LC-MS/MS.

Protein	0 nM T3												100 nM T3											
	TRα1						TRβ1						TRα1						TRβ1					
	1st			2nd			1st			2nd			1st			2nd			1st			2nd		
	UPC	% Cov	% Prob	UPC	% Cov	% Prob	UPC	% Cov	% Prob	UPC	% Cov	% Prob	UPC	% Cov	% Prob	UPC	% Cov	% Prob	UPC	% Cov	% Prob	UPC	% Cov	% Prob
ADNP	9	11.7	100.0	7	10.7	100.0	3	4.3	100.0	12	18.4	100.0	1	1.1	12.3	0	0	0	0	0	0	0	0	0
ANKRD11	3	2.8	100.0	17	11.4	100.0	1	0.4	99.7	7	4.3	100.0	1	0.3	8.6	0	0	0	0	0	0	0	0	0
ASH2L	0	0	0	0	0	0	0	0	0	0	0	0	2	3.8	99.9	3	6.4	100.0	0	0	0	0	0	0
CCDC101	0	0	0	0	0	0	0	0	0	0	0	0	2	8.9	100.0	2	8.2	100.0	3	13.3	100.0	3	10.6	100.0
CCNC	0	0	0	0	0	0	0	0	0	0	0	0	3	9.9	100.0	3	8.5	100.0	4	14.5	100.0	5	20.1	100.0
CDK19	0	0	0	0	0	0	0	0	0	0	0	0	4	16.7	100.0	8	31.5	100.0	8	26.7	100.0	10	36.5	100.0
CDK8	0	0	0	0	0	0	0	0	0	0	0	0	8	19.4	100.0	8	23.5	100.0	8	22.4	100.0	8	25.2	100.0
CHD4	4	2.8	100.0	6	5.7	100.0	5	4.9	100.0	6	4.4	100.0	3	3.5	100.0	12	11.5	100.0	4	4.1	100.0	1	1.15	98.7
CPVL	2	4.2	100.0	6	13.9	100.0	2	3.8	100.0	7	16.8	100.0	0	0	0	0	0	0	0	0	0	0	0	0
EP400	0	0	0	0	0	0	0	0	0	0	0	0	8	4.0	100.0	0	0	0	1	1.0	16.8	1	0.5	39.8
EXOSC10	1	1.1	27.1	2	3.3	100.0	0	0	0	0	0	0	0	0	0	2	3.3	99.9	0	0	0	0	0	0
FOXK1	9	20.9	100.0	10	22.0	100.0	2	3.7	100.0	8	18.0	100.0	2	4.1	99.8	0	0	0	0	0	0	0	0	0
FOXK2	4	7.0	100.0	6	14.8	100.0	0	0	0	4	14.1	100.0	0	0	0	0	0	0	0	0	0	0	0	0
GATAD2A	0	0	0	0	0	0	0	0	0	0	0	0	1	3.8	99.4	3	7.6	100.0	0	0	0	0	0	0
GON4L	0	0	0	0	0	0	0	0	0	0	0	0	20	13.8	100.0	18	11.9	100.0	5	3.4	100.0	3	2.2	100.0
GPS2	9	41.9	100.0	8	42.5	100.0	3	15.9	100.0	6	24.5	100.0	1	2.5	87.4	0	0	0	0	0	0	0	0	0
HDAC2	0	0	0	1	3.3	87.6	0	0	0	1	9.0	92.70	1	1.6	87.4	3	11.1	100.0	0	0	0	2	5.5	99.9
HDAC3	17	48.4	100.0	21	66.4	100.0	15	42.8	100.0	15	44.6	100.0	7	25.9	100.0	7	27.6	100.0	0	0	0	0	0	0
HMBOX1	0	0	0	0	0	0	0	0	0	0	0	0	0	0	0	1	4.5	100.0	3	10.2	100.0	2	8.6	100.0
HOOK2	0	0	0	0	0	0	0	0	0	0	0	0	1	1.0	38.7	2	3.3	93.1	0	0	0	1	1.0	39.3
INSM2	13	38.9	100.0	13	40.6	100.0	7	19.8	100.0	18	57.2	100.0	0	0	0	0	0	0	0	0	0	0	0	0

Protein	0 nM T3												100 nM T3											
	TRα1						TRβ1						TRα1						TRβ1					
	1st			2nd			1st			2nd			1st			2nd			1st			2nd		
	UPC	% Cov	% Prob	UPC	% Cov	% Prob	UPC	% Cov	% Prob	UPC	% Cov	% Prob	UPC	% Cov	% Prob	UPC	% Cov	% Prob	UPC	% Cov	% Prob	UPC	% Cov	% Prob
KAT2A	0	0	0	0	0	0	0	0	0	0	0	0	3	4.7	100.0	1	1.3	75.7	1	2.3	97.7	2	3.1	99.9
KDM1A	3	4.5	100.0	10	17.0	100.0	0	0	0	5	8.6	100.0	0	0	0	0	0	0	0	0	0	0	0	0
KDM6A	0	0	0	0	0	0	0	0	0	0	0	0	3	3.9	100.0	3	4.1	100.0	0	0	0	0	0	0
KMT2E	3	2.9	100.0	9	6.9	100.0	0	0	0	1	1.3	40.7	0	0	0	0	0	0	0	0	0	0	0	0
MBD3	0	0	0	0	0	0	0	0	0	0	0	0	2	8.9	99.8	5	19.9	100.0	1	5.5	67.1	0	0	0
MED10	0	0	0	0	0	0	0	0	0	0	0	0	7	60.0	100.0	6	57.8	100.0	7	59.3	100.0	6	57.8	100.0
MED11	0	0	0	0	0	0	0	0	0	0	0	0	4	55.6	100.0	4	55.6	100.0	3	49.6	100.0	4	55.6	100.0
MED12	0	0	0	0	0	0	0	0	0	0	0	0	53	33.6	100.0	58	32.7	100.0	52	32.2	100.0	61	39.2	100.0
MED13	0	0	0	0	0	0	0	0	0	0	0	0	49	30.6	100.0	52	31.7	100.0	51	32.0	100.0	46	29.5	100.0
MED13L	0	0	0	0	0	0	0	0	0	0	0	0	25	20.5	100.0	39	31.4	100.0	35	27.9	100.0	40	31.9	100.0
MED14	0	0	0	0	0	0	0	0	0	0	0	0	34	31.7	100.0	43	37.6	100.0	42	36.1	100.0	41	37.9	100.0
MED15	0	0	0	0	0	0	0	0	0	0	0	0	12	23.0	100.0	13	23.9	100.0	12	23.0	100.0	12	21.1	100.0
MED17	0	0	0	0	0	0	0	0	0	0	0	0	24	43.8	100.0	28	50.8	100.0	28	51.2	100.0	27	45.3	100.0
MED18	0	0	0	0	0	0	0	0	0	0	0	0	3	15.4	100.0	3	15.4	100.0	3	15.4	100.0	3	15.4	100.0
MED19	0	0	0	0	0	0	0	0	0	0	0	0	4	32.4	100.0	3	21.7	100.0	6	42.2	100.0	3	21.7	100.0
MED20	0	0	0	0	0	0	0	0	0	0	0	0	6	31.1	100.0	5	26.9	100.0	5	29.2	100.0	5	29.2	100.0
MED21	0	0	0	0	0	0	0	0	0	0	0	0	3	39.6	100.0	4	53.5	100.0	4	53.5	100.0	4	53.5	100.0
MED22	0	0	0	0	0	0	0	0	0	0	0	0	3	12.0	100.0	3	14.0	100.0	3	18.5	100.0	5	23.0	100.0
MED23	0	0	0	0	0	0	0	0	0	0	0	0	11	10.8	100.0	20	17.6	100.0	24	24.7	100.0	20	17.4	100.0
MED24	0	0	0	0	0	0	0	0	0	0	0	0	17	23.2	100.0	23	28.9	100.0	23	29.5	100.0	21	26.8	100.0
MED25	0	0	0	0	0	0	0	0	0	0	0	0	6	19.0	100.0	5	17.4	100.0	5	13.4	100.0	6	20.2	100.0
MED26	0	0	0	0	0	0	0	0	0	0	0	0	13	29.7	100.0	13	36.5	100.0	8	19.7	100.0	11	25.2	100.0

Protein	0 nM T3												100 nM T3											
	TRα1						TRβ1						TRα1						TRβ1					
	1st			2nd			1st			2nd			1st			2nd			1st			2nd		
	UPC	% Cov	% Prob	UPC	% Cov	% Prob	UPC	% Cov	% Prob	UPC	% Cov	% Prob	UPC	% Cov	% Prob	UPC	% Cov	% Prob	UPC	% Cov	% Prob	UPC	% Cov	% Prob
MED27	0	0	0	0	0	0	0	0	0	0	0	0	9	28.6	100.0	11	39.5	100.0	10	27.7	100.0	10	30.5	100.0
MED28	0	0	0	0	0	0	0	0	0	0	0	0	7	47.8	100.0	6	41.0	100.0	8	46.1	100.0	8	48.9	100.0
MED29	0	0	0	0	0	0	0	0	0	0	0	0	2	13.0	100.0	3	19.0	100.0	2	13.0	100.0	4	34.0	100.0
MED30	0	0	0	0	0	0	0	0	0	0	0	0	1	5.1	96.2	1	5.1	96.2	1	5.1	96.4	2	11.8	100.0
MED31	0	0	0	0	0	0	0	0	0	0	0	0	2	24.4	100.0	3	38.9	100.0	3	31.3	100.0	4	40.5	100.0
MED4	0	0	0	0	0	0	0	0	0	0	0	0	10	43.0	100.0	9	39.6	100.0	10	43.3	100.0	9	39.6	100.0
MED6	0	0	0	0	0	0	0	0	0	0	0	0	8	30.1	100.0	10	37.8	100.0	11	40.7	100.0	13	45.1	100.0
MED7	0	0	0	0	0	0	0	0	0	0	0	0	2	15.0	100.0	2	15.0	100.0	3	24.5	100.0	3	24.5	100.0
MED8	0	0	0	0	0	0	0	0	0	0	0	0	6	29.9	100.0	4	20.9	100.0	6	28.4	100.0	6	32.5	100.0
MED9	0	0	0	0	0	0	0	0	0	0	0	0	2	17.8	100.0	2	12.3	99.9	1	12.3	96.4	5	40.4	100.0
MTA1	0	0	0	0	0	0	0	0	0	0	0	0	6	15.1	100.0	15	29.4	100.0	5	14.4	100.0	3	10.9	100.0
MTA2	0	0	0	0	0	0	0	0	0	0	0	0	3	8.1	100.0	9	21.7	100.0	5	11.8	100.0	1	2.4	69.3
NCOA1	0	0	0	0	0	0	0	0	0	0	0	0	36	34.4	100.0	25	26.2	100.0	29	32.8	100.0	29	31.9	100.0
NCOA2	0	0	0	0	0	0	0	0	0	0	0	0	12	12.5	100.0	3	2.7	100.0	6	5.5	100.0	4	4.8	100.0
NCOA3	0	0	0	0	0	0	0	0	0	0	0	0	12	12.6	100.0	0	0	0	5	5.4	100.0	4	4.5	100.0
NCOR1	105	52.8	100.0	96	50.5	100.0	81	43.6	100.0	86	45.3	100.0	54	32.6	100.0	29	17.3	100.0	2	1.4	100.0	1	0.7	95.6
NCOR2	35	22.2	100.0	26	17.3	100.0	2	3.0	98.0	10	7.1	100.0	1	2.9	71.1	0	0	0	0	0	0	0	0	0
NSD1	5	2.5	100.0	1	0.5	53.8	0	0	0	0	0	0	3	1.8	100.0	0	0	0	0	0	0	0	0	0
NT5C1A	2	7.3	98.6	0	0	0	2	9.2	100.0	1	4.6	96.8	0	0	0	0	0	0	0	0	0	0	0	0
PATZ1	0	0	0	1	1.9	96.8	0	0	0	0	0	0	1	1.9	96.2	2	2.9	99.9	0	0	0	0	0	0
PDE4D	0	0	0	0	0	0	0	0	0	0	0	0	0	0	0	0	0	0	1	3.2	96.4	2	5.9	100.0
PNMA2	2	14.0	100.0	3	16.5	100.0	0	0	0	0	0	0	6	22.3	100.0	6	23.4	100.0	8	27.5	100.0	6	23.4	100.0

Protein	0 nM T3												100 nM T3											
	TRα1						TRβ1						TRα1						TRβ1					
	1st			2nd			1st			2nd			1st			2nd			1st			2nd		
	UPC	% Cov	% Prob	UPC	% Cov	% Prob	UPC	% Cov	% Prob	UPC	% Cov	% Prob	UPC	% Cov	% Prob	UPC	% Cov	% Prob	UPC	% Cov	% Prob	UPC	% Cov	% Prob
POLR2A	0	0	0	0	0	0	0	0	0	0	0	0	34	18.8	100.0	37	21.8	100.0	25	17.3	100.0	28	18.7	100.0
POLR2B	1	1.6	76.6	0	0	0	2	2.4	99.5	4	4.9	100.0	25	25.3	100.0	28	25.0	100.0	21	19.9	100.0	21	17.9	100.0
POLR2C	2	12.0	100.0	0	0	0	0	0	0	2	13.5	100.0	10	52.7	100.0	13	69.5	100.0	9	46.9	100.0	10	56.7	100.0
POLR2D	0	0	0	0	0	0	0	0	0	0	0	0	3	28.2	100.0	3	34.5	100.0	1	11.3	98.7	4	40.8	100.0
POLR2E	0	0	0	0	0	0	0	0	0	0	0	0	3	17.1	100.0	4	21.4	100.0	3	17.1	100.0	2	9.1	97.3
POLR2G	0	0	0	0	0	0	0	0	0	0	0	0	1	12.8	78.0	3	23.8	100.0	1	12.8	96.4	2	17.4	99.9
POLR2H	0	0	0	0	0	0	0	0	0	0	0	0	3	34.7	100.0	3	34.7	100.0	3	34.7	100.0	2	16.7	99.5
POLR2I	0	0	0	0	0	0	0	0	0	0	0	0	5	56.8	100.0	5	56.8	100.0	3	40.8	100.0	4	46.4	100.0
POLR2K	0	0	0	0	0	0	0	0	0	0	0	0	2	13.8	94.3	2	13.8	93.7	1	12.1	89.8	1	12.1	39.3
PROX1	0	0	0	5	8.3	100.0	0	0	0	2	3.8	99.9	18	34.6	100.0	28	48.6	100.0	14	28.4	100.0	13	22.4	100.0
RBBP4	0	0	0	1	3.8	96.8	0	0	0	1	3.8	81.4	5	29.9	100.0	10	61.2	100.0	2	14.1	100.0	2	12.0	100.0
RBBP5	0	0	0	0	0	0	0	0	0	0	0	0	3	7.6	100.0	2	5.8	100.0	0	0	0	0	0	0
RBBP7	0	0	0	0	0	0	0	0	0	0	0	0	2	12.2	85.8	4	30.4	100.0	0	0	0	1	5.7	99.8
RECQL5	0	0	0	0	0	0	0	0	0	0	0	0	12	14.0	100.0	18	24.8	100.0	8	11.6	100.0	10	16.0	100.0
RPAP2	0	0	0	0	0	0	0	0	0	0	0	0	3	8.0	100.0	4	6.7	100.0	0	0	0	0	0	0
RPL5	1	3.4	93.6	0	0	0	0	0	0	0	0	0	3	18.5	100.0	0	0	0	1	11.8	96.4	2	16.5	100.0
RXRB	14	41.3	100.0	8	33.8	100.0	2	6.6	100.0	5	22.7	100.0	18	52.7	100.0	14	49.9	100.0	9	38.3	100.0	7	28.9	100.0
SETD5	2	2.8	100.0	7	9.3	100.0	0	0	0	1	1.8	49.7	0	0	0	0	0	0	0	0	0	0	0	0
SUPT20H	0	0	0	0	0	0	0	0	0	0	0	0	5	10.8	100.0	5	10.4	100.0	5	8.6	100.0	7	17.3	100.0
SUPT7L	0	0	0	0	0	0	0	0	0	0	0	0	5	14.3	100.0	4	11.8	100.0	4	12.3	100.0	5	14.3	100.0
TADA1	0	0	0	0	0	0	0	0	0	0	0	0	2	8.4	100.0	2	8.7	90.2	1	3.9	73.4	4	17.3	100.0
TADA3	0	0	0	0	0	0	0	0	0	0	0	0	4	11.1	100.0	2	7.6	100.0	4	14.6	100.0	2	7.6	100.0

Protein	0 nM T3												100 nM T3											
	TRα1						TRβ1						TRα1						TRβ1					
	1st			2nd			1st			2nd			1st			2nd			1st			2nd		
	UPC	% Cov	% Prob	UPC	% Cov	% Prob	UPC	% Cov	% Prob	UPC	% Cov	% Prob	UPC	% Cov	% Prob	UPC	% Cov	% Prob	UPC	% Cov	% Prob	UPC	% Cov	% Prob
TAF10	0	0	0	0	0	0	0	0	0	0	0	0	1	11.5	96.2	1	11.5	65.8	1	11.5	85.5	2	17.9	100.0
TAF5L	0	0	0	0	0	0	0	0	0	0	0	0	7	13.6	100.0	3	6.1	100.0	4	8.0	100.0	6	12.1	100.0
TAF6L	0	0	0	0	0	0	0	0	0	0	0	0	4	10.5	100.0	3	7.2	100.0	3	7.2	100.0	1	2.4	98.3
TBL1X	10	39.3	100.0	13	54.2	100.0	5	32.1	100.0	12	56.5	100.0	0	0	0	1	19.9	100.0	0	0	0	0	0	0
TBL1XR1	27	74.7	100.0	25	80.2	99.7	22	65.8	100.0	24	80.2	100.0	16	59.5	100.0	17	60.7	100.0	3	14.6	100.0	4	16.9	100.0
TCF12	0	0	0	1	4.11	95.4	0	0	0	2	5.0	99.9	0	0	0	1	2.8	96.2	2	6.5	100.0	1	2.8	96.3
TCF4	0	0	0	0	0	0	0	0	0	1	2.4	96.8	1	3.8	99.8	1	2.4	96.2	1	3.8	99.8	1	2.4	96.3
TFAP2A	0	0	0	1	4.6	96.8	1	4.6	97.9	2	6.6	100.0	0	0	0	1	4.6	96.2	2	6.6	100.0	1	4.6	96.3
THRA	25	60.6	100.0	25	61.2	100.0	2	11.2	100.0	1	8.37	99.7	27	59.2	100.0	20	54.7	100.0	1	6.7	99.7	1	8.4	99.9
THRB	1	6.9	100.0	1	6.9	100.0	26	59.9	100.0	32	66.6	100.0	2	10.8	100.0	2	8.5	100.0	29	63.6	100.0	28	65.9	100.0
TIAM2	0	0	0	0	0	0	0	0	0	0	0	0	0	0	0	0	0	0	2	1.2	92.1	1	0.8	28.6
TRRAP	0	0	0	0	0	0	0	0	0	0	0	0	17	5.5	100.0	16	6.3	100.0	20	7.2	100.0	17	6.8	100.0
WIZ	0	0	0	0	0	0	0	0	0	1	1.2	29.1	2	2.2	99.6	1	1.0	9.5	0	0	0	1	1.2	99.0
ZKSCAN1	0	0	0	0	0	0	2	3.7	99.5	3	7.1	100.0	2	5.3	100.0	2	4.6	98.9	2	3.7	99.9	2	5.0	100.0
ZNF512	2	5.5	99.8	1	2.3	32.3	0	0	0	0	0	0	2	4.9	100.0	0	0	0	0	0	0	0	0	0
ZNF629	1	1.5	97.5	0	0	0	0	0	0	0	0	0	4	6.0	100.0	2	3.0	97.3	2	2.7	100.0	1	1.5	89.5

UPC, exclusive unique peptide count; **%Cov**, percent coverage; **%Prob**, percent probability

Supplementary Table S2. Identified TR-interacting proteins are associated in large protein complexes.

Protein complex	Identified proteins	Associated condition
NCoR/SMRT corepressor	NCoR1; SMRT (NCoR2); HDAC3; TBL1X; TBL1XR1; GPS2	Unliganded TRα and β
Wnt/β-catenin signalling	FOXK1; FOXK2	Unliganded TRα and β
RNA polymerase II	POLR2A, B, C, D, E, G, H, I, K; RECQL5; RPAP2	Liganded TRα and β
Mediators	CCNC; CKD8, 19; MED 4, 6-15, 17-31, 13L	Liganded TRα and β
MLL/SET methyltransferase	ASH2L; KDM6A; RBBP5	Liganded TRα only
NuRD (Nucleosome Remodeling Deacetylase)	GATAD2A*; MBD3; MTA1, 2; CHD4**; RBBP4, 7	Liganded TRα and β
SAGA (Spt-Ada-Gcn5-Acetyltransferase)	CCDC101 (SGF29); KAT2A (GCN5); SUPT20H; SUPT7L; TADA3; TAF5L, 6L, 10; TRRAP	Liganded TRα and β

*TRα1 only; **predominant with unliganded TRs

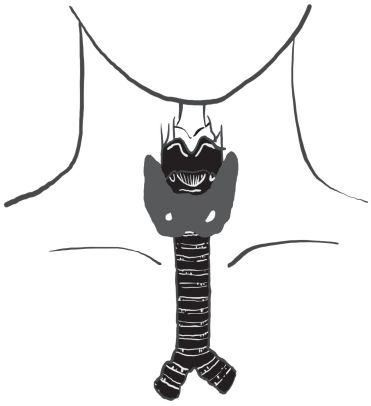

CHAPTER 7

General Discussion

7

Overview

Genomic actions of thyroid hormone (TH) are regulated by the binding of TH to thyroid hormone receptors (TRs). Mutations of the genes encoding TRα and TRβ lead to resistance to thyroid hormone (RTH) α and β, respectively. In the first part of this thesis, we describe two novel mutations identified in an RTHα and RTHβ patient. *In silico* and *in vitro* studies confirmed the pathogenic impact of the amino acid substitutions on receptor function. In addition, these studies allowed us to gain more insight into the role of particular amino acid residues in TR functions. In the second part, we focus on the genotype-phenotype correlation in RTHα (1,2). Based on our observations, the severity of the clinical phenotype of these patients is not solely explained by the degree of impairment in T3 binding affinity. Therefore, we conducted studies to evaluate the diverse functional impairment of mutant TRs to correlate the *in vitro* functional impairment to the severity of the phenotype of reported patients. The last part of this thesis focuses on nuclear coregulatory proteins that are involved in TR functions. We asked whether the nuclear coregulatory protein recruitment by TRs have tissue- and isoform-specific patterns. In this chapter, we discuss the relevance of our studies to the current knowledge gaps and further research strategies to confirm our findings and broaden the understanding of the complexity of TR actions.

Role of specific amino acid residue on TR function: lessons from mutated TRs

Pathogenic mutations in TRs that cause RTH are located in the ligand binding domain (LBD) and adjacent hinge region of the receptors and lead to a reduced affinity for TH. The LBD shares a high sequence homology between isoforms and among species (3). However, not all amino acids in the LBD are equally important for T3 binding and T3-induced transcriptional activity. For instance, a study of Hayashi et al. on sixteen TRβ1 mutations located in the LBD (six patient-derived and ten artificial mutations) showed that six artificial mutations did not significantly affect T3 binding affinity (4), suggesting that only certain residues in the LBD play a role in T3 binding and are sensitive to amino acid changes. Subsequent crystal structures of TRα1 and TRβ1 showed that amino acid residues located at the surface of the ligand-binding pocket interact with T3 and mainly determine T3 binding affinity (3,5). This was confirmed by mutations of TRα1 and TRβ1 identified in RTH patients that reduce T3 binding affinity of the receptor (6-8).

In addition to the affinity for T3, studies of mutated TRs also emphasized the role of particular amino acid residues in interaction between TRs and cofactor proteins. For example, Arg243, Arg383, and Pro453 of TRβ1 seem to be important for the interaction with corepressor proteins because mutations at these residues (R243Q and R243W (9), R383H (10), and P453S (11)) impair interaction with the corepressor NCoR1. In addition, Thr277 and

Leu454 of TRβ1 are likely involved in the interaction with coactivator proteins, since mutations of these residues (T277A (12) and L454V (13)) affect interaction with the coactivator SRC1. Therefore, functional studies of the mutant TRs do not only confirm the pathogenicity of a mutation in the diagnosis of RTH in patients, but also allow us to gain more understanding about the role of specific amino acid residues in TR function.

Role of Leu341 in T3 binding affinity of TRβ

In **chapter 2**, we describe the role of Leu341 in TRβ1 function, prompted by the identification of a novel L341V mutation in RTHβ patients. Another mutation at this residue (L341P) has been reported as a cause of RTHβ (14,15). However, the functional importance of this amino acid residue has never been established. Our in-depth inspection of wild-type (WT) TRβ crystal structure showed that Leu341 lines the ligand-binding pocket of TRβ1 and form a direct hydrophobic interaction with the outer ring of the T3 molecule, which is in agreement with previous reports (16-18). This residue also interacts with the surrounded residues such as Phe272 and Leu346 to stabilize the microarchitecture of the ligand-binding pocket. The leucine to valine substitution (L341V) in the *in silico* model showed that the consequential shortening of the aliphatic amino acid side-chain alters the shape of the ligand-binding pocket and abolishes the direct hydrophobic interaction of the side-chain with T3. The functional impairment of TRβ1-L341V predicted by the *in silico* model was confirmed by the *in vitro* studies. The mutant has reduced T3 binding affinity, impaired T3-induced transcriptional activation, and a dominant-negative effect on WT receptor function. The importance of Leu341 was further confirmed by three artificial mutations, L341A, L341I and L341F, which were created based on the *in silico* prediction. The side-chains of these three amino acids (alanine, isoleucine, and phenylalanine) have similar hydrophobic properties but different in size and orientation, resulting in a variable distance to the T3 molecule. We also demonstrated a correlation between the degree of receptor impairment and the side-chain size and orientation of these artificial mutants. Based on this study, we suggested that the direct interaction between Leu341 and T3 and the microarchitecture formed by interactions between Leu341 and its surrounding residues are required for optimal T3 binding affinity and T3-induced transcriptional activation of TRβ1.

Role of TRα1-Met256 and TRβ1-Met310 in T3 versus T4 recognition of TRs

The concept that T4 is a prohormone which has to be converted to the biologically active form T3 to activate TRs in target tissues has been established for several decades based on the seminal studies showing that T3 has a greater biological potency than T4 (19-22). However, molecular and structural mechanisms underlying this concept have never been thoroughly examined. In **chapter 3**, we highlight the role of residues Met256 of TRα1 and Met310 of TRβ1 in determining the differential biological potency of T3 versus T4, by characterizing a novel mutation (TRα1-M256T) identified in an RTHα patient and a mutation at the corresponding position (TRβ1-M310T) identified in RTHβ patients (23-25). The crystal

structure previously showed that the ligand-binding pocket of WT TRβ1 can accommodate both T3 and T4, but that it is more tightly packed in the case of T3 binding than T4 binding (26). Helix 12 of T4-bound TRβ1 is more mobile than that of T3-bound TRβ1. Therefore, T4 is less stably retained in the LBD, resulting in a higher ligand dissociation rate and a lower binding affinity of T4-bound TRβ1. By focusing on Met256 of TRα1, we demonstrated that this residue forms a direct (hydrophobic) interaction with 5' carbon of the outer ring of T3 and interacts with surrounding residues to create a niche that allows the accommodation of T3. The bulky 5' iodine of T4 abolishes these direct interactions between the ligand and Met256 and, consequently, affects the stability of T4 in this niche. Therefore, we predicted based on our *in silico* models that Met256 in TRα1 plays a pivotal role in discriminating between T3 and T4. This prediction was confirmed by the studies on threonine and alanine substitutions. We demonstrated that TRα1-M256T and the artificial mutant TRα1-M256A have a more pronounced distortion of the hydrophobic niche accommodating the outer ring of T3 than that of T4, which suggests a greater impact on the affinity for T3 of these two mutations. The *in vitro* studies confirmed that threonine and alanine substitutions at Met256 selectively reduced the affinity for T3 and had a greater impact on T3- versus T4-dependent transcriptional activation. The naturally occurring mutation at the corresponding residue in the TRβ1 (M310T) also showed the same result. In contrast, amino acid substitutions at other residues of TRα1 (D211G (27), A263S, and R384H (28)) equally affect the transactivation potency of both T3 and T4. These findings confirm that Met256 in TRα1 and Met310 in TRβ1 are important for T3 versus T4 discrimination and shed light on the underlying molecular and structural basis for the role of T4 as a prohormone and T3 as a biologically active hormone in a widely accepted concept of TH physiology.

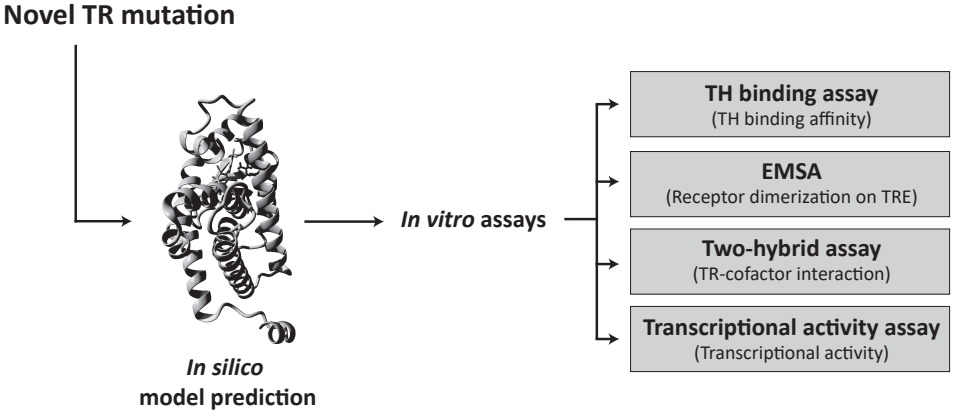

Figure 1. A pipeline of assays for confirming functional impairment of mutant TRs. The assay details are described in chapters 2-4 of this thesis. (EMSA, electrophoretic mobility shift assay; TRE, thyroid hormone response elements)

These studies in **chapters 2 and 3** are based on the identification of novel mutations in RTHα and β patients. Our studies showed that the combination of *in silico* model prediction and the creation of artificial mutations is a highly relevant approach to further explore the role of mutated amino acid residues of TRs in RTH patients and expand the knowledge about underlying structural and molecular basis for interactions of TR with its ligands and protein co-partners. In addition to the *in silico* prediction, we have applied a pipeline of assays, including *in vitro* TH binding assay, electrophoretic mobility shift assay (EMSA), TR-cofactor (two-hybrid) interaction assay, and transcriptional activity assay, in order to rapidly and extensively confirm functional impairment of mutant TRs (Figure 1).

Diverse functional impairment of TRα1 mutants and phenotype variability in RTHα

RTHα caused by mutations of the *THRA* gene was first identified in 2012 (1,2). To date, 25 mutations (in a total of 40 patients) have been reported. These mutations can be categorized into two groups based on the type of mutation. The first group consists of nonsense and frameshift mutations that generate premature stop codons. These mutations lead to truncated receptors that exhibit negligible T3 binding and a lack T3-induced gene expression (1,2,28-32). The second group consists of missense mutations that result in amino acid substitutions (7,27,28,33-39). These missense mutants can bind T3 but with a lower affinity than WT receptors.

The common phenotype of RTHα patients includes growth retardation, delayed bone maturation, macrocephaly, constipation, delayed cognitive and motor development, anemia, and a high (F)T3/(F)T4 ratio (7). An increase in the number of RTHα patients identified and their clinical characterization allows us to investigate the variability in the phenotype of RTHα patients. In general, patients with truncating mutations have more severe phenotype than patients with missense mutations that can still bind T3 (7). However, there are specific differences in the phenotype of patients in each group. For instance, the neurological phenotype of patients with truncating mutations varies from mild cognitive and motor impairment (F397fsx406 (2) and E403X (1)) to severe mental retardation and in some cases inability to walk and no developed speech (C380fsx387 (28), A382fsx388 (33), R384fsx388, and C392X (29)) (Table 1). Likewise, some patients with missense mutations displayed clear motor and cognitive impairment, whereas in a large family with patients carrying an A263S mutation, the affected members only showed mild symptoms and even partially overlapped with unaffected members for some characteristics (Table 2). So far, the underlying molecular mechanism to explain these observations has not yet been clearly established.

In **chapter 4**, we evaluated the differences in the degree of functional impairment of seven TRα1 missense mutants, four of which were derived from RTHα patients (D211G (27),

M256T (37), A263S, and R384H (28)) and the other three were derived from RTHβ patients (P398H, T223A, and L287V). These mutations covered the three CpG-rich regions of the LBD of TRα1 that are homologous to the mutation-prone hotspots of the TRβ1, namely R384H and P398H in cluster 1, M256T, A263S and L287V in cluster 2, and D211G and T223A in cluster 3 (Figure 2). Studies in patient-derived TRβ1 mutants showed that some mutants have severe transcriptional impairment despite only mild T3 binding defect. This finding would be explained by either impaired dimerization (40-42) or defective TR-cofactor interaction (9-13). In addition, a subset of TRβ1 mutants showed a defective transcriptional activation only on specific TRE configurations (12). Since TRα1 and TRβ1 are highly homologous, we asked whether impaired dimerization, defective TR-cofactor interaction, and configuration of TREs (DR4, IR0, and ER6) could contribute to the functional impairment of TRα1 mutants. Our results showed that in these seven TRα1 missense mutants it is predominantly the reduced T3 binding affinity that determines the severity of impaired transcriptional activation and defective interactions with the cofactors (NCoR1 and SRC1). There is no substantial evidence that suggests an additional TRE-specific transcriptional impairment of these mutants.

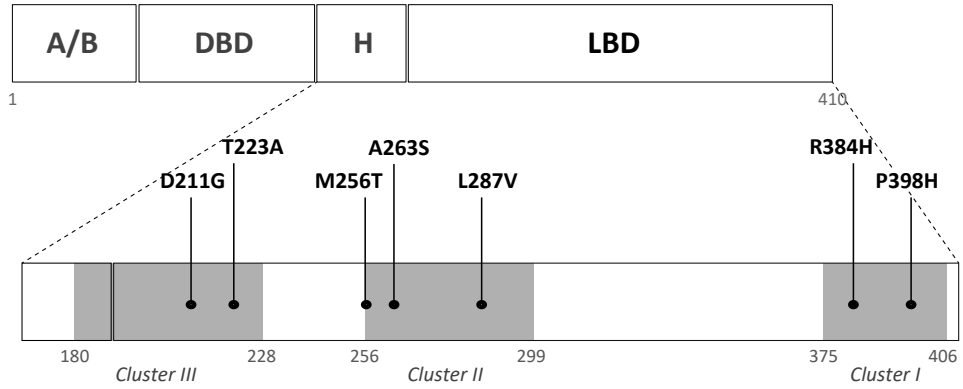

Figure 2. The diagram shows the location of selected mutations in the three CpG-rich regions of the LBD of TRα1 (adapted from Rebai M et al. 2012(43)) [A/B, A/B domain; DBD, DNA-binding domain; H, Hinge region; LBD, ligand binding domain]

The degree of reduced T3 binding affinity and impaired transcriptional activation of the mutants seems to be correlated with the phenotype of the patients. For instance, as previously mentioned, patients carrying D211G and R384H mutations have a more severely impaired motor development than patients carrying the A263S mutation. This is in agreement with the more prominent transcriptional impairment that we showed for the D211G and R384H mutants than for the A263S mutant. This finding is in line with the report of Moran et al. that showed that the degree of transcriptional impairment of two TRα1 missense mutations,

A263V and L274P, correlates with the severity of the clinical phenotype of the patients (36). However, there is an exception. The M256T mutation exhibited the most severe transcriptional impairment, but the available clinical information showed that patient carrying this mutation does not have severe cognitive impairment and delayed motor development (Table 2). There is no clear explanation yet for this paradox. Since our studies did not take the dominant-negative effect of the mutant on WT receptor function into account, it might be that this is one of the factors that further complicates the phenotype of the patients.

In addition to the variation between different mutations, the severity of clinical phenotype is also diverse between patients who carry the same mutation (28). This phenomenon has also been reported in RTHβ patients who belong to the same family and carry a similar mutation (44-48). The mechanisms underlying this finding is unknown. This may very well be explained by other factors beyond TRs such as genetic variability or epigenetic modification that might modulate the phenotype of RTH patients.

As previously mentioned, the diversity in phenotype severity was also observed in RTHα patients carrying truncating mutations. In **chapter 5**, we analyzed gene transcription regulated by two TRα1 truncating mutations, C380fsx387 and F397fsx406, both of which lack T3-induced gene expression (1,2) but result in a different degree in cognitive impairment of the patient (Table 1). The patient who carries the TRα1-C380fsx387 mutation was severely handicapped and unable to communicate at 12 years of age, suggesting severe cognitive impairment (28). In contrast, the index patient who carries the TRα1-F397fsx406 mutation had borderline cognitive impairment (IQ score 90 at 11 years old) (2). The transcriptome analysis was performed in a human neuronal cell line (SH-SY5Y) overexpressing Flag- and Hemagglutinin double-epitope tagged TRα1 (FHTRα1) to focus on neurological phenotype. The results showed that overexpressing FHTRα1-C380fsx387 and -F397fsx406 mutants altered the transcriptomes when compared to cells overexpressing FHTRα1 WT and abolished T3-induced gene expression. In addition, the transcriptomes of these two mutants were very different from each other, suggesting a differential effect of these two mutations on gene transcription. The genes that were differentially expressed in the two mutant cells were related to nervous system development and neuronal pathfinding. For instance, we identified many genes (*SEMA3A*, *SEMA3C*, *SLIT1*, *EFNB2*, *UNC5A*, and *UNC5D*) that encode proteins that act as extracellular guidance cues for axonal/dendritic growth (49,50). We also identified many genes that are related to cell adhesion molecules (e.g., *NRCAM*, *CNTNs*, *PCDHs*, *ITGs*, and *ASTNs*) and neural growth factor receptors (*NGFR*, *NTRK3*, and *GFRA2*), which are essential for neural growth and migration (51-56). Additionally, the expression of *ASCL1* and *NEUROG2*, which encode two master proteins for neuronal differentiation, Achaete-scute homolog 1 and Neurogenin 2, respectively, was different between the two mutant cells. Evidence in murine models showed that Neurog2 assigns neuron progenitor cells to differentiate into excitatory (glutamatergic) neurons, whereas Ascl1 assigns progenitor cells to differentiate into inhibitory (GABAergic) neurons (57-61). Progenitor cells that highly express Ascl1 also keep proliferating rather than differentiate into a mature neuron. Since the expression of *NEUROG2* and *ASCL1*

was respectively lower and higher in SH-SY5Y/FHTRα1-C380fsx387 cells compared to both SH-SY5Y/FHTRα1-F397fsx406 and SH-SY5Y/FHTRα1 WT cells, this may keep more cells in a proliferating phase or drive them into becoming inhibitory neurons, thereby contribute to the more severe neurological phenotype in the C380fsx387 patient.

The studies in **chapters 4 and 5** showed a relationship between functional impairment of the mutant TRs and the neurological phenotype of the patients. However, the limitation of our studies is that the neurological phenotype of patients was not systematically evaluated, which leads to difficulty in phenotype comparison. For instance, cognitive and motor function was assessed at a different age and by different tests/scores or described only as a qualitative observation in some publications. The test was also performed and interpreted by different investigators without standardization. In addition, the effect of treatments/interventions which had been given to some patients before the RTH diagnosis and might improve the cognitive and motor function were not taken into account. Therefore, our results need to be interpreted cautiously, and further studies with standardized assessment methods are required in order to solve this issue and confirm our findings.

Recruitment of nuclear coregulatory protein by TRs

TRs regulate gene transcription by interacting with nuclear coregulatory proteins that modify local chromatin structure and accessibility of the promotor region of target genes. In the absence of T3, TRs repress gene transcription by binding to the main corepressor proteins, NCoR (nuclear receptor corepressor) and SMRT (silencing mediator of retinoid and thyroid hormone receptors), that form complexes with other nuclear proteins to promote histone deacetylation and nucleosome compaction. Binding of TH to TRs creates a closed-conformation of TR-LBD, leading to the dissociation of the corepressor complex and the association of coactivator proteins. Steroid hormone receptor coactivator 1, 2, and 3 (SRC-1, -2, and -3) directly bind to TRs and recruit other proteins such as histone acetyltransferase (HAT), resulting in histone acetylation, chromatin accessibility, and gene transcription.

Apart from the classical TR cofactors, other nuclear proteins have been identified as corepressors or coactivators. There is evidence indicates that TRs recruit cofactor proteins in a tissue- and isoform-dependent manner, which may further explain the diverse transcriptional regulation of TRs in different tissues (62-65). Understanding the complexity in TR-cofactor interactions will gain more insight into the impact of TR mutations in RTH syndromes in addition to the effect on T3 binding. Therefore, in **chapters 6a and 6b**, we used an unbiased approach to identify TR-interactomes by using a tandem-affinity protein purification method.

In **chapter 6a**, we compared the unliganded and liganded TRα1-interactomes in a human liver cell model (HepG2) and a human neuronal cell model (SH-SY5Y). The main objective was to evaluate the tissue-dependency of TR-cofactor interactions. FHTRα1 WT

was stably expressed in these two cell types by lentiviral transduction. To identify nuclear proteins that interact with TRα1 in the absence and presence of T3, we purified FHTRα1 and its associated proteins from the nuclear extracts of HepG2 and SH-SY5Y (after stimulating with 0 or 100 nM T3) using a tandem-affinity purification. The TRα1-interactomes were identified by LC-MS/MS and confirmed by co-immunoprecipitation. By this approach, we were able to identify several proteins and protein complexes that are associated with TRα1. The number of hits is larger than in previous TR-interactome studies (63,65). The composition of TRα1-interactomes is strongly dependent on ligand-binding state and largely overlapped between HepG2 and SH-SY5Y cells, suggesting that TRα1 uses common nuclear coregulatory proteins to regulate gene transcription in these two cell types. However, some proteins are likely to interact with TRα1 in a cell-type specific manner, including nuclear receptor interacting protein 1 (NRIP), as known as RIP140, in HepG2 cells and transcription factor 4 (TCF4) in SH-SY5Y cells. Given that NRIP and TCF4 are exclusively expressed in HepG2 and SH-SY5Y cells, respectively, the cell-type specific TR-cofactor recruitment found in our study may be mainly explained by the differential availability of these particular cofactors and may not necessarily prove a tissue-specific interaction.

In addition to the cell-type specificity, we also identified a novel putative binding partner, transcription factor Prospero homeobox 1 (Prox1), in both HepG2 and SH-SY5Y cells. The interaction of this transcription factor with TR was increased in the presence of T3. Prox1 is known to be involved in cell fate specification and metabolism. Prox1 can interact with many nuclear receptors, including chicken ovalbumin upstream promoter transcription factor II (COUP-TFII) in lymphatic endothelial cells (66), and hepatic nuclear factor 4 alpha (HNF4α), liver receptor homologue-1 (LRH-1), and Retinoid Orphan Receptor (ROR) α and γ in the liver (67-69). The interaction between TR and Prox1 had not previously been described, although Broekema et al. recently showed the interaction between TRs and a binding motif of Prox1 by using the Microarray Assay for Realtime Coregulator-Nuclear Receptor Interaction (MARCoNI) technology (70). Our finding further confirms that Prox1 may work as TR coregulatory protein to regulate gene transcription. In addition, we identified several proteins belonging to multisubunit chromatin remodelling complexes that help to rearrange local chromatin architecture and regulate gene transcription. The most notable one was the nuclear remodelling and deacetylase (NuRD) complex that was identified in both HepG2 and SH-SY5Y cells. The NuRD complex was initially identified as a transcriptional repression complex (71-73). However, it was later shown that this complex can also be involved in transcriptional gene activation (74), which is in line with our finding that components of the NuRD complex identified in our study were slightly enriched in the presence of T3.

In **chapter 6b**, we studied the isoform-specific recruitment of coregulatory proteins for TRs in SH-SY5Y cells in order to understand the complexity of TR actions in the brain. Since previous studies in other cell models showed that TRs recruit a subset of coregulatory proteins in an isoform-specific manner (63,65), we asked whether the isoform-specific coregulatory protein recruitment exists in SH-SY5Y cells as well. Therefore, we compared

the interactomes for the two major TR isoforms (TRα1 and TRβ1) using the same tandem-affinity purification method and LC-MS/MS analysis as in chapter 6a. The result showed that the majority of identified proteins were associated with both TRα1 and TRβ1, suggesting that both TR isoforms associate with common nuclear coregulatory proteins to regulate gene transcription. However, a subset of nuclear proteins interacted with TRs in an isoform-specific manner. The interesting hits are lysine-specific demethylase 6A (KDM6A, as known as UTX), set1/Ash2 histone methyltransferase complex subunit ASH2 (ASH2L), and retinoblastoma-binding protein 5 (RBBP5), all of which were identified exclusively with TRα1 in the presence of T3. These proteins are likely to work together to establish transcriptional permissive chromatin for many key developmental genes such as HOX genes (75-78).

In agreement with the study in chapter 6a, we identified many components of multisubunit chromatin remodelling complexes that regulate gene transcription together with both TR isoforms in SH-SY5Y cells, such as the NuRD complex and the Spt-Ada-Gcn5-Acetyltransferase (SAGA) complex, both of which seems to interact with TR more prominently in the presence of T3. Identifying the NuRD complex again in this study confirms that this protein complex is a common co-partner that plays a crucial role in TR actions, regardless of TR isoform and tissue context. The proteins in the SAGA complex were also co-purified with TRs exclusively in the presence of T3, suggesting the role of this complex in transcriptional activation. To our knowledge, this is the first study suggesting a relationship between SAGA complex and TRs. Other novel binding co-partners of TRs, Foxhead box transcription factor K1 and K2 (FOXK1 and FOXK2), were identified in the absence of T3. The FOXK1 and FOXK2 are the proteins that positively regulate the Wnt/β-catenin signaling pathway (79). These studies indicate crosstalk between TH-TR and the Wnt/β-catenin pathway at multiple levels, such as an effect of TH on the Wnt and β-catenin protein expression, a physical interaction between TRs and β-catenin in specific tissues, and synergistic effect of TH-TRs and Wnt/β-catenin signaling on cell proliferation and differentiation (80). However, the role of FOXK1 and FOXK2 in this crosstalk has not yet been established. Our finding suggests that these proteins may also take part in the interaction between TRs and Wnt/β-catenin signaling.

In summary, our results in **chapters 6a and 6b** showed that TRs interact with not only classic nuclear coregulatory proteins, such as NCoR/SMRT and SRC complexes, but also several potential novel binding partners. TRs also interact with a number of transcription factors and chromatin remodeling complexes, which highlights the role of TRs in local chromatin accessibility. Although the majority of identified proteins are able to interact with both TR isoforms and regardless of cellular context, we also found that a small subset of nuclear proteins seems to interact with TRs in tissue- and isoform-specific manner. These findings expand the knowledge about the interaction between TRs and cofactor proteins in transcriptional gene regulation and may lead to a more understanding of the impact of TR mutations in RTH syndrome.

Concluding remarks and future perspective

TRs are key controllers for transcriptional regulation (genomic actions) by TH. Research on molecular functions of TRs provides more understanding about the physiology of TR actions which are more complicated than merely binding of TH to TRs.

The knowledge of TR actions has been broadened by the identification of mutations in RTH patients. All identified mutants help to confirm a crucial role of that particular residue/domain in TR functions, which includes interactions with TH in the ligand-binding pocket and interactions with regulatory proteins, such as RXR, corepressors, and coactivators. In this thesis, we provide more information about the importance of particular amino acid residues in TR functions prompted by identifying two RTH patients who carry novel mutations. The combination of *in silico* model prediction and *in vitro* studies of mutated TRs allows us to understand not only the effect of the mutation but also the role of the residue of interest in TR function. We, therefore, suggest using this approach to further explore the role of mutated amino acid residues of TRs in RTH patients. According to this, we have applied a pipeline of assays for a novel TR mutation by combining all of the techniques we have used, including *in silico* protein modeling and several *in vitro* functional assays. Since we are now capable of performing TR transcriptome and interactome analyses, we could also incorporate these techniques in order to explore all aspects of transcriptional regulation by TRs and effect of TR mutations in RTH syndromes.

One of the interesting issues is the factor that determine the functional impairment of the mutated TRs and the severity of phenotype of RTHα patients. Our study with the TRα missense mutants showed that the reduced affinity for T3 is the main factor that determines the severity of impaired transcriptional activity of mutants and seems to define patients' phenotypes. However, the transcriptome analysis of two TRα1 truncating mutations (C380fsx387 and F397fsx406), both of which exhibit negligible T3 binding, showed that there is a difference in baseline RNA expression between mutants. This finding suggests that additional factors, apart from the affinity for T3, could also influence the severity of patients' phenotype in RTH, which is confirmed by the diversity of the cognitive phenotype in these patients. We are aware that our studies have some limitations. For instance, the *in vitro* overexpression system we used may not perfectly represent the *in vivo* situation. The system also not allow us to study the effect of the mutant on WT receptor function (i.e., dominant-negative effect) since it was difficult to mimic heterozygosity. For this, other cell models, such as patient-derived primary cells or CRISPR-Cas9 genome editing, need to be developed. There is also a difficulty in phenotype comparison of RTHα patients since the phenotype description is often incomplete, and clinical assessment methods sometimes vary among publications. This may affect the reliability of the relationship between genotype and phenotype we reported. A patient registry for RTH syndrome, which provides a guideline and standardized methods for clinical assessment should overcome this limitation and will lead to a more comprehensive understanding of the genotype-phenotype correlation in RTH syndromes.

Interaction between TR and cofactors is important for transcriptional gene regulation by TH. Our studies showed that TRs interact with not only classical nuclear coregulatory proteins but also several potential novel binding partners to regulate gene transcriptions. A small subset of proteins interacts with TRs in tissue- and isoform-specific manner. These findings provide more insight into the complexity of TR actions and may expand the understanding about the impact of mutated TRs on phenotype of RTH patients, especially in patients who carry mutated TRs that have a greater impaired transcriptional activation than the degree of T3 binding defect. However, further studies are still needed to confirm the interaction between WT TRs and novel binding protein copartners and the functional importance of these interactions in both the physiological actions of TRs and RTH syndromes.

Table 1. Clinical characteristics and thyroid function tests (TFTs) of RTHα patients (index cases) carrying **truncating mutation** in the *THRA* gene.

Phenotype	C380fs387X	A382fs388X	R384fs388X	C392X	E395X	E403X	F397fs406X
Sex	F	F	F	M	M	F	F
Age (year)	1.3	45	19	18	2	6	6
GA (week)	Term	N/A	Term	41	Term	N/A	N/A
Birth weight (gm)	3200	N/A	N/A	**4200**	**4000**	N/A	N/A
Skeletal							
-Ht SDS or percentile (P)	**-2.46**	**-2.34**	**<P3**	**-6**	**<P3**	**Ht deficit**	**Ht deficit**
-Sitting/ total Ht SDS	N/A	+0.29	N/A	N/A	N/A	N/A	N/A
-Subischial length SDS	N/A	**-3.87**	N/A	N/A	N/A	**<P3**	N/A
-HC SDS or percentile (P)	**+2.29**	**+9.0**	**Macrocephaly**	**Macrocephaly**	No	N/A	**+1.65**
-Delayed bone maturation	N/A	N/A	N/A	N/A	**Yes**	**Yes**	**Yes**
-Delayed dentition	**Yes**	N/A	N/A	N/A	N/A	**Yes**	**Yes**
Appearance							
-Coarse facies	**Yes**	**Yes**	**Yes**	**Yes**	N/A	N/A	N/A
-Skin tags	N/A	**Yes**	N/A	N/A	No	N/A	N/A
-Macroglossia	**Yes**	**Yes**	**Yes**	N/A	No	N/A	**Yes**
-Umbilical hernia	**Yes**	**Yes**	**Yes**	N/A	N/A	N/A	N/A
Gastrointestinal							
-Constipation	**Yes**	**Yes**	N/A	**Yes**	**Yes**	**Yes**	**Yes**
Neurocognitive							
-Delayed milestone	**Yes**	**Yes**	**Yes**	N/A	**Yes**	**Yes**	**Yes**
-Cognitive impairment	**Severe***	**Yes** (IQ 52)	**Severe**	**Severe** (IQ 22)	N/A	**Yes**	**Mild** (IQ 90)
-Delayed motor development	**Severe***	**Yes**	**Yes**	N/A	**Yes**	**Yes**	**Yes**

Phenotype	C380fs387X	A382fs388X	R384fs388X	C392X	E395X	E403X	F397fs406X
Hematological							
-Anemia	**Yes**	No	N/A	**Yes**	**Yes**	N/A	**Yes**
Additional phenotype	Hoarse-sounding cry, Hypertrophic obstructive cardiomyopathy, pericardial effusion, nephrolithiasis	Epilepsy	Atonic seizure, myelination disorder, dysgerminoma, hypertelorism, smooth philtrum, thin upper lip, wide nasal base/ ridge, downslant palpebral fissure	Hypertelorism, palpebral ptosis, flat nasal bridge, elongated thorax, club foot, tortusity of arteries, puffy hands, rough skin texture	Disproportionate short stature, short arm span, broad face and nasal bridge	Mild hypermobility, ligamentous laxity, wormian bones, femoral epiphyseal dysgenesis, restrict adaptive behavior	Congenital hip dislocation
TFTs [NR]							
-TSH (mU/L)	1.4 [0.4-4.3]	**5.8** [0.35-5.5]	N/A	2.76	1.37 [0.38-7.31]	1.04 [0.8-6.2]	Normal
-FT4 (pmol/L)	**5.1** [11-25]	10.0 [10.0-19.8]	N/A	10.0 [9.0-11.6]	**11.2** [15.4-22.3]	**6.5** [10.3-21.9]	**Low**
-TT4 (nmol/L)	**53** [58-128]	85 [69-141]	N/A	N/A	101.8 [66.7-157.7]	**42.5** [95.3-155.8]	Low normal
-FT3 (pmol/L)	**12.4** [3.8-7.6]	4.9 [3.5-6.5]	N/A	**7.96** [2.23-5.38]	**8.06** [4.22-7.18]	6.1 [4.6-7.7]	**High**
-TT3 (nmol/L)	**2.76** [1.4-2.5]	1.7 [0.9-2.8]	N/A	N/A	3.34 [1.52-3.49]	2.4 [2.0-3.4]	N/A
-rT3 (nmol/L)	N/A	**0.15** [0.17-0.49]	N/A	N/A	N/A	**0.11** [0.32-0.57]	**Low**
-T3/T4 ratio	N/A	N/A	N/A	N/A	N/A	N/A	**High**
Reference	*(28)*	*(30)*	*(31)*	*(29)*	*(32)*	*(1)*	*(2)*

Abnormal values are indicated in bold. [GA, gestational age; Ht, height; HC, head circumference; SDS, standard deviation score; M, male; F, female; NR, normal range; N/A, data not available]

*Severely handicapped (unable to walk and communicate) at the age of 12.7 years

Table 2. Clinical characteristics and thyroid function tests (TFTs) of RTHα patients (index cases) carrying **missense mutation** in the *THRA* gene.

Phenotype	D211G	M256T	A263S	A263V	L274P	G291S	N359Y	R384H	P398R	E403K
Sex	F	M	M	M	M	M	F	M	F	F
Age (year)	1.4	19	2.6	17	15	4	27	0.9	8	12
GA (week)	Term	**43**	Term	39	41	38	37	N/A	42	42
Birth weight (gm)	**4000**	**5000**	3000	**4580**	3260	2900	N/A	3400	3450	3650
Skeletal										
-Ht SDS or percentile (P)	**-2.77**	-1	-1.18	P50	**P0.4**	**-2.47**	**-6**	-0.63	-0.5	**-3**
-Sitting/ total Ht SDS	N/A	**+2.5**	**+2.71**	N/A	N/A	N/A	**Short limbs**	-1.00	**Short limbs**	**Short limbs**
-Subischial length SDS	N/A	-1	N/A	+1	**-2**	N/A	N/A	N/A	N/A	N/A
-HC SDS or percentile (P)	0	**+2.5**	+1.14	**P99**	**P99**	**+2.08**	**Macrocephaly**	**+2.02**	N/A	**Macrocephaly**
-Delayed bone maturation	N/A	N/A	**Yes**	**Yes**	**Yes**	**Yes**	N/A	**Yes**	N/A	**Yes**
-Delayed dentition	N/A	**Yes**	**Yes**	**Yes**	**Yes**	**Yes**	No	No	N/A	N/A
Appearance										
-Coarse facies	**Yes**	**Yes**	N/A	**Yes**	**Yes**	**Yes**	No	**Yes**	**Yes**	**Yes**
-Skin tags	No	**Yes**	No	**Yes**	**Yes**	N/A	N/A	No	N/A	N/A
-Macroglossia	No	N/A	No	**Yes**	**Yes**	N/A	N/A	**Yes**	No	No
-Umbilical hernia	N/A	**Yes**	No	**Yes**	**Yes**	**Yes**	N/A	No	N/A	N/A
Gastrointestinal										
-Constipation	**Yes**	**Yes**	**Yes**	**Yes**	**Yes**	**Yes**	N/A	No	**Yes**	**Yes**

Phenotype	D211G	M256T	A263S	A263V	L274P	G291S	N359Y	R384H	P398R	E403K
Neurocognitive										
-Delayed milestone	**Yes**	N/A	No	**Mild**	**Severe**	**Yes**	N/A	**Yes**	**Yes**	**Yes**
-Cognitive impairment	No	**Mild (Special school)**	No	Regular school	**Special needs school**	**Yes**	No (obtained an advanced academic degree)	**Moderate**	Normal (IQ 95)	**Mild** (IQ 80)
-Delayed motor development	**Severe**	**Yes**	No	**Mild**	**Moderate**	**Yes**	N/A	**Severe**	**Yes**	**Yes**
Hematological										
-Anemia	**Yes**	**Yes**	**Yes**	**Yes**	**Yes**	**Yes**	**Yes**	**Yes**	**Yes**	**Yes**
Additional phenotype	-	Mild hypertelo-rism, striking blue eyes, mild learning problems, mild autistic spectrum disorder	-	Bilateral inguinal hernia	Genu valgum, coxa valga, femoral epiphyseal dysgenesis, mesomelic short limbs	-	Hypertelorism, clavicular & 12th ribs agenesis, humero-radial synostosis, syndactyly, scoliosis, hip dislocation, hypercalcemia	-	Hypertelo-rism, wide valgus foot with sandal gap, puffy hands	Hypertelorism, micrognathia, short neck, wide valgus foot with sandal gap, puffy hands
TFTs [NR]										
-TSH (mU/L)	4.40 [0.5-5.0]	1.83 [0.4-4.3]	2.10 [0.4-4.3]	3.6 [0.35-5.50]	2.07 [0.35-5.50]	3.89 [0.35-5.5]	**0.34** [0.4-3.6]	1.89 [0.4-4.3]	0.45 [0.4-0.6]	1.89 [0.4-0.6]
-FT4 (pmol/L)	**9.0** [10-23]	**10.6** [11-25]	16.4 [11-25]	10 [10-19.8]	**8.4** [10-19.8]	12.0 [11.4-22.7]	10.3 [9.0-15.4]	13.9 [11-25]	9.05 [12.5-21.5]	13.35 [12.6-21.5]
-TT4 (nmol/L)	110 [70-150]	67 [58-128]	85 [58-128]	N/A	N/A	N/A	N/A	107 [58-128]	N/A	N/A

Phenotype	D211G	M256T	A263S	A263V	L274P	G291S	N359Y	R384H	P398R	E403K
-FT3 (pmol/L)	N/A	N/A	7.28 [3.8-7.6]	**7.6** [3.5-6.5]	**9.1** [3.5-6.5]	**7.7** [3.5-6.5]	6.14 [3.07-6.14]	**8.08** [3.8-7.6]	5.62 [3.88-8.02]	6.94 [3.93-7.70]
-TT3 (nmol/L)	**3.6** [1.3-2.7]	**2.9** [1.4-2.5]	**3.65** [1.4-2.5]	N/A	N/A	N/A	N/A	**5.20** [1.4-2.5]	N/A	N/A
-rT3 (nmol/L)	**0.09** [0.11-0.44]	**0.18** [0.22-0.54]	0.31 [0.22-0.52]	**<0.07** [0.12-0.36]	**<0.07** [0.12-0.36]	N/A	0.26 [0.22-0.83]	0.31 [0.22-0.52]	N/A	N/A
-T3/T4 ratio	**0.033** [0.01-0.04]	**0.043** [0.01-0.03]	**0.043** [0.01-0.03]	N/A	N/A	N/A	N/A	**0.049** [0.01-0.03]	N/A	N/A
Reference	*(27)*	*(37)*	*(28)*	*(36)*	*(36)*	*(39)*	*(34)*	*(28)*	*(29)*	*(29)*

Abnormal values are indicated in bold. [GA, gestational age; Ht, height; HC, head circumference; SDS, standard deviation score; M, male; F, female; NR, normal range; N/A, data not available]

References

1. Bochukova E, Schoenmakers N, Agostini M, Schoenmakers E, Rajanayagam O, Keogh JM, Henning E, Reinemund J, Gevers E, Sarri M, Downes K, Offiah A, Albanese A, Halsall D, Schwabe JW, Bain M, Lindley K, Muntoni F, Vargha-Khadem F, Dattani M, Farooqi IS, Gurnell M, Chatterjee K. A mutation in the thyroid hormone receptor alpha gene. *N Engl J Med.* 2012;**366**(3):243-249.
2. van Mullem A, van Heerebeek R, Chrysis D, Visser E, Medici M, Andrikoula M, Tsatsoulis A, Peeters R, Visser TJ. Clinical phenotype and mutant TRalpha1. *N Engl J Med.* 2012;**366**(15):1451-1453.
3. Wagner RL, Huber BR, Shiau AK, Kelly A, Cunha Lima ST, Scanlan TS, Apriletti JW, Baxter JD, West BL, Fletterick RJ. Hormone selectivity in thyroid hormone receptors. *Mol Endocrinol.* 2001;**15**(3):398-410.
4. Hayashi Y, Sunthornthepvarakul T, Refetoff S. Mutations of CpG dinucleotides located in the triiodothyronine (T3)-binding domain of the thyroid hormone receptor (TR) beta gene that appears to be devoid of natural mutations may not be detected because they are unlikely to produce the clinical phenotype of resistance to thyroid hormone. *J Clin Invest.* 1994;**94**(2):607-615.
5. Wagner RL, Apriletti JW, McGrath ME, West BL, Baxter JD, Fletterick RJ. A structural role for hormone in the thyroid hormone receptor. *Nature.* 1995;**378**(6558):690-697.
6. Dumitrescu AM, Refetoff S. The syndromes of reduced sensitivity to thyroid hormone. *Biochim Biophys Acta.* 2013;**1830**(7):3987-4003.
7. van Gucht ALM, Moran C, Meima ME, Visser WE, Chatterjee K, Visser TJ, Peeters RP. Resistance to Thyroid Hormone due to Heterozygous Mutations in Thyroid Hormone Receptor Alpha. *Curr Top Dev Biol.* 2017;**125**:337-355.
8. Concolino P, Costella A, Paragliola RM. Mutational Landscape of Resistance to Thyroid Hormone Beta (RTHbeta). *Mol Diagn Ther.* 2019;**23**:353-368.
9. Safer JD, Cohen RN, Hollenberg AN, Wondisford FE. Defective release of corepressor by hinge mutants of the thyroid hormone receptor found in patients with resistance to thyroid hormone. *J Biol Chem.* 1998;**273**(46):30175-30182.
10. Clifton-Bligh RJ, de Zegher F, Wagner RL, Collingwood TN, Francois I, Van Helvoirt M, Fletterick RJ, Chatterjee VK. A novel TR beta mutation (R383H) in resistance to thyroid hormone syndrome predominantly impairs corepressor release and negative transcriptional regulation. *Mol Endocrinol.* 1998;**12**(5):609-621.
11. Yoh SM, Chatterjee VK, Privalsky ML. Thyroid hormone resistance syndrome manifests as an aberrant interaction between mutant T3 receptors and transcriptional corepressors. *Mol Endocrinol.* 1997;**11**(4):470-480.
12. Collingwood TN, Wagner R, Matthews CH, Clifton-Bligh RJ, Gurnell M, Rajanayagam O, Agostini M, Fletterick RJ, Beck-Peccoz P, Reinhardt W, Binder G, Ranke MB, Hermus A, Hesch RD, Lazarus J, Newrick P, Parfitt V, Raggatt P, de Zegher F, Chatterjee VK. A role for helix 3 of the TRbeta ligand-binding domain in coactivator recruitment identified by characterization of a third cluster of mutations in resistance to thyroid hormone. *EMBO J.* 1998;**17**(16):4760-4770.
13. Collingwood TN, Rajanayagam O, Adams M, Wagner R, Cavailles V, Kalkhoven E, Matthews C, Nystrom E, Stenlof K, Lindstedt G, Tisell L, Fletterick RJ, Parker MG, Chatterjee VK. A natural transactivation mutation in the thyroid hormone beta receptor: impaired interaction with putative transcriptional mediators. *Proc Natl Acad Sci U S A.* 1997;**94**(1):248-253.
14. Chiesa A, Olcese MC, Papendieck P, Martinez A, Vieites A, Bengolea S, Targovnik HM, Rivolta CM, Gruneiro-Papendieck L. Variable clinical presentation and outcome in pediatric patients with resistance to thyroid hormone (RTH). *Endocrine.* 2012;**41**(1):130-137.
15. Rivolta CM, Olcese MC, Belforte FS, Chiesa A, Gruneiro-Papendieck L, Iorcansky S, Herzovich V, Cassorla F, Gauna A, Gonzalez-Sarmiento R, Targovnik HM. Genotyping of resistance to thyroid hormone in South American population. Identification of seven novel missense mutations

in the human thyroid hormone receptor beta gene. *Mol Cell Probes.* 2009;**23**(3-4):148-153.

16. Hangeland JJ, Friends TJ, Doweyko AM, Mellstrom K, Sandberg J, Grynfarb M, Ryono DE. A new class of high affinity thyromimetics containing a phenyl-naphthylene core. *Bioorg Med Chem Lett.* 2005;**15**(20):4579-4584.
17. Li F, Xie Q, Li X, Li N, Chi P, Chen J, Wang Z, Hao C. Hormone activity of hydroxylated polybrominated diphenyl ethers on human thyroid receptor-beta: in vitro and in silico investigations. *Environ Health Perspect.* 2010;**118**(5):602-606.
18. Nascimento AS, Dias SM, Nunes FM, Aparicio R, Ambrosio AL, Bleicher L, Figueira AC, Santos MA, de Oliveira Neto M, Fischer H, Togashi M, Craievich AF, Garratt RC, Baxter JD, Webb P, Polikarpov I. Structural rearrangements in the thyroid hormone receptor hinge domain and their putative role in the receptor function. *J Mol Biol.* 2006;**360**(3):586-598.
19. Gross J, Pitt-Rivers R. Physiological activity of 3:5:3'-L-triiodothyronine. *Lancet.* 1952;**1**(6708):593-594.
20. Lerman J. The contribution of triiodothyronine to thyroid physiology. *J Clin Endocrinol Metab.* 1954;**14**(6):690-693.
21. Mussett MV, Pitt-Rivers R. The thyroid-like activity of triiodothyronine analogues. *Lancet.* 1954;**267**(6850):1212-1213.
22. Pitt-Rivers R. Metabolic effects of compounds structurally related to thyroxine in vivo: thyroxine derivatives. *J Clin Endocrinol Metab.* 1954;**14**(11):1444-1450.
23. Kim HK, Kim D, Yoo EH, Lee JI, Jang HW, Tan AH, Hur KY, Kim JH, Kim KW, Chung JH, Kim SW. A case of resistance to thyroid hormone with thyroid cancer. *J Korean Med Sci.* 2010;**25**(9):1368-1371.
24. Mitchell CS, Savage DB, Dufour S, Schoenmakers N, Murgatroyd P, Befroy D, Halsall D, Northcott S, Raymond-Barker P, Curran S, Henning E, Keogh J, Owen P, Lazarus J, Rothman DL, Farooqi IS, Shulman GI, Chatterjee K, Petersen KF. Resistance to thyroid hormone is associated with raised energy expenditure, muscle mitochondrial uncoupling, and hyperphagia. *J Clin Invest.* 2010;**120**(4):1345-1354.
25. Takeda K, Weiss RE, Refetoff S. Rapid localization of mutations in the thyroid hormone receptor-beta gene by denaturing gradient gel electrophoresis in 18 families with thyroid hormone resistance. *J Clin Endocrinol Metab.* 1992;**74**(4):712-719.
26. Sandler B, Webb P, Apriletti JW, Huber BR, Togashi M, Cunha Lima ST, Juric S, Nilsson S, Wagner R, Fletterick RJ, Baxter JD. Thyroxine-thyroid hormone receptor interactions. *J Biol Chem.* 2004;**279**(53):55801-55808.
27. van Gucht AL, Meima ME, Zwaveling-Soonawala N, Visser WE, Fliers E, Wennink JM, Henny C, Visser TJ, Peeters RP, van Trotsenburg AS. Resistance to Thyroid Hormone Alpha in an 18-Month-Old Girl: Clinical, Therapeutic, and Molecular Characteristics. *Thyroid.* 2016;**26**(3):338-346.
28. Demir K, van Gucht AL, Buyukinan M, Catli G, Ayhan Y, Bas VN, Dundar B, Ozkan B, Meima ME, Visser WE, Peeters RP, Visser TJ. Diverse Genotypes and Phenotypes of Three Novel Thyroid Hormone Receptor-alpha Mutations. *J Clin Endocrinol Metab.* 2016;**101**(8):2945-2954.
29. Tylki-Szymanska A, Acuna-Hidalgo R, Krajewska-Walasek M, Lecka-Ambroziak A, Steehouwer M, Gilissen C, Brunner HG, Jurecka A, Rozdzynska-Swiatkowska A, Hoischen A, Chrzanowska KH. Thyroid hormone resistance syndrome due to mutations in the thyroid hormone receptor alpha gene (THRA). *J Med Genet.* 2015;**52**(5):312-316.
30. Moran C, Schoenmakers N, Agostini M, Schoenmakers E, Offiah A, Kydd A, Kahaly G, Mohr-Kahaly S, Rajanayagam O, Lyons G, Wareham N, Halsall D, Dattani M, Hughes S, Gurnell M, Park SM, Chatterjee K. An adult female with resistance to thyroid hormone mediated by defective thyroid hormone receptor alpha. *J Clin Endocrinol Metab.* 2013;**98**(11):4254-4261.
31. Stampfer M, Beck-Wodl S, RieB A, Haack T. Most severe case of thyroid-alpha-receptor deficiency in a female patient with severe growth and mental retardation, macrocephaly, pubertas tarda and dysgerminoma. Poster presented at The European Society of Human Genetics 28 May, 2017;P08.65A (abstract).

32. Sun H, Wu H, Xie R, Wang F, Chen T, Chen X, Wang X, Flamant F, Chen L. New Case of Thyroid Hormone Resistance alpha Caused by a Mutation of THRA /TRalpha1. *J Endocr Soc.* 2019;**3**(3):665-669.

33. Moran C, Agostini M, Visser WE, Schoenmakers E, Schoenmakers N, Offiah AC, Poole K, Rajanayagam O, Lyons G, Halsall D, Gurnell M, Chrysis D, Efthymiadou A, Buchanan C, Aylwin S, Chatterjee KK. Resistance to thyroid hormone caused by a mutation in thyroid hormone receptor (TR)alpha1 and TRalpha2: clinical, biochemical, and genetic analyses of three related patients. *Lancet Diabetes Endocrinol.* 2014;**2**(8):619-626.

34. Espiard S, Savagner F, Flamant F, Vlaeminck-Guillem V, Guyot R, Munier M, d'Herbomez M, Bourguet W, Pinto G, Rose C, Rodien P, Wemeau JL. A Novel Mutation in THRA Gene Associated With an Atypical Phenotype of Resistance to Thyroid Hormone. *J Clin Endocrinol Metab.* 2015;**100**(8):2841-2848.

35. Yuen RK, Thiruvahindrapuram B, Merico D, Walker S, Tammimies K, Hoang N, Chrysler C, Nalpathamkalam T, Pellecchia G, Liu Y, Gazzellone MJ, D'Abate L, Deneault E, Howe JL, Liu RS, Thompson A, Zarrei M, Uddin M, Marshall CR, Ring RH, Zwaigenbaum L, Ray PN, Weksberg R, Carter MT, Fernandez BA, Roberts W, Szatmari P, Scherer SW. Whole-genome sequencing of quartet families with autism spectrum disorder. *Nat Med.* 2015;**21**(2):185-191.

36. Moran C, Agostini M, McGowan A, Schoenmakers E, Fairall L, Lyons G, Rajanayagam O, Watson L, Offiah A, Barton J, Price S, Schwabe J, Chatterjee K. Contrasting Phenotypes in Resistance to Thyroid Hormone Alpha Correlate with Divergent Properties of Thyroid Hormone Receptor alpha1 Mutant Proteins. *Thyroid.* 2017;**27**(7):973-982.

37. Wejaphikul K, Groeneweg S, Hilhorst-Hofstee Y, Chatterjee VK, Peeters RP, Meima ME, Visser WE. Insight into molecular determinants of T3 vs. T4 recognition from mutations in thyroid hormone receptor alpha and beta. *J Clin Endocrinol Metab.* 2019;**104**(8):3491-3500.

38. Kalikiri MK, Mamidala MP, Rao AN, Rajesh V. Analysis and functional characterization of sequence variations in ligand binding domain of thyroid hormone receptors in autism spectrum disorder (ASD) patients. *Autism Res.* 2017;**10**(12):1919-1928.

39. Korkmaz O, Ozen S, Ozdemir TR, Goksen D, Darcan S. A novel thyroid hormone receptor alpha gene mutation, clinic characteristics, and follow-up findings in a patient with thyroid hormone resistance. *Hormones (Athens).* 2019;**10.1007/s42000-019-00094-9**.

40. Kitajima K, Nagaya T, Jameson JL. Dominant negative and DNA-binding properties of mutant thyroid hormone receptors that are defective in homodimerization but not heterodimerization. *Thyroid.* 1995;**5**(5):343-353.

41. Flynn TR, Hollenberg AN, Cohen O, Menke JB, Usala SJ, Tollin S, Hegarty MK, Wondisford FE. A novel C-terminal domain in the thyroid hormone receptor selectively mediates thyroid hormone inhibition. *J Biol Chem.* 1994;**269**(52):32713-32716.

42. Sasaki S, Nakamura H, Tagami T, Miyoshi Y, Nakao K. Functional properties of a mutant T3 receptor beta (R338W) identified in a subject with pituitary resistance to thyroid hormone. *Mol Cell Endocrinol.* 1995;**113**(1):109-117.

43. Rebai M, Kallel I, Rebai A. Genetic features of thyroid hormone receptors. *J Genet.* 2012;**91**(3):367-374.

44. Geffner ME, Su F, Ross NS, Hershman JM, Van Dop C, Menke JB, Hao E, Stanzak RK, Eaton T, Samuels HH, et al. An arginine to histidine mutation in codon 311 of the C-erbA beta gene results in a mutant thyroid hormone receptor that does not mediate a dominant negative phenotype. *J Clin Invest.* 1993;**91**(2):538-546.

45. Adams SO, Mutter SH, Daley BA, Bordic ME. Military RDs improve oral liquid diets. How to ensure nutritious meals for patients with maxillofacial and oral injuries. *J Am Diet Assoc.* 1994;**94**(1):24.

46. Gurnell M, Rajanayagam O, Agostini M, Clifton-Bligh RJ, Wang T, Zelissen PM, van der Horst F, van de Wiel A, Macchia E, Pinchera A, Schwabe JW, Chatterjee VK. Three novel mutations at serine 314 in the thyroid hormone beta receptor differentially impair ligand binding in the syndrome of resistance to thyroid hormone. *Endocrinology.* 1999;**140**(12):5901-5906.

47. Lee JH, Kim EY. Resistance to thyroid hormone due to a novel mutation of thyroid hormone receptor beta gene. *Ann Pediatr Endocrinol Metab.* 2014;**19**(4):229-231.

48. Liang AC, Mandeville ET, Maki T, Shindo A, Som AT, Egawa N, Itoh K, Chuang TT, McNeish JD, Holder JC, Lok J, Lo EH, Arai K. Effects of Aging on Neural Stem/Progenitor Cells and Oligodendrocyte Precursor Cells After Focal Cerebral Ischemia in Spontaneously Hypertensive Rats. *Cell Transplant.* 2016;**25**(4):705-714.

49. Dickson BJ. Molecular mechanisms of axon guidance. *Science.* 2002;**298**(5600):1959-1964.

50. Bashaw GJ, Klein R. Signaling from axon guidance receptors. *Cold Spring Harb Perspect Biol.* 2010;**2**(5):a001941.

51. Ayala R, Shu T, Tsai LH. Trekking across the brain: the journey of neuronal migration. *Cell.* 2007;**128**(1):29-43.

52. Short CA, Suarez-Zayas EA, Gomez TM. Cell adhesion and invasion mechanisms that guide developing axons. *Curr Opin Neurobiol.* 2016;**39**:77-85.

53. Stoeckli ET. Understanding axon guidance: are we nearly there yet? *Development.* 2018;**145**(10).

54. Huang EJ, Reichardt LF. Neurotrophins: roles in neuronal development and function. *Annu Rev Neurosci.* 2001;**24**:677-736.

55. Bernd P. The role of neurotrophins during early development. *Gene Expr.* 2008;**14**(4):241-250.

56. Ceni C, Unsain N, Zeinieh MP, Barker PA. Neurotrophins in the regulation of cellular survival and death. *Handb Exp Pharmacol.* 2014;**220**:193-221.

57. Chouchane M, Costa MR. Instructing neuronal identity during CNS development and astroglial-lineage reprogramming: Roles of NEUROG2 and ASCL1. *Brain Res.* 2019;**1705**:66-74.

58. Wilkinson G, Dennis D, Schuurmans C. Proneural genes in neocortical development. *Neuroscience.* 2013;**253**:256-273.

59. Guillemot F, Hassan BA. Beyond proneural: emerging functions and regulations of proneural proteins. *Curr Opin Neurobiol.* 2017;**42**:93-101.

60. Schuurmans C, Armant O, Nieto M, Stenman JM, Britz O, Klenin N, Brown C, Langevin LM, Seibt J, Tang H, Cunningham JM, Dyck R, Walsh C, Campbell K, Polleux F, Guillemot F. Sequential phases of cortical specification involve Neurogenin-dependent and -independent pathways. *EMBO J.* 2004;**23**(14):2892-2902.

61. Berninger B, Guillemot F, Gotz M. Directing neurotransmitter identity of neurones derived from expanded adult neural stem cells. *Eur J Neurosci.* 2007;**25**(9):2581-2590.

62. Flamant F, Gauthier K. Thyroid hormone receptors: the challenge of elucidating isotype-specific functions and cell-specific response. *Biochim Biophys Acta.* 2013;**1830**(7):3900-3907.

63. Fozzatti L, Lu C, Kim DW, Cheng SY. Differential recruitment of nuclear coregulators directs the isoform-dependent action of mutant thyroid hormone receptors. *Mol Endocrinol.* 2011;**25**(6):908-921.

64. Paul BD, Buchholz DR, Fu L, Shi YB. Tissue- and gene-specific recruitment of steroid receptor coactivator-3 by thyroid hormone receptor during development. *J Biol Chem.* 2005;**280**(29):27165-27172.

65. Hahm JB, Schroeder AC, Privalsky ML. The two major isoforms of thyroid hormone receptor, TRalpha1 and TRbeta1, preferentially partner with distinct panels of auxiliary proteins. *Mol Cell Endocrinol.* 2014;**383**(1-2):80-95.

66. Lee S, Kang J, Yoo J, Ganesan SK, Cook SC, Aguilar B, Ramu S, Lee J, Hong YK. Prox1 physically and functionally interacts with COUP-TFII to specify lymphatic endothelial cell fate. *Blood.* 2009;**113**(8):1856-1859.

67. Song KH, Li T, Chiang JY. A Prospero-related homeodomain protein is a novel co-regulator of hepatocyte nuclear factor 4alpha that regulates the cholesterol 7alpha-hydroxylase gene. *J Biol Chem.* 2006;**281**(15):10081-10088.

68. Qin J, Gao DM, Jiang QF, Zhou Q, Kong YY, Wang Y, Xie YH. Prospero-related homeobox (Prox1) is a corepressor of human liver receptor homolog-1 and suppresses the transcription of the cholesterol 7-alpha-hydroxylase gene. *Mol Endocrinol.* 2004;**18**(10):2424-2439.

69. Takeda Y, Jetten AM. Prospero-related homeobox 1 (Prox1) functions as a novel modulator of retinoic acid-related orphan receptors alpha- and gamma-mediated transactivation. *Nucleic Acids Res.* 2013;**41**(14):6992-7008.

70. Broekema MF, Hollman DAA, Koppen A, van den Ham HJ, Melchers D, Pijnenburg D, Ruijtenbeek R, van Mil SWC, Houtman R, Kalkhoven E. Profiling of 3696 Nuclear Receptor-Coregulator Interactions: A Resource for Biological and Clinical Discovery. *Endocrinology.* 2018;**159**(6):2397-2407.

71. Xue Y, Wong J, Moreno GT, Young MK, Cote J, Wang W. NURD, a novel complex with both ATP-dependent chromatin-remodeling and histone deacetylase activities. *Mol Cell.* 1998;**2**(6):851-861.

72. Tong JK, Hassig CA, Schnitzler GR, Kingston RE, Schreiber SL. Chromatin deacetylation by an ATP-dependent nucleosome remodelling complex. *Nature.* 1998;**395**(6705):917-921.

73. Zhang Y, LeRoy G, Seelig HP, Lane WS, Reinberg D. The dermatomyositis-specific autoantigen Mi2 is a component of a complex containing histone deacetylase and nucleosome remodeling activities. *Cell.* 1998;**95**(2):279-289.

74. Bornelov S, Reynolds N, Xenophontos M, Gharbi S, Johnstone E, Floyd R, Ralser M, Signolet J, Loos R, Dietmann S, Bertone P, Hendrich B. The Nucleosome Remodeling and Deacetylation Complex Modulates Chromatin Structure at Sites of Active Transcription to Fine-Tune Gene Expression. *Mol Cell.* 2018;**71**(1):56-72 e54.

75. Sengoku T, Yokoyama S. Structural basis for histone H3 Lys 27 demethylation by UTX/KDM6A. *Genes Dev.* 2011;**25**(21):2266-2277.

76. Shpargel KB, Starmer J, Wang C, Ge K, Magnuson T. UTX-guided neural crest function underlies craniofacial features of Kabuki syndrome. *Proc Natl Acad Sci U S A.* 2017;**114**(43):E9046-E9055.

77. Steward MM, Lee JS, O'Donovan A, Wyatt M, Bernstein BE, Shilatifard A. Molecular regulation of H3K4 trimethylation by ASH2L, a shared subunit of MLL complexes. *Nat Struct Mol Biol.* 2006;**13**(9):852-854.

78. Froimchuk E, Jang Y, Ge K. Histone H3 lysine 4 methyltransferase KMT2D. *Gene.* 2017;**627**:337-342.

79. Wang W, Li X, Lee M, Jun S, Aziz KE, Feng L, Tran MK, Li N, McCrea PD, Park JI, Chen J. FOXKs promote Wnt/beta-catenin signaling by translocating DVL into the nucleus. *Dev Cell.* 2015;**32**(6):707-718.

80. Skah S, Uchuya-Castillo J, Sirakov M, Plateroti M. The thyroid hormone nuclear receptors and the Wnt/beta-catenin pathway: An intriguing liaison. *Dev Biol.* 2017;**422**(2):71-82.

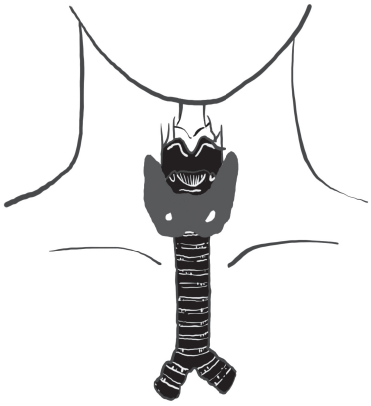

CHAPTER 8

Summary/Samenvatting

8

SUMMARY

Thyroid hormone (TH) is indispensable for normal growth, development, and metabolic homeostasis. The principal action of TH is transcriptional gene regulation (genomic actions), which is mediated by binding of TH to thyroid hormone receptors (TRs). Two major forms of TH are produced from the thyroid gland under tight regulation of the hypothalamic-pituitary-thyroid (HPT) axis, namely 3,3',5,5'-tetraiodothyronine or thyroxine (T4), and 3,3',5-triiodothyronine (T3). T3 is the bioactive hormone, whereas T4 is a prohormone, since T3 binds to TRs with a higher affinity than T4. However, the mechanism underlying this difference in affinity has received marginal attention.

There are three functional isoforms of TRs that are capable of binding T3 and controlling gene transcription, namely TRα1, TRβ1, and TRβ2. TRα1 is encoded by the *THRA* gene on chromosome 17, and TRβ1 and TRβ2 are encoded by the *THRB* gene on chromosome 3. TRs mainly heterodimerize with the retinoid X receptor (RXR) and bind to thyroid hormone response elements (TREs) to regulate gene transcription. In the absence of T3, the TRs recruit corepressor proteins to repress transcription of positively regulated genes. In the presence of T3, TRs then release the corepressors and recruit coactivators to induce gene transcriptional activation. Mutations of the TRs cause resistance to thyroid hormone (RTH) that results in two distinct disorders; RTHα and RTHβ, dependent on *THRA* and *THRB* mutations, respectively.

This thesis focuses on the complexity of the genomic actions of TH. **Chapter 1** provides a general introduction of TH actions, especially the function of TRs and genetic abnormalities that cause RTH. The general aims and outline of this thesis are also presented in this chapter. **Chapter 2** describes the role of Leu341 in TRβ function, prompted by the identification of a novel mutation, TRβ1-L341V, as a cause of RTHβ. By using an *in silico* prediction model and a pipeline of *in vitro* studies (T3 binding assays, electromobility shift assays, transcriptional activity assays, and protein-protein interaction [two-hybrid] assays). Our study shows that the direct interaction between Leu341 and T3 and the microarchitecture formed by interactions between Leu341 and its surrounding residues are required for optimal T3 binding affinity and T3-induced transcriptional activity of TRβ1. **Chapter 3** unravels the molecular and structural mechanism underlying the differences in biological activity of T3 and T4, prompted by the identification of a novel TRα1-M256T mutation and the previously reported TRβ1-M310T mutations in RTHα and RTHβ patients, respectively. We found that these mutations have a greater impact on the affinity of T3 than of T4 for the receptors. This finding suggests that Met256 in TRα1 and the equivalent Met310 in TRβ1 are important for T3 versus T4 discrimination and may partially explain the underlying molecular and structural basis for the role of T4 as a prohormone and T3 as a biologically active hormone in a widely accepted concept of TH physiology.

To date, 25 mutations (in a total of 40 patients) have been identified as a cause of RTHα. The increase in the number of patients allowed us to study the variability in patients' phenotype. So far, the underlying molecular mechanisms to explain this variation have not yet been clearly established. In **chapter 4**, we investigate the factors that contribute to the differential impaired transcriptional activity of seven TRα missense mutations, four of which are derived from RTHα patients. The results show that reduced T3 binding affinity is the predominant factor that determines the severity of impaired transcriptional activation and defective interactions with the cofactor NCoR1 and SRC1. In addition, the degree of reduced T3 binding affinity and impaired transcriptional activation of the mutants seems to be related to the phenotype of the patients. In **chapter 5**, we study the difference of the neurological phenotype found in two RTHα patients carrying TRα1-C380fsx387 and TRα1-F397fsx406 truncating mutations that both entirely abolish T3 binding affinity. The transcriptomes of these two mutants in a human neuronal cell line show that the TRα1-C380fsx387 mutant alters baseline gene expression to a larger and different extent than the TRα1-F397fsx406 mutant, which is in agreement with the more severe cognitive impairment of the patient carrying the TRα1-C380fsx387 mutation. This finding suggests that the effect of the mutants on gene expression is not only due to the reduced T3 binding, but that other defects in receptor function may contribute to the differences in the phenotype of patients.

As mentioned previously, nuclear coregulatory proteins are important in transcriptional gene regulation by TRs. Understanding the complexity of TR-cofactor interactions will gain more insight into mechanisms of disease in RTH. In **chapter 6**, we used an unbiased approach using a tandem-affinity TR purification technique to identify the interactomes of TRs. **Chapter 6a** focuses on the cell-type specific coregulatory protein recruitment of TRα1 by performing the experiments in human liver and neuronal cell lines. In general, TRα1 uses common nuclear coregulatory proteins to regulate gene transcription in these two cell types. However, some proteins are likely to interact with TRα1 in a cell-type specific manner. **Chapter 6b** focuses on the isoform-dependent (TRα1 versus TRβ1) coregulatory protein recruitment by TRs in a human neuronal cell line in order to understand the complexity of TR actions in the brain. We show that the majority of identified proteins were associated with both TRα1 and TRβ1, suggesting that both TR isoforms associate with common nuclear coregulatory proteins to regulate gene transcription. However, a subset of nuclear proteins interacts with TRs in an isoform-specific manner. These findings expand the knowledge about the interaction between TRs and coregulatory proteins in transcriptional gene regulation and may provide more understanding about the impact of TR mutations in RTH syndromes.

Finally, in **chapter 7**, we discuss the findings presented in this thesis in light of the currently available literature. The possible implications of these studies and future perspective are also suggested.

SAMENVATTING

Schildklierhormoon (TH) is onmisbaar voor normale groei, ontwikkeling en metabole homeostase. De belangrijkste actie van TH is transcriptionele genregulatie (genomische acties) dat wordt gemedieerd door binding van TH aan schildklierhormoonreceptoren (TRs). Twee belangrijke vormen van TH worden geproduceerd door de schildklier onder strikte regulering door de hypothalamus-hypofyse-schildklier (HPT) as, namelijk 3,3',5,5' tetraiodothyronine of thyroxine (T4), en 3,3',5- triiodothyronine (T3). T3 is het biologisch actieve hormoon, terwijl T4 een prohormoon is, aangezien T3 met een hogere affiniteit aan de TR bindt dan T4. Het mechanisme dat aan dit verschil in affiniteit ten grondslag ligt heeft echter slecht beperkte aandacht gekregen.

Er zijn drie functionele TR isovormen die in staat zijn om T3 te binden en gentranscriptie te reguleren, namelijk TRα1, TRβ1 en TRβ2. TRα1 wordt gecodeerd door het THRA-gen op chromosoom 17 en TRβ1 en TRβ2 worden gecodeerd door het THRB-gen op chromosoom 3. TRs heterodimeriseren voornamelijk met retinoïde X-receptoren (RXR) en reguleren gentranscriptie via binding aan schildklierhormoon respons elementen (TRE's). Bij afwezigheid van T3 binden de TRs aan corepressor-eiwitten waardoor de transcriptie van positief gereguleerde genen wordt onderdrukt. In de aanwezigheid van T3 worden de corepressoren uitgewisseld voor co-activatoren, wat vervolgens gentranscriptie te induceert. Mutaties in de TRs zijn de oorzaak van twee verschillende vormen van resistentie tegen schildklierhormoon (RTH), namelijk RTHα en β door mutaties in respectievelijk THRA en THRB.

Dit proefschrift gaat over de complexiteit van de genomische acties van TH. **Hoofdstuk 1** geeft een algemene inleiding over TH werking, met name de functie van TRs en genetische afwijkingen in TRs die RTH veroorzaken. De algemene doelstellingen en de rode draad van dit proefschrift worden ook in dit hoofdstuk gepresenteerd. **Hoofdstuk 2** beschrijft de rol van Leu341 in de werking van TRβ, naar aanleiding van de identificatie van een nieuwe mutatie, TRβ1-L341V gevonden in een RTHβ patiënt. Deze mutatie is getest door gebruik te maken van een voorspellend in silico model en een pijplijn van in vitro-onderzoeken (T3-bindingsassays, elektroforetische mobiliteit shift assay, transcriptionele activiteit assays en eiwit-eiwit interacties [twee-hybride] assays). Onze studie toont aan dat de directe interactie tussen Leu341 en T3 en de microarchitectuur gevormd door interacties tussen Leu341 en de omliggende residuen vereist zijn voor een optimale bindingsaffiniteit voor T3 en T3-geïnduceerde transcriptionele activiteit van TRβ1. **Hoofdstuk 3** ontrafelt het moleculaire en structurele mechanisme dat ten grondslag ligt aan de verschillen in de biologische activiteit van T3 en T4, naar aanleiding van de identificatie van respectievelijk een nieuwe TRα1-M256T mutatie en de eerder gemelde TRβ1-M310T-mutatie in RTHα- en RTHβ-patiënten. We vonden dat deze mutaties een grotere impact hebben op de affiniteit van de receptoren voor T3 dan voor T4. Deze bevinding suggereert dat Met256 in TRα1 en de equivalente Met310 in TRβ1 belangrijk zijn voor het T3- versus T4-onderscheid en kan deels de onderliggende moleculaire

en structurele basis voor de rol van T4 als een prohormoon en T3 als een biologisch actief hormoon verklaren, binnen een algemeen geaccepteerd concept van TH fysiologie.

Tot op heden zijn 25 mutaties (in totaal 40 patiënten) geïdentificeerd die RTHα veroorzaken. Een toename van het aantal patiënten stelt ons in staat de variabiliteit van het fenotype van de patiënten te bestuderen. Tot dusverre is het onderliggende moleculaire mechanisme om de variatie te verklaren nog niet duidelijk opgehelderd. In **hoofdstuk 4** hebben we de factoren onderzocht die bijdragen aan de differentieel gestoorde transcriptionele activiteit van zeven TRα-mutaties, waarvan er vier zijn afgeleid van RTHα-patiënten. De resultaten tonen aan dat verminderde T3-bindingsaffiniteit de belangrijkste factor is die de mate van de verminderde transcriptionele activiteit en interacties met de cofactoren NCoR1 en SRC1 bepaalt. Bovendien lijkt de mate van verminderde bindingsaffiniteit voor T3 en verminderde transcriptionele activiteit van de mutanten gerelateerd te zijn aan het fenotype van de patiënten. In **hoofdstuk 5** bestuderen we het verschil in het neurologisch fenotype gevonden in twee RTHα-patiënten, één met een TRα1-C380fsx387 mutatie en één met een TRα1-F397fsx406 truncerende mutatie, die beide de binding van T3 volledig opheffen. De transcriptomen van deze twee mutanten in een menselijke neuronale cellijn laten zien dat de TRα1-C380fsx387 mutant de baseline genexpressie in een grotere mate verandert dan de TRα1-F397fsx406 mutant, wat in overeenstemming is met de ernstigere cognitieve stoornissen van de patiënt met de TRα1-C380fsx387 mutatie. Deze bevinding suggereert dat het effect van de mutanten op genexpressie niet enkel wordt veroorzaakt door een verminderde T3-binding, maar dat andere defecten in receptor functie kunnen bijdragen aan de verschillen in het fenotype van patiënten.

Zoals eerder vermeld, zijn nucleaire coregulatoire eiwitten belangrijk voor de transcriptionele regulatie door TRs. Het begrijpen van de complexiteit van de TR-cofactor interacties kan verder inzicht geven in de impact van TR-mutaties bij RTH-syndromen, naast het effect op T3-binding. In **hoofdstuk 6** hebben we een hypothese vrije benadering gebruikt door middels een tandem-affiniteitszuiveringstechniek de interactomen van TRs te identificeren. **Hoofdstuk 6a** is gericht op de celtype specifieke associatie van coregulatoire eiwitten met TRα1 door de identificatie van de interactomen in zowel een menselijke lever als neuronale cellijn. Over het algemeen gebruikt TRα1 dezelfde nucleaire coregulatoire eiwitten om gentranscriptie in deze twee celtypen te reguleren. Het is echter waarschijnlijk dat sommige eiwitten interacties aangaan met TRα1 op een celtype specifieke manier. **Hoofdstuk 6b** is gericht op de isovorm-afhankelijke (TRα1 versus TRβ1) coregulatoire eiwit interacties in een menselijke neuronale cellijn, om de complexiteit van TR-werking in de hersenen te begrijpen. We laten zien dat de meerderheid van de geïdentificeerde eiwitten geassocieerd was met zowel TRα1 als TRβ1, wat suggereert dat beide TR-isovormen associëren met dezelfde nucleaire coregulatoire eiwitten om gentranscriptie te reguleren. Een aantal nucleaire eiwitten bindt echter aan TRs op een isovormspecifieke manier. Deze bevindingen vergroten de kennis over de interactie tussen TRs en coregulatoire eiwitten tijdens transcriptionele genregulatie en kunnen meer inzicht verschaffen in het effect van TR-mutaties bij RTH-syndromen, naast het effect op T3-binding.

Tot slot bespreken we in **hoofdstuk 7** de bevindingen uit dit proefschrift in het kader van de momenteel beschikbare literatuur. De mogelijke implicaties van deze studies en het toekomstperspectief worden ook besproken.

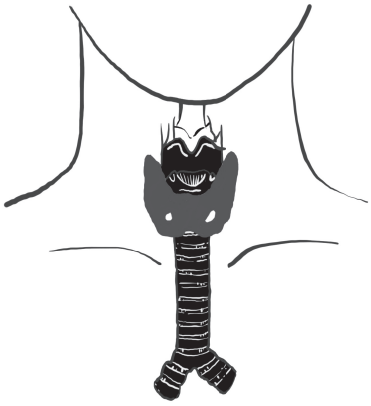

CHAPTER 9

Appendix

- *Authors' affiliations*
- *List of publications and manuscripts*
- *Erasmus MC PhD portfolio*
- *Acknowledgments*
- *About the author*

9

Authors' Affiliations

Erasmus MC, Department of Internal Medicine, Academic Center for Thyroid Diseases, Rotterdam, the Netherlands

Karn Wejaphikul, Anja L.M. van Gucht, Stefan Groeneweg, Selmar Leeuwenburgh, Theo J. Visser, W. Edward Visser, Marcel E. Meima, Robin P. Peeters

Erasmus MC, Department of Neurology, Rotterdam, the Netherlands

Lona Zeneyedpour, Lennard J.M. Dekker, Theo M. Luider

Erasmus MC, Center of Biomics, Rotterdam, the Netherlands

Wilfred F.J. van IJcken

Wellcome-MRC Institute of Metabolic Science, University of Cambridge, United Kingdom

V. Krishna Chatterjee, W. Edward Visser

Department of Clinical Genetics, Leiden University Medical Center, Leiden, the Netherlands

Yvonne Hilhorst-Hofstee

Department of Pediatrics, Faculty of Medicine, Chiang Mai University, Chiang Mai, Thailand

Karn Wejaphikul, Prapai Dejkhamron, Kevalee Unachak

List of Publications and Manuscripts

Wejaphikul K, Groeneweg S, Dejkhamron P, Unachak K, Visser WE, Chatterjee VK, Visser TJ, Meima ME, Peeters RP. Role of Leucine 341 in Thyroid Hormone Receptor Beta Revealed by a Novel Mutation Causing Thyroid Hormone Resistance. *Thyroid 2018;28(12):1723-1726.*

Wejaphikul K, Groeneweg S, Hilhorst-Hofstee Y, Chatterjee VK, Peeters RP, Meima ME, Visser WE. Insight into molecular determinants of T3 vs T4 recognition from mutations in thyroid hormone receptor α and β. *J Clin Endocrinol Metab 2019;104(8):3491-3500.*

Wejaphikul K, Van Gucht ALM, Groeneweg S, Visser WE, Visser TJ, Peeters RP, Meima ME. The *in vitro* functional impairment of thyroid hormone receptor alpha 1 isoform mutants is mainly dictated by reduced ligand-sensitivity. *Thyroid 2019 (in press).*

Wejaphikul K, Visser WE, Leeuwenbrugh S, Van IJcken WFJ, Peeters RP, Meima ME. The effect of thyroid hormone receptor truncating mutants on gene transcription in neuronal cells. *Manuscript in preparation*

Meima ME, **Wejaphikul K**, Leeuwenburgh S, Van Gucht ALM, Zeneyedpour L, Dekker LJM, Visser WE, Luider TM, Peeters RP. Human liver and neuronal interactomes reveal novel binding partners for the T3 receptor isoform α1. *Submitted*

Wejaphikul K, Zeneyedpour L, Visser WE, Leeuwenburgh S, Luider TM, Peeters RP, Meima ME. Coregulatory protein recruitment by thyroid hormone receptors in neuronal cells. *Manuscript in preparation*

Publications not in this Thesis

Dejkhamron P, **Wejaphikul K**, Mahatumarat T, Silvilairat S, Charoenkwan P, Saekho S, Unachak K. Vitamin D deficiency and its relationship with cardiac iron and function in patients with transfusion dependent thalassemia at Chiang Mai University Hospital. *Pediatr Hematol Oncol 2018;35(1):52-59.*

Choeyprasert W, Yansomdet T, Netesirinilkul R, **Wejaphikul K**, Charoenkwan P. Adverse effects of imatinib in children with chronic myelogenous leukemia. *Pediatr Int 2017;59(3):286-292.*

Wejaphikul K, Cho SY, Huh R, Kwun Y, Lee J, Ki CS, Jin DK. Hypoparathyroidism in a 3-year-old Korean Boy with Sotos Syndrome and a Novel Mutation in NSD1. *Ann Clin Lab Sci 2015;45(2):215-8.*

PhD Portfolio

PhD Student: **Karn Wejaphikul**

Erasmus MC Department: Internal Medicine, Academic Center for Thyroid Diseases

Research School: Molecular Medicine

PhD period: 2015-2019

Promotor: Prof.dr. Robin P. Peeters

Co-promotors: Dr. Marcel E. Meima

Dr. W. Edward Visser

PhD Training	Year	Workload	ECTs
Courses & Workshops			
Stralingsbeschermings-deskundigheidsniveau 5B	2015	3 days	1.0
Introduction to GraphPad Prism	2015	1 day	0.3
The Basic Human Genetic course: Genetics for Dummies	2015	2 days	0.5
The Course Biomedical Research Techniques XIV	2015	5 days	1.5
The Annual Course on Molecular Medicine	2016	2 days	0.7
Biostatistic course CCO2A 2016	2016	4 days	2.0
The 6th course Basic and Translational Endocrinology: “Emerging Technologies in Endocrine Research”	2016	3 days	1.0
Research Integrity	2017	1day	0.3
The Workshop on Photoshop & Illustrator CS6 for PhD-students and other researchers	2017	1 day	0.3
The SNP Course XIV: SNPs and Human Diseases	2017	5 days	2.0
The course in English Biomedical Writing and Communication	2017	10 weeks	3.0
The Ensembl Workshop	2018	2 days	0.6
The Workshop on NCBI & other open source software	2018	3 days	1.0
The Workshop on InDesign CC 2019 for PhD-students and other researchers	2019	1 day	0.3
Oral presentations			
Dutch Endocrine Society Meeting 2016, Noordwijkerhout, The Netherlands: *The Activity of T3 Receptor Mutants on Different T3 Response Elements*	2016		0.7
39th Annual Meeting of the European Thyroid Association (ETA), Copenhagen, Denmark: *Variably Defective Transcriptional Activity of T3 Receptor TRα1 Mutants in Different Thyroid Hormone Response Elements*	2016		0.7

PhD Training	Year	Workload	ECTs
9th Biennial Scientific Meeting of the Asia Pacific Pediatric Endocrine Society (APPES): *Comprehensive Steroid Profile in Classic 21-Hydroxylase Deficiency: Clinical and Hormonal Correlation*	2016		0.7
3rd JNVE conference 2016, Leiden, The Netherlands: *A Novel L341V Mutation of the Thyroid Hormone (TH) Receptor β Gene in a Girl with Resistance to TH*	2016		0.7
Wetenschapsdagen (Science Day) 2017, Antwerp, Belgium: *A Novel L341V Mutation of the Thyroid Hormone (TH) Receptor β Gene in a Girl with Resistance to TH*	2017		0.7
Dutch Endocrine Society Meeting 2017, Noordwijkerhout, The Netherlands: *A Novel L341V Mutation of the Thyroid Hormone (TH) Receptor β Gene in a Girl with Resistance to TH*	2017		0.7
The Internal Medicine Research Symposium: *Diverse Functional Impairment of Thyroid Hormone Receptor Alpha (TRα) Mutations*	2017		0.4
40th Annual Meeting of the European Thyroid Association (ETA), Belgrade, Serbia: *Diverse Functional Impairment of Thyroid Hormone Receptor Alpha Mutations* (Topic Highlight)	2017		0.7
4th JNVE conference 2017, Leiden, The Netherlands: *Diverse Functional Impairment of Thyroid Hormone Receptor Alpha Mutations*	2017		0.7
33rd Workshop on Experimental Thyroid Research (Arbeitstagung Experimentelle Schilddrüsenforschung, AESF), Berlin, Germany: *How to Study Functions of Mutated Thyroid Hormone Receptors (TRs)?* (invited speaker)	2018		0.7
13th International Workshop on Resistance to Thyroid Hormone (IWRTH) Meeting 2018, Doorn, The Netherlands: *Naturally Occuring Mutations in Thyroid Hormone Receptors Highlight T3 versus T4 Recognition*	2018		0.7
41st Annual Meeting of the European Thyroid Association (ETA), Newcastle, United Kingdom: *A Novel THRA M256T Mutation in Resistance to Thyroid Hormone Alpha Highlights T3 versus T4 Recognition of Thyroid Hormone Receptors*	2018		0.7
10th Asia Pacific Paediatric Endocrine Society (APPES) Scientific Meeting, Chiang Mai, Thailand: *A Resistance to Thyroid Hormone α Patient with a Novel THRA M256T Mutation Lacking T3 versus T4 Discrimination*	2018		0.7
Dutch Thyroid Club Meeting, Nijmegen, Rotterdam: *Coregulatory Protein Recruitment by Thyroid Hormone Receptors in Neuronal Cells*	2019		0.7
Dutch Endocrine Society Meeting 2019, Noordwijkerhout, The Netherlands: *Coregulatory Protein Recruitment by Thyroid Hormone Receptors in Neuronal Cells*	2019		0.7

PhD Training	Year	Workload	ECTs
Poster presentations			
Wetenschapsdagen (Science Day) 2016, Antwerp, Belgium: *The Activity of T3 Receptor Mutants on Different T3 Response Elements*	2016		0.7
20th Molecular Medicine Day 2016: *The Activity of T3 Receptor Mutants on Different T3 Response Elements*	2016		0.7
12th International Workshop on Resistance to Thyroid Hormone (IWRTH), Colorado, USA: *Diverse Transcriptional Activation Patterns of Thyroid Hormone Receptor Alpha Mutations on Different Thyroid Response Elements*	2016		0.7
86th Annual Meeting of the American Thyroid Association (ATA), Denver, USA: *A Novel L341V Mutation of the Thyroid Hormone (TH) Receptor β Gene in a Girl with Resistance to TH* (Basic poster award winner)	2016		0.7
9th Biennial Scientific Meeting of the Asia Pacific Pediatric Endocrine Society (APPES): *GnRH-independent Precocious Puberty in a Thai Boy with NR0B1 Novel Mutation Causing X-linked Adrenal Hypoplasia Congenita*	2016		0.7
The 10th Benelux Nuclear Receptor meeting, Leuven, Belgium: Variably *Defective Functional Properties of Thyroid Hormone Receptor Alpha Mutations*	2017		0.7
Wetenschapsdagen (Science Day) 2018, Antwerp, Belgium: *Resistance to Thyroid Hormone due to Novel THRA M256T Mutation*	2018		0.7
10th Asia Pacific Paediatric Endocrine Society (APPES) Scientific Meeting, Chiang Mai, Thailand: *Clinical Features and Genetic Analysis of Patients with Resistance to Thyroid Hormone β: A single-center experience*	2018		0.7
Wetenschapsdagen (Science Day) 2019, Sint-Michielsgestel, the Netherlands: *Coregulatory Protein Recruitment by Thyroid Hormone Receptors in Neuronal Cells*	2019		0.7
Conferences			
54th Annuals European Society for Paediatric Endocrinology (ESPE) Meeting, Barcelona, Spain	2016	3 days	
The 8th Benelux Nuclear Receptor meeting, Leiden, The Netherlands	2016	1 day	
Wetenschapsdagen (Science Day) 2016, Antwerp, Belgium	2016	2 days	
Dutch Endocrine Society Meeting 2016, Noordwijkerhout, The Netherlands	2016	2 days	
20th Molecular Medicine Day 2016	2016	1 day	
39th Annual Meeting of the European Thyroid Association (ETA), Copenhagen, Denmark	2016	4 days	

PhD Training	Year	Workload	ECTs
12th International Workshop on Resistance to Thyroid Hormone (IWRTH), Colorado, USA	2016	4 days	
86th Annual Meeting of the American Thyroid Association, Denver, USA	2016	5 days	
9th Biennial Scientific Meeting of the Asia Pacific Pediatric Endocrine Society (APPES)	2016	4 days	
3rd JNVE conference 2016, Leiden, The Netherlands	2016	2 days	
Wetenschapsdagen (Science Day) 2017, Antwerp, Belgium	2017	2 days	
Dutch Endocrine Society Meeting 2017, Noordwijkerhout, The Netherlands	2017	2 days	
40th Annual Meeting of the European Thyroid Association, Belgrade, Serbia	2017	4 days	
4th JNVE conference 2017, Leiden, The Netherlands	2017	2 days	
The10th Benelux Nuclear Receptor meeting, Leuven, Belgium	2017	1 day	
Wetenschapsdagen (Science Day) 2018, Antwerp, Belgium	2018	2 days	
33rd Workshop on Experimental Thyroid Research (Arbeitstagung Experimentelle Schilddrüsenforschung, AESF), Berlin, Germany	2018	3 days	
13th International Workshop on Resistance to Thyroid Hormone (IWRTH) Meeting 2018, Doorn, The Netherlands	2018	4 days	
41st Annual Meeting of the European Thyroid Association, Newcastle, United Kingdom	2018	4 days	
10th Asia Pacific Paediatric Endocrine Society Scientific Meeting, Chiang Mai, Thailand	2018	4 days	
Wetenschapsdagen (Science Day) 2019, Sint-Michielsgestel, the Netherlands	2019	2 days	
Dutch Thyroid Club Meeting, Nijmegen, Rotterdam	2019	½ day	
Dutch Endocrine Society Meeting 2019, Noordwijkerhout, The Netherlands	2019	2 days	
Seminars and Meetings			
Thyroid Laboratory Meeting	2015-2019		1.0
Annual Symposium of the Dutch Thyroid Research Foundation	2015-2019		0.7
The Internal Medicine Research Symposium	2016-2019		0.4
Teaching Activities			
6th course Basic and Translational Endocrinology: “Emerging Technologies in Endocrine Research” (Lecturing: Thyroid Hormone Resistance due to Mutations in Thyroid Hormone receptors)	2016	1 day	0.3

PhD Training	Year	Workload	ECTs
Other Academic Activities			
Co-chair of oral presentation session in Wetenschapsdagen (Science Day) 2018, Antwerp, Belgium	2018		
Judging committee for poster-prize in Wetenschapsdagen (Science Day) 2019, Sint-Michielsgestel, the Netherlands	2019		
Grants and Awards			
ETA Travel Award Grant (for Young Investigator) 2016 (500€)	2016		
ATA Travel Grant 2016	2016		
ATA Trainee Poster Award 2016 (The winner of Basic Poster)	2016		
ETA Travel Award Grant 2017 (500€)	2017		
ETA Travel Award Grant 2018 (500€)	2018		

Acknowledgments

This PhD trajectory has been such a long rough road. Without the great support from my mentors, colleagues, friends, and family, I could never have come this far. Therefore, I would like to take this opportunity to express my gratitude to each of them.

First of all, I would like to express my deepest gratitude to my promotor, **Prof.dr. R.P. Peeters**. Dear Robin, thank you for accepting me as a member of your group. Since our first Skype call and the first meet-up in Thailand, I knew already that I am in good hands. Four years in your lab has proved I was correct. You always supported me and guided me to stay on track. “Keep focusing on the goal” was always the conclusion of our discussion, which improves how I work. You also concerned about my future academic career and gave me valuable advice, which I very much appreciate. Apart from that, I immensely enjoy all the dinners and social events we had together as a group. The performance of you in the middle of the dance floor was epic! Thank you for being a great mentor and a good role model for me.

The completion of my PhD would not have been possible without the support of my co-promotor and daily supervisor, **Dr. M.E. Meima**. Dear Marcel, how can I find enough words to thank you for all the things you have done for me? I have learned a lot from you, especially the laboratory skills that I had no experience before. Not only that, you always be there to support me whenever I want, which made me feel very secure. You also helped me to improve my writing and presenting skills, which are vital for my future career. Thank you for your patient guidance and all of your brilliant ideas and suggestions. I also appreciate your sense of humor and easy-going personality, which made me (and everybody in the lab) feel very comfortable to work with you. It was very fortunate for me to have you as my supervisor.

I am also extremely grateful to my second co-promotor, **Dr. W.E. Visser**. Dear Edward, thank you very much for your significant contribution to my research. It was an excellent opportunity for me to work with you. Thanks also for your kindness and your profound belief in my work. I really appreciate it.

I would like to extend my deepest gratitude to **Prof.dr.ir. T.J. Visser**, who unfortunately passed away during my PhD period. Dear Theo, it was a great honor for me to work under your supervision and to know you as a person. I much admire your wide-range of knowledge and creativity. You always came up with brilliant and eye-opening questions and comments during the work-discussion, which were one hand difficult to response, but on the other hand, broaden my point of view. Your dedication to the thyroid field also inspired me. Thank you very much for everything. I will always miss you.

I am also extremely grateful to the reading committee members, **Prof.dr. A.J. van der Lelij**, **Prof.dr. A.C.S. Hokken-Koelega**, and **Prof.dr. A.S.P. van Trotsenburg**, Thank you for accepting the responsibility to read and evaluate my thesis. I greatly appreciate it and look forward to discussing my work with you. I would also like to extend my deepest gratitude to the plenary committee members, **Prof.dr. O.C. Meijer**, **Dr. A. Boelen**, and **Dr. T.M. Luider**.

Thank you for agreeing to be a member of the committee. It will be my pleasure to discuss my work with you.

Without the invaluable contribution of all co-authors, this thesis would not have been completed. I would like to thank **Prof.dr. V.K.K. Chatterjee** from Wellcome-MRC Institute of Metabolic Science, University of Cambridge, UK. It was an honor to collaborate with you. I am also glad to have an opportunity to attain your lecture and discuss with you in person. Thank you very much for sharing your expertise in the thyroid research field with us. I also wish to thank **Dr. Y. Hilhorst-Hofste** from Department of Clinical Genetics, Leiden University Medical Center. I very much appreciate your helpful contribution and constructive advice. Thanks also to **L. Zeneyedpour** and **L.J.M Dekker** form Department of Neurology, Erasmus MC for your contribution in proteomic projects and **W.F.J. van IJcken** from Center of Biomics, Erasmus MC for your assistance and helpful advice in RNAseq project.

Special thanks should also go to all co-authors and colleagues in the thyroid lab, **Dr. S. Groeneweg**, **Dr. A.L.M. van Gucht**, and **S. Leeuwenburgh**. Dear Stefan, thanks for sharing your expertise in protein modeling in my works. Your incredible inputs made this thesis stronger in every way. It was enjoyable working with you in the lab and traveling together to several international conferences. I wish you all the best with your PhD trajectory and your future career. Dear Anja, thanks for your contribution to RTHα projects and everything you taught me since the beginning of my PhD. Having you as a friend and colleague is fantastic. I wish you lots of success in your medical training. Dear Selmar, I appreciate your effort on RNAseq and proteomic projects and also your general assistance. Thanks also for being around in the lab and create such a fun vibe.

I would not have survived in the lab without the support from all thyroid lab members (and ex-members). Dear **Elaine**, thank you so much for your unwavering support and encouragement. Your way of working is very organized, which I took as a role model. Without you, the beginning of my lab life would have been more difficult. Dear **Stefania**, thanks for all the great times (and of course, delicious food) we had together. You are such a wonderful friend. I look forward to seeing the success of your PhD. The final year will be tough, but believe me, you can do it! Dear **Zhongli**, thanks for accepting to be my paranymph. Thanks also for being my good friend. You made working in the weekend not so suffering (at least I knew I was not the only one). I will not forget all the cookies and chocolate we shared. Wish you great success in your PhD (with high IF publications as you want). Dear **Ramona**, **Melitza**, **Celia**, **Ferdy**, **Nilhan**, **Linda**, **Rutchanna**, and **Wouter**, I enjoyed working with you guys in the lab. Thanks for all of your help and also all the inputs you gave me in our work-discussion. Thanks also to all students and visitors that have been a part of our lab. I wish you all the best!

The thyroid group would not be complete without colleagues from the clinical part. Dear **Layal**, **Tim**, **Elske**, **Mirijana**, and **Arjola**, I am so glad that I have got to know you guys. Your epidemiological and clinical researches helped me to maintain my clinical knowledge.

It was also fun being together as a group at many conferences. Dear **Evert**, **Deborah**, **Arash**, **Tessa**, **Caroline**, **Oscar**, and **Mathe,** thank you for creating a pleasant atmosphere not only in the work-discussion but also at all conferences we have been together. I wish you all the best in your PhD trajectory. Dear **Marco** and **Laura**, thank you for all the valuable suggestion during the work-discussion. Special thanks to **Anneke** for your help to arrange all documents and also my flights back home every year. My thanks also to **people on the Ee 5th** (Gonaden lab, Bone lab, Neuro-endo lab, and Genetics lab) who always be very friendly. Good luck with your research!

I would also like to acknowledge all of the support from Thailand. I cannot even begin to express my gratitude to my beloved mentors, **Dr. K. Unachak** and **Dr. P. Dejkhamron**. Dear Ajarn Kevalee and Ajarn Prapai, you are the wind beneath my wings since I was a pediatric resident. Thank you very much for believing in me and for allowing me to pursue my PhD in the Netherlands with no hesitation. I will keep my promise to go back and help to develop our division and department. Many thanks also to all assistants: **P'Kai**, **P'Laddawan**, **P'Pook**, and **P'Danil**. I very much appreciate the help that I received from you guys during my stay in the Netherlands. I would like to extend my gratitude to **Chiang Mai University** and **the Faculty of Medicine,** who awarded me a scholarship to accomplish my PhD degree. Thanks also to **the Department of Pediatrics, CMU**, who gave me this great opportunity. Last but foremost, I am deeply indebted to my mentors at King Chulalongkorn Memorial Hospital, **Dr. T. Sahakitrungruang**, **Prof.dr. V. Supornsilchai**, and **Prof.dr. S. Wacharasindhu**. Dear P'Dao, P'Tee, and Ajarn Suttipong, thanks for all of your support and for providing me this incredible connection with Erasmus MC. Without you, it would not have been possible for me to be here.

Four and a half years in Rotterdam would have been worse than this if I had not had these lovely Thai people around. Dear **Aung**, you were such a fantastic roommate. I believe it was a destiny that brought us to reunite and had memorable moments together. It was always fun to talk nonsense and watch Toey-Taew-Thai (and so on) together. You were also the one who dragged me to the gym and built my exercise habits. Thanks for sharing with me all the good and the bad. Thanks also for the beautiful thesis cover. I wish you all the best in your PhD. Keep in touch and see you in CM soon. Dear **P'Ann**, thank you so much for all of your help and practical advice since my first day in R'dam. Although we did not hang out together so much afterward (because you were always super busy), you still kept concerning about me and all Thai students. See you in CM very soon. Dear **Keng**, I was so lucky to have you on the same floor and extremely happy to have you as a paranymph. You were very supportive and always tried your best to help me and everybody to solve all the issues we have, which I very much appreciate. Now you are approaching the finish line, and I am sure you will do great. Good luck with that. Dear **Dew**, thank you so much for being a kind and supportive sister. I have to congratulate you as well for your magnificent achievement. Next chapter now officially begins. I wish you lots of success. Dear **Utt**, although we had hardly talked when we were in med school together, we managed to be very close now. It is brillant to see you are doing

better and better in your PhD trajectory. Do not give up. You will rock it. Dear **Nook, Jan, Kib,** and **Ply**, you guys made my days in R'dam more enjoyable. I wish you all the best for your PhD and your future career. Please stay in touch and see you again in Thailand.

Not only Thai friends, but I was very fortunate in having many foreign friends in Rotterdam. Dear **Monique**, I could not find enough words to thank you for everything. You were so kind to me since my very first days in R'dam without knowing each other before. You also helped me and Aung to find this amazing apartment (Ter Hooch), which therefore brought us to become neighbors. Thanks also for your support and encouragement in my bad days. You will always be part of my Rotterdam family. I promise to come back to revisit you, or we can also meet up in Thailand. "Kob-kun-mak-mak-kub". Dear **Mathijs**, thanks for all the nice dinners we had together and also for the yummy bread. "Aroy-mak-mak-mak-mak." Thanks should also go to **Kru Monique**, my Dutch teacher in CM. Thank you very much for introducing me to Monique (now I am getting confused). Sorry that, eventually, I still could not speak Dutch, but at least I remember this word, "Be dank". Dear **Martin**, thanks for the lively conversation and also nice coffee and delicious Chinese food we had together in Den Haag. Dear **Do**, thank you for your companion in the gym, very useful advice for my PhD defense, and also for our friendship. I wish you all the best in your future career. Dear **Claudia**, thanks for all of your help and for being such an amazing landlord. Dear **Wilson**, **Christian**, **Bas**, **Ferran**, **Yi Chien**, **Pascal**, **Shatavisha**, **Faymah**, **Mladen**, and **Grazia**, thanks for your friendship. I am so glad that I have got to know you guys. Good luck with your PhD and/or your future. Last, dear **Henk**, thank you so much for always being with me and cheering me up. We do not know what the future holds, but I am sure it will be great. A big hug goes to you.

Finally, but yet importantly, many thanks to my family (**Papa**, **Mama**, **Ae-Muay**, **Lawan**, and **Wut**) who always be there and support me. Your immense unconditional love has kept me moving forward. Love you guys so much. Thanks also to my friends (**Apple**, **Taew**, **Sueb**, **Jip**, and **P'Poy**) who kept pressuring me to finish my PhD as fast as possible. Four years apart was too long; now it is time to reunite.

About the Author

Karn Wejaphikul was born on 6 May 1983 in Chiang Mai, Thailand. In 2001, he graduated from Chiang Mai University Demonstration School in his home town. He started his Medical Training at Faculty of Medicine, Chiang Mai University and obtained his medical degree (First-Class Honors, Gold Medal) in 2007. After that, he completed a four-year Pediatrics training at Chiang Mai University Hospital, Chiang Mai, Thailand and obtained the Thai Board of Pediatrics in 2011. He then attained a two-year Pediatric Endocrinology training at King Chulalongkorn Memorial Hospital, Chulalongkorn University, Bangkok, Thailand and received his Thai Subboard of Pediatric Endocrinology in 2013. Afterward, he started working as an instructor in Pediatric and Pediatric Endocrinologist at Chiang Mai University Hospital. During that time (2014), Karn was awarded a scholarship from Samsung Medical Center to be a visiting fellow in Pediatric Endocrinology and Medical Genetics for three months at Samsung Medical Center, Seoul, Republic of Korea. In 2015, he started his PhD project at the Academic Center for Thyroid Diseases, Erasmus MC, under the supervision of Prof.dr. Robin P. Peeters, Dr. Marcel E. Meima, and Dr. W. Edward Visser. The results of his research are presented in this PhD thesis entitled “Complexity of genomic actions controlled by thyroid hormone receptors”.